FUNDAMENTAL RESEARCH OF THE SOLVENT ROLE IN THE IONOTHERMAL SYNTHESIS OF MICROPOROUS MATERIALS

by

XIN SUN

B.S., Dalian University of Technology, 2006

AN ABSTRACT OF A DISSERTATION

Submitted in partial fulfillment of the requirements for the degree

DOCTOR OF PHILOSOPHY

Department of Chemical Engineering
College of Engineering

KANSAS STATE UNIVERSITY
Manhattan, Kansas

2012

Abstract

Zeolites and zeolite-like materials are a group of porous materials with many applications in industry including but not limited to detergent builders and catalyst in the oil refining and petrochemical industry, due to their unique properties such as uniform pore size, large surface area and ion-exchange capacity. Researchers are constantly seeking new methods to synthesize zeolites. Zeolites are commonly synthesized in water. Then in 2004, a new method called ionothermal synthesis was invented by Dr. Morris and his colleagues, using ionic liquids (ILs) and eutectic mixtures as the solvent. In contrast to water, ILs and eutectic mixtures have negligible vapor pressure, thus making the use of high-pressure vessel unnecessary. In addition, they have various structures which could render new structures to frameworks of zeolite. Furthermore, since the cations of some ILs have structures which are similar to common structure directing agents, they theoretically could be used both as solvent and structure directing agent in ionothermal synthesis, possibly simplifying the synthesis process.

This project is aimed at investigating the behavior of precursors of zeolites in ionic liquids and the interaction between precursors and ionic liquids in ionothermal synthesis because these fundamental properties could be useful in the current and future synthesis of zeolites. First, solubilities of different precursors, including Syloid 63 silica particles, aluminium isopropoxide ($Al(OiPr)_3$) and phosphoric acid (H_3PO_4) in ILs with different structures are reported. Parameters such as activity coefficient and Henry's constant are calculated from the solubility result. Second, interaction between precursors and ILs are studied. It is found that the addition of ILs in $Al(OiPr)_3$ could change the structure of $Al(OiPr)_3$, especially with the presence of H_3PO_4. Both ILs' structures and temperature are capable of influencing the structure change of $Al(OiPr)_3$. Third, hydrochloric acid is used for the first time as the mineralizer to synthesize aluminophosphates in ILs and it could lead to both dense and porous materials. Regardless of the acid used, frameworks synthesized after several hours always undergo a dramatic change after further heating. A slightly longer alkyl chain of ILs could accelerate the formation of crystalline materials. Increasing concentration of precursors in the reaction gel could increase the yield, but the same framework is not retained. Researches have also been done on stability of ILs in the synthesis process and it is found that heat and the presence of H_3PO_4 could decompose ILs, but the decomposed amount is extremely small.

FUNDAMENTAL RESEARCH OF THE SOLVENT ROLE IN THE IONOTHERMAL SYNTHESIS OF MICROPOROUS MATERIALS

by

XIN SUN

B.S., Dalian University of Technology, 2006

A DISSERTATION

Submitted in partial fulfillment of the requirements for the degree

DOCTOR OF PHILOSOPHY

Department of Chemical Engineering
College of Engineering

KANSAS STATE UNIVERSITY
Manhattan, Kansas

2012

Approved by:

Major Professor
Jennifer L. Anthony

Copyright

Abstract

Zeolites and zeolite-like materials are a group of porous materials with many applications in industry including but not limited to detergent builders and catalyst in the oil refining and petrochemical industry, due to their unique properties such as uniform pore size, large surface area and ion-exchange capacity. Researchers are constantly seeking new methods to synthesize zeolites. Zeolites are commonly synthesized in water. Then in 2004, a new method called ionothermal synthesis was invented by Dr. Morris and his colleagues, using ionic liquids (ILs) and eutectic mixtures as the solvent. In contrast to water, ILs and eutectic mixtures have negligible vapor pressure, thus making the use of high-pressure vessel unnecessary. In addition, they have various structures which could render new structures to frameworks of zeolite. Furthermore, since the cations of some ILs have structures which are similar to common structure directing agents, they theoretically could be used both as solvent and structure directing agent in ionothermal synthesis, possibly simplifying the synthesis process.

This project is aimed at investigating the behavior of precursors of zeolites in ionic liquids and the interaction between precursors and ionic liquids in ionothermal synthesis because these fundamental properties could be useful in the current and future synthesis of zeolites. First, solubilities of different precursors, including Syloid 63 silica particles, aluminium isopropoxide ($Al(OiPr)_3$) and phosphoric acid (H_3PO_4) in ILs with different structures are reported. Parameters such as activity coefficient and Henry's constant are calculated from the solubility result. Second, interaction between precursors and ILs are studied. It is found that the addition of ILs in $Al(OiPr)_3$ could change the structure of $Al(OiPr)_3$, especially with the presence of H_3PO_4. Both ILs' structures and temperature are capable of influencing the structure change of $Al(OiPr)_3$. Third, hydrochloric acid is used for the first time as the mineralizer to synthesize aluminophosphates in ILs and it could lead to both dense and porous materials. Regardless of the acid used, frameworks synthesized after several hours always undergo a dramatic change after further heating. A slightly longer alkyl chain of ILs could accelerate the formation of crystalline materials. Increasing concentration of precursors in the reaction gel could increase the yield, but the same framework is not retained. Researches have also been done on stability of ILs in the synthesis process and it is found that heat and the presence of H_3PO_4 could decompose ILs, but the decomposed amount is extremely small.

Table of contents

List of figures

List of tables

Acknowledgements

First, I would like to thank my primary advisor Dr. Jennifer Anthony for her continuous support of my research and my personal life during these years. She has given me a lot of guidance on my work, especially when I am stuck with my research. Her strict attitude towards research and her nice personality makes it a pleasure for me to work with her. Under her instruction and support, I have learned how to use different scientific instruments, how to present my work professionally in conferences and in papers, and how to criticize and improve my research.

I would also like to thank all of the professors and staff in the Chemical Engineering Department. They are really nice to international students and are willing to help us whenever we need their help. The whole department also maintains a high teaching level. Class taught by each professor is very rewarding and useful. Staff in Chemical Engineering Department often organizes parties and events to unite the persons in the department, including pizza party to celebrate graduation of a student, potluck at the end of each semester and welcome party for the new students joining the department. I really enjoy these activities.

My husband is another person I owe gratitude to. PhD research for many years is sometimes boring and challenging. Without the love and support from him, the completion of my work will be an impossible task. His optimistic personality and tolerance towards my bad temper (seldom) can always melt my tension from the research. He is really a person with a sense of humor, intelligence and knowledge. I have learned a lot from him. My eldest son (Yixiong Cong, a teddy bear), my unborn son (Yixin Cong), my husband and I make up a happy family and I always feel lucky to own all of you.

I am also lucky to have many friends in Manhattan, including Yi Zhang, Li Du, Fan Zhang, Wei Gao, etc. After my graduation, I will definitely miss the happy time with you, playing poker, having hot pot and barbecue, shopping and eating in Kansas City and exchanging ideas on food & clothes.

Dedication

TO MY PARENTS

PEIFA SUN AND **YUFENG XIN**

To MY HUSBAND

WEILONG CONG

Chapter 1 - Introduction to the Project

Molecular sieves (or zeolites) are a group of microporous minerals which have been used extensively in a variety of industrial application including us as detergent builders and as catalyst in the oil refining and petrochemical industry. Currently, 197 zeolites with unique framework structures have been synthesized. The recipes to produce them are found empirically, and it still is not possible to intentionally design a new framework structure. The lack of a full understanding of the formation mechanism such as interactions between solvent/precursor or precursor/precursor is one of the challenges inhibiting the rationally design of a specific framework of zeolite. This lack of understanding is especially pronounced in synthesizing zeolites in ionic liquids since this is a recently invented method, first proposed in 2004.[1] Synthesizing zeolites in ionic liquids is called ionothermal synthesis as compared to conventional hydrothermal synthesis where water is the solvent. In the past eight years, more than 15 microporous aluminophosphate zeolites and two silica-based zeolites have been synthesized. One of the reasons why ionothermal synthesis of zeolites is interesting is that ionic liquids with various chemical structures can be used as the solvent which may lead to zeolites with different framework structures that cannot be synthesized by hydrothermal synthesis. In fact, several new aluminophosphate zeolites which have never been produced in water are readily synthesized in ionic liquids. However, only a few papers talk about the mechanism of zeolites' formation in ionic liquids. As a result, this research focuses on the early stages of zeolitic formation, mainly in the field of solubility and stability of precursors in ionic liquids, and interaction between ionic liquids and precursors, in the hope that the findings could be used for further ionothermal synthesis of zeolites. For example, the maximum solubility of phosphoric acid in 1-hexyl-3-methylimidazolium is around 45 wt %; this experimental result promoted the author to systematically increase the concentration of precursors in the reaction gel to maximize yield of the product. The hypothesis and objective of this project are listed below.

Hypothesis

It is hypothesized that, in the nucleation and growth process of microporous materials, the solvent plays an important role. Understanding the interactions between the precursors and the solvent could help the researchers direct the synthesis of zeolites. The precursors should be

soluble or stabilized in the solvent; then the dissolved precursors could approach each other and initiate the reaction. However, if the solubility of precursor in a solvent is too high, likely denoting a strong interaction between the solvent and the precursor, this interaction will compete with the interactions between precursors and thus inhibit the formation of microporous materials. As a result, interactions between precursor and solvent and precursors' solubilities in solvents need to be investigated.

Objective

The goal of my research is to investigate the interactions between room temperature ionic liquids (RTILs) and precursors of microporous zeolite and aluminophosphate (AlPOs) in the hope that the findings could be used to direct current and future synthesis of these materials in RTILs. Different recipes to ionothermally synthesize aluminophosphates have also been created and tried to investigate the effects of different synthesis parameters (such as solvent structure, prolonged heating time, different mineralizers, concentration of precursors, structure directing agent) on the frameworks structure formed. The interaction between ILs and precursors, and the interaction between different precursors determined by solid NMR will also be used to explain the experimentally-found effect of different parameters on the frameworks. These precursors, which are used to synthesize zeolites and aluminophosphates, include silicon dioxide, aluminium isopropoxide, phosphoric acid and phosphorus pentoxide. The ionic liquids used in this project are all 1-alkyl-3-methylimidazolium-based RTILs with different anions and different sizes of cations, since most of the microporous materials synthesized ionothermally utilize these ionic liquids as solvent and often also as structure directing agent.

Objectives of this project are achieved by experiments and theoretical models. Following this introduction chapter, Chapter 2 gives a detailed background on the basic concepts involved in zeolites and zeolites synthesis, and Chapter 3 presents experimental description and introduction to different instruments used in this project. Experimental results and the theoretical models are presented in detail from Chapter 4 to Chapter 6 and recommendations to the future work are presented in Chapter 7.

Chapter 2 Literature review

Chapter 2 introduces zeolite and zeotype materials, ionic liquids, ionothermal synthesis, and describes which framework structures have been synthesized ionothermally (meaning synthesized in ionic liquids), and summarizes the effects synthesis parameters on the framework structures formed. Finally, the conformation of aluminium isopropoxide (one of the important precursors for zeolite and zeotype materials) is discussed.

Chapter 3 Synthesis and characterization techniques

Chapter 3 presents the techniques to synthesize ionic liquids and zeolites in ionic liquids. Characterization methods for ionic liquids ionic liquids and zeolites are introduced following the synthesis techniques. In addition, methods to test solubility of precursors in ionic liquids and techniques to test interaction between IL and precursors are also discussed in Chapter 3.

Chapter 4 Solubility and stability of precursors in ionic liquids

Chapter 4 deals with solubility and stability of zeolites' precursors in ionic liquids. First, Syloid 63 silica particles which is an important precursor to synthesize silica-based zeolites, are mixed with different types of ionic liquids. It is found that both cation and anion of ILs could influence the saturation of silica particles in ionic liquids. The volume fraction of silica particles ranges from 0.61 to 0.69 depending on the ionic liquid used, and these particles are stable in ionic liquids for a long time. Second, aluminium isopropoxide and phosphoric acid which are precursors of aluminophosphates are dissolved in ionic liquids. The solubility of aluminium isopropoxide in bromide-based ionic liquids is very low, lower than its concentration in a reaction gel, indicating the reaction is a heterogeneous reaction. But pure phosphoric acid dissolves in bromide-based ionic liquids easily. After reaching 44 wt%, phase split begins to show up in the mixture of IL and pure phosphoric acid. This result is used in the synthesis of aluminophosphate to increase the yield of products. Solubility of $Al(OiPr)_3$ in ionic liquids at different temperatures is compared with ideal solubility of $Al(OiPr)_3$. Parameters such as activity coefficient and Henry's constant are given. Finally, the stability of ionic liquids in the presence of phosphoric acid was investigated. After a time from 16 hours to 426 hours, ionic liquids can be decomposed by phosphoric acid, but the amount of decomposed products is small and does

not increase significantly with the increase of time at 50 ^{o}C. Even at 150 ^{o}C, with the presence of other ingredients, phosphoric acid with a lower concentration does not lead to decomposition of ILs after five days. As a result, the decomposition of ionic liquids by phosphoric acid should not be a concern.

Chapter 5 Interactions between precursors and solvent

Chapter 5 presents an investigation into the interaction of precursors with bromide-based ionic liquids. ^{27}Al solid NMR is used to investigate influence of ionic liquid and phosphoric acid on the conformation of Al atoms in $Al(OiPr)_3$. When $Al(OiPr)_3$ is mixed with an ionic liquid, at a higher temperature (70 ^{o}C), Al(VI) begins to change to Al(IV) and Al(V). But Al(VI) is still the dominant conformation as seen in pure $Al(OiPr)_3$. At lower temperature (20 ^{o}C), the change is not remarkable. When H_3PO_4 is added into the mixture, at a higher temperature (70 ^{o}C), tetrahedral-coordination becomes the dominant conformation of Al atoms. In addition, the peak location of Al(IV) is the same with the Al atoms in zeolites, indicating the confirmation of Al atoms in ionic liquid is the same as the Al confirmation in as-synthesized molecular sieves. Regardless if there is H_3PO_4 in the mixture or not, ratio of Al(IV) to Al(VI) increases with increase of alkyl chain length in the imidazolium ring of ionic liquids, suggesting long alkyl chain could possibly accelerates the formation of aluminophosphates, and this hypothesis is proved by the experimental result in section 6.1.3.3. Moreover, temperature has a great influence on the conformation of $Al(OiPr)_3$ in ionic liquids. With the increase of temperature from 20 ^{o}C to 70 ^{o}C, the ratio of Al(IV) to Al(VI) increases dramatically and the influence of temperature is enhanced with the addition of H_3PO_4.

Chapter 6 Effect of ionic liquid (molten salts) and other factors on hydrothermal synthesis of aluminosilicate and on ionothermal synthesis of aluminophosphates

Chapter 6 presents the effect of ionic liquid and molten salts in ionothermal synthesis of aluminophosphates and in hydrothermal synthesis of aluminosilicate. First, some new discoveries on ionothermal synthesis of zeolites, especially porous aluminophosphates have been found. Hydrochloric acid is a promising mineralizer to synthesize crystalline materials, but the choice of the mineralizing agent (e.g. hydrochloric acid versus hydrofluoric acid) affects the final zeolite framework structure at short synthesis times. After heating from several hours to several

days, frameworks undergo dramatic changes, regardless of the acid. Third, a slightly longer alkyl chain in the imidazolium ring of ILs accelerates the formation of crystalline materials, which is consistent with the finding of interaction between ILs and $Al(OiPr)_3$. Finally, increasing the percentage of precursor in the reaction gel leads to a higher yield of crystalline materials, but different types of frameworks are synthesized, from SIZ-4 to AEL to berlinite. The formation of berlinite when concentration of precursors reaches a limit is possibly due to increase of water content in the reaction gel.

In addition, the role of different molten salts with common ionic liquid cations and anions is studied in the hydrothermal synthesis of silicate-based molecular sieves. Pure-silica ZSM-5 is formed with tripropylammonium bromide ([TPA][Br]) as the structure directing agent (SDA). However, when tributylammonium bromide, tributylammonium hexafluorophosphate, tributylammonium nitride or 1-ethyl-3-methylimidazolium bromide is used as the SDA, magadiite is formed, which does not need any SDA in the formation. These results demonstrate the importance of appropriate van der Waals force between precursor and structure directing agent. Also, the addition of tetraalkylammonium salts to the reaction mixture does not inhibit the silica chemistry involved in the formation of magadiite which is one of dense materials, while these materials are precursors to useful porous materials.

Chapter 7 Conclusion and recommendation

At the end of the dissertation, in Chapter 7, the findings from this project are summarized and future research on ionothermal synthesis of molecular sieves is proposed.

References

1. Cooper, E. R.; Andrews, C. D.; Wheatley, P. S.; Webb, P. B.; Wormald, P.; Morris, R. E. *Nature* **2004**, *430*, 1012-1016.

Chapter 2 - Literature Review

2.1 Introduction to Zeolite and Zeotype Materials

2.1.1 General introduction

The first zeolite was discovered about 250 years ago by a Swedish mineralogist Cronstedt. By heating the mineral, a large amount of steam was given off, giving the impression that the stone was boiling. So he made the name "zeolite" for this kind of mineral from the Greek words "zeo" (meaning boil) and "lithos" (meaning stones).[1] Although the Cronstedt did not identify the structure of the zeolite he found, the material was reported as stilbite.[2] For quite a long time after the first zeolite was discovered, the definition of zeolite was restricted to crystalline aluminosilicates which are constructed from AlO_4 tetrahedral and SiO_4 tetrahedral where Al and Si are tetrahedral atoms.[3] There are also pure-silica zeolites where all of the tetrahedral atoms (T atoms) are silicon. However, many similar crystalline materials have been discovered or synthesized with T-atoms being aluminium, phosphorus, titanium, cobalt, etc. Dyer called these materials zeotypes, and this name was accepted by researchers.[4] The terms zeolites, molecular sieves and microporous are not strictly defined and are often used as synonyms.

Besides dividing the family of molecular sieves into zeolites and zeotypes, molecular sieves can also be divided into dense materials and microporous zeolites. They are differentiated by the number of TO_4 tetrahedral per nm^3 ($T/1000Å^3$).[5,6] If the number of TO_4 tetrahedral per nm^3 is larger or equal to 21, these materials are classified as dense zeolites. On the contrary, if the number is less than 21, meaning the pore size in the zeolites are large enough for guest molecular to go through, these materials are classified as porous zeolites.[5,6]

According to the rules given by the *Commission of the International Zeolite Association* (IZA), each zeolite structure is given by a 3 capital letter code in order to separate one from another.[7] For example, AEL stands for the structure of AlPO-11, which has a 10-member ring and framework density 19.1 $T/1000Å^3$ and CHA stands for the framework of Linde Type A zeolite which has a 8-member ring and framework density 12.9 $T/1000\ Å^3$. Figure 2.1 shows the structure of AEL and CHA.[7] The current IZA database (www.iza-structure.org) contains 197

distinctive structures of zeolites (each with a 3 capital letter code), most of which are synthesized, instead of occurring naturally.

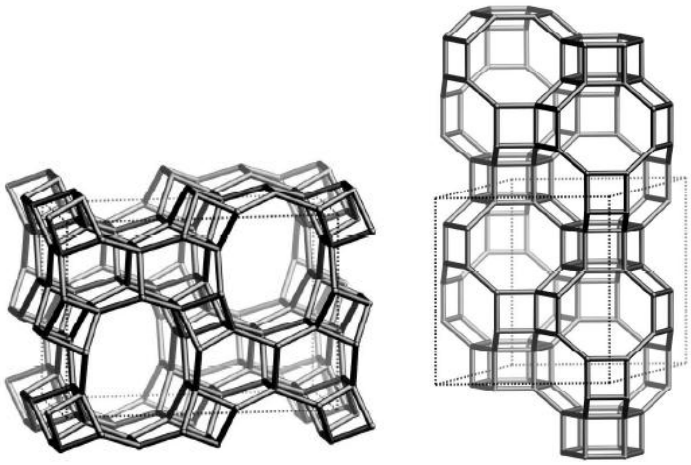

Figure 2.1 Frameworks of AEL and CHA. (www.iza-structure.org)

There is a group of zeotypes which are particularly important in this dissertation. They are aluminophosphate ($AlPO_4$) molecular sieves that are composed of AlO_4 tetrahedral and PO_4 tetrahedral. The first $AlPO_4$ was discovered by Flanigen, Wilson, Patton and others of Union Carbide.[8] Since then, every year, $AlPO_4$'s with new frameworks are reported by IZA. They are an important family of the zeolite and have similar frameworks with those of aluminosilicates. It is the first class of molecular sieves without silica in framework oxide compositions.

2.1.2 Hydrothermal synthesis of zeolites

Zeolites are prepared in a solvent. The recipe to produce a specific framework is often empirically found. The formation of zeolite composes gel formation and evolution, nucleation and crystal growth. In each process, several parameters could influence the shape, morphology and surface area of zeolites, such as solvent type, the reaction pH, heating temperature, and the existence of structure directing agent. As a result, in order to reproduce a structure reported in literature, every synthetic parameter should be exactly the same with what is reported in literature.

Zeolites are commonly prepared in water, since it is cheap and environmentally friendly. If the water is used as the solvent, the synthesis process is only called hydrothermal synthesis. Several steps are involved in formation of frameworks. They will be discussed in detail.

(1) Formation of gel

This process involves mixing ingredients of zeolites into a homogeneous gel, including precursors of the T-atom, the structure directing agent, and acid or base to adjust pH of the reaction gel. Depending on the composition of framework desired, different forms of precursors could be used, such as fumed silica, aluminium salts, alkoxides of aluminium and phosphoric acid. The Si/Al ratio is an important number to decide if a zeolite is suitable for a specific application, especially used as catalysts. Zeolites of low Si/Al ratio can be prepared in the presence of inorganic cations. On the contrary, zeolites of high Si/ Al ratio should be prepared using bulky organic alkylammonium cations as structure directing agent. Zeolites with a low ratio of silicon to aluminium are preferred since they have more capacity to ion exchange and higher adsorption properties. But these zeolites are less hydrothermally stable than zeolites with high ratio of silica to aluminium.[9]

Alkali and alkaline earth metal cations are also reported to facilitate zeolite syntheses. The literature reports that some structure types are favored when a specific cation is used, such as LTA and FAU for Na, whereas ERI and CHA are not favored when Na is present in the reaction gel.[10,11] Those metal cations are commonly added in the form of soluble hydroxide, which at the same time adjust the pH values to 12-13, suitable for the crystallization process to occur.[12]

Organic cations, usually called structure directing agent (SDA) in synthesis of zeolites, are also useful in the formation of zeolite frameworks, first found by Barrer and Denny[13], and Kerr and Kokotailo.[14] Functions of SDAs vary; sometimes they serve as space-holders or pore-filling agents, sometimes they have specific interactions with the zeolite precursors and promote formations of micropores and sometimes they can truly function as templates for the final materials.[15,16] The common organic structure directing agents are tetramethylammonium (TMA), tetraethylammonium (TEA), tetrapropylammonium (TPA), etc.[10] However, all of the zeolitic silicas tested are only 7- 14 kJ/mol less stable in enthalpy than quartz.[17] As a result, the author concluded that the main function of the metal and organic cations is not to stabilize open silicate

frameworks compared to dense silicates, but to "fulfill a kinetic or entropic role by directing the path of the reaction".[17]

Since the solubility of silica and alumina are not high, bases are added into the reaction mixture to increase the solubility of precursors. At high pH, alumina exists as $Al(OH)_4^-$ and silica exists as oligomeric species.

(2)Nucleation and crystal growth

Figure 2.2 shows a typical hydrothermal crystallization process. Initially, particles are dissolved in solution and begin to form small units as the nuclei. Then the crystallization process proceeds rapidly. After the reactants are almost exhausted, crystallization is complete.

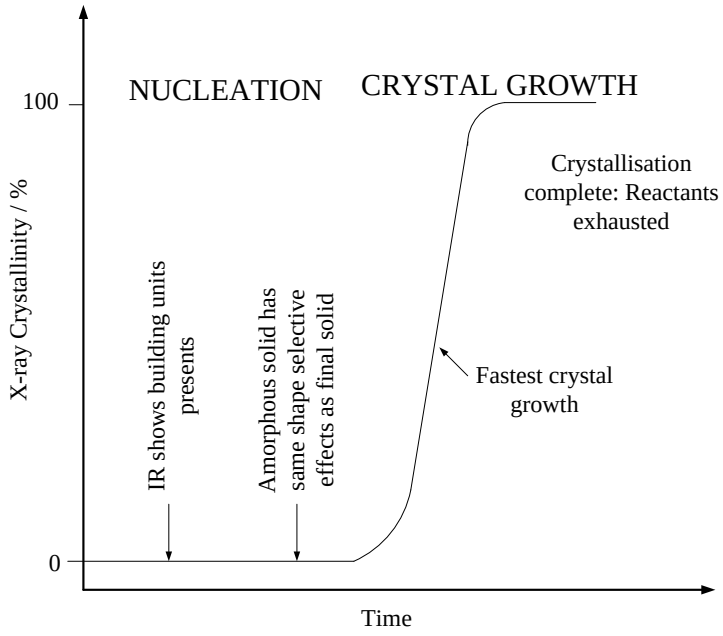

Figure 2.2 Process of crystal growth in solution.[12]

Temperature is one of the most important factors in determining the time required for the nucleation and crystal growth process. Generally speaking, increasing the temperature will make the time shorter. Christensen et al[18] found that crystallization is governed by thermally activated reactions instead by rates of diffusion. However, heating the reaction gel at a high temperature can cause unfavorable dense phase materials to form. The reasons might be loss of water of crystallization, or decomposition of organic structure directing agents.[12] Similar to the effect of temperature, pH also influences the crystallization process.[19] High pH increases the rate of

crystallization, but when pH reaches a limit, it will lead to dissolution of the crystal and reaction to dense phases. As a result, a medium range of pH is preferred. For example, a pH between 11.5 and 13.0 is best to form modernite. [19]

Although 197 zeolites and zeolitic materials have been synthesized,[7] the full mechanism of self-assembly process of these materials is not fully understood. However, there have been a few breakthroughs in this field. Davis and his coworkers investigated the interaction between a structure directing agent (tetrapropylamine) and a silica precursor in the synthesis. They found during the heating of the zeolite synthesis gel, short-range intermolecular interactions on the order of van der Waals interactions are formed, initiating the self-assembly process. Then the silica precursors surrounded the SDA, aggregate, nucleate and grow into the final crystals.[20] This process is illustrated in Figure 2.3. A few years later, Tsapatsis and colleagues confirmed the final aggregation through crystal growth steps after a few years.[21]

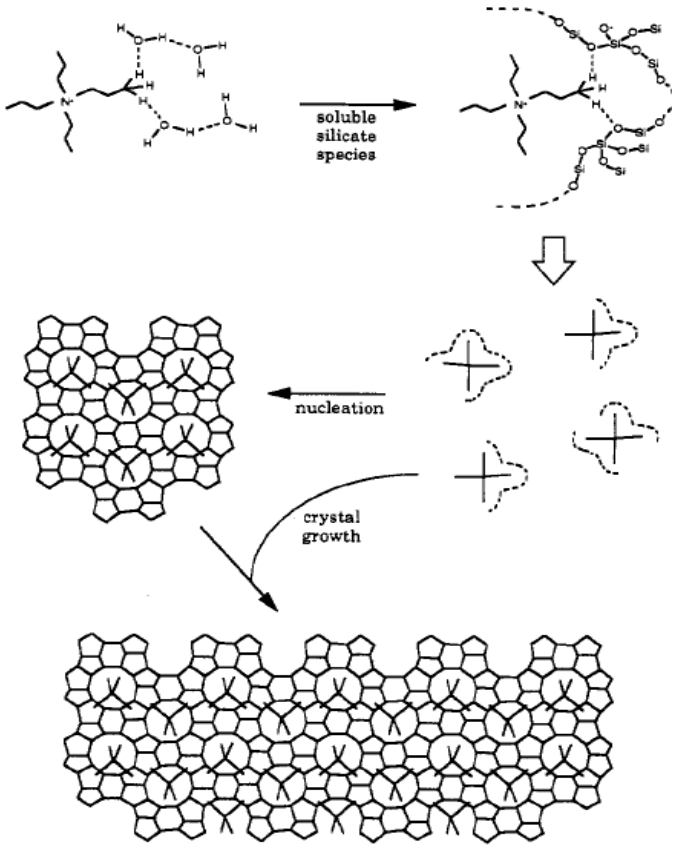

Figure 2.3 Illustration of the proposed growth mechanism in the TPA-mediated synthesis of Si-ZSM-5.[20]

In 2005, Grandjean and his coworks proposed a three-stage, one-dimensional crystallization mechanism for hydrothermal synthesis of CoAPO-5 molecular sieves, one of the aluminophosphate frameworks.[22] They proposed the first step of aluminophosphate formation is an initial reaction between aluminium and phosphate units forming a primary amorphous phase, the second step is progressive condensation of linear Al-O-P chains forming a poorly ordered structure separated by template molecules up to 155 ^{o}C and the last step is rapid internal reorganization of the aluminophosphate network leading to crystallization of the crystal structure.[22] This process is illustrated in Figure 2.4. Note the silicate formation studies by Davis were not the same as the aluminophosphate formation mechanism studies by Grandjean.

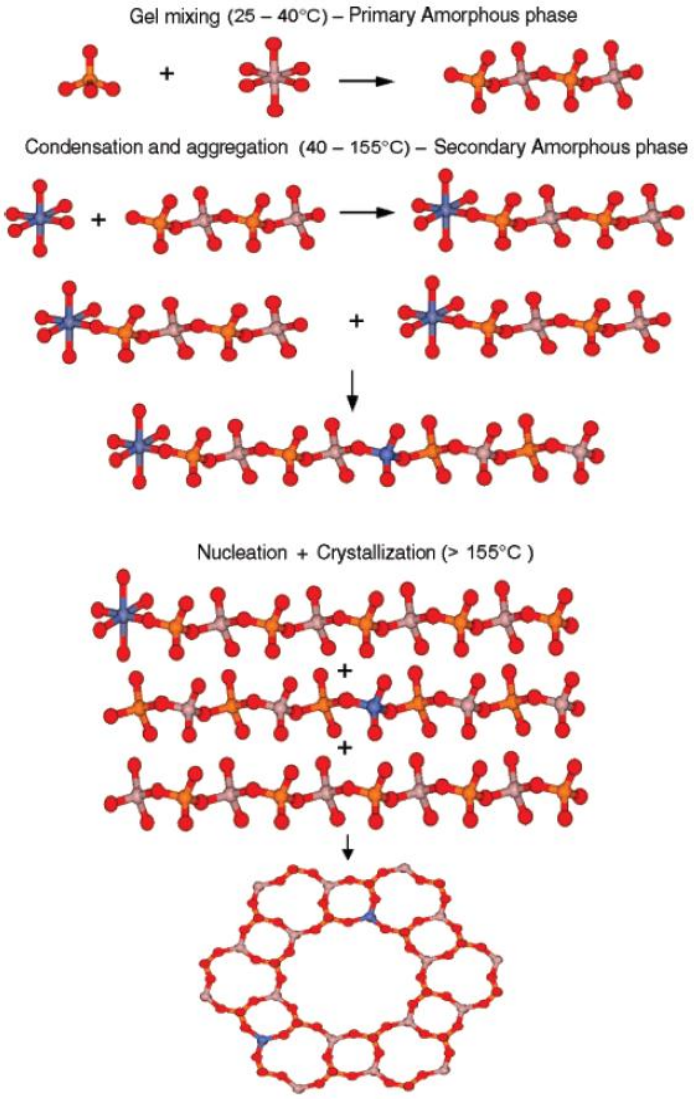

Figure 2.4 Schematic of the three-stage crystallization model.[22]

However until now, no one knows what exactly occurs in the first phase of reaction, especially when the solvent is not water. No one is sure if the interaction between precursors and solvents, or interaction between precursors and structure directing agent, or interaction between two precursors initiates the reaction. Nevertheless, the interactions between the solvent and the precursors in the early stages of the reaction are likely very important.

2.1.3 Properties of zeolites

One important property of zeolite is that it has large cavities and entry channels. These pores are only filled with water. If water is removed by heating, the cavities or pores in the zeolite will be empty. Then, molecules with diameters smaller than the size of cavity can pass through, whereas bigger molecules are excluded from the pores. Therefore, zeolites can be used to separate big molecules from small molecules.[23] That's the reason why zeolites are also called "molecular sieves". However, the separation process is often companied by adsorption process mentioned in the next paragraph.

In zeolites, for tetrahedral composed of one Al atom and four O atoms, there is a negative charge on each of the Al atoms. If the T-atom is Zn, there will be two negative charges on the Zn atom. The charges in the framework attract species with permanent dipole moments. Zeolites are adsorbents for some gases. For example, they can be used to purify natural gas by absorbing CO_2 and they are used to adsorb N_2 from air.[24]

Another important property of zeolite is that it has ion–exchange capacity. As mentioned in the previous paragraph, in zeolites there is charge deficiency on the tetrahedral frameworks. The excessive negative charges are balanced by cations, such as Na^+ and K^+. These cations are often loosely bonded to the framework and thus easy to be ion-exchanged by other cations. The process can be done by washing them with a concentrated solution of another ion. In theory, the bigger the Al/Si ratio, the more free cations in the framework and thus has better ion-exchange capacity. This property is useful in many applications of zeolites.[25,26]

2.1.4 Applications of zeolites

In order to commercially use zeolites, large amount of zeolites with low price should be available. In the1950's, natural zeolites were discovered as major constituents of numerous volcanic tuffs in saline-lake deposits of the western United States and of marine tuffs of Japan and Italy. Since then, more than 40 countries have found zeolites from sedimentary rocks. These zeolites are easy to mine in large quantities, arousing the interest of researchers to commercially use them.[27]

When zeolites are used as adsorbents or catalysts, large pore sizes are preferred; only those with a minimum of eight tetrahedral atoms rings are considered. These qualified zeolites can generally be divided into three categories.[28]

1. Small pore zeolites which have eight member ring pore apertures and have free diameters of 0.30 – 0.45 nm.
2. Medium pore zeolites which have ten member ring pore apertures and have free diameters of 0.45 – 0.60 nm.
3. Large pore zeolites which have 12 membered-ring apertures and have free diameters of 0.6 – 0.8 nm.
4. Besides the zeolites mentioned above, zeolites with ultralarge pores have also been synthesized, such as $AlPO_4$-8 (with 14 membered-ring aperture),[29] VPI-5 (with 18 membered-ring aperture)[29] and Cloverite (with 20 membered-ring aperture).[30]

Zeolites can be used in the following applications.

(1) Catalysts

Their use as catalysts is the most important application of zeolites in industry. However, natural zeolites are not directly used as catalysts, despite their abundance and variety. The reasons are (a) they have impurity phases, (b) their chemical and physical properties are different from one deposit to another deposit and (c) their properties are not optimal for the usage of catalysts. As a result, synthetic zeolites are produced and until now about 150 frameworks have been synthesized. They are mainly used as catalyst in the oil refining and petrochemical industry because (1) zeolites have high concentration of active sites (2) they have thermal and

hydrothermal stability and (3) the pore sizes of zeolites can direct the reaction pathway towards formation of desired products.[28] These catalysts are used in fluid catalytic cracking,[31,32] hydrocracking,[33,34] C4-C6 alkane isomerization,[35,36] base oil production and processing,[37] paraxylene manufacturing,[38,39] aromatic alkylation,[40-42], and conversion of methanol to olefins,[43] etc.

(2) Use as detergent builders

Sodium tripolyphosphate was used as a detergent builder and to soften hard water in powdered laundry detergent. However, it causes eutrophication in lake and sea. Zeolites are a good substitute for tripolyphosphate and it has already been used in large amounts each year. In laundry detergent the calcium and magnesium ions in water thus softening the water. It has the same function of sodium tripolyphosphate.[44] The use of zeolites in laundry detergent is the largest market of zeolites in terms of weight consumed each year.

(3) Application of natural zeolites in Animal Science

Most research of natural zeolites in Animal Science is done in Japan. Natural zeolites can first increase feed efficiency. For example: montmorillonite clay was added to the food of poultry, swine and cattle as dietary supplement to slow down the passage of nutrients in the digestive system of chickens, thereby increasing caloric efficiency.[45] When clinoptilolite and modernite are added to the normal protein diets of pigs, chickens, and ruminants, for per unit of feed consumed, the grain of body weight is increased remarkably.[46] Natural zeolites could also control the malodor and moisture in poultry houses. Farm owners and researchers in Japan found that if the chicken droppings are mixed with one-third zeolite, water content, maggot population, and ammonia productions are all decreased to a great extent.[46-48] These positive results are due to good adsorption properties of zeolites towards water and reaction of ammonia with hydrous zeolite, to form ammonium ions which are held in the pores of zeolites.[49] Similar results are also seen in swine breeding.[48,50]

(4) Application of natural zeolites in aquaculture

In aquacultural systems, unconsumed food could produce NH_4^+ which could lead to disease and mortality of fish. As a result, a method to control the concentration of NH_4^+ is required.

Zeolite ion-exchange is capable of regulating the NH_4^+ content and could remove 97 to 99 % of the NH_4^+ produce in a recirculating system.[51] Moreover, activated zeolites can also produce oxygen-enrich air by selectively adsorbing nitrogen. Goldfish living in oxygen-rich environments are reported to be livelier and have greater appetites.[52]

Zeolites also have applications in other fields. They are used to remove and trap many fission products from nuclear waste[53,54], to slowly release phosphorus fertilizer for plant production,[55] and as solar thermal collectors.[56] Sandbags filled with zeolite are being used to adsorb cesium in the sea after the explosion of Fukushima Daiichi nuclear plant in Japan.[57]

2.2 Introduction to Ionic Liquids

2.2.1 General introduction

Ionic liquids are chemicals which are solely composed of ions and generally have melting points lower than 100 ^oC, with a few as low as -96 ^oC. They include a vast number of chemicals. The low melting points are largely due to the low lattice energies between ILs' asymmetric cations and sometimes irregular anions. The wide liquid range, in some cases as large as 400 ^oC, make them ideal for applications where common solvents would not be operable. [58-60]

The first true ionic liquid, ethylammonium nitrate (with melting point 12 ^oC) was synthesized by Pal Walden in 1914.[61] However, since then, not many studies are conducted in this field. Beginning in the middle of 1990's, publications on ionic liquids have increased exponentially each year. From 1995 to 1998, publications containing "ionic liquid" are less than 50 each year. However, beginning 1999, the number increases to around 80 and in 2002, the number is more than 450. There are already 1495 papers published in the first half year of 2011. These data were obtained from database of "Web of Science". Ionic liquids have already become a "hot topic" due to the appeal of eco-friendly solvents in industry.

2.2.2 Structures and synthesis of ionic liquids

The cations of ionic liquids are usually bulk organic ions with low symmetry. The center of cation often has a positively charged nitrogen or phosphorus. There are various types of cations, a few of which are shown in Figure 2.5 as examples. Among them, ammonium cation, phosphonium cation and imidazolium cations are the mostly used because of their simplicity to synthesize. Functionalized ionic liquids have recently been synthesized and expanding the applications of ionic liquids.

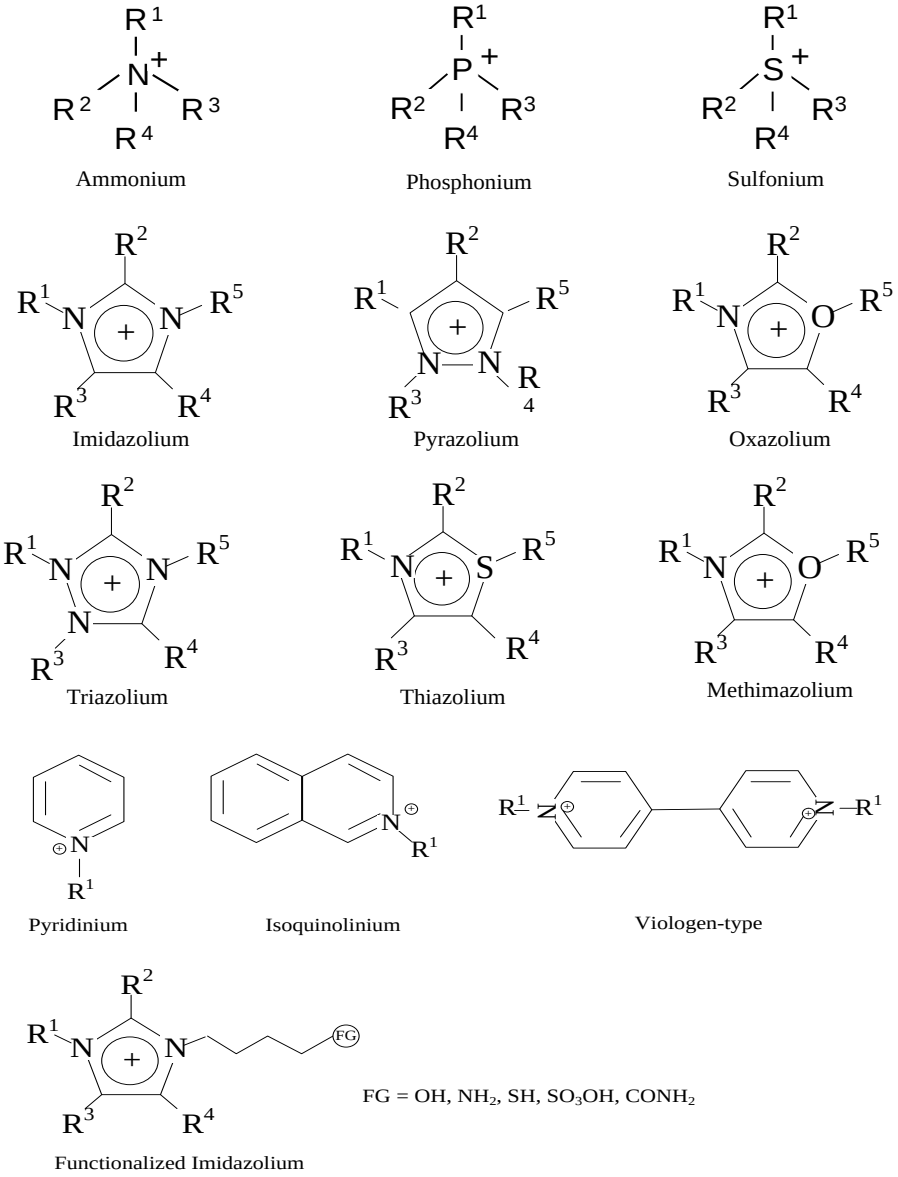

Figure 2.5 Examples of cations which can be used in ionic liquids.

Figure 2.6 shows a few common anions of ionic liquids. They vary from simple bromide and chloride anions to complicated tris(trifluoromethanesulfonyl)methanide. There are many more complicated anions which will not be discussed here. It is not difficult to imagine that by combining different anions and cations, a large number of ionic liquids can be synthesized. Theoretically, at least a million binary ionic liquids and 10^{18} ternary ionic liquids can be synthesized.[62]

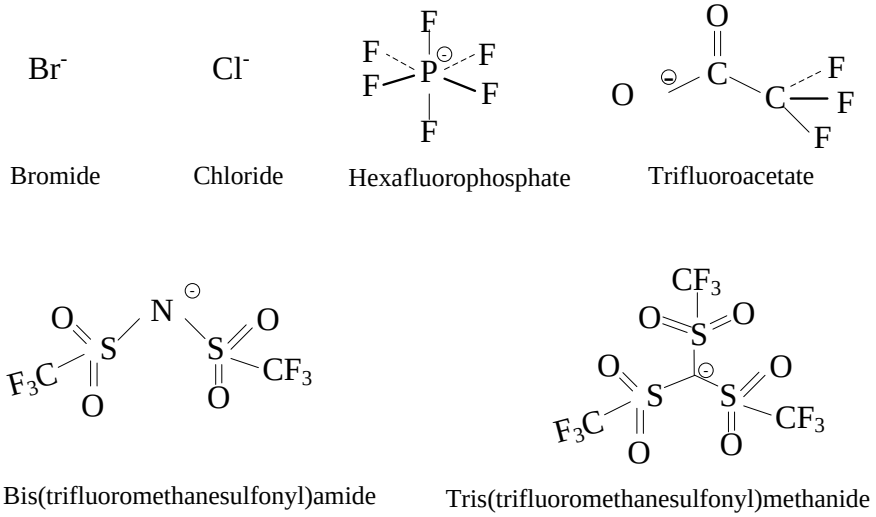

Figure 2.6 Examples of anions which can be used in ionic liquids.

Because all of the ionic liquids used in the synthesis of zeolites are imidazolium-based ionic liquids, only methods to synthesized imidazolium-IL are introduced in this literature review. They are synthesized by two main methods; the metathesis of an imidazolium halide IL into another imidazolium IL, and halogen free synthesis.

(1) In the metathesis method, first an imidazolium bromide or imidazolium chloride is synthesized by reacting alkyl bromide with alkyl-imidazole for a certain time, depending on the alkyl length of the alkyl bromide. From this 1-alkyl-3-alkylimidazolium halide ($[C_nC_n\text{mim}][X]$), different methods can be used to produce various types of ILs. If the desired IL is immiscible with water, the $[C_nC_n\text{mim}][X]$ can be reacted with a chemical containing the anion needed. For example, dialkylimidazolium bis(triflyl)amides and dialkylimidazolium nonafluorobutanesulphonate can be synthesized by reacting dialkylimidazolium halide with lithium bis(triflyl)amide or potassium nonafluorobutanesulphonate in water. The products are washed with dichloromethane several times in order to get high purity ILs.[63] However, for those

ionic liquids which are miscible with water or organic solvent, another method is used. This technique involves reacting $[C_nC_n mim][X]$ with Ag salt, whose products are AgX (solid) and the desired IL. However, Ag salts are always expensive and the price of the ILs synthesized in this way is costly. As a result, this route to synthesize ILs could only be produced in small amount. [64] Lastly, a route to synthesize ILs by ion-exchange is proposed and it was perceived to be able to synthesize IL in large scale. The $[C_nC_n mim][X]$ is passed through a column which is compacted with ion exchange materials.[65] The ion exchange materials are salts with desired ions exchangeable and the counter ions fixed in a stationary phase. If the column is long enough, the ion exchange process will be complete and only the desired IL will be eluted.

(2) The metathesis method introduced above is relatively easy and could produce many kinds of ionic liquids with good quality. However, there is inevitably a certain amount of residual halide left in the IL which will change the physical properties of the IL and cause catalytic poisoning and deactivation.[66] As result, several synthetic strategies have been provided to directly synthesize ILs without the presence of halide.[67-69] The route proposed by Dupont et al. is shown in Figure 2.7. They synthesized $[C_4C_1im][BF_4]$, $[C_4C_4im][BF_4]$ and $[C_1C_1im][BF_4]$ by a one-step procedure.[67]

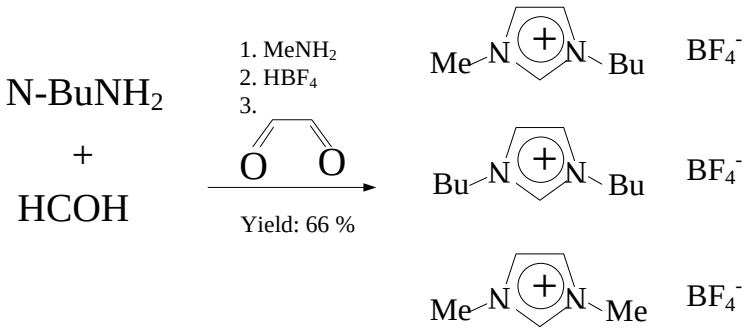

Figure 2.7 Route to synthesize $[C_nC_n mim][BF_4]$ by a one-step procedure.[67]

2.2.3 Properties of ionic liquids

Properties of ionic liquids can be changed dramatically by altering cations or anions. In order to choose ionic liquids for a specific reaction, the relationship between structure and properties is discussed here.

(1) Melting points

One of the interest properties of ionic liquids is their low melting points compared to common salts, such as sodium chloride. Melting points are governed by van der Waals forces and electrostatic interaction.[70-72] It is shown that the influence of cations on melting points of ionic liquids is dependent on the symmetry of cations. If the cations are asymmetric, cations and anions could not pack closely and form crystal, thus lowering the melting points. On the contrary, if the cations of ionic liquids are symmetrical, melting points of ionic liquids are usually higher.[73] Figure 2.8 shows the influence of alkyl chain on melting points of several ionic liquids. It is important to note that reported melting point of any ionic liquid is not exactly the same with each other, possibly due to the trace impurities in the IL tested.

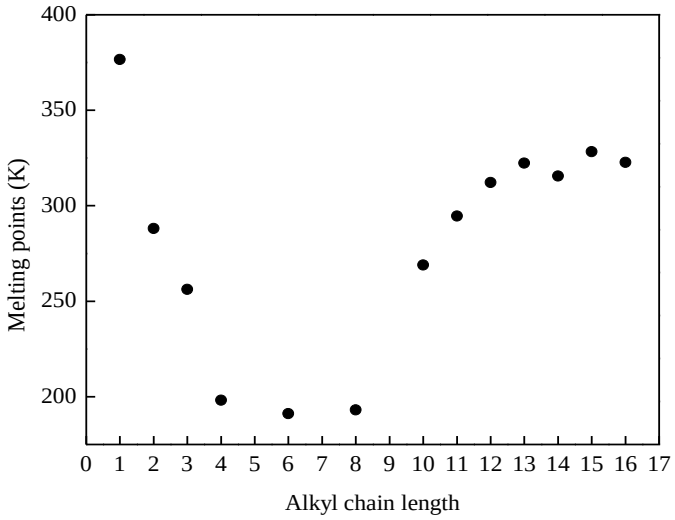

Figure 2.8 Influence of alkyl chain length on melting points of $[C_nC_1im][BF_4]$ (data retrieved from [74]).

From Figure 2.8, it can be seen that with the increase of carbon number in alkyl chain from one to sixteen, melting points decrease due to the increase of asymmetry in cations of ILs. However, with the further increase carbon number in alkyl chain, liquid crystalline regions are formed and increase the melting points.

The influence of anions on ionic liquids is mainly determined by their sizes. The larger the anion, the less charge density on the surface of the anion, thus lowering the interaction between cations and anion and lowering melting points. For example, with the increase of anion size,

melting points of $[C_2C_1im][Cl]$, $[C_2C_1im][Br]$, $[C_2C_1im][PF_6]$ and $[C_2C_1im][Tf_2N]$ are 362.15 K, 352.15 K, 332.15 K and 258.15 K, respectively.[74]

(2) Decomposition temperature

It is preferred that a solvent to have high decomposition temperature in order to operate at high temperature and reuse the solvent. As a result, decomposition temperatures of ILs need to be investigated. Imidazolium ionic liquids usually have onset decomposition temperature from 280 ^oC to a temperature higher than 450 ^oC. Before reaching the decomposition temperature, they maintain low vapor pressure. The large liquid range of ionic liquids makes them suitable for some applications where high temperature operation conditions are required. There are some trends can be drawn from experiments. (1) Ionic liquids based on imidazolium cations are generally more thermal stable than ionic liquids based on tetraalkyl ammonium cations. (2) Increasing alkyl chain length of imidazolium ring slightly increases the decomposition temperature. (3) Anions have great influence on the decomposition temperatures and the trend is hexafluoropohosphate > bis-(trifluoromethanesulfonyl) imide ≈ tetrafluoroborate > tris-(trifluoromethanesulfonyl) methanide ≈ tetrafluoroarsenic >> iodine, bromide, chloride. (4) The presence of oxygen does not influence the onset decomposition temperature.[73,75]

(3) Vapor pressure

Low vapor pressure is one of the merits of ILs which make them considered green solvents. However, there are not many published papers analyzing the effect of ILs' structures on vapor pressures. Here are a few of the published works on vapor pressures of ILs. When the pressure is kept at 10^{-3} Pa, the vapor pressures of $[C_4mim][Tf_2N]$ are 122 Pa at 457.66K, 874 Pa at 487.54 K and 4660 Pa at 517.45 K.[76] Saturated vapor pressures for $[C_4mim][PF_6]$ are $1 * 10^{-10}$ Pa at 298.15 K, $2 * 10^{-4}$ Pa at 400 K and $5 * 10^{-1}$ at 500 K.[77]

(4) Density

The density of an ionic liquid is also influenced by bhe structures of ILs and by temperature. Densities of ILs are larger than the density of water. At room temperature, the number is in the range of 1.05 to 1.64 g/cm^3. With the increase of temperature, density decreases accordingly, but not much, as shown in Figure 2.9. In addition, Increase of alkyl chain length of the imidazolium ring decreases density, as shown in Figure 2.10.[78]

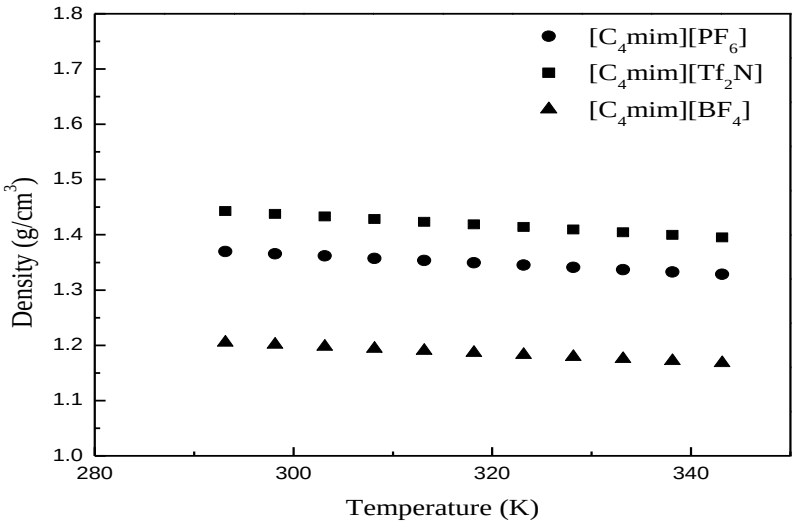

Figure 2.9 Influence of temperature on density of several ionic liquids.[78]

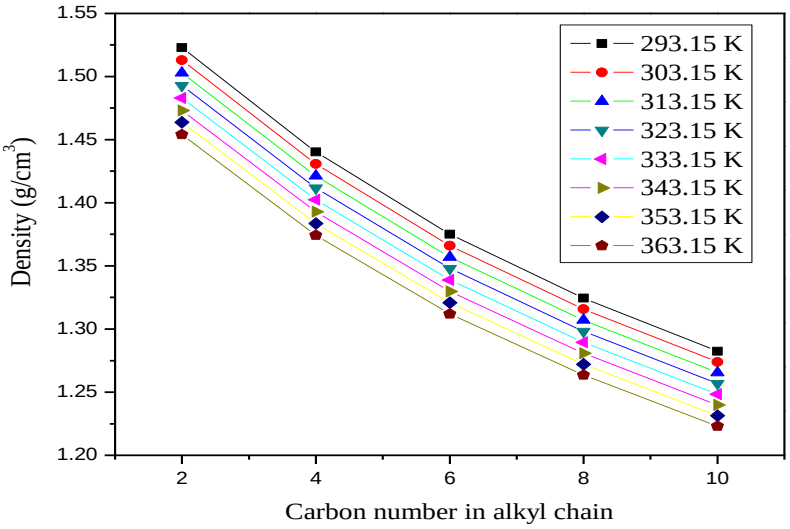

Figure 2.10 Influence of alkyl chain length on density of [$C_n$mim][Tf_2N] at different temperatures.[78]

(5) Viscosity

Viscosity is influenced by intermolecular interactions. When ionic liquids are used in large-scale application, viscosity is an important factor to consider. Generally, low viscosity is preferred to minimize pumping costs and increase mass transfer. However, when it is used as

lubricant oil, low viscosity is not required. Viscosities vary remarkably between different ionic liquids. Nevertheless, almost all of ILs have viscosities higher than common organic solvents at room temperature. Common organic solvents have viscosities between 0.2 cP to 10 cP, whereas ILs have viscosities between 10 to 726 cP at room temperature. Figure 2.11 shows the influence of cation and anions on viscosity of ILs.

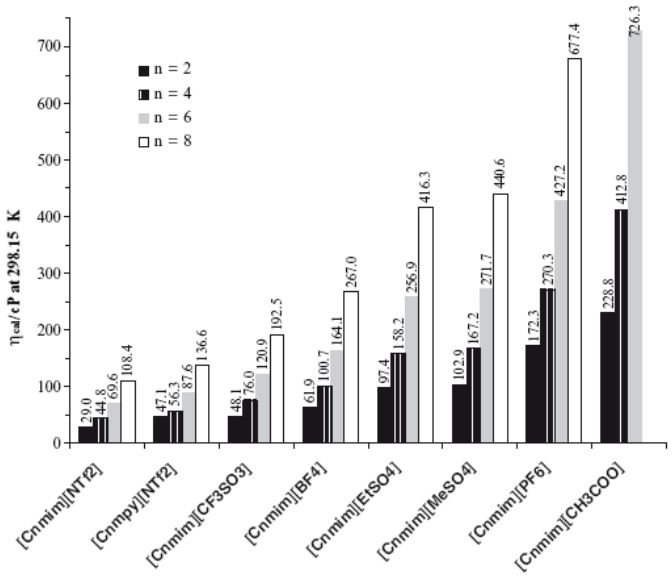

Figure 2.11 Influence of cations and anions on viscosity of ILs.[79]

From Figure 2.11, it can be seen that with the increase of alkyl chain length, viscosity increases due to the increase of van der Waals force. Anions also have great influence on the result, with the trend $[CH_3COO]^- > [PF_6]^- > [MeSO_4]^- > [EtSO_4]^- > [BF_4]^- > [CF_3SO_3]^- > [Tf_2N]^-$. Researches show that hydrogen bonding, Van der Waal forces, molecular weight and mobility are the main factors deciding the magnitude of viscosity.[80-83] In addition, temperature influences viscosities dramatically. Take $[C_4mim][PF_6]$ for example, its viscosity is 312 cP at 30 ^oC and 28.5 cP at 70 ^oC.[74]

2.2.4 Applications of ionic liquids

The use of ionic liquids includes but is not limited to the following applications.

(1) Use of ionic liquids as lubricants

The first paper published on using ionic liquids as a novel versatile lubricant was published in 2001 by Ye and his colleagues.[84] The author proposed that alkylimidazolium tetrafluoroborates are promising as versatile lubricants for contact of steel/steel, steel/aluminium, steel/copper, steel/SiO_2, Si_3N_4/SiO_2, steel/Si (100), steel/sialon ceramics and Si_3N_4/sialon ceramics. Since then, many papers have been published on exploiting pure ionic liquids to achieve friction reduction, antiwear performance and high load carrying capacity.[84-94] In the first phase of investigation, most commonly-seen ionic liquids such as alkylimidazolium tetrafluoroborate or alkylimidazolium hexafluorophosphate were used as pure lubricants. In order to give better properties, chemists synthesized more complicated ones, such as new IL with alkylimidazolium attached by tributylalkylphosphonium and Alpha, Omega - Diimidazoliumalkylene Hexafluorophosphate.[87,95-98] Although some of these new ILs are less stable in air, they generally show less wear volume and wear scar diameter than pure ILs and they can solve problems of commonly-used lubricants, such as evaporation loss and oxidation degradation under vacuum, and non-versatility.

(2) Dissolution of cellulose

Cellulose is investigated extensively recently as a potential renewable source of fuel. However, traditional cellulose dissolution process is expensive or cumbersome and the solvent could not be used. As a result, a "green" method to dissolved cellulose is studied by Rogers and his group, and followed by other researchers.[99,100] They found cellulose can be dissolved in hydrophilic ionic liquids, such as [C_4C_1im][Cl] and [$C_nC_1$im][Cl]. Under microwave heating, up to 25 wt% cellulose can be dissolved in [C_4C_1im][Cl]. Then cellulose in the solution could be easily precipitated by addition of water, ethanol or acetone. It is proposed that the high chloride concentration and activity in [C_4C_1im][Cl] is good at breaking the hydrogen bonding in cellulose, thus dissolving it in ILs. Because ILs could dissolve cellulose, this property could be used in (1) fraction of lignocellulosic materials, (2) preparation of cellulose derivatives and (3)

preparation of cellulose composites.[101]

(3) As solvent for extraction and separation

ILs can also be used as solvent for extraction and separation of metal ions, organic and biological compounds. Extraction in ionic liquid/water two phase systems has better extraction efficiency and better selectivity than most of organic solvents. This feature has been used to detect ultra-trace metal ions.[102]

There are many other applications of ionic liquids, which will not be discussed in detail here. These applications include but not limited to (1) use of amino acid-based green ionic liquids as catalyst in the cycloaddition of cyclopentadiene to methyl acrylate, [103] (2) application as reaction media for polymerization processes,[104,105] (3) use of ionic liquids as electrolyte or electrolyte additive,[106] and (4) application of ionic liquid to replace conventional solvents.[107]

2.3 Ionothermal Synthesis

2.3.1 Definition

As introduced in the section of zeolite synthesis, zeolites are usually prepared in water, except a few in alcohols, hydrocarbons and other organic solvents. Zeolites are commonly heated at an elevated temperature, usually from 150 ^{o}C to 200 ^{o}C. The solvents vaporize at this temperature and they generate great pressure, often up to 15 bar. This high pressure necessitates the use of specially designed high pressure vessel, which makes the operation expensive and unsafe.

Because of the low pressure of ILs at elevated temperature, ionic liquids are considered as the solvent to synthesize crystalline materials. When ionic liquid is used as the solvent to synthesize crystalline material, this method is called ionothermal synthesis, as compared to conventional hydrothermal synthesis. In ionothermal synthesis, a high pressure vessel is not required and sometimes structure directing agent can be avoided since it is believed that ILs could function as SDA because they often have structures similar to commonly used SDA in hydrothermal synthesis.[108] As a result, porous materials could be synthesized in a common container, such as a round bottom flask. Moreover, it was believed that no $AlPO_4$ molecular

sieves could be formed without addition of organic molecules as template in hydrothermal synthesis. "The action of a template appears to have both electronic and steric components. In AlPO4 molecular sieve synthesis the steric component appears to dominate."[109,110] However, in the ionothermal synthesis, sometimes a separate structure directing agent is not required, which simplifies the synthesis process.

2.3.2 Crystalline materials synthesized in ionic liquids

Many crystalline materials have been synthesized ionothermally, including aluminophosphate zeolites, silicon-based zeolites, metal organic frameworks and coordination polymers, etc. Since this project is only concerned on aluminophosphate zeolite and silicon-based zeolites, a list of almost all of the aluminophosphate zeolites and silicon-based zeolites synthesized in ionic liquids are shown in Table 2-1. From table 2-1, it can be seen that the first zeolite synthesized in ionic liquid was SIZ-1 and since then, zeolites with different frameworks are synthesized in ionic liquids nearly each year. Most ILs used are imidazolium-based ILs. Crystalline materials could be formed by heating from 20 mins to 14 days. Heating temperature also has a large range, from 90 ^{o}C to 280 ^{o}C. There are basically two heating method, one with microwave heating and one with conventional heating method, such as oven and oil bath.

Table 2-1 Published recipes to ionothermally synthesize crystalline zeolites. (collected from ISI Web of Knowledge)

No.	Name	Year	Framework source	Acid	SDA	IL	Heat	Time	Temp (^{o}C)	Ref.
1	SIZ-1	2004	$Al(OiPr)_3$, H_3PO_4	No	No	$[C_2mim][Br]$	oven	66 hrs	150	[111]
2	SIZ-3	2004	$Al(OiPr)_3$, H_3PO_4	HF	No	$[C_2mim][Br]$	oven	68 hrs	150	[111]
3	SIZ-4 (CHA)	2004	$Al(OiPr)_3$, H_3PO_4	HF	No	$[C_2mim][Br]$	oven	68 hrs	150	[111]
4	SIZ-5 (AFO)	2004	$Al(OiPr)_3$, H_3PO_4	No	No	$[C_2mim][Br]$	oven	19 hrs	150	[111]
5	SIZ-7	2005	$Al(OiPr)_3$,$Co(OH)_2$, H_3PO_4,$Co(OH)_2$	HF	No	$[C_2mim][Br]$	oven	3 days	170	[112]
6	SIZ-8 (AEI)	2005	$Al(OiPr)_3$,$Co(OH)_2$, H_3PO_4,$Co(OH)_2$	HF	No	$[C_2mim][Br]$	oven	3 days	170	[112]
7	SIZ-9 (SOD)	2005	$Al(OiPr)_3$,$Co(OH)_2$, H_3PO_4,$Co(OH)_2$	HF	No	$[C_2mim][Br]$	oven	3 days	170	[112]
8	SIZ-4	2006	$Al(OiPr)_3$, H_3PO_4	HF	No	$[C_2mim][Br]$	oven	68 hrs	150	[113]
9	SIZ-6	2006	$Al(OiPr)_3$, H_3PO_4	No	No	$[C_2mim][Br]$	oven	96 hrs	200	[113]
10	SIZ-10	2006	$Al(OiPr)_3$, H_3PO_4	HF	No	$[C_3mim][Br]$	oven	72 hrs	150	[113]
11	SIZ-10	2006	$Al(OiPr)_3$, H_3PO_4	HF	No	$[C_4mim][Br]$	oven	96 hrs	200	[113]
12	SIZ-10	2006	$Al(OiPr)_3$, H_3PO_4	HF	No	$[C_5mim][Br]$	oven	240 hrs	170	[113]
13	SIZ-10	2006	$Al(OiPr)_3$, H_3PO_4	HF	No	dication	oven	45 hrs	170	[113]
14	SIZ-10	2006	$Al(OiPr)_3$, H_3PO_4	HF	No	[iPrmim][Br]	oven	96 hrs	150	[113]
15	SIZ-11	2006	$Al(OiPr)_3$, H_3PO_4	No	No	[iPrmim][Br]	oven	96 hrs	150	[113]
16	$Al(H_2PO_4)_2F$	2006	$Al(OiPr)_3$, H_3PO_4	HF	No	$[C_2mim][Tf_2N]$	oven	96 hrs	170	[114]
17	AEL	2006	$Al(OiPr)_3$, H_3PO_4	HF	No	$[C_2mim][Br]$	oven	68 hrs	150	[115, 116]
18	AEL	2006	$Al(OiPr)_3$, H_3PO_4	HF	No	$[C_2mim][Br]$	microwave	20 mins	150	[115,116]
19	AEL	2006	$Al(OiPr)_3$, H_3PO_4	HF	No	$[C_2mim][Br]$	microwave	1 hr	150	[115,116]
20	AEL	2006	$Al(OiPr)_3$, H_3PO_4, TEOS	HF	No	$[C_2mim][Br]$	oven	1 hr	150	[115,116]
21	AEL	2006	$Al(OiPr)_3$, H_3PO_4	HF	No	$[C_4mim][Br]$	oven	4 hrs	190	[117, 116]
22	AFI	2006	$Al(OiPr)_3$, H_3PO_4	HF	or(n-DPA,i-DPA,MIA,PRD,n-BTA,DEA,TEA)	$[C_4mim][Br]$	oven	1 hr	190	[116,117]
23	AEL	2006	$Al(OiPr)_3$, H_3PO_4	HF	n-DPA	$[C_4mim][Br]$	oven	8 hrs	190	[116,117]
24	AFI	2006	$Al(OiPr)_3$, H_3PO_4	HF	n-DPA	$[C_4mim][Br]$	oven	0.5 hr	280	[116,117]
25	ATV	2006	$Al(OiPr)_3$, H_3PO_4	HF	n-DPA	$[C_4mim][Br]$	oven	3 hrs	280	[116,117]

26	SIZ-6	2006	$Al(OiPr)_3$, H_3PO_4	No	No	$[C_2mim][Br]$	oven	4 days	200	[118]
27	SOD	2008	$Al(OiPr)_3$, H_3PO_4,$CoCl_2.6H_2O$ or $Fe(NO_3)_3.9H_2O$	HF	No	$[C_2mim][Br]$ or $[C_4mim][Br]$	oven	3 or 5 days	150, 160, 170, 180, 190, 200	[119]
28	AEL film	2008	$Al(OiPr)_3$, H_3PO_4	HF	No	$[C_2mim][Br]$	microwave	age 4 hrs	100	[120]
29	LTA	2008	$Al(OiPr)_3$, H_3PO_4	HF	No	$[C_2mim][Br]$	oven	5 days	180 or 170	[121]
30	Quartz	2008	$Al(OiPr)_3$, H_3PO_4	HF	No	$[C_2mim][Br]$	oven	5 days	180	[121]
31	LTA	2008	Ga_2O_3, H_3PO_4	HF	No	$[C_2mim][Br]$	oven	5 days	150, 160, 170, 180, 190	[121]
32	Quartz	2008	Ga_2O_3, H_3PO_4	HF	No	$[C_2mim][Br]$	oven	5 days	180	[121]
33	AFI	2009	$Al(OiPr)_3$, H_3PO_4	HF	No	TEA Br and pentaerythritol	oven	3 days	180	[122]
34	GaPO4-a	2009	GaOOH, H_3PO_4	No	No	$[C_2mim][Br]$	oven	2 days	150	[123]
35	CLO	2009	GaOOH, H_3PO_4	HF	No	$[C_2mim][Br]$	oven	12 days	150	[123]
36	LTA	2009	GaOOH, H_3PO_4	HF	No	$[C_2mim][Br]$	oven	8 days	180	[123]
37	LTA	2009	GaOOH, H_3PO_4	HF	No	$[C_3mim][Br]$	oven	2 days	180	[123]
38	LTA	2009	GaOOH, H_3PO_4	HF	No	$[C_4mim][Br]$	oven	2 days	180	[123]
39	LTA	2009	GaOOH, H_3PO_4	HF	No	$[C_5mim][Br]$	oven	2 days	150	[123]
40	LTA	2009	GaOOH, H_3PO	HF	No	$[C_6mim][Br]$	oven	2 days	150	[123]
41	AEL	2009	Al(OiPr)3, H3PO4	HF	No	[C4mim][Br]	oven	4 hrs	160	[124]
42	AFI, AEL	2009	Al(OiPr)3, H3PO4	HF	n-DPA	[C4mim][Br]	oven	4 hrs	160	[124]
43	AFI	2009	Al(OiPr)3, H3PO4	HF	n-DPA	[C4mim][Br]	oven	4 hrs	160	[124]
44	LTA, AFI	2009	Al(OiPr)3, H3PO4	HF	n-DPA	[C4mim][Br]	oven	4 hrs	160	[124]
45	LTA	2009	Al(OiPr)3, H3PO4	HF	n-DPA, or n-BA, or TriBA, or DEA, or CHA, or HMTA, or Imidazole, or Pyridine	[C4mim][Br]	oven	4 hrs, 8 hrs, 12 hrs, 16 hrs	160	[124]
46	LTA	2010	$Al(OiPr)_3$, H_3PO_4	HF	No	[Benzmim][Cl]	oven	10 hrs	160	[125]
47	LTA+AFI	2010	$Al(OiPr)_3$, H_3PO_4	HF	No	[Benzmim][Cl]	oven	15 hrs	160	[125]
48	AFI	2010	$Al(OiPr)_3$, H_3PO_4	HF	No	[Benzmim][Cl]	oven	24 hrs	160	[125]
49	LTA	2010	$Al(OiPr)_3$, H_3PO_4	HF	TMA	[Benzmim][Cl]	oven	10 hrs	160	[125]
50	LTA	2010	$Al(OiPr)_3$, H_3PO_4	HF	TMA	[Benzmim][Cl]	oven	24 hrs	160	[125]

51	Cristobalite	2010	$Al(OiPr)_3$, H_3PO_4	HF	Morpholine	$[C_4mim][Br]$	oven	30 mins	80	[126]
52	MFI	2010	TEOS	HF		$[C_4mim][OH_{0.65}Br_{0.35}$ and H_2O	oven	14 days	170	[127]
53	AFI	2010	$Al(OiPr)_3$, H_3PO_4, $C_6H_9MnO_6.2(H_2O)$	No	No	$[C_2C_1mim][Br]$	oven	90 hrs	150	[128]
54	MFI	2010	SiO_2	No	TPAOH , EtOH	$[C_4mim][Br]$ and H_2O	microwave	3 hrs	175	[129]
55	LTA	2010	$Al(OiPr)_3$, H_3PO_4	HF	n-DPA	$[C_4mim][Br]$	oven	4 hrs	160	[130]
56	LTA	2010	$Al(OiPr)_3$, H_3PO_4	HF	n-DPA	$[C_4mim][Br]$	oven	2 hrs	190	[130]
57	LTA	2010	$Al(OiPr)_3$, H_3PO_4	HF	CHA	$[C_4mim][Br]$	oven	4 hrs	160	[130]
58	LTA	2010	$Al(OiPr)_3$, H_3PO_4	HF	DEA	$[C_4mim][Br]$	oven	4 hrs	160	[130]
59	LTA	2010	$Al(OiPr)_3$, H_3PO_4	HF	TBA	$[C_4mim][Br]$	oven	4 hrs	160	[130]
60	LTA	2010	$Al(OiPr)_3$, H_3PO_4	HF	HMTA	$[C_4mim][Br]$	oven	14 hrs	160	[130]
61	LTA	2010	$Al(OiPr)_3$, H_3PO_4	HF	TETA	$[C_4mim][Br]$	oven	8 hrs	160	[130]
62	LTA	2010	$Al(OiPr)_3$, H_3PO_4	HF	imidazole	$[C_4mim][Br]$	oven	2 hrs	160	[130]
63	LTA	2010	$Al(OiPr)_3$, H_3PO_4	HF	pyridine	$[C_4mim][Br]$	oven	2 hrs	160	[130]
64	AEL	2010	$Al(OiPr)_3$, H_3PO_4	HF	TBA^+	$[C_4mim][Br]$	oven	8 hrs	160	[131]
65	AEL	2010	$Al(OiPr)_3$, H_3PO_4	HF	TPA^+	$[C_4mim][Br]$	oven	8 hrs	160	[131]
66	AFI	2010	$Al(OiPr)_3$, H_3PO_4	HF	$Choline^+$	$[C_4mim][Br]$	oven	10 hrs	160	[131]
67	AFI	2010	$Al(OiPr)_3$, H_3PO_4	HF	n-DPA	$[C_4mim][Br]$	oven	4 hrs	160	[131]
68	AFI	2010	$Al(OiPr)_3$, H_3PO_4	HF	TEA^+	$[C_4mim][Br]$	oven	2 hrs	160	[131]
69	LTA	2010	$Al(OiPr)_3$, H_3PO_4	HF	TMA^+	$[C_4mim][Br]$	oven	2 hrs	160	[131]
70	AEL	2010	$Al(OiPr)_3$, H_3PO_4	HF	none	$[C_4mim][Br]$	oven	4 hrs	160	[131]
71	DNL-1	2010	$Al(OiPr)_3$, H_3PO_4	HF	HAD	$[C_2mim][Br]$	oven	2 hrs	210	[132]
72	Sodalite	2010	$NaAlO_2$, $Na_2SiO_3.9H_2O$, NaOH, KOH	No	No	$[C_2mim][Br]$ and H_2O	oil bath	15 hrs	90	[133]
73	CHA	2010	Al(OiPr)3, H3PO4	HF	No	1-Methylimidazole, or pyridine, or 4-methylpyridine	oven	3 days	150	[134]
74	SOD in amorphous	2010	$Al(OiPr)_3$, H_3PO_4	HF	No	1-methylpyrrolidine	oven	3 days	150	[134]
75	AEL, CHA	2010	$Al(OiPr)_3$, H_3PO_4	HF	No	$[C_n mim][Br]$ or EPB	oven	3 days	150	[134]
76	AlPO-5	2010	$Al(OiPr)_3$, H_3PO_4	HF	No	N-methyl-N-butyl-pyrollidinium bromide	oven	3 days	150	[134]
77	Unknown or dense	2010	$Al(OiPr)_3$, H_3PO_4	HF	No	1-Butyl-4-methylpyridinium	oven	3 days	150	[134]

						bromide				
78	AlPO-CJ12	2010	$Al(OiPr)_3$, H_3PO_4	No	No	1-Methylimidazole	oven	3 days	150	[134]
79	Layered structure	2010	$Al(OiPr)_3$, H_3PO_4	No	No	Pyridine	oven	3 days	150	[134]
80	Layer phase	2010	$Al(OiPr)_3$, H_3PO_4	No	No	4-Methylpyridine	oven	3 days	150	[134]
81	SIZ-1, SIZ-6	2010	$Al(OiPr)_3$, H_3PO_4	No	No	n-Alkylimidazoliums	oven	3 days	150	[134]
82	Chain structure	2010	$Al(OiPr)_3$, H_3PO_4	No	No	n-Alkyl pyridiunium bromides	oven	3 days	150	[134]
83	SIZ-6	2010	$Al(OiPr)_3$, H_3PO_4	No	No	1-Butyl-4-methylpyridinium bromide	oven	3 days	150	[134]
84	AlPO chain	2010	$Al(OiPr)_3$, H_3PO_4	No	No	1-ethylpyridinium bromide	oven	3 days	150	[135]
85	AlPO chain, SIZ-1	2010	$Al(OiPr)_3$, H_3PO_4, $Zn(Oac)_2$	No	No	$[C_2mim][Br]$	oven	1 days	150	[135]
86	AlPO chain	2010	$Al(OiPr)_3$, H_3PO_4	No	tripropylamine	$[C_2mim][Br]$	oven	3 days	150	[135]
87	SIZ-4, AlPO chain	2010	$Al(OiPr)_3$, H_3PO_4	HF	TEAOH	$[C_2mim][Br]$	oven	1 day	150	[135]
88	AlPO chain, hexagonal GaPO	2010	$Al(OiPr)_3$, H_3PO_4	No	No	$[C_2mim][Br]$	oven	1 day	150	[135]
89	CHA	2010	$Al(OiPr)_3$, H_3PO_4	HF	2-methylimidazole, or N-methylimidazole, or 4-methylpyridine	$[C_4mim][Br]$	oven	1 hrs, 2 hrs, 4 hrs, 16 hrs	130, 140, 150, 160	[136]
90	ZSM-5	2011	$NaAlO_2$, TEOS	KOH	TPAOH	$[C_4mim][Cl]$, H_2O	Oil bath	5-20 mins	150	[137]

Not only powders of zeolites could be synthesized. Dr. Yan and his group in 2008 synthesized oriented zeolite AEL films in ionic liquids at ambient pressure and with microwave heating. These films can be used as corrosion-resistant coatings after adding sealing agent on them, such as silane.[120]

2.3.3 Effect of different synthesis parameters in ionothermal synthesis

Since ionothermal synthesis was discovered fairly recently, there is not much synthesis mechanism proposed. However, researchers found effects of a few variables on the synthesized frameworks.

(1) Effect of heating source

From Table 1, it can be seen that several frameworks could be synthesized by heating with microwave instead of conventional oven. Commonly, crystallization time is greatly reduced from conventional oven to microwave heating, which is preferred. The possibility to use microwave as a heating source is due to good microwave absorbing capacity of ionic liquids and low vapor pressure during the heating process. However, heating reaction gel by microwave and by conventional oven could influence the framework formed. For example, Ma and his group report the synthesis of AlPO4-11 in the case of microwave heating, while Dr. Morris synthesize SIZ-6 using conventional heating.[118,138]

(2) Effect of water

There are two main papers discussing effects of water on ionothermal synthesis of zeolites.[138,139] Both found water plays an important role in deciding the crystallization rate and phase selection. In the common ionothermal synthesis process, little amount of water is present from the aqueous acid solution and from the aqueous phosphoric acid solution. As a result, when they are added into the reaction mixture, water is introduced in the reaction gel. In the first paper published on ionothermal synthesis of zeolites in 2004, Dr. Morris found if no measure is done to evaporate the water in the reaction mixture, SIZ-3 is formed. However, if the reaction mixture is heated at 50 ^{o}C for 2 hrs to remove water and isopropanol formed during the initial reaction before heating it to 150 ^{o}C, SIZ-4 is the product.[111] In addition, he found at intermediate water

concentration, materials with dense phase are formed and when molar ratio of ionic liquid/water is 1: 2.5, product is SIZ-5(AlPO-41) framework with a little dense phase impurity.[111] Then in 2009, Dr. Morris did a systematic experiment to investigate what frameworks could be formed by systematically changing molar ratio of water to ionic liquid.[139] The result of materials synthesized in $[C_2C_1im][Br]$ (heated by microwave) is shown in Figure 2.12. Similar results are obtained when 1-ethylpyridiunium is used as the solvent.

From the results shown in Figure 2.12, Dr. Morris concluded that water played an important role in deciding the frameworks synthesized, but the water content is not a reliable way to select between SIZ-3 and SIZ-4.[139]

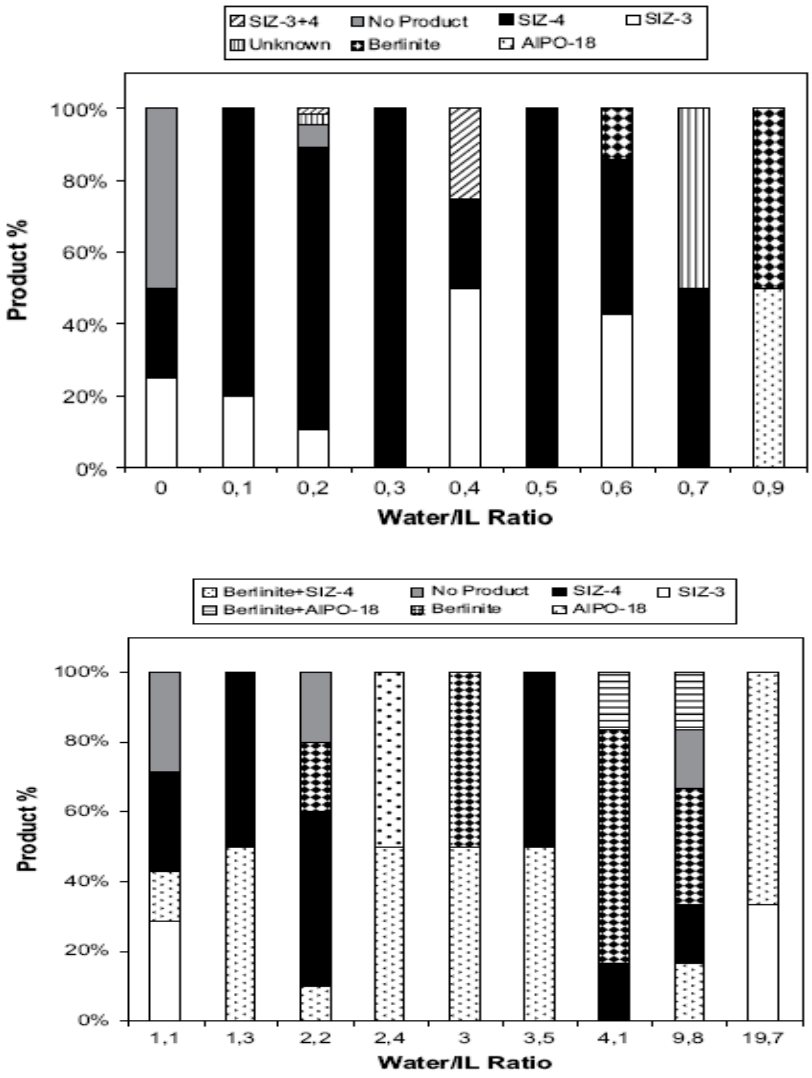

Figure 2.12 Products synthesized by changing ratio of water to IL.[139]

There is another paper dealing with effect of water on the frameworks formed.[138] The author found with initial gel composition: $1AlOOH:3NH_4H_2PO_4$: $0.5NH_4F:yH_2O$:40 $[C_2C_1im][Br]$ (molar ratio), when y is equal to 0 (meaning no water in the reaction gel), crystallinity of the material is about 25 % and about 50 % after heating for 20 mins and 30 mins. As a comparison, crystallinities are about 75 % and 80 % when y is equal to 0.5. Similarly, with initial gel composition: $1AlOOH$: $1.2NH_4H_2PO_4$: yH_2O: $40[C_4C_1im][Br]$, crystallinities of $AlPO_4$-11 are 0 % and 30 % after 60 mins and 180 mins, whereas the number are 40 % and 60 %, respectively when y is equal to 4. The ratio of water to ionic liquid (4:40) is about the same as the ratio in an ionothermal synthesis reaction gel where water comes only from hydrofluoric acid and phosphoric acid. As a result, the author claims that water is involved in the crystallization of the molecular sieves. The reason is because water could improve hydrolysis reaction and accelerate the formation of solution active species.[140]

(3) Effect of structure directing agent

In Ma's paper, the authors also did research on effect of F^- on formation of frameworks. With the absence of NH_4F in the reaction gel, $AlPO_4$-11 is obtained. Whereas, if NH_4F is present in the reaction gel, $AlPO_4$-5 or a mixture of $AlPO_4$-5 and $AlPO_4$-11 are synthesized. As a result, the authors concluded that NH_4F may play as a structure directing agent to direct formation of $AlPO_4$-5. From Figure 2.13, authors claim that NH_4F also plays as a mineralizer to promote crystallization process under microwave heating at 200 ^oC. However, this trend does not hold under conventional heating at 200 ^oC, as shown in Figure 2.14. The reason is not explained in the paper.

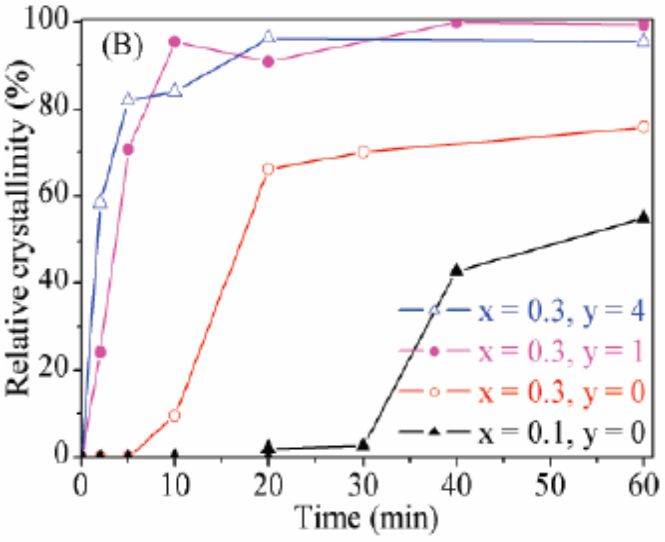

Figure 2.13 Crystallization curves of products obtained in $[C_4C_1im][Br]$ under microwave heating at 200 ℃.[138]

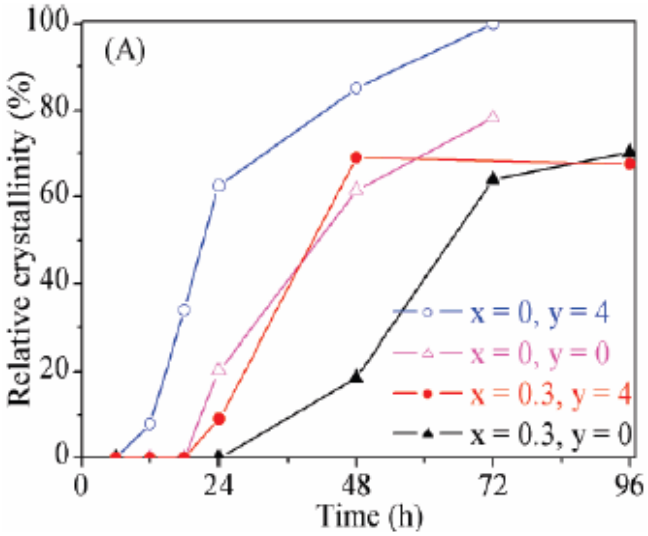

Figure 2.14 Crystallization curves of products obtained in $[C_4C_1im][Br]$ under conventional heating at 200 ℃.[138]

A paper published in 2010 provides evidence for the importance of F^-. With the same reaction composition, after heating for 10 hours, LTA is formed with the presence of F^-, whereas amorphous phase if formed with the absence of F^-.[141] Xu found that in the nucleation stage, organic anion, such as morpholine, connected with $[C_4C_1im][Br]$ through hydrogen bonding and

the hybrid functions as structure directing agent to form AFI structure. Then $[C_4C_1im][Br]$ acts as pore-filling agents in the process of crystal growth.[142] Fayad claims that [Benzmim][Cl] and TMA^+ and F^- can function as co-templating agent to stabilize $AlPO_4$-LTA framework.[141] AFI is formed when $[C_4C_1im][Br]$ is used as solvent, while AEL and CHA are preferred when $[C_2C_1im][Br]$ is used.[115] AFI contains a 12-membered ring, whereas AEL has 10-membered ring and CHA has 8-membered rings, shown in Figure 2.15. As a result, the author concluded that ionic liquid with longer alkyl chain length act as structure directing agent and leads to zeolites with larger pores.[115]

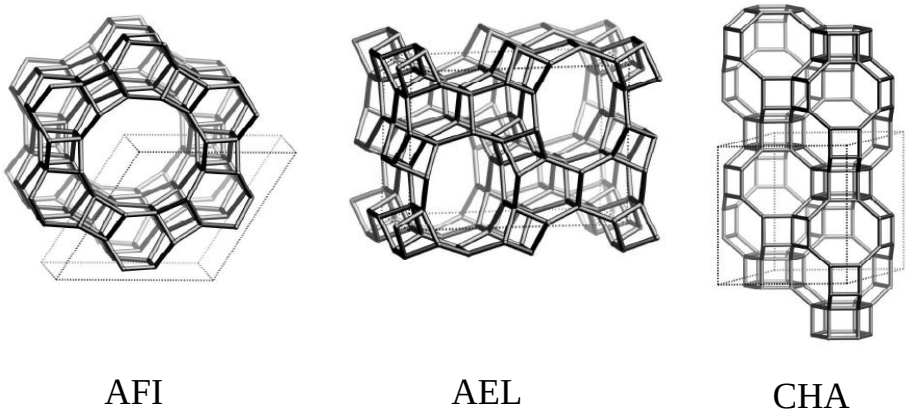

Figure 2.15 Frameworks of AFI, AEL and CHA (www.iza-structure.org).

2.4 Conformation of precursors

Since aluminium isopropoxide is an important precursor in the ionothermal synthesis of microporous materials, its structure needs to be investigated. The formula for aluminium isopropoxide is $Al(OiPr)_3$. However, it does not exist in the monomer state. Actually, many experiments have been done on the conformation of this material.[143-146] They found Al has a tendency to maximize its coordination number, resulting in materials containing tetrahedral and octahedral metal centers.[146] commonly, freshly distilled aluminium alkoxide is supposed to be a trimer, but after aging for a certain time, it rearranges to tetramer. The formula for a tetrameric aluminium isopropoxide is $Al[(\mu\text{-}O^iPr)_2Al(O^iPr)_2]_3$. [145]

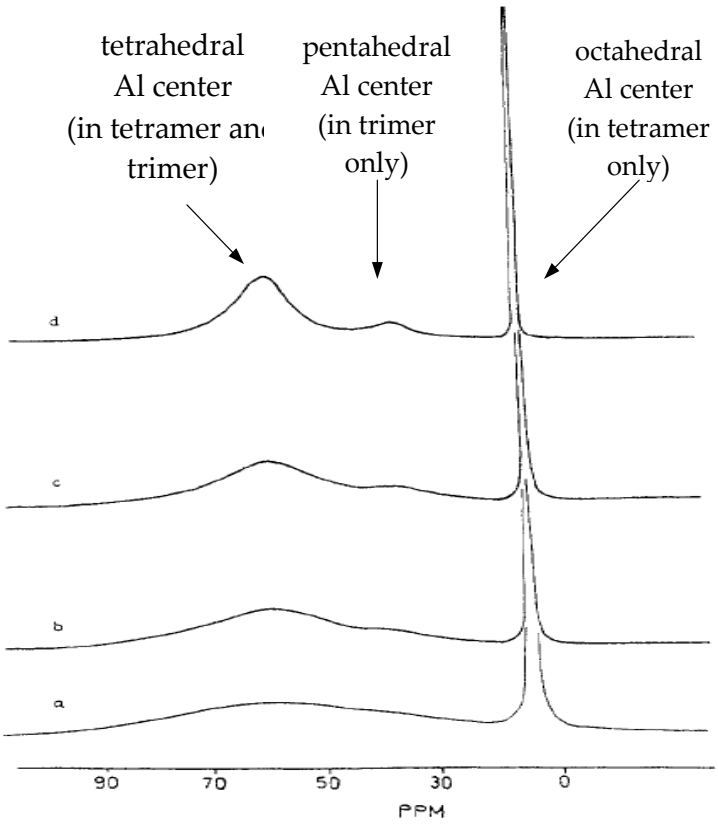

Figure 2.16 ^{27}Al NMR spectra of Al(OiPr)$_3$ in toluene: (a) 3.5 M at 297K; (b) 6.2*10^{-1} M at 297 K; (c) 6.2*10^{-1} M at 309 K; (d) 6.2*10^{-1} M at 349 K.

Ropson et al. used ^{27}Al NMR to investigate the state of aluminium isopropoxide in toluene. The patterns they got were in Figure 2.16. The broader peak and the sharp narrow peaks correspond to tetrahedral-coordinated aluminium atoms (Al(IV)) and octahedral-coordinated aluminium atoms (Al(VI)).[147]

As mentioned above, in molecular sieves or zeolites, aluminium is tetrahedral-coordinated, which indicates each aluminium atom is bonded to four oxygen atoms and forms AlO_4. As a result, almost all of the aluminium in molecular sieves should have the structure of Al(IV). The ^{27}Al MAS NMR results of zeolites have been reported and prove this statement. For example, Sakthivel and his coworkers published the ^{27}Al MAS-NMR spectra of as-synthesized Na-AlMCM-41, shown in Figure 2.17.[148] In Figure 2.17, only one peak corresponding to Al(IV) is shown. But after calcination at around 500 oC for several hours, some of the AlO_4 structures will be destroyed and a small peak corresponding to Al(IV) will show up.[148-150]

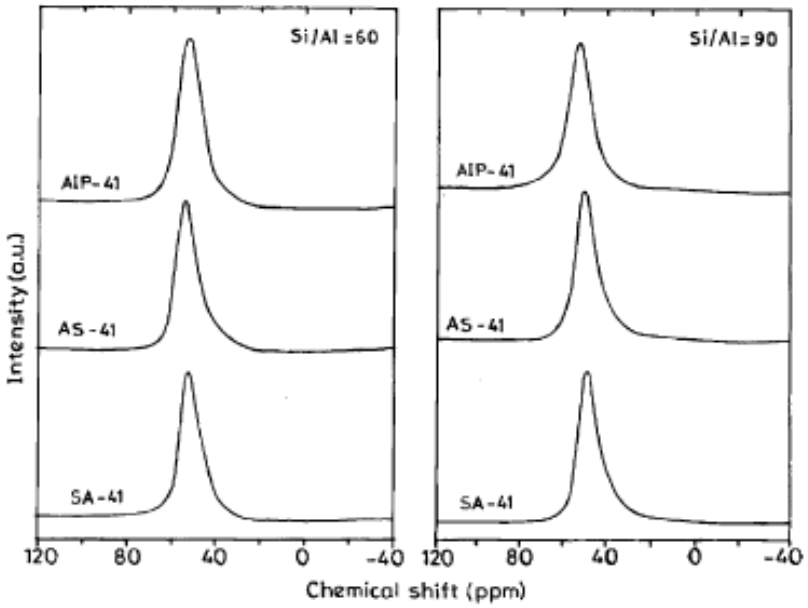

Figure 2.17 ^{27}Al MAS-NMR spectra of as-synthesized Na-AlMCM-41 synthesized from different aluminium sources with various silicon-to-aluminium ratos.[148]

In Chapter 2, different empirically-derived recipes to synthesize molecular sieves in ionic liquids are listed and effects of synthesis parameters in ionothermal synthesis, such as heating source, water and structure directing agent, have been summarized. But these works are not enough to fully understand the formation mechanism of molecular sieves in ionic liquids and more works are needed. So in this project, research was done to investigate the behaviors of precursors in ionic liquids and the interactions between room temperature ionic liquids (RTILs) and precursors of microporous zeolite and aluminophosphate (AlPOs) in the hope that the findings could be used to direct current and further synthesis of these materials in RTILs. Different recipes to ionothermally synthesize aluminophosphates have also been created and used to investigate the effects of other synthesis parameters (such as solvent structure, prolonged heating time, different mineralizers, concentration of precursors) on the frameworks structure formed.

2.5 References

1. Cronstedt, A. F. *Kongl Vetenskaps Academiens Handlingar Stockholm* **1756**, *17*, 120.
2. Breck, D. W. *Zeolite Molecular Sieves: Structure, Chemistry, and Use*; john Wiley & Sons: new York, 1974.
3. Davis, M. E. *Industrial & Engineering Chemistry Research* **1991**, *30*, 1675-1683.
4. Dyer, A. *An Introduction to Zeolite Molecular Sieves*; John Wiley and Sons: Chichester, 1988.
5. Liebau, F. *Structural Chemistry of Silicates: Structure, Bonding, and Classification*; Springer-Verlag: Berlin, Heidelberg, New York, Tokyo, 1985.
6. Liebau, F.; Gies, H.; Gunawardane, R. P.; Marler, B. **1986**, *6*, 373.
7. Baerlocher, C.; Meier, W. M.; Olson, D. H. *Atlas of zeolite framework types*; Elsevier: Amsterdam, NY, USA, 2001.
8. Wilson, S. T.; Lok, B. M.; Messina, C. A.; Cannan, T. R.; Flanigen, E. M. *Acs Symposium Series* **1983**, *218*, 79-106.
9. Weitkam, J.; Kleinschmit, P.; Kiss, A.; Berke, C. H. the Ninth International Zeolite Conference, 1993, Boston.
10. Robson, H. *Verified Syntheses of Zeolitic Materials*, 2 ed.; Elsevier Science B. V.: Amsterdam, 2001.
11. Barrer, R. M. *Hydrothermal Chemisry of Zeolites*; Academic Press: London, 1982.
12. Wright, P. A. *Microporous Framework Solids*; The Royal Society of Chemistry: Cambridge, 2008.
13. Barrer, R. M.; Denny, P. J. *Journal of Chemical Society* **1961**, 971-982.
14. Kerr, G. T.; Kokotailo, G. T. *Journal of American Chemical Society* **1961**, *83*, 4675.
15. Sastre, G. *Physical Chemistry Chemical Physics* **2007**, *9*, 1052-1058.
16. Bonilla, G.; Diaz, I.; Tsapatsis, M.; Jeong, H. K.; Lee, Y.; Vlachos, D. G. *Chemistry of Materials* **2004**, *16*, 5697-5705.
17. Petrovic, I.; Navrotsky, A.; Davis, M. E.; Zones, S. I. *Chemistry of Materials* **1993**, *5*, 1805-1813.
18. Christensen, A. N.; Jensen, T. R.; Norby, P.; Hanson, J. C. *Chemistry of Materials* **1998**, *10*, 1688-1693.

19. Domine, D.; Quobex, J. *Molecular Sieves*; Society of Chemical Industry: London, 1968.
20. Burkett, S. L.; Davis, M. E. *Journal of Physical Chemistry* **1994**, *98*, 4647-4653.
21. Drews, T. O.; Katsoulakis, M. A.; Tsapatsis, M. *Journal of Physical Chemistry B* **2005**, *109*, 23879-23887.
22. Grandjean, D.; Beale, A. M.; Petukhov, A. V.; Weckhuysen, B. M. *Journal of the American Chemical Society* **2005**, 127, 14454-14465.
23. Jia, W.; Murad, S. *Journal of Chemical Physics* **2005**, *122*.
24. Lopes, F. V. S.; Grande, C. A.; Ribeiro, A. M.; Loureiro, J. M.; Evaggelos, O.; Nikolakis, V.; Rodrigues, A. E. *Separation Science and Technology* **2009**, *44*, 1045-1073.
25. Hedstrom, A. *Journal of Environmental Engineering-Asce* **2001**, *127*, 673-681.
26. Pansini, M. *Mineralium Deposita* **1996**, *31*, 563-575.
27. Mumpton, F. A. *Commercial utilization of natural zeolites*, 4 ed.New York, 1975.
28. Guisnet, M.; Gilson, J. P. *Zeolites for Cleaner Technologies*; Imperial College Press: London, 2002.
29. Casci, J. L. The Preparation and Potential Applications of Ultra-Large Pore Molecular-Sieves - a Review. In *Advanced Zeolite Science and Applications*, 1994; Vol. 85; pp 329-356.
30. Wei, Y.; Tian, Z. J.; Gies, H.; Xu, R. S.; Ma, H. J.; Pei, R. Y.; Zhang, W. P.; Xu, Y. P.; Wang, L.; Li, K. D.; Wang, B. C.; Wen, G. D.; Lin, L. W. *Angewandte Chemie-International Edition* **2010**, *49*, 5367-5370.
31. Chen, Y. M. *Powder Technology* **2006**, *163*, 2-8.
32. Letzsch, W. S.; Mauleon, J. L.; Long, S. *Abstracts of Papers of the American Chemical Society* **1983**, *186*, 11-PETR.
33. Zhang, W. M.; Smirniotis, P. G. *Journal of Catalysis* **1999**, *182*, 400-416.
34. Sato, K.; Iwata, Y.; Yoneda, T.; Nishijima, A.; Miki, Y.; Shimada, H. *Catalysis Today* **1998**, *45*, 367-374.
35. Maesen, T. L. M.; Krishna, R.; van Baten, J. M.; Smit, B.; Calero, S.; Sanchez, J. M. C. *Journal of Catalysis* **2008**, *256*, 95-107.
36. Guisnet, M.; Gnep, N. S. *Applied Catalysis a-General* **1996**, *146*, 33-64.
37. Schuster, H.; Rios, L. A.; Weckes, P. P.; Hoelderich, W. F. *Applied Catalysis a-General* **2008**, *348*, 266-270.

38. Fong, Y. Y.; Abdullah, A. Z.; Ahmad, A. L.; Bhatia, S. *Chemical Engineering Journal* **2008**, *139*, 172-193.
39. Bhat, Y. S.; Das, J.; Halgeri, A. B. Conversion of n-pentane to benzene toluene and para-xylene over pore size controlled Ga2O3 incorporated ZSM-5 zeolite. In *Progress in Zeolite and Microporous Materials, Pts a-C*; Chon, H., Ihm, S. K., Uh, Y. S., Eds., 1997; Vol. 105; pp 1309-1316.
40. Musilova, Z.; Zilkova, N.; Park, S. E.; Cejka, J. *Topics in Catalysis* **2010**, *53*, 1457-1469.
41. Zilkova, N.; Bejblova, M.; Gil, B.; Zones, S. I.; Burton, A. W.; Chen, C. Y.; Musilova-Pavlackova, Z.; Kosova, G.; Cejka, J. *Journal of Catalysis* **2009**, *266*, 79-91.
42. Smirniotis, P. G.; Ruckenstein, E. *Industrial & Engineering Chemistry Research* **1995**, *34*, 1517-1528.
43. Cui, Z. M.; Liu, Q.; Ma, Z.; Bian, S. W.; Song, W. G. *Journal of Catalysis* **2008**, *258*, 83-86.
44. Quisenberry, J. H. *Clay & Clay Minerals* **1968**, *16*, 267.
45. Minato; Hideo. *Koatsugasu* **1968**, *5*.
46. Minato; Hideo "utilization of natural zeolites in Japan," 1971.
47. Torii; Kazuo "utilization of sedimentary zeolites in Japan," 1974.
48. Onagi, T. *Rep. yamagata Stock Raising inst.* **1965**, 11-22.
49. Nishimura; Yoichi. *Journal of Clay Society* **1973**, *13*, 23.
50. Peter, M. D.; Bose, R. J. *Fish and marine Tech* **1975**, 12.
51. Koyo kaihatsu Co., L. *Company Brochure* **1974**, 4.
52. Lancaster, M. *Green Chemistry: An Introductory Text*; The Royal Society of Chemistry: Cambridge, 2010.
53. Yoo, T. S.; Frank, S. M.; Simpson, M. F.; Hahn, P. A.; Battisti, T. J.; Phongikaroon, S. *Nuclear Technology, 171*, 306-315.
54. Faghihian, H.; Kabiri-Tadi, M.; Ahmadi, S. J. *Journal of Radioanalytical and Nuclear Chemistry, 285*, 499-504.
55. Pickering, H. W.; Menzies, N. W.; Hunter, M. N. *Scientia Horticulturae* **2002**, *94*, 333-343.
56. Marmottant, B.; Mhimid, A.; Elgolli, S.; Grenier, P. *Revue Generale De Thermique* **1992**, *31*, 97-105.
57. Levels of Radioactive Materials Rise near Japanese Plant, 2011.
58. Chiappe, C.; Pieraccini, D. *J. Phys. Org. Chem.* **2005**, *18*, 275-297.

59. Ngo, H. L.; LeCompte, K.; Hargens, L.; McEwen, A. B. *Thermochim. Acta* **2000**, *357*, 97-102.

60. Seddon, K. R. *J. Chem. Technol. Biotechnol.* **1997**, *68*, 351-356.

61. Walden, P. *Bulletin of the Russian Academy of Sciences* **1914**, 405-422.

62. Sedden, K. R. "Ionic liquids: designer solvents?" International George Papatheodorou Symposium, 1999, Institute of Chemical Engineering and High Temperature Processes, Patras, Greece.

63. Bonhote, P.; Dias, A. P.; Papageorgiou, N.; Kalyanasundaram, K.; Gratzel, M. *Inorganic Chemistry* **1996**, *35*, 1168-1178.

64. Wilkes, J. S.; Zaworotko, M. J. *Journal of the Chemical Society-Chemical Communications* **1992**, 965-967.

65. Lall, S. I.; Mancheno, D.; Castro, S.; Behaj, V.; Cohen, J. L. I.; Engel, R. *Chemical Communications* **2000**, 2413-2414.

66. Seddon, K. R.; Stark, A.; Torres, M. J. *Pure and Applied Chemistry* **2000**, *72*, 2275-2287.

67. De Souza, R. F.; Rech, V.; Dupont, J. *Advanced Synthesis & Catalysis* **2002**, *344*, 153-155.

68. Siriwardana, A. I.; Crossley, I. R.; Torriero, A. A. J.; Burgar, I. M.; Dunlop, N. F.; Bond, A. M.; Deacon, G. B.; MacFarlane, D. R. *Journal of Organic Chemistry* **2008**, *73*, 4676-4679.

69. Holbrey, J. D.; Reichert, W. M.; Tkatchenko, I.; Bouajila, E.; Walter, O.; Tommasi, I.; Rogers, R. D. *Chemical Communications* **2003**, 28-29.

70. Stegemann, H.; Rohde, A.; Reiche, A.; Schnittke, A.; Fullbier, H. *Electrochimica Acta* **1992**, *37*, 379-383.

71. Elaiwi, A.; Hitchcock, P. B.; Seddon, K. R.; Srinivasan, N.; Tan, Y. M.; Welton, T.; Zora, J. A. *Journal of the Chemical Society-Dalton Transactions* **1995**, 3467-3472.

72. Seddon, K. R. *Journal of Chemical Technology and Biotechnology* **1997**, *68*, 351-356.

73. Ngo, H. L.; LeCompte, K.; Hargens, L.; McEwen, A. B. *Thermochimica Acta* **2000**, *357*, 97-102.

74. Zhang, S. J.; Sun, N.; He, X. Z.; Lu, X. M.; Zhang, X. P. *Journal of Physical and Chemical Reference Data* **2006**, *35*, 1475-1517.

75. Ohtani, H.; Ishimura, S.; Kumai, M. *Analytical Sciences* **2008**, *24*, 1335-1340.

76. Paulechka, Y. U.; Zaitsau, D. H.; Kabo, G. J.; Strechan, A. A. *Thermochimica Acta* **2005**, *439*, 158-160.

77. Paulechka, Y. U.; Kabo, G. J.; Blokhin, A. V.; Vydrov, O. A.; Magee, J. W.; Frenkel, M. *Journal of Chemical and Engineering Data* **2003**, *48*, 457-462.

78. Jacquemin, J.; Ge, R.; Nancarrow, P.; Rooney, D. W.; Gomes, M. F. C.; Padua, A. A. H.; Hardacre, C. *Journal of Chemical and Engineering Data* **2008**, *53*, 716-726.

79. Rooney, D.; Jacquemin, J.; Gardas, R. L. Thermophysical Properties of Ionic Liquids. In *Ionic Liquids*, 2009; Vol. 290; pp 185-212.

80. Li, H. L.; Ibrahim, M.; Agberemi, I.; Kobrak, M. N. *Journal of Chemical Physics* **2008**, *129*.

81. Jacquemin, J.; Husson, P.; Padua, A. A. H.; Majer, V. *Green Chemistry* **2006**, *8*, 172-180.

82. Tokuda, H.; Hayamizu, K.; Ishii, K.; Susan, M.; Watanabe, M. *Journal of Physical Chemistry B* **2005**, *109*, 6103-6110.

83. Tokuda, H.; Hayamizu, K.; Ishii, K.; Abu Bin Hasan Susan, M.; Watanabe, M. *Journal of Physical Chemistry B* **2004**, *108*, 16593-16600.

84. Chengfeng Ye; Weimin Liu; Yunxia Chen; Yu, L. *Chem. Commun.* **2001**, 2244-2245.

85. A.E. Jimenez; M.D. Bermudez; P. Iglesias; F.J. Carrion; G. Martinez-Nicolas. *Wear* **2006**, *260*, 766-782.

86. Akihito Suzuki; Yoshihiro Shinka; Masabumi Masuko. *Tribol. Lett.* **2007**, *27*, 307-313.

87. Guiqin Yu; Shiqiang Yan; Feng Zhou; Xuqing Liu; Wenmin Liu; Liang, Y. *Tribology Letters* **2007**, *25*, 197-205.

88. Manuel Palacio; Bharat Bhushan. *Adv. Mater.* **2008**, *20*, 1194-1198.

89. Weimin liu; Chengfeng Ye; Qingye Gong; Haizhong Wang; Peng Wang. *Tribol. Lett.* **2002**, *13*, 81-85.

90. X. Q. Liu; F. Zhou; Y. M. Liang; W. M. Liu. *Wear* **2006**, *261*.

91. Yu, G. Q.; Zhou, F.; Liu, W. M.; Liang, Y. M.; Yan, S. Q. *Wear* **2006**, *260*, 1076-1080.

92. Qu, J.; Truhan, J. J.; Dai, S.; Luo, H.; Blau, P. J. *Tribology Letters* **2006**, *22*, 207-214.

93. Sanes, J.; Carrion, F. J.; Bermudez, M. D.; Martinez-Nicolas, G. *Tribology Letters* **2006**, *21*, 121-133.

94. Wang, H. Z.; Lu, Q. M.; Ye, C. F.; Liu, W. M.; Cui, Z. J. *Wear* **2004**, *256*, 44-48.

95. Yu, B.; Zhou, F.; Pang, C. J.; Wang, B.; Liang, Y. M.; Liu, W. M. *Tribology International* **2008**, *41*, 797-801.

96. Mu, Z. G.; Wang, X. X.; Zhang, S. X.; Liang, Y. M.; Bao, M.; Liu, W. M. *Journal of Tribology-Transactions of the Asme* **2008**, *130*.

97. Mu, Z. G.; Zhou, F.; Zhang, S. X.; Liang, Y. M.; Liu, W. M. *Tribology International* **2005**, *38*, 725-731.

98. Zhu, M.; Yan, J.; Mo, Y.; Bai, M. *Tribology Letters* **2008**, *29*, 177-183.

99. Swatloski, R. P.; Spear, S. K.; Holbrey, J. D.; Rogers, R. D. *Journal of the American Chemical Society* **2002**, *124*, 4974-4975.

100. Zhang, H.; Wu, J.; Zhang, J.; He, J. S. *Macromolecules* **2005**, *38*, 8272-8277.

101. Zhu, S. D.; Wu, Y. X.; Chen, Q. M.; Yu, Z. N.; Wang, C. W.; Jin, S. W.; Ding, Y. G.; Wu, G. *Green Chemistry* **2006**, *8*, 325-327.

102. Li, Z. J.; Chang, J.; Shan, H. X.; Pan, J. M. *Reviews in Analytical Chemistry* **2007**, *26*, 109-153.

103. Tao, G. H.; He, L.; Liu, W. S.; Xu, L.; Xiong, W.; Wang, T.; Kou, Y. *Green Chemistry* **2006**, *8*, 639-646.

104. Biedron, T.; Kubisa, P. *Polymer International* **2003**, *52*, 1584-1588.

105. Kubisa, P. *Progress in Polymer Science* **2009**, *34*, 1333-1347.

106. Galinski, M.; Lewandowski, A.; Stepniak, I. *Electrochimica Acta* **2006**, *51*, 5567-5580.

107. Marsh, K. N.; Deev, A.; Wu, A. C. T.; Tran, E.; Klamt, A. *Korean Journal of Chemical Engineering* **2002**, *19*, 357-362.

108. Lobo, R. F.; Zones, S. I.; Davis, M. E. *Journal of Inclusion Phenomena and Molecular Recognition in Chemistry* **1995**, *21*, 47-78.

109. Daniels, R. H.; Kerr, G. T.; Rollmann, L. D. *Journal of the American Chemical Society* **1978**, *100*, 3097-3100.

110. Flanigen, E. M. *Advances in Chemistry Series* **1973**, 119-139.

111. Cooper, E. R.; Andrews, C. D.; Wheatley, P. S.; Webb, P. B.; Wormald, P.; Morris, R. E. *Nature* **2004**, *430*, 1012-1016.

112. Parnham, E. R.; Morris, R. E. *Journal of the American Chemical Society* **2006**, *128*, 2204-2205.

113. Parnham, E. R.; Morris, R. E. *Chemistry of Materials* **2006**, *18*, 4882-4887.

114. Parnham, E. R.; Morris, R. E. *Journal of Materials Chemistry* **2006**, *16*, 3682-3684.

115. Xu, Y. P.; Tian, Z. J.; Wang, S. J.; Hu, Y.; Wang, L.; Wang, B. C.; Ma, Y. C.; Hou, L.; Yu, J. Y.; Lin, L. W. *Angewandte Chemie-International Edition* **2006**, *45*, 3965-3970.

116. Xu, R. S.; Shi, X. C.; Zhang, W. P.; Xu, Y. P.; Tian, Z. J.; Lu, X. B.; Han, X. W.; Bao, X. H. *Physical Chemistry Chemical Physics*, *12*, 2443-2449.

117. Wang, L.; Xu, Y. P.; Wei, Y.; Duan, J. C.; Chen, A. B.; Wang, B. C.; Ma, H. J.; Tian, Z. J.; Lin, L. W. *Journal of the American Chemical Society* **2006**, *128*, 7432-7433.

118. Parnham, E. R.; Wheatley, P. S.; Morris, R. E. *Chemical Communications* **2006**, 380-382.

119. Han, L. J.; Wang, Y. B.; Li, C. X.; Zhang, S. J.; Lu, X. M.; Cao, M. J. *Aiche Journal* **2008**, *54*, 280-288.

120. Cai, R.; Sun, M. W.; Chen, Z. W.; Munoz, R.; O'Neill, C.; Beving, D. E.; Yan, Y. S. *Angewandte Chemie-International Edition* **2008**, *47*, 525-528.

121. Han, L. J.; Wang, Y. B.; Zhang, S. J.; Lu, X. M. *Journal of Crystal Growth* **2008**, *311*, 167-171.

122. Liu, L.; Li, X. P.; Xu, H.; Li, J. P.; Lin, Z.; Dong, J. X. *Dalton Transactions* **2009**, 10418-10421.

123. Ma, H. J.; Xu, R. S.; You, W. S.; Wen, G. D.; Wang, S. J.; Xu, Y.; Wang, B. C.; Wang, L.; Wei, Y.; Xu, Y. P.; Zhang, W. P.; Tian, Z. J.; Lin, L. W. *Microporous and Mesoporous Materials* **2009**, *120*, 278-284.

124. Pei, R. Y.; Wei, Y.; Li, K. D.; Wen, G. D.; Xu, R. S.; Xu, Y. P.; Wang, L.; Ma, H. J.; Wang, B. C.; Tian, Z. J.; Zhang, W. P.; Lin, L. W. *Dalton Transactions*, *39*, 1441-1443.

125. Fayad, E. J.; Bats, N.; Kirschhock, C. E. A.; Rebours, B.; Quoineaud, A. A.; Martens, J. A. *Angewandte Chemie-International Edition*, *49*, 4585-4588.

126. Xu, R. S.; Zhang, W. P.; Han, X. W.; Bao, X. H. *Chinese Journal of Catalysis* **2010**, *31*, 776-780.

127. Wheatley, P. S.; Allan, P. K.; Teat, S. J.; Ashbrook, S. E.; Morris, R. E. *Chemical Science* **2010**, *1*, 483-487.

128. Ng, E. P.; Itani, L.; Sekhon, S. S.; Mintova, S. *Chemistry-a European Journal* **2010**, *16*, 12890-12897.

129. Cai, R.; Liu, Y.; Gu, S.; Yan, Y. S. *Journal of the American Chemical Society* **2010**, *132*, 12776-12777.

130. Pei, R. Y.; Xu, Y. P.; Wei, Y.; Wen, G. D.; Li, K. D.; Wang, L.; Ma, H. J.; Tian, Z. J.; Lin, L. W. *Chinese Journal of Catalysis* **2010**, *31*, 1083-1089.

131. Pei, R. Y.; Tian, Z. J.; Wei, Y.; Li, K. D.; Xu, Y. P.; Wang, L.; Ma, H. J. *Materials Letters* **2010**, *64*, 2118-2121.

132. Wei, Y.; Tian, Z. J.; Gies, H.; Xu, R. S.; Ma, H. J.; Pei, R. Y.; Zhang, W. P.; Xu, Y. P.; Wang, L.; Li, K. D.; Wang, B. C.; Wen, G. D.; Lin, L. W. *Angewandte Chemie-International Edition*, *49*, 5367-5370.

133. Ma, Y. C.; Wang, S. J.; Song, Y.; Xu, Y. P.; Tian, Z. J.; Yu, J. Y.; Lin, L. W. *Chinese Journal of Inorganic Chemistry* **2010**, *26*, 1923-1926.

134. Wragg, D. S.; Fullerton, G. M.; Byrne, P. J.; Slawin, A. M. Z.; Warren, J. E.; Teat, S. J.; Morris, R. E. *Dalton Transactions*, *40*, 4926-4932.

135. Wragg, D. S.; Le Ouay, B.; Beale, A. M.; O'Brien, M. G.; Slawin, A. M. Z.; Warren, J. E.; Prior, T. J.; Morris, R. E. *Journal of Solid State Chemistry*, *183*, 1625-1631.

136. Pei, R. Y.; Tian, Z. J.; Wei, Y.; Li, K. D.; Xu, Y. P.; Wang, L.; Ma, H. J. *Materials Letters*, *64*, 2384-2387.

137. Hoang, P. H.; Park, H.; Kim, D. P. *Journal of the American Chemical Society*, *133*, 14765-14770.

138. Ma, H. J.; Tian, Z. J.; Xu, R. S.; Wang, B. C.; Wei, Y.; Wang, L.; Xu, Y. P.; Zhang, W. P.; Lin, L. W. *Journal of the American Chemical Society* **2008**, *130*, 8120-+.

139. Wragg, D. S.; Slawin, A. M. Z.; Morris, R. E. *Solid State Sciences* **2009**, *11*, 411-416.

140. Oliver, S.; Kuperman, A.; Ozin, G. A. *Angewandte Chemie-International Edition* **1998**, *37*, 47-62.

141. Fayad, E. J.; Bats, N.; Kirschhock, C. E. A.; Rebours, B.; Quoineaud, A. A.; Martens, J. A. *Angewandte Chemie-International Edition* **2010**, *49*, 4585-4588.

142. Xu, R. S.; Zhang, W. P.; Guan, J.; Xu, Y. P.; Wang, L.; Ma, H. J.; Tian, Z. J.; Han, X. W.; Lin, L. W.; Bao, X. H. *Chemistry-a European Journal* **2009**, *15*, 5348-5354.

143. Fieggen, W.; Gerding, H. *Recueil Des Travaux Chimiques Des Pays-Bas* **1971**, *90*, 410-&.

144. Fieggen, W.; Gerding, H.; Nibberin.Nm. *Recueil Des Travaux Chimiques Des Pays-Bas* **1968**, *87*, 377-&.

145. Folting, K.; Streib, W. E.; Caulton, K. G.; Poncelet, O.; Hubertpfalzgraf, L. G. *Polyhedron* **1991**, *10*, 1639-1646.

146. Wengrovius, J. H.; Garbauskas, M. F.; Williams, E. A.; Going, R. C.; Donahue, P. E.; Smith, J. F. *Journal of the American Chemical Society* **1986**, *108*, 982-989.

147. Ropson, N.; Dubois, P.; Jerome, R.; Teyssie, P. *Macromolecules* **1993**, *26*, 6378-6385.

148. Sakthivel, A.; Dapurkar, S. E.; Gupta, N. M.; Kulshreshtha, S. K.; Selvam, P. *Microporous and Mesoporous Materials* **2003**, *65*, 177-187.

149. Majano, G.; Mintova, S.; Ovsitser, O.; Mihailova, B.; Bein, T. *Microporous and Mesoporous Materials* **2005**, *80*, 227-235.

150. Li, Y.; Zhang, W. H.; Zhang, L.; Yang, Q. H.; Wei, Z. B.; Feng, Z. C.; Li, C. *Journal of Physical Chemistry B* **2004**, *108*, 9739-9744.

Chapter 3 - Synthesis and Characterization Techniques

3.1 Synthesis

3.1.1 Synthesis of ionic liquids

Ionic liquids used in this work are synthesized according to literature.[1] 1-alkyl-3-methylimidazolium bromide ([$C_n$mim][Br]) is used directly or as the starting chemical to synthesize ILs with other cations. Steps to synthesize specific ILs are elaborated upon in the following sections.

(1) Synthesis of [$C_n$mim][Br]

The reagents used to synthesize [$C_n$mim][Br] include 1-bromoalkane, 1-methylimidazole and a solvent (such as acetonitrile and methanol). They are bought from the website of Fisher Scientific and their labeled impurities are 99+%. 1-bromoalkane and 1-methylimidazole are distilled before use in order to ensure purity. Then they are mixed by a molar ratio of 1 methylimidazole : 1.05 bromoalkane : 5 solvent in a 500 mL round bottom flask and blow argon into the flask before it is sealed by a cap. Excess solvent is added in order to help control the temperature and excess bromoalkane is used to ensure the complete consumption of methylimidazole which is not easy to separate from the final product because its melting point is 198 ^{o}C. When melting point of 1-bromoalkane increases as alkyl chain in 1-bromoalkane increase, the molar ratio of methylimidazole and bromoalkane used in reaction approaches 1:1. The mixture in the round bottom flask is then stirred at 40 ^{o}C for several days depending on the length of alkyl chain in 1-bromoalkane. For example, [C_2mim][Br] needs one or two days and [C_4mim][Br] needs three to four days. The process to synthesize [$C_n$mim][Br] is illustrated in Figure 3.1.

After the synthesis is complete after several days, the mixture is first dried by a rotary evaporator for four hours to evaporate most of the solvent in the mixture. Then the flask with mixture is then placed on a manifold with strong pump and vacuum trap. The drying process takes about 4 days under vacuum. At the same time, the flask is kept in a water bath at a higher temperature, first at 50 ^{o}C and then increased to 65 ^{o}C. Temperature is maintained below 70 ^{o}C since imidazolium can begin to decompose at a temperature higher than 70 ^{o}C.

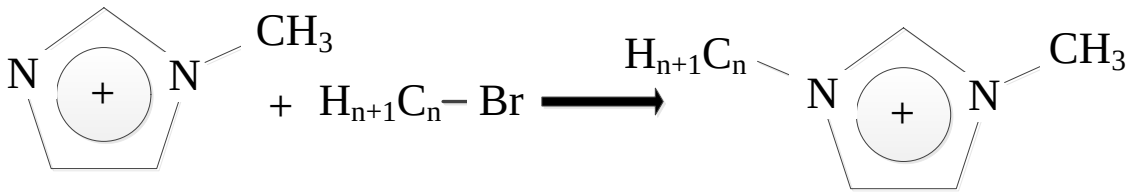

Figure 3.1 Illustration of process to synthesize [$C_n$mim][Br].

(2) Synthesis of [C_4mim][Tf_2N]

[C_4mim][Tf_2N] is synthesized by metathesis reaction. First, [C_4mim][Br] is mixed with two times DI water, and lithium bis(trifluoromethanesulfonyl)imide is mixed with two times DI water separately. The two mixtures are then poured into a separatory funnel and shaken vigorously for 30 minutes. The new mixture is left overnight and will split into two layers with the bottom [C_4mim][Tf_2N] and top water/LiBr. The dense IL is removed and washed with water. It needs to be washed at least 10 times. In order to test if all of the bromide has been separated from [C_4mim][Tf_2N] , a little portion of [C_4mim][Tf_2N] is then mixed with silver nitrate solution in order to determine if more washes are needed. If there is precipitate, more washes are needed until there is no precipitate.

(3) Purification of ILs

In order to remove color and impurities of the synthesized ionic liquids, two processes are followed after the synthesis. First, ionic liquids is mixed with 10 % granular activate carbon and stirred for 24 hours. After the carbon is filtered out, ionic liquid is run through an acidic activate aluminum oxide column. After these processes, these ionic liquids changes from clear yellow liquid to a clear white liquid or a clear yellowish liquid.

3.1.2 Synthesis of zeolites

3.1.2.1 Hydrothermal synthesis of zeolites

Zeolites are synthesized in a standard way.[2] First, precursors (such as $Al(OiPr)_3$, H_3PO_4, SiO_2) are added into water. The mixture is then added by structure directing agent and base (such as KOH and NaOH) if necessary. The mixture is then stirred at room temperature for two hours until a homogenous gel is formed. The mixture is then charged into a liner and the liner is then put into an autoclave. After the autoclave is well sealed, it is put into a conventional oven and heated at 150 ^{o}C for several days. The powders synthesized in the liner is then filtered and washed with water and acetone. The powders are dried at 50 ^{o}C for 12 hours and are ready to be characterized by different techniques.

3.1.2.2 Ionothermal synthesis of zeolites

The ionothermal synthesis of microporous aluminophosphates (AlPOs) uses a process very similar to the traditional hydrothermal techniques,[2] with the primary difference being the solvent (IL vs water) used. A schematic illustration of the procedure to produce microporous materials in ILs is shown in Figure 3.2.

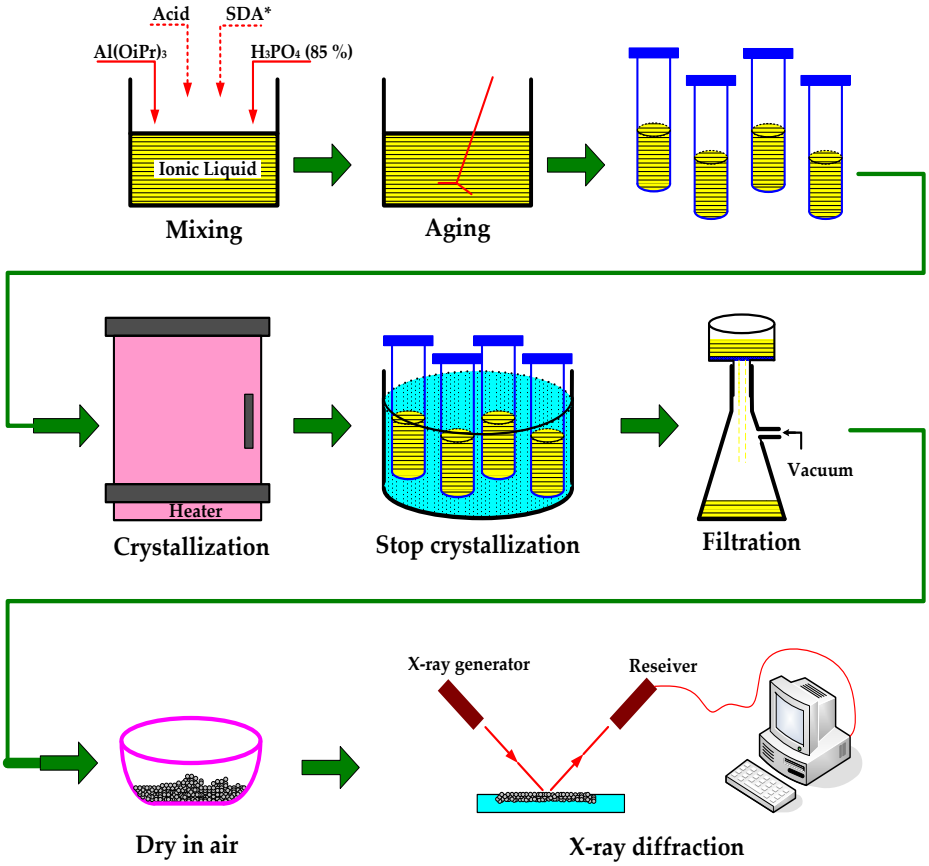

Figure 3.2 Schematic illustration of the procedure to synthesize microporous materials.

First, the precursors ($Al(OiPr)_3$, acid, SDA and phosphoric acid) are added into the ionic liquid. Then the mixture is stirred at a high temperature (usually 100 ^oC) for 40 minutes. After mixing the homogeneous gel is charged into several liners and put into an oven which is set at an elevated temperature (100 ^oC, 150 ^oC, or 190 ^oC). After heating for several hours or several days, the liners are quenched into cold water to stop crystallization of materials inside the liners. Then the powders are filtered and washed with water and acetone. The white powders left on the filter paper are dried on a crucible for several hours at 50 ^oC. The final dry powders are scanned by XRD and the framework synthesized is determined. Each recipe to synthesize AlPO is used at least two times to make sure the result is reproducible.

3.1.2.3 Calcination of zeolites

During the synthesis process, structure directing agents and some guest molecular are left in the pores of zeolites. They interact with zeolite frameworks through hydrogen bonding or van der Waals' force and could not be washed away by water and acetone. As a result, calcination is needed to decompose and oxidize the organic molecules left in the pores.

Zeolites are calcined in an oven heated at 500 ^oC for 5 hours. This process is done in air. After calcination, the powders are scanned by XRD again to ensure no decomposition of frameworks by this method.

3.2 Characterization Techniques

After ILs and zeolite are synthesized, they need to be characterized in order to check purity and properties. These techniques will be introduced in detail in the following sections.

3.2.1 Characterization of ILs

3.2.1.1 Nuclear magnetic resonance spectroscopy (NMR)-liquid NMR

Liquid NMR is used to identify the structure of ILs synthesized. Each IL has a specific NMR pattern. Pure IL shows no extra peak than a standard NMR pattern of the same IL.

The first commercial NMR instrument was Varian HR-30 which was installed in 1952 at the Humble Oil Company in Baytown, Texas. Since then, it has developed quite rapidly. If a nucleus of some combined atoms in a molecular is located in a magnetic field, it absorbs radiowaves. Radiowaves are low energy electromagnetic radiation which are too small to vibrate, rotate, or electronically excite an atom or molecule, however, it can affect the nuclear spin of atoms. As a result, spinning nuclei can absorb radiofrequency radiation and change the direction of the spinning axis. If any nucleus possesses a magnetic moment, the atom in a molecule will have a different absorption frequency also called resonance. Overall, NMR is used to investigate the shape and structure of molecules. Affected by different chemical environments of the nuclei in a molecule, the nuclei will show peaks at different frequency, thus the structure of the molecule can be determined. In addition, if the structures of molecular in a sample are known, from area of peaks shown in NMR pattern, the amount of the molecule could be calculated. As a result, NMR is both a qualitative and quantitative instrument. The set-up of a liquid NMR is shown in Figure 3.3.[3]

The nuclei which could be analyzed by NMR must have a nonzero spin quantum number and have a magnetic dipole moment. They include but not limited to ^{13}C, ^{17}O, ^{1}H, ^{2}H, ^{3}H, ^{19}F, ^{31}P, ^{29}Si, ^{33}S and ^{35}S.[3]

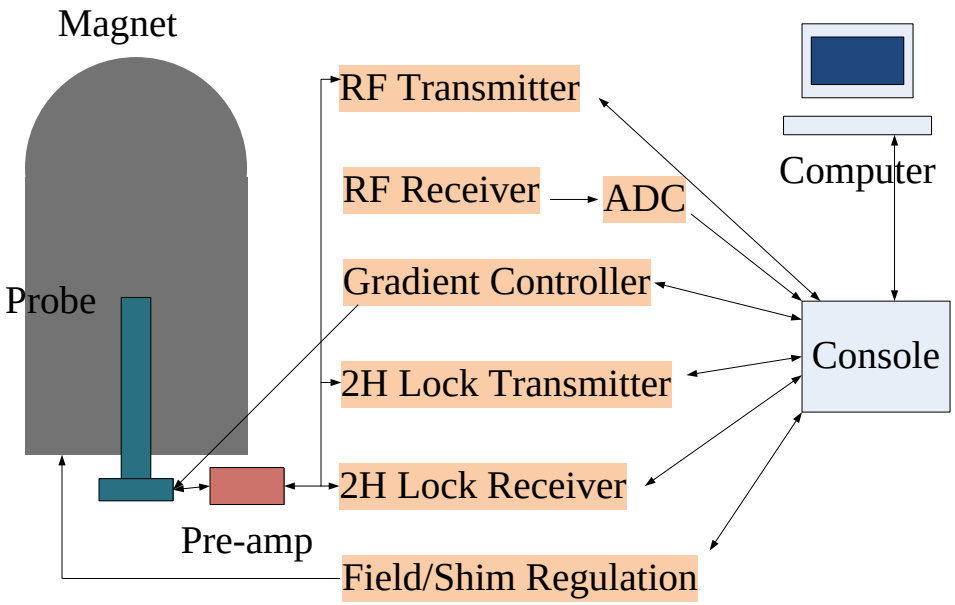

Figure 3.3 Schematic illustration of liquid NMR system.[3]

The type of NMR used in this dissertation is INOVA 400. It operates at 400 MHz frequency and is only useful to test liquid samples. This instrument is equipped with pulse field gradients and a variable temperature controller. But most of the tests in this project are done at room temperature. Chloroform-d is used as the solvent to test samples. Each ionic liquid synthesized is analyzed by ^{1}H NMR to confirm its chemical structure and compare the NMR pattern with literature.

Typically, to aid in the NMR analysis, a deuterated solvent such as deuterated-chloroform, is added to the solution to dissolve the analyzed chemicals of interest. Since deuterated solvent does not show peaks in NMR pattern, it does not interfere the NMR patterns of chemicals interested.

3.2.1.2 Karl-Fischer titrator (KFT)

In this project, coulometric KFT is used to measure the water content in ionic liquids.

Karl Fischer titration is a direct and easy method to measure the concentration of water in a solution. It is especially useful for samples with low water concentration (< 1 %). Water-containing samples are added to an anhydrous methanol solution containing iodine, sulfur dioxide and excess pyridine. The presence of water causes the iodine and sulfur dioxide to react. By measuring how much iodine is consumed during titration, the water content can be calculated.[4]

$$I_2 - Pyr + SO_2 - Pyr + H_2O \rightarrow SO_3 - Pyr + 2PyrH^+ I^- \qquad \textbf{Equation 3-1}$$

where Pyr is pyridine. $SO_3 - Pyr$ is then reacted with methanol to form methylsulfate anions.

$$SO_3 - Pyr + CH_3OH \rightarrow PyrH^+ CH_3SO_4^- \qquad \textbf{Equation 3-2}$$

From equations 3-1 and 3-2, it can be seen that reacting one mole of I_2 requires one mole of water. The method to detect the endpoint is done electrometrically. [4]

There are basically two types of KFT: coulometric KFT and volumetric KFT. Coulometric KFT measures the amount of water which undergoes a reaction at an electrode by measuring the amount of electricity necessary to finish the complete reaction, while volumetric KFT measures the volume of a standard solution that must be added to react with the water present. Coulometric KFT is more accurate and does not need to prepare standard solution, but it is only suitable for

low water content solution and is more expensive than volumetric KFT. As a contrary, volumetric KFT can be used to measure solution whose water content is from 10 ppm up to 100 %.[4]

The KFT used in this project is a coulometric KFT made by Denver Instrument, Inc. The model is 270, called PH · ISE · Conductivity titration controller. The weight of IL injected into KFT is measured and input into the KFT monitor. At the titration endpoint, water content is given directly to the user in the units of ppm.

3.2.2 Characterization of zeolites

3.2.2.1 X-ray diffraction (XRD)

X-ray diffraction is used extensively in this project to determine the structures of frameworks synthesized.

X-ray diffraction or X-ray diffractometry (XRD) is a common technique to analyze the solid crystalline or semicrystalline materials. Inorganic or organic materials with different structures of unit cell have distinctive XRD standard patterns. After analyzing the material with XRD, the spectrum is compared with standard pattern and conclusions such as crystallinity and structures of the substances analyzed could be obtained. XRD can not only give the qualitative and quantitative identification of the molecules in pure powders, but also mixtures of crystalline powders.[3]

The main components of XRD include an X-ray tube which generates X-ray, a sample specimen, and a detector which rotates in an arc. The schematic illustration of XRD is shown in Figure 3.4. Manufacturers of X-ray diffraction have different designs. Some fix the position of sample specimen and rotate both of X-ray source and detector simultaneously. Some fix the position of X-ray source, but rotate sample specimen and detector at the same time. The principles are the same. When the angle between sample and the source is θ degree, angle between detector and plane of x-ray source is 2θ degree.[3]

Sample preparation is particularly important for XRD identification of powder samples. In order to prevent particles from orienting in the same direction, the samples are ground with pestle and mortar into extremely fine powders and pressed into a sample holder to form a flat

surface. The fine powders are tens of micrometers in size. If the particles are not prepared properly and oriented in the same direction, some of the peaks will be lost in the XRD pattern. Samples should be packed at the same height with the height of sample holder since any change to the height of samples will shift the locations of peaks.[3]

The XRD used in the lab is Rigaku MiniFlex II benchtop XRD system. Its X-ray source is fixed; only sample holder and detector rotate in the process of scanning powders. Typical range of 2θ is from 5 degrees to 50 degrees. Scan speed is 2 degrees/minute. As a result, one XRD spectrum is achieve within in 30 minutes. For powders whose XRD patterns are not with sharp peaks and with background of high intensities, slower scan speed is used, 0.25 degree/minute. This XRD use Cu to generate X-ray with 30 kV and 15 mA. The sample holder is 0.5 mm glass plate. The DivSlit is 1.25 degree, SctSlit is 1.25 degree, RecSlit is 0.3mm and Monochro RS is 0.8mm.

Identification of frameworks is done by software called PDXL. This software is used to subtract background and match XRD pattern of the specimen with standard XRD patterns of other crystals. XRD patterns of zeolites with different unique structures are available through the international zeolite association (www.iza-structure.org/databases/).

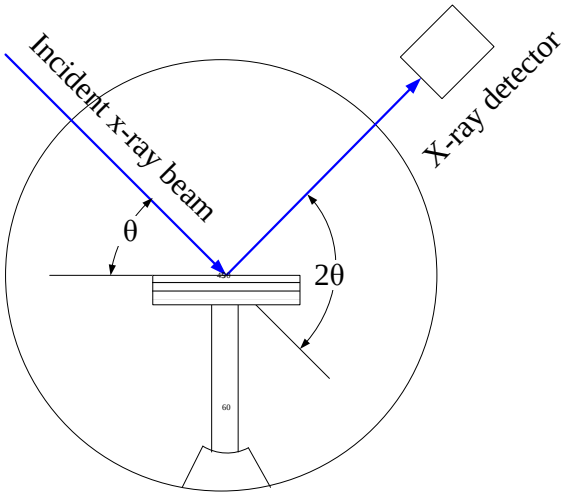

Figure 3.4 Schematic illustration of XRD.[3]

3.2.2.2 BET

In order to measure the surface area of zeolite powders synthesized, a BET instrument is used. This instrument measures surface area and pore distribution of porous materials by gas adsorption on a cold sample. BET is named after Stephen Brunauer, Paul Emmett, and Edward Teller, who published this method first in an article in 1938. This technique is the standard method to test surface area of a solid. BET theory assumes that the surface of absorbent is uniform and the energy of each absorption center is the same. The intermolecular force between adsorptives is negligible. At a certain condition, rates and adsorption and desorption are the same, so an equilibrium is established. The most common absorptive is nitrogen and absorption temperature is fixed at 77 K using a cold reservoir or liquid nitrogen. Cold temperature could prevent chemical adsorption. Relative pressure is fixed at 0.05-0.35. In this range, only one-layer absorption will occur, which is preferred for BET technique. [5]

BET equation is

$$\frac{P}{X(P_0 - P)} = \frac{1}{X_m C}\left[1 + \frac{P}{P_0}(C-1)\right] \qquad \textbf{Equation 3-3}$$

where P_0 is the saturation or equilibrium pressure of adsorbate, P is the measured partial pressure of adsorbate, C is a constant relating to the adsorption enthalpy, X is the mass of gas adsorbed at pressure P, and X_m is the amount of gas adsorbed to form a saturated surface of one atomic layer thick.[5]

X is measured at different P, a line will be obtained by plotting $\frac{P}{X(P_0 - P)}$ versus $\frac{P}{P_0}$.

Then

$$X_m = \frac{1}{\text{slope of the line} + \text{intercept of the line}} \qquad \textbf{Equation 3-4}$$

Finally the specific surface area of a sample is:

$$S_{BET} = \frac{X_m N_0 A_0}{WM} \qquad \textbf{Equation 3-5}$$

where M is the molecular weight of the adsorbate, N_0 is the Avogadro's number and W is equal to the weight of the sample. [5]

The BET analyzer is an AUTOSORB-1. It is used to measure the surface area of porous aluminophosphates before and after calcination. Before the measurement, all of the samples are loaded into an outgassing station, which heats the sample at low pressure to remove adsorbed molecules in the samples. When samples are cooled down to room temperature after the outgassing process, samples are analyzed using the AUTOSORB-1. Nitrogen is the adsorbing gas to test surface area of zeolites. The analysis uses multipoint 11 point BET method. After weight of the desorbed zeolite is entered into the computer, AUTOSORB-1 will give the surface area of zeolite automatically after several hours.

3.2.2.3 Scanning electron microscope (SEM)

SEM is used to investigate surface topography, morphology, compositions or particles sizes of zeolites and their precursors. It has a higher magnification and greater depth of field than conventional microscope. It can image bulk samples and can produce images of the 3-D structure of the tested samples. Schematic diagram of a scanning electron microscope is shown in Figure 3.5. A high voltage is applied to a hot tungsten filament, and then an electron beam is produced and delivered by an electron gun to magnetic field lenses, which focuses the electron beam to a spot of 100 nm or less on the sample. The primary electron beam will excite the secondary electrons and makes them emit from the sample surface. By detecting these secondary electrons, SEM produces the images of samples. [6]

The SEM used in this project is a Hitachi S-3500 scanning electron microscope. It is used to detect morphology of zeolites and arrangement of silica particles which are stabilized in ionic liquids. Probe current is kept at 20 kV and magnification is adjusted to enlarge zeolite powders from several micrometers in diameter to several nanometers in diameter.

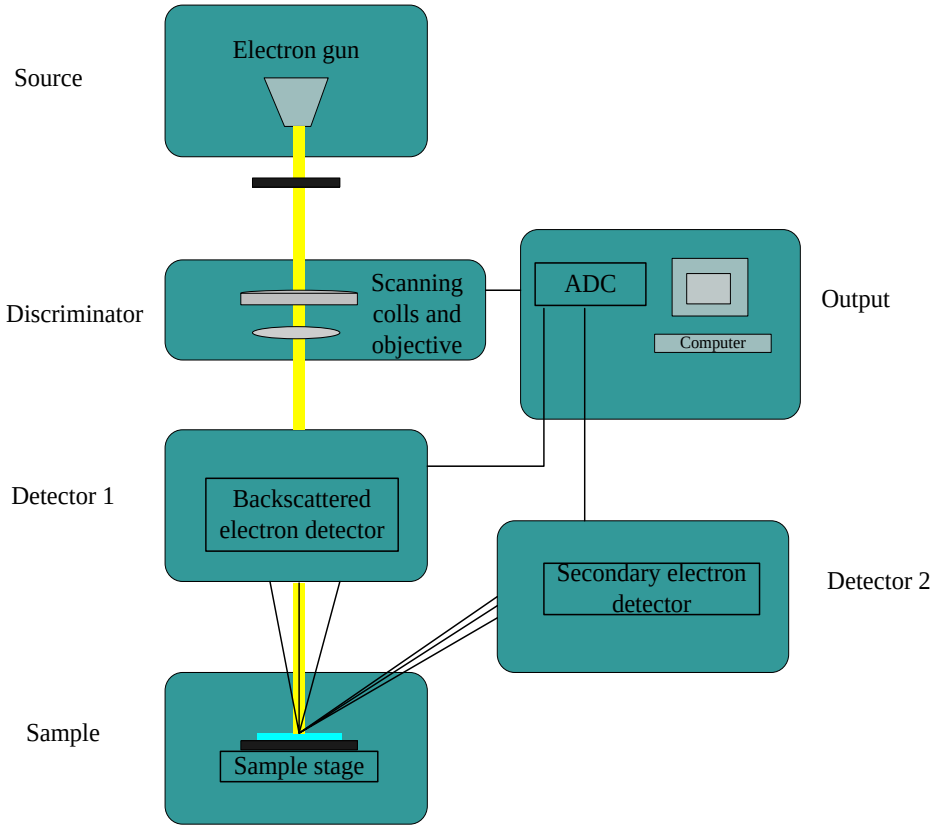

Figure 3.5 Schematic illustration of SEM.[6]

3.3 Other Techniques

3.3.1 Techinque to test solubility of precursors

3.3.1.1 Centrifuge

Centrifuge is used to separate the un-dissolved particles from a mixture of IL & $Al(OiPr)_3$. After centrifugation, the top layer of the solution is clear with dissolved $Al(OiPr)_3$ and the un-dissolved $Al(OiPr)_3$ is left at bottom. Then the concentration of Al in the top lay could be analyzed in order to find the equilibrium concentration of $Al(OiPr)_3$ in IL at different temperatures.

Model of centrifuge used in this project is Eppendorf 5810 R. All of the samples are centrifuged for 3 hours (1.5 hours for 2 times due to the limitation of the machine) at 3000 rpm. Temperatures are set either at 20 ^oC or 40 ^oC depending on the requirement of the experiment.

3.3.1.2 Atomic absorption spectrometry (AAS)

Atomic absorption spectrometry is used to analyze the concentration of $Al(OiPr)_3$ in ionic liquids. After a mixture of $Al(OiPr)_3$ and IL are centrifuged at different temperatures to remove the undissolved $Al(OiPr)_3$ powders, the concentration of $Al(OiPr)_3$ in ILs are analyzed by AAs. AAS is an elemental analysis technique to provide the concentration information of about 70 elements in all kinds of samples. Most all of these elements are metal or metalloid elements, since nonmetal elements require great amount of energy to reach the first excited state, which could not be reached by normal UV radiation. The principle of AAS involves first transforming solid or liquid samples into gas phase, then changing the gas phase samples into free atoms by an "atomizer" at higher temperature, finally exciting free atoms from ground state to a higher state by absorbing a defined quantity of energy. Figure 3.6 shows a schematic block diagram of the instrumentation used for AAS.[3]

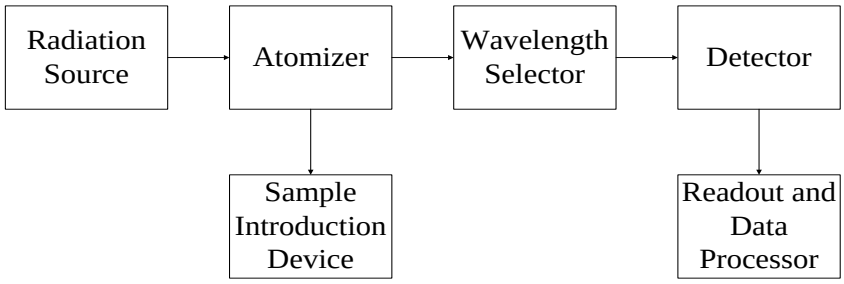

Figure 3.6 Schematic block diagram of the instrumentation used for AAS.[3]

Several standard solutions with known concentrations need to be prepared and tested by AAS in order to set up a relationship between absorption and concentration. This relationship is used to make a calibration curve with x-axis to be concentration and y-axis to be absorbance. As a result, given an absorbance, concentration can be calculated from this curve. The samples to be tested are first diluted in order to have concentration in the range of samples used to make calibration curve. Then they are analyzed by AA which shows their absorbance. The absorbance is used to calculate concentration of samples using the calibration curve. One of the calibration curves is shown in Figure 3.7.

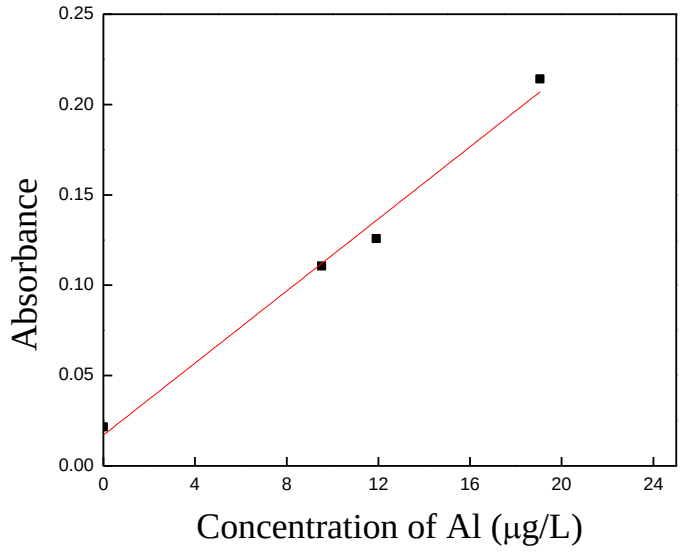

Figure 3.7 One of the calibration curves used to calculate concentration of diluted samples.

The AAS used in this dissertation is AA 240 manufactured by Varian, Inc with a GTA 120 graphite tube atomizer and a cold vapor generation accessory Varian Model VGA65. When multiple samples are analyzed at the same time, a programmable sample dispenser is used. Before the samples are added to the sample holder, they are diluted. If the concentration of the diluted sample is out of the concentration range of calibration curve, they will be diluted automatically by the machine. The absorbance of the sample is given after the analysis and concentration can also be calculated from the calibration curves by the machine. AAS is only used to analyze concentration of aluminum in this project. Current of Al lamp is 10.0 mA, wavelength is 385 nm, and slit is 0.5 nm.

3.3.1.3 Inductively coupled plasma optical emission spectrometer (ICP-OES)

Inductively coupled plasma optical emission spectrometer (ICP-OES) is used to detect the concentration of phosphorus in ionic liquids. This technique is very sensitive and could determine a range of metals and non-metals. ICP-OES is composed of two parts. The first one is inductively coupled plasma which could produce ions of the detected elements and the second one is optical emission spectrometer to detect the ions.

Similar to the operation of AAS, firstly, several standard solutions with known concentrations need to be prepared and tested by ICP-OES to set up a relationship between absorption and concentration. This relationship is then used to make a calibration curve with x-axis to be concentration and y-axis to be absorbance. The samples to be tested are first diluted in order to have concentration in the range of samples used to make calibration curve. Then they are analyzed by ICP-OES which shows their absorbance. The absorbance is used to calculate concentration of samples using the calibration curve.

The model of ICP-OES used in this project is ICP-OES 730, manufactured by Varian Inc. It is used at a wavelength of 178.222nm.

3.3.1.4 Cone and plate rheometer

In order to test the maximum concentration of silica particles in ionic liquids and analyze the final states of systems, cone and plate rheometer is applied to test viscosities of the systems.

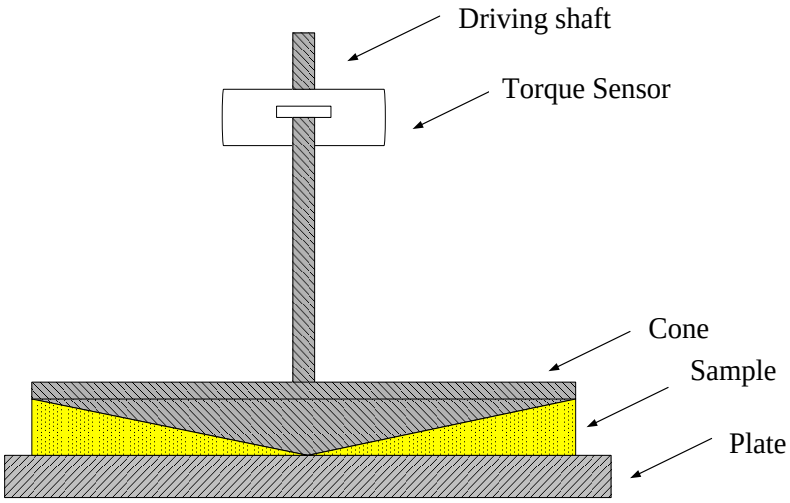

Figure 3.8 Schematic diagrams of the cone and plate system.[8]

Cone and plate rheometer is used to measure the rheology of the fluid. It measures how fluid, suspension or slurry flows in response to applied forces. Non-newtonian fluids could not be represented only by a single value of viscosity, because viscosity of non-newtonian fluid is also dependent on shear rate or shear rate history. The set-up of a cone and plate rheometer is shown in Figure 3.8.[7]

The cone and plate rheometer is composed of a flat plate and a cone rotates on the plate. There is a small gap between the flat plate and a cone (commonly tens or hundreds of micrometers). The fluid or suspension tested is in the gap. There is a force applied on the cone for it to rotate and a torque sensor to record the magnitude of the force. Shear rate of the cone does not change since

$$\gamma = \frac{r\Omega}{r\theta} = \frac{\Omega}{\theta}$$

Equation 3-6

where Ω is the linear velocity, θ is the angle between plate and cone, and r is the distance between the axis of rotation to a single point of the cone. In another word, the shear rate is uniform across the gap. Then viscosities can be calculated from torque and shear rate. The change of viscosity with time is obtained.[7]

Rheological measurements of the concentrated samples are performed by using a Bohlin CVOR 150 rheometer (Malvern Instruments). The distance between cone and plate is set to 500 μm for all measurements. Experiments are conducted under steady shear flow at 80 ^{o}C. Shear rates range from 10 to 240 s-1, at 20 s-1 increment. Data are recorded after the machine runs 100 s. All experiments are done in duplicate, and average values are reported.

3.3.1.5 Dynamic light scattering (DLS)

In order to understand the status of silica particle after it is stabilized in ionic liquid, dynamic light scattering is used to determine the particle size.

Dynamic light scattering is a technique to measure hydrodynamic diameter of particles from the dynamic changes of the scattered light intensity. "The intensity of the scattered light by an assembly of particles is measured at a given angle as a function of time. The Brownian motion of the dispersed particles determines the rate of change of the scattered light intensity."[9] It measures diffusion coefficient of the particles and from it, calculate particle size by Stokes-Einstein equation. The concentration of particles in liquid should be extremely low in order to avoid particle-particle interactions and multiple scatterings.[9] Typical set up of a dynamic light scattering instrument is shown in Figure 3.9.

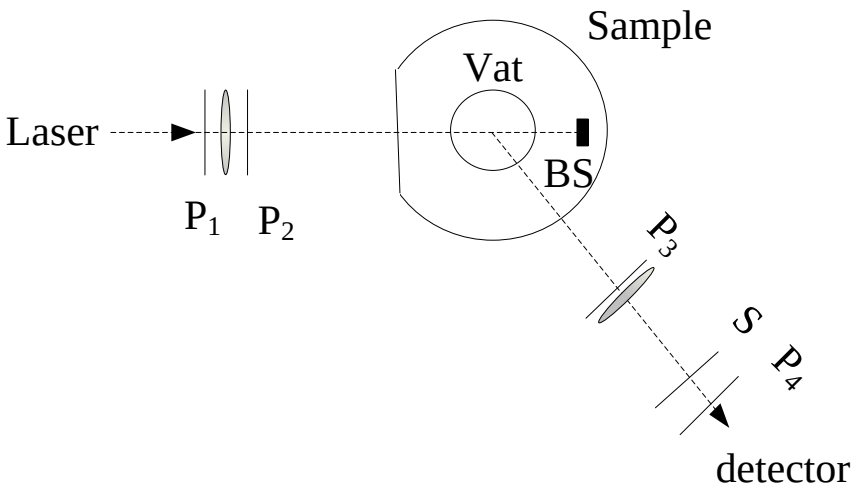

Figure 3.9 Typical set-up of a dynamic light scattering instrument.[9]

After the scattered light is measured over a time, a graph of scattering can be achieved. A general graph is shown in Figure 3.10.

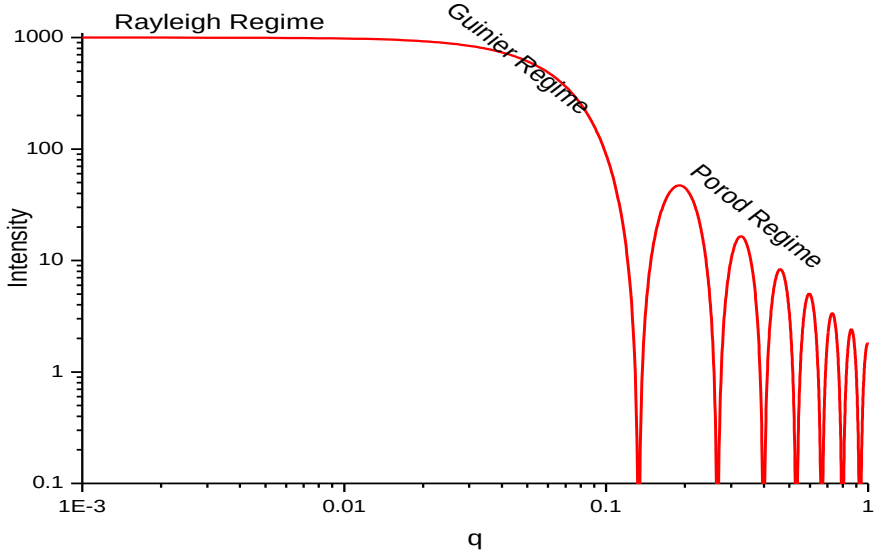

Figure 3.10 A typical scattering pattern given by DLS.

The graph of scattering can be divided into three regimes: (1) Rayleigh regime: when the particle radius is smaller than wavelength of light. (2) Guinier regime: when the product of particle radius and q is small. (3) Porod regime: when the product of particle radius and q is very

large. The regime of Guinier is used to calculate the silica particle size in small range of q, where $q = \frac{4\pi}{\lambda}\sin(\theta)$, unit is length^{-1} In the Guinier regime: I(q) is proportional to $1 - \frac{1}{3}q^2 R_g^2$,and

$$I(0)/I(q) \approx 1 + \frac{1}{3}q^2 R_g^2 \qquad \textbf{Equation 3-7}$$

If a graph of I(0)/ I(q) and q^2 is made, a line is obtained, the slope of which is equal to $\frac{1}{3}R_g^2$. Figure 3.11 is a typical linear line drawn from the data in the regime of Guinier. I(0) is the all of the scattered lights are in the same direction, which is the value in the Rayleigh regime and R_g is a radius of gyration. The relationships between radius and R_g are different according to the shape of the particle. For spherical particles, $a = 0.77R_g$. Then the radius of the particle can be calculated.

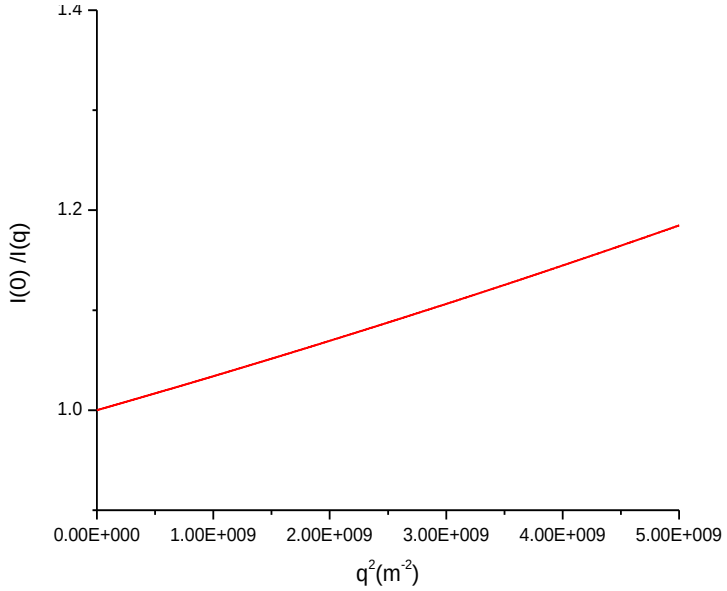

Figure 3.11 A typical linear line drawn from the data in the regime of Guinier.

DLS is performed at room temperature with an argon ion laser operating at 488 nm. It uses an ALV 5000 as dynamic light scattering correlator. The sample contains silica particles suspended in ionic liquid (5 wt %).

3.3.2 Technique to test interaction between IL/precursors

3.3.2.1 Solid NMR

In order to investigate interaction between IL/precursors, mixture of ILs with precursors are prepared and scanned first by liquid NMR. However, liquid NMR shows a very broad peak which is not useful at all. As a result, another instrument is used.

The phenomenon that solid has broad peaks due to different orientation is called chemical shift anisotropy. A technique is developed to avoid chemical shift anisotropy. It is theoretically calculated and experimentally proved that by spinning the sample at an angle of 54.76 ^{o}C, instead of 90 ^{o}C as in liquid NMR, the chemical shift anisotropy could be eliminated and narrow line spectra could be obtained. Solid NMR has special probes which automatically position the sample at an angle of 54.76 ^{o}C, thus solid NMR could be used to analyze solid or highly viscous samples.[3]

Solid state NMR spectra were acquired on a Bruker Avance III 400 spectrometer (Bruker Biospin, Billerica, MA) operating at 400.1 MHz for ^{1}H and 104.26 MHz for ^{27}Al. The probe is a Bruker 2 channel probe with a 4 mm spinning system. The spectrometer setup used $Al(OH)_6$ as a secondary external chemical shift reference at 0 ppm. Each sample was packed into a Kel-F insert and inserted into a 4.0 mm zirconia rotor (Bruker Biospin, Billerica, MA). Magic angle spinning used a sample spinning rate of 4 kHz. Excitation times of 0.60 us were used for direct excitation. A pulse delay of 1.0 second was used. The spectral width was 50 kHz and the acquisition time was 20 ms. Proton decoupling was performed with a proton decoupling field of 64 kHz. Each data set is the sum of 14400 transients. A spectrum was acquired for each sample at room temperature and at 70 ^{o}C.

Since a few samples are liquid at room temperature which could spill from the probe when it is spun at a high speed in solid NMR, a special wax is used to seal the samples at the top and bottom of the sample. All of the samples are tested both at 23 ^{o}C and a higher temperature (either 70 ^{o}C or 80 ^{o}C).

3.4 References

1. Barbara, K. *Ionic liquids*; Springer: Germany, 2009.
2. Cundy, C. S.; Cox, P. A. *Chemical Reviews* **2003**, *103*, 663-701.
3. Robinson, J. W.; M., S. F. E.; Frame II, G. M. *Undergraduate Instrumental Analysis*, 6 ed.; Marcel Dekker, Inc.: New York, 2005.
4. Wrolstad, R. E.; Decker, E. A.; Schwartz, S. J.; Sporns, P.; Decker, E. A.; Schwartz, S. J. *Handbook of Food Analytical Chemistry, Water, Proteins, Enzymes, Lipids, and Carbohydrates*; John Wiley & Sons, Inc.: Hoboken, New Jersey, 2004.
5. Randall, M. G.; Seong, J. P. *Handbook of Mathematical Relations in Particulate Materials Processing*; John Wiley & Sons, Inc.: Hoboken, New Jersey, 2008.
6. Mcmahon, G. *Analytical Instrumentation A Guide to Laboratory, Portable and miniaturized Instruments*; John Wiley & Sons Ltd: Chichester, West Sussex, England, 2007.
7. Tadros, T. F. *Colloids in Paints*; WILEY-VCH Verlag GmbH & Co.: Weinheim, 2010.
8. Lipták, B. G. *Instrument Engineers' Handbook: Process measurement and analysis*, 4 ed.; CRC Press LLC.: Boca Raton, Florida, 2003.
9. Merkus, H. G. *Particle Size Measurements: Fundamentals, Practice, Quality*; Springer Science+Business Media B. V.: Dordrecht, 2009.

Chapter 4 - Solubility and Stability of Precursors in Ionic Liquids

4.1 Influences of Side Chain Length of 1-Alkyl-3-methylimidazolium Bromide on Silica Saturation

4.1.1 Introduction

Room temperature ionic liquids (RTILs), a group of novel solvents, have received significant attention in the last 20 years. In recent work, ionic liquids have been utilized in the synthesis of molecular sieves, taking advantage of the RTIL thermal stability and negligible vapor pressure.[1-3] A molecular sieve is a material containing tiny pores of a precise and uniform size. They can be used as absorbents, desiccants, water softeners, reaction media, etc.[4-7] Molecular sieves are commonly synthesized hydrothermally, which means that in order to get crystals of molecular sieves, the mixture of precursors, water, structure directing agent, and mineralizing agent needs to be heated at an elevated temperature.[8, 9] A challenge with this method results since the reaction temperature is typically above the boiling point of the solvent (i.e. water), thus necessitating the use of a pressurized reaction vessel. However, if ionic liquids are substituted as the solvents, molecular sieves can be synthesized at ambient pressure. Morris and coworkers have published several papers on the synthesis of aluminophosphates (AlPOs), a group of molecular sieves, in imidazolium based ionic liquids.[2, 3, 10, 11] In these studies, the ionic liquids not only served as the reaction solvent, but the ILs also served as structure directing agents (SDA), which play a significant role in determining the final zeolite structure. These systems generated several new framework structures. The successful synthesis of these AlPOs suggests the possibility of synthesizing silica-based zeolites, another group of molecular sieves, in ionic liquids.

It has been only in the recent literature that researchers are beginning to report applications of ionic liquids with silica-based advanced materials. For example, Itoh and coworkers developed an electrochemical light-emitting gel using a ruthenium complex, an ionic liquid, and fumed silica nanoparticles. The gel produced can be used in flexible displays, three-dimensional displays, and other lighting applications.[12] Other groups have synthesized silica xerogels with highly distinct morphologies in the presence of ionic liquids.[13, 14] Our group recently reported

the synthesis of porous silicate materials in the presence of ionic liquids and similar molten salts.[15] Watanabe and co-workers have been one of the only groups to consider the behavior of silica particles in ionic liquids.[16, 17] They investigated colloidal stability and rheology of the dispersions of hydrophilic and hydrophobic silica nanoparticles in different ionic liquids.[16, 17] However, there is still a lack of systematic studies investigating the saturation solubility of silica as a function of ionic liquid properties. In this work, we report results on the solubility of fumed silica particles in ionic liquids and the influence of cation alkyl-chain length on the solubility.

4.1.2 Experiment

4.1.2.1 Ionic liquids

The ionic liquids used in this paper are of the family 1-alkyl-3-methylimidazolium bromide [$C_n$mim][Br] where n = 2, 4, 6, 8, 10, and 12. Their names and abbreviations are listed in Table 4-1. These ILs were selected as both [C_2mim][Br] and [C_4mim][Br] have been successfully used in the synthesis of zeolitic molecular sieves.[2, 3, 10]

Each [$C_n$mim][Br] was synthesized in the lab according to methods reported in the literature.[18] This typically involves reacting 1-methylimidazole and bromoalkane in acetonitrile for 2-8 days and drying the mixture for another 3 days. All of the reactants are distilled before the reaction to ensure the purity of ionic liquids. The products were passed through columns of granular activated carbon and also acidic activated aluminum oxide column to remove color. Before each trial, the ionic liquid was dried for 6-12 hrs at 60 ^{o}C – 100 ^{o}C to reduce the water content below 200 ppm, which was tested by Karl-Fischer titration.

Table 4-1 Ionic liquids used.

Name of ionic liquids	*Abbreviation*
1-ethyl-3-methylimidazolium bromide	[C_2mim][Br]
1-butyl-3-methylimidazolium bromide	[C_4mim][Br]
1-hexyl-3-methylimidazolium bromide	[C_6mim][Br]
1-octyl-3-methylimidazolium bromide	[C_8mim][Br]
1-decyl-3-methylimidazolium bromide	[C_{10}mim][Br]
1-dodecyl-3-methylimidazolium bromide	[C_{12}mim][Br]

4.1.2.2 Silica source

Syloid 63FP (from GRACE Davison Company) was the source of silica used in this work. Syloid 63 is pure, fumed silicon dioxide and has been used as the silica source for the hydrothermal synthesis of silica-based zeolites. Silica particles were dried at 100 ^{o}C for 2 hrs and grounded into fine power. The average diameter of single silica particle is 9 μm, which is confirmed through SEM analysis.

4.1.2.3 Determination of the saturation point

The saturation point of the silica in the ionic liquid was determined gravimetrically by slowly adding the silicon dioxide powder in approximately 0.05 g increments to the initial 5 g sample of ionic liquid. The silica was mixed until fully dissolved in the ionic liquid (i.e. became a homogenous clear solution) before continuing with subsequent additions. The viscosity of the solution would increase until the saturation point was reached and the SiO_2/IL mixture became a gel. At this point, any additional silica would just remain in a second solid phase. All measurements were made at 80 ^{o}C, which is above the melting points for all of the ILs used.

4.1.3 Results and discussion

4.1.3.1 Solution behavior

The saturation solubility of silicon dioxide particles was measured in six ionic liquids. Table 4-2 summarized the results in terms of mole fraction and weight percent. In each case, a rather large amount of silicon dioxide could be added to the ionic liquid before the saturation/gelation point was reached. The largest amount of silica could be added to [C_8mim][Br]: a ratio of 3.58 moles silicon dioxide to every 1 mole ionic liquid (equivalent to 44 wt% SiO_2 in [C_8mim][Br]**)**. This ability of ionic liquids to stabilize SiO_2 particles in such high concentrations bodes well for the use of ILs in the synthesis of silica-based materials. Preliminary characterization efforts on dilute SiO_2/IL solutions dynamic light scattering indicate that the size of the silica particles usually remains unchanged; however these investigations are still ongoing. These early DLS results suggest that these saturated gels are stable colloid systems.

Table 4-2 Silica saturation solubility result

Ionic liquid	*Mole ratio of silica to IL*	*Mole fraction (%)*	*Weight percentage of silica (%)*
[C_2mim][Br]	1.95	66.10	40.16
[C_4mim][Br]	2.65	72.60	42.09
[C_6mim][Br]	3.10	75.61	42.98
[C_8mim][Br]	3.58	78.17	43.88
[C_{10}mim][Br]	3.05	75.31	37.68
[C_{12}mim][Br]	1.81	64.41	24.72

4.1.3.2 Influence of side chain length

The solubility of silica particles in bromide-based ionic liquids with different side chain lengths were tested to elucidate the influence of cation. The relationship is shown in Figure 4.1. As the alkyl chain increases from an ethyl group to an octyl group, the amount of silica that could be added increased from 66 mol% to 78 mol%. Then, increasing the chain length any more resulted in a decrease in affinity for the SiO_2 particles, reaching 64 mol% at a chain length of twelve carbons.

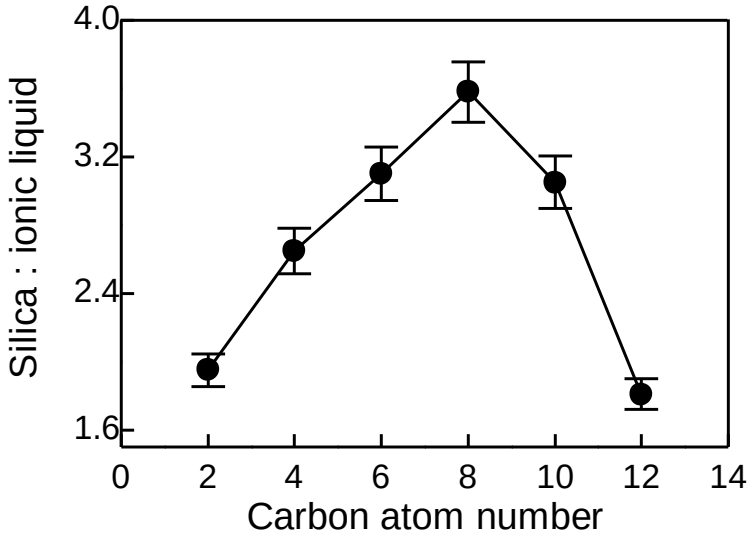

Figure 4.1 Relationship between silica molar saturation solubility and number of carbon atoms in the side chain at 80 ^{o}C.

4.1.3.3 Comparison to trends seen with melting points

The observation of an optimum solubility when the alkyl chain contains eight carbons is similar to trends previously observed with ionic liquid melting points.[19-26] The reported melting point values for the [$C_n$mim][Br] family are summarized in Table 4-3. Figure 4.2 illustrates the trends as a function of chain length. It has been observed that the same intermolecular interactions governing the pure ionic liquid melting points are affecting the ionic liquid's affinity for the SiO_2 particles. Melting points of 1-alkyl-3-methylimidazolium ionic liquids are mainly influenced by the packing ability of cations and anions, which is a function of the cation symmetry.[27, 28] Symmetric cations and anions facilitate better crystal packing, leading to stronger cation-anion interaction and thus higher melting points. When the alkyl chain has only one or two carbon atom, the imidazolium ring is symmetrical and the melting points are higher for [C_1mim][Br] and [C_2mim][Br]. However, with the increase in alkyl chain length, the symmetry is broken and the melting points are lower. After eight carbons, researchers attribute the increase in melting point to the increase of van der Waals forces.[29] The increased van der Waals force between cations and anions also leads to smaller silica affinity in ionic liquids after the side chain length is 8 carbons long.

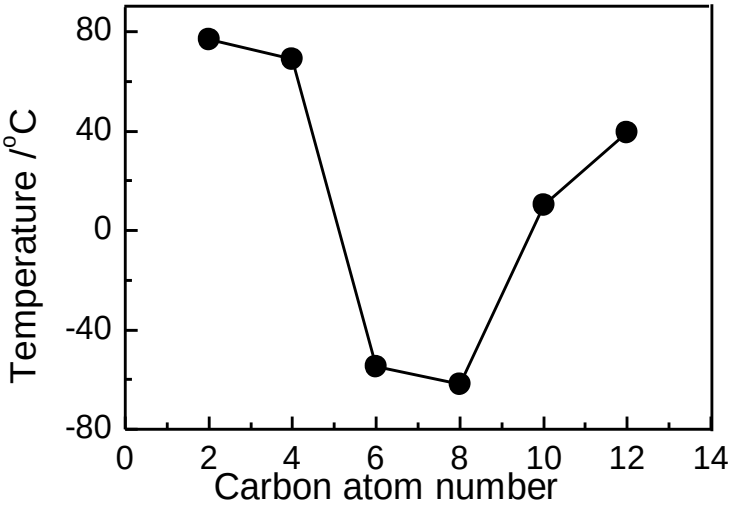

Figure 4.2 Melting points of 1-alkyl-3-methylimidazolium bromide.

Table 4-3 Observed melting points of [$C_n$mim][Br].

Ionic liquids	*Melting point observed*	*Lit.*
[C_2mim][Br]	76.9	19
[C_4mim][Br]	69	20
[C_6mim][Br]	-54.9	21
[C_8mim][Br]	-61.9	21
[C_{10}mim][Br]	10.5	21
[C_{12}mim][Br]	39.7	22

4.1.3.4 Intermolecular forces driving SiO_2 solubility

The relative solubility of the silica particles in the ionic liquids tested trends with the degree of interactions between the cation and anion expected within pure ionic liquids (exhibited by the melting point). The stronger the cation/anion interactions are, the lower the observed solubility of silica particles becomes. The primary intermolecular interactions in ionic liquid systems are electrostatic forces, hydrogen bonding and van der Waals forces.[30-32] The electrostatic forces occur between the negative charge of anion and positive charge on the imidazolium ring. Hydrogen bonding can occur with the hydrogen on the carbon between the two nitrogen atoms in the cation. This hydrogen has been shown to be acidic due to the electron-withdrawing effect of the two nitrogen atoms in the imidazolium ring; it can form strong hydrogen bonds with halide ions, such as bromide and chloride.[33-35] The final significant category of intermolecular interactions include the van der Waals forces which can occur between cation and anion, the cation and cation, and the ionic liquid and solute.

When carbon number of the side chain increases from two to eight, the silica solubility also increases. This trend is explained with the decrease of electrostatic force with longer alkyl chains. According to Coulomb's law, which states that the electrostatic force is proportional to the magnitudes of positive and negative charge, and inversely proportional to the square distance between charges, the distance between charges is the primary influence on electrostatic force. The positive imidazolium ring not only has attractive interaction with the negative bromide ion next to it, but also attracts bromide anions next to other rings. When the side chain is with one or two carbons, the symmetry of anion and cation allows the ions to pack very closely, which means that the electrostatic attractive force is larger. But when the side chain becomes longer, the steric effects hinders the packing ability, decreasing the attractive forces between ions. This decrease in attractive forces leads to bigger free volume cavities and enables the increase of dissolution of

silica particles.

Although much weaker than the electrostatic forces for the shorter alkyl chains, the van der Waals forces and hydrogen bonding are also worthy of addressing. With the increase in side chain length, the van der Waal force also increase. Additionally, since the side chain is an electron-donor group, with the increase in alkyl chain length, nitrogen atoms in the imidazolium ring become more electronegative and accordingly the hydrogen on the carbon is more positive, thus leading to stronger hydrogen bonding. Although an increase in chain length from two carbons to eight carbons will increase the effective van der Waal forces and hydrogen bonding ability (and therefore increase the strength of interactions between the anion and cation), the influence of these forces compared to electrostatic effects do not become relevant in terms of silica particle solubility until the chain length is increased beyond eight carbons.

After the carbon number reaches eight, electrostatic force between imidazolium ring and bromide ions around it becomes small since the distance between them is far. Increasing the alkyl chain length from eight to ten to twelve will not have as large of effect as that from two to four. At this time, van der Waals forces and hydrogen bonding begin to dominate silica solubility. When side chain becomes longer, the larger, more dispersed electron clouds lead to increased polarizability of the cation, thus increasing the van der Waals force. Hydrogen bonding strength also increases due to the increase in the electron-withdrawing capability of nitrogen atoms in the imidazolium ring. As a result, when the distance between cation and anions are separated at a far distance, the increased strengths of van der Waals force and hydrogen bonding overrides the decreased strength of electrostatic force in determining the overall force between cations and anions. With the increase in the overall interaction between cations and anions, it becomes much harder for silica particle to overcome the force and become solubilized in liquid phase.

4.1.4 Conclusion

Silica saturations in 1-alkyl-3-methylimidazolium bromide ionic liquids are greatly influenced by the side chain length. Silica saturation increases with the increase in carbon number of the side chain at first. However, when the carbon number reaches 8, it begins to decrease. Change in solubility is explained with respect to electrostatic interaction, van der Waals force and hydrogen bonding between cations and anions. When the side chain of imidazolium

ring is with 2-8 carbon atoms, the decreased electrostatic interaction overrides the increased hydrogen bonding and Van der Waals force, which results in the increased silica solubility. However, when the chain becomes longer, effect of electrostatic force becomes smaller and the increased hydrogen bonding and Van der Waal force begin to dominate the silica solubility.

4.1.5 References

1. Han, L. J.; Wang, Y. B.; Li, C. X.; Zhang, S. J.; Lu, X. M.; Cao, M. J., Simple and safe synthesis of microporous aluminophosphate molecular sieves by inothermal approach. *AIChE J.* , **2008,** 54, 280.
2. Parnham, E. R.; Morris, R. E., Ionothermal synthesis of zeolites, metal-organic frameworks, and inorganic-organic hybrids. *Acc. Chem. Res.*, **2007,** 40, 1005.
3. Xu, L.; Choi, E. Y.; Kwon, Y. U., Ionothermal syntheses of six three-dimensional zinc metal-organic frameworks with 1-alkyl-3-methylimidazolium bromide ionic liquids as solvents. *Inorg. Chem.* , **2007,** 46, 10670.
4. Cooney, E. L.; Booker, N. A.; Shallcross, D. C.; Stevens, G. W., Ammonia removal from wastewaters using natural Australian zeolite. I. Characterization of the zeolite. *Sep. Sci. Technol.*, **1999,** 34, 2307.
5. Lin, C. F.; Lo, S. S.; Lin, H. Y.; Lee, Y. C., Stabilization of cadmium contaminated soils using synthesized zeolite. *J. Hazard. Mater.*, **1998,** 60, 217.
6. Oshima, K.; Yamazaki, M.; Takewaki, T.; Kakiuchi, H.; Kodama, A., Application of novel FAM adsorbents in a desiccant system. *Kagaku Kogaku Ronbunshu*, **2006,** 32, 518.
7. Yang, J.; Ma, L. L.; Shen, B.; Zhu, J. H., Capturing nitrosamines in environment by zeolite. *Mater. Manuf. Processes*, **2007,** 22, 750.
8. Corma, A.; Davis, M. E., Issues in the synthesis of crystalline molecular sieves: Towards the crystallization of low framework-density structures. *Chemphyschem*, **2004,** 5, 304.
9. Cundy, C. S.; Cox, P. A., The hydrothermal synthesis of zeolites: Precursors, intermediates and reaction mechanism. *Microporous and Mesoporous Mater.*, **2005,** 82, 1.
10. Parnham, E. R.; Morris, R. E., The ionothermal synthesis of cobalt aluminophosphate zeolite frameworks. *J. Am. Chem. Soc.*, **2006,** 128, 2204.
11. Parnham, E. R.; Wheatley, P. S.; Morris, R. E., The ionothermal synthesis of SIZ-6 - a layered aluminophosphate. *Chem. Commun.*, **2006**, 380.
12. Itoh, N., Electrochemical light-emitting gel made by using an ionic liquids as the electrolyte. *J. Electrochem. Soc.*, **2009,** 156, J37.
13. Donato, R. K.; Migliorini, M. V.; Benvegnu, M. A.; Stracke, M. P.; Gelesky, M. A.; Pavan,

F. A.; Schrekker, C. M. L.; Benvenutti, E. V.; Dupont, J.; Scherekker, H. S., Synthesis of silica xerogels with highly distinct morphologies in the presence of imidazolium ionic liquids. *J. Sol-Gel Sci. Technol*, **2009**, 71.

14. Gelesky, M. A.; Chiaro, S. S. X.; Pavan, F. A.; dos Santos, J. H. Z.; Dupont, J., Supported ionic liquid phase rhodium nanoparticle hydrogenation catalysts. *Dalton Transactions*, **2007**, 5549.
15. Sun, X.; King, J.; Anthony, J. L., Molecular sieve synthesis in the presence of tetraalkylammonium and dialkylimidazolium molten salts. *Chem. Eng. J.*, **2009,** in press, in press.
16. Ueno, K.; Lnaba, A.; Kondoh, M.; Watanabe, M., Colloidal stability of bare and polymer-grafted silica nanoparticles in ionic liquids. *Langmuir*, **2008,** 24, 5253.
17. Ueno, K.; Imaizumi, S.; Hata, K.; Watanabe, M., Colloidal interaction in ionic liquids: effects of ionic structures and surface chemistry on rheology of silica colloidal dispersions. *Langmuir*, **2009,** in press, in press.
18. Gaillon, L.; Sirieix-Plenet, J.; Letellier, P., Volumetric study of binary solvent mixtures constituted by amphiphilic ionic liquids at room temperature (1-alkyl-3-methylimidazolium bromide) and water. *J. Solution Chem.*, **2004,** 33, 1333.
19. Golovanov, D. G.; Lyssenko, K. A.; Vygodskii, Y. S.; Lozinskaya, E. I.; Shaplov, A. S.; Antipin, M. Y., Crystal structure of 1,3-dialkyldiazolium bromides. *Russ. Chem. Bull.*, **2006,** 55, 1989.
20. Golovanov, D. G.; Lyssenko, K. A.; Antipin, M. Y.; Vygodskii, Y. S.; Lozinskaya, E. I.; Shaplov, A. S., Cocrystal of an ionic liquid with organic molecules as a mimic of ionic liquid solution. *Cryst. Growth Des.*, **2005,** 5, 337.
21. Wang, J. J.; Wang, H. Y.; Zhang, S. L.; Zhang, H. H.; Zhao, Y., Conductivities, volumes, fluorescence, and aggregation behavior of ionic liquids [C(4)mim][BF4] and [C(n)mim]Br(n = 4, 6, 8, 10, 12) in aqueous solutions. *J. Phys. Chem. B*, **2007,** 111, 6181.
22. Yan, F.; Texter, J., Surfactant ionic liquid-based microemulsions for polymerization. *Chem. Commun.*, **2006**, 2696.
23. Nishida, T.; Tashiro, Y.; Yamamoto, M., Physical and electrochemical properties of 1-alkyl-3-methylimidazolium tetrafluoroborate for electrolyte. *J. Fluorine Chem.*, **2003,** 120, 135.
24. Ruiz-Angel, M. J.; Berthod, A., Reversed phase liquid chromatography of alkyl-

imidazolium ionic liquids. *J. Chromatogr. A*, **2006,** 1113, 101.

25. Holbrey, J. D.; Seddon, K. R., The phase behaviour of 1-alkyl-3-methylimidazolium tetrafluoroborates; ionic liquids and ionic liquid crystals. *J. Chem. Soc. , Dalton Trans.*, **1999**, 2133.
26. Reichert, W. M.; Holbrey, J. D.; Swatloski, R. P.; Gutowski, K. E.; Visser, A. E.; Nieuwenhuyzen, M.; Seddon, K. R.; Rogers, R. D., Solid-state analysis of low-melting 1,3-dialkylimidazolium hexafluorophosphate salts (ionic liquids) by combined x-ray crystallographic and computational analyses. *Cryst. Growth Des.*, **2007,** 7, 1106.
27. Krossing, I.; Slattery, J. M.; Daguenet, C.; Dyson, P. J.; Oleinikova, A.; Weingartner, H., Why are ionic liquids liquid? A simple explanation based on lattice and solvation energies. *J. Am. Chem. Soc.*, **2006,** 128, 13427.
28. Trohalaki, S.; Pachter, R., Prediction of melting points for ionic liquids. *QSAR Comb. Sci.*, **2005,** 24, 485.
29. Lopez-Martin, I.; Burello, E.; Davey, P. N.; Seddon, K. R.; Rothenberg, G., Anion and cation effects on imidazolium salt melting points: A descriptor modelling study. *Chemphyschem*, **2007,** 8, 690.
30. Tsuzuki, S.; Tokuda, H.; Hayamizu, K.; Watanabe, M., Magnitude and directionality of interaction in ion pairs of ionic liquids: Relationship with ionic conductivity. *Journal of Physical Chemistry B*, **2005,** 109, 16474.
31. Lynden-Bell, R. M.; Del Popolo, M. G.; Youngs, T. G. A.; Kohanoff, J.; Hanke, C. G.; Harper, J. B.; Pinilla, C. C., Simulations of ionic liquids, solutions, and surfaces. *Accounts of Chemical Research*, **2007,** 40, 1138.
32. Del Popolo, M. G.; Kohanoff, J.; Lynden-Bell, R. M.; Pinilla, C., Clusters, liquids, and crystals of dialkyimidazolium salts. A combined perspective from a initio and classical computer simulations. *Accounts of Chemical Research*, **2007,** 40, 1156.
33. Crowhurst, L.; Mawdsley, P. R.; Perez-Arlandis, J. M.; Salter, P. A.; Welton, T., Solvent-solute interactions in ionic liquids. *Phys. Chem. Chem. Phys.*, **2003,** 5, 2790.
34. Morrow, T. I.; Maginn, E. J., Molecular dynamics study of the ionic liquid 1-n-butyl-3-methylimidazolium hexafluorophosphate. *J. Phys. Chem. B*, **2002,** 106, 12807.
35. Hardacre, C.; McMath, S. E. J.; Nieuwenhuyzen, M.; Bowron, D. T.; Soper, A. K., Liquid structure of 1, 3-dimethylimidazolium salts. *J. Phys-Condens. Mater.*, **2003,** 15, S159.

4.2 Influence of Structural Variation in Imidazolium-based Ionic Liquids on Saturation Points of Syloid 63 Silica Particles

4.2.1 Introduction

Due to the desirable properties of many ionic liquids (ILs), such as low vapor pressure, wide liquidus range, tunable structures and reasonable cost,[1-3] ILs recently have shown great potential for the synthesis of a variety of organic and inorganic, porous and non-porous materials.[4-8] In the ionothermal synthesis (i.e. ionic liquid used as the solvent) of porous crystalline materials such as silicates, phosphates and other molecular sieves,[9-11] the ionic liquid often serves as both the solvent and a structure directing agent (SDA) that participates in the formation of the pores.[6,12] One advantage over conventional hydrothermal synthesis (i.e. water is used as the solvent) is that synthesizing molecular sieves in ionic liquids at high temperature typically generates much less pressure and thus does not require a high-pressure vessel.[13] A variety of porous aluminophosphates with zeolitic frameworks have been successfully synthesized in ionic liquids,[10,14,15] however, there have been few examples of silica-based materials. Morris and coworkers reports the successful synthesis of siliceous zeolites Silicalite-1 and Theta-1 in an IL mixture of $[C_4mim][OH_{0.65}Br_{0.35}]$.[16,17] Xu and coworkers reported synthesizing sodalite in $[C_2mim][Br]$,[18] although the reaction mixture does contain a significant amount of water. The synthesis of true aluminosilicate zeolite or even pure silica zeolites has been limited likely by the solubility of silica in the ionic liquids.

In addition to use in zeolite synthesis, colloids of silica particles in ionic liquids have been used as electrochemical light-emitting gel and for synthesizing silica xerogels.[19-21] In their work on the stability of silica nanoparticle colloids in ionic liquids, Wantanabe and coworkers found that bare silica particles coagulated easily in dilute solutions of silica particles and ionic liquids, unless a polymer was grafted onto collide surface.[22,23]

In this work, silica particles of Syloid 63 type were mixed with ionic liquids to investigate the relationship between their saturation points and structures of ionic liquids. Syloid 63, a fumed silica, has been used as a pure source of silica in hydrothermal synthesis of zeolitic materials, such as VPI-9.[24] The saturated point was determined as the point when the addition of more silica particles formed a second phase; it was found to correlate with a limiting volume or

packing fraction which depends on the pure ionic liquid properties. Since the majority of ionothermally synthesized porous materials have been made in methylimidazolium-based ionic liquids, such as 1-ethyl-3-methylimidazolium bromide and 1-butyl-3-methylimidazolium bromide,[14,25] this work focuses on ionic liquids with the methylimidazolium cations $[C_n mim]^+$.

4.2.2 Experiment

4.2.2.1 Preparation of ionic liquids

1-alkyl-3-methylimidaozlium bromide ($[C_n mim][Br]$) ionic liquids were synthesized according to standard procedures.[26] The general synthesis procedure involves reacting 1-methylimidazole and bromoalkane in acetonitrile at 40 ^oC for 2-8 days, followed by passing it through a granular activated carbon column and an acidic activated aluminum oxide column to remove impurities, and drying the mixture for another 3 days. The products are tested by liquid NMR to check purity. All of the reactants are distilled before the reaction. $[C_4mim][Tf_2N]$ was synthesized by mixing $[C_4mim][Br]$ solution and lithium bis(trifluoromethylsulfonyl)imide ($[Li][Tf_2N]$) solution.[27] The dense ionic liquid phase was repeatedly washed with water to remove any residual LiBr, which was confirmed by reacting the ionic liquid solution with silver nitrate. 1-butyl-3-methylimidazolium trifluoroacetate ($[C_4mim][CF_3CO_2]$) was bought from EMD Company and used as received (high purity). 1-butyl-3-methylimidazolium chloride ($[C_4mim][Cl]$), 1-ethyl-3-methylimidazolium chloride ($[C_2mim][Cl]$) and 1-butyl-3-methylimidazolium hexafluorophosphate ($[C_4mim][PF_6]$) were bought from Fischer. Labeled purity of $[C_4mim][PF_6]$ is 98%. 1-ethyl-2,3-dimethylimidazolium bromide ($[C_2mmim][Br]$) was bought from Acros Organics. The labeled purity is 97%. Before use, each ionic liquid was dried for 6-12 hrs at 60 ^oC under vacuum to ensure the water content is lower than 500 ppm, which was confirmed by Karl-Fischer titration.

4.2.2.2 Silica source

Syloid 63 (GRACE Davison Company) was used as the silica particle. Syloid 63 has a reported particle size of about 9 microns and a surface area of about 675 m^2/g. The average pore diameter of Syloid 63 is 25 Angstroms. It has a strong affinity for moisture even at very low

humidity levels. The surface of the Syloid 63 silica particles is covered with hydroxyl groups. Before use, the silica particles were dried at 100 ^{o}C for 2 hrs and ground into fine powders.

4.2.2.3 Determination of the saturation point

The saturation point was found by adding the silica particles in 0.05 g increments to approximately 5 g ionic liquid until the point when any additional silica remained in a separate phase. All measurements were made at 80^{o}C, except for [C_2mim][Cl], [C_2mim][Br], [C_4mim][Br] and [C_2mmim][Br], where higher temperatures (90^{o}C and 125^{o}C) were maintained in order to be above the ILs' melting point.

4.2.2.4 Characterization methods

The size of the silica particles in dilute solutions (typically 5 % of the saturation value) was measured using dynamic light scattering (DLS).The light source was an Argon ion laser with a wave length of λ = 488 nm. ALV 5000 correlator was used to measure the correlation function of the scattering light. A Hitachi S-3500 scanning electron microscope (SEM) was used to check the configuration and size of silica particles in ionic liquids at saturation as well as those recovered from the IL via an acetone and water wash. The recovered particles were dried in an oven at 100 ^{o}C for 5 hrs prior to being scanned by SEM.

Table 4-4 Properties of Pure Ionic Liquids and Silica Particle – Ionic Liquid Mixtures.

		Pure IL Properties						*Silica – IL Mixture Properties*		
IL	*Temperature* (^oC)	*Melting point* (^oC)	*Viscosity* (*cP*)	*Molar vol.* (cm^3/mol)	*Cation volume* (cm^3/mol)	*Anion volume* (cm^3/mol)	*Free vol.* (cm^3/mol)	*Mol. ratio of Si to IL*	*Mass ratio of Si to IL*	*Volume fraction of silica*
[C_2mim][Br]	80	76.9[28]		141 ± 1	90 ± 12[29]	34 ± 8[30]	17 ± 4	2.13 ± 0.10	0.67 ± 0.03	0.67 ± 0.03
	90			141 ± 1			17 ± 5	2.16 ± 0.10	0.68 ± 0.03	0.68 ± 0.03
	125			142 ± 1			18 ± 5	2.25 ± 0.10	0.71 ± 0.03	0.68 ± 0.03
[C_4mim][Br]	80	69.0[31]		178 ± 0	119 ± 12[29]	34 ± 8[30]	25 ± 7	2.65 ± 0.10	0.73 ± 0.03	0.67 ± 0.03
	125			181 ± 1			28 ± 7	2.74 ± 0.10	0.75 ± 0.03	0.67 ± 0.03
[C_6mim][Br]	80	-54.9[32]		212 ± 1	148 ± 12[29]	34 ± 8 [30]	30 ± 8	3.16 ± 0.10	0.77 ± 0.02	0.67 ± 0.02
[C_8mim][Br]	80	-61.9[32]		243 ± 1	176 ± 12[29]	34 ± 8[30]	33 ± 8	3.58 ± 0.10	0.78 ± 0.02	0.67 ± 0.02
[C_{10}mim][Br]	80	10.5[32]		274 ± 1	205 ± 12[29]	34 ± 8[30]	35 ± 9	3.14 ± 0.10	0.62 ± 0.02	0.61 ± 0.02
[C_{12}mim][Br]	80	39.7[33]						1.81 ± 0.10	0.33 ± 0.02	
[C_2mmim][Br]	125			158 ± 1	105 ± 12[29]	34 ± 8[30]	19 ± 5	2.38 ± 0.10	0.70 ± 0.03	0.67 ± 0.03
[C_2mim][Cl]	90	89.0[2]						1.57 ± 0.10	0.64 ± 0.04	
[C_4mim][Cl]	80	68.8[34]		166 ± 0[35]	119 ± 12[29]	28 ± 8[30]	19 ± 5	2.38 ± 0.10	0.82 ± 0.03	0.66 ± 0.03
[C_4mim][Tf_2N]	33	-4.0[36]	35.45[37]	293 ± 0[38]	119 ± 12[29]	138 ± 12[29]	36 ± 5	3.78 ± 0.10	0.54 ± 0.01	0.64 ± 0.02
	51		19.10[37]	296 ± 0[39]			39 ± 5	4.38 ± 0.10	0.63 ± 0.01	0.67 ± 0.02
	74		10.52[37]	302 ± 0[40]			45 ± 6	4.74 ± 0.10	0.68 ± 0.01	0.68 ± 0.01
	80		9.27 [37]	302 ± 0[40]			45 ± 6	4.80 ± 0.10	0.69 ± 0.01	0.68 ± 0.01
	90		7.59[37]	305 ± 0[40]			47 ± 6	5.06 ± 0.10	0.73 ± 0.01	0.69 ± 0.01
	110		5.42[37]	309 ± 0[40]			52 ± 7	5.25 ± 0.10	0.75 ± 0.01	0.69 ± 0.01
[C_4mim][PF_6]	30	11.0[39]	187.51[37]	209 ± 0[40]	119 ± 12[29]	65 ± 5[29]	25 ± 3	2.44 ± 0.10	0.52 ± 0.02	0.62 ± 0.03
	50		67.33[37]	211 ± 0[40]			28 ± 3	2.86 ± 0.10	0.61 ± 0.02	0.65 ± 0.02
	65		38.00 [37]	214 ± 0[41]			31 ± 4	3.06 ± 0.10	0.65 ± 0.02	0.66 ± 0.02
	80		24.00[37]	215 ± 0[40]			32 ± 4	3.27 ± 0.10	0.69 ± 0.02	0.68 ± 0.02
	100		14.74[37]	218 ± 0[40]			35 ± 4	3.37 ± 0.10	0.71 ± 0.02	0.68 ± 0.02
	120		10.01[37]					3.41 ± 0.10	0.72 ± 0.02	
[C4mim][CF_3CO_2]	80	23.2[42]		215 ± 1[41]	119 ± 12[29]	65 ± 12[29]	31 ± 6	3.43 ± 0.10	0.82 ± 0.02	0.69 ± 0.02

4.2.3 Silica particle saturation points

Saturation points and volume fractions of Syloid 63 particles in different ionic liquids along with the properties of the ionic liquids are listed in Table 4-4. The volume fractions were calculated using a Syloid 63 fumed silica density of 0.44 g/cm^3 (provided by manufacturer) and densities of ILs at different temperatures. The molar volumes or densities of [C_4mim][Tf_2N], [C_4mim][PF_6], [C_4mim][Cl] and [C_4mim][CF_3CO_2] at 80 ^{o}C were obtained from literature.[35,43-48] Densities of other ILs at 80 ^{o}C, 90 ^{o}C or 125 ^{o}C were measured with this work. Free volumes were calculated by subtracting anion and cation volume[29] from molar volume of ILs at the specific temperature. There is a clear relationship between silica saturation point and molar volume of ILs (or free volume), as shown in Figure 4.3-(a) and Figure 4.3-(b), where the 80 ^{o}C data from Table 4-4 are plotted. The magnitude of molar volume and free volume in ionic liquids is influenced by the intermolecular forces of ionic liquids and thus not surprisingly affects the silica saturation point. The influence of structural variation in imidazolium-based ILs on Syloid 63 silica particles are discussed in detail in the following sections.

(a)

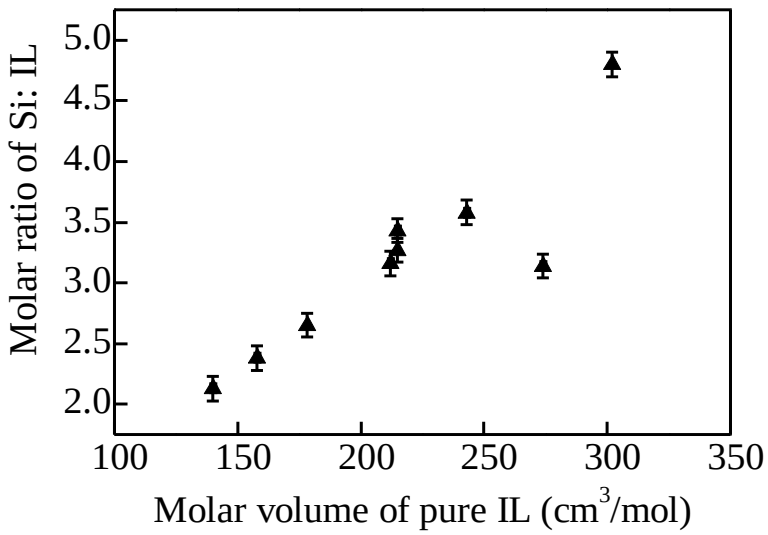

(b)

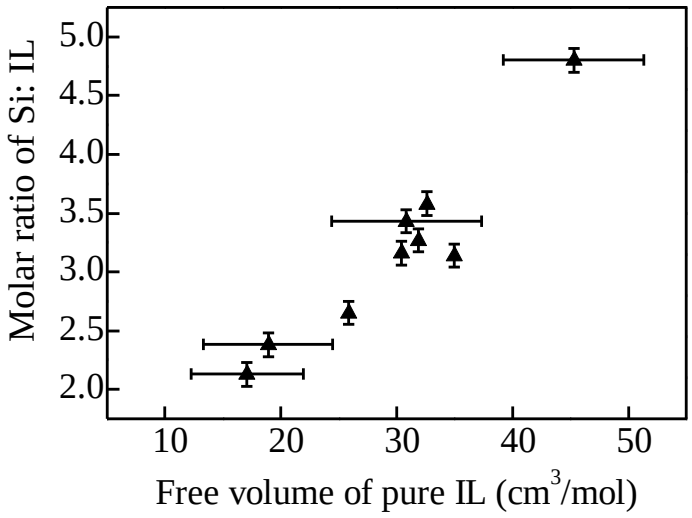

Figure 4.3 Relationship between silica saturation point and (a) molar volume of pure IL at 80 °C, and (b) free volume of pure ILs at 80 °C.

The saturation points for the silica particles in the ionic liquid (i.e. when any additional silica remained in a separate phase) range from 1.5 to 5.3 mol SiO_2/mol IL (90.15 to 318.53 g SiO_2/mol IL), whereas the volume fractions fall in a narrow range (ranging from 0.61 to 0.69) suggesting that this limiting volume fraction determines the saturation point. The range of volume fractions is consistent with the packing fraction one would expect for a closely packed system. For spherical particles, the volume fraction for a maximally random jamming system should be 0.64.[49] Volume fractions for body-centered cubic, face-centered cubic and hexagonal close packed structures are 0.68, 0.74 and 0.74, respectively.[50] Most of the silica-ILs systems have volume fractions from 0.67 to 0.69, similar to the packing factor of body-centered cubic structure and slightly less than packing fractions of face-centered cubic and hexagonal close packed structures. In addition, a few ILs which are saturated with silica particles at lower temperature have volume fractions from 0.62 to 0.66. Among all of the systems, [C_{10}mimBr] has the lowest volume fraction (0.61 ± 0.02), which is outside the packing factor ranges of close packing systems. Although Syloid 63 silica particles are not strictly spherical and therefore not expected to be a true maximally random jamming or BCC system, the fact that all the ionic liquids systems exhibited similar volume fractions at their silica saturation points suggests that these particles are packed closely within the ionic liquid, thus limiting the maximum saturation point.

4.2.3.1 Influence of side chain length connected to C1

Syloid 63 silica particles were mixed with ionic liquids based on [$C_n$mim][Br] (n=2,4,6,8,10,12) to determine the influence of alkyl chain length on silica saturation points. The relationship between silica molar solubility and number of carbon atoms in the alkyl chain is shown in Figure 4.4. At 80 ^oC, with the increase of carbon number in alkyl chain, molar ratios of silica to ionic liquid increase from 1.95 to 3.58 when the number of carbon atoms in side chain is increased from two to eight, then decreases from 3.58 to 1.81 when the carbon number is increased from eight to twelve. The maximum saturation point is achieved when the carbon number in the alkyl chain is eight. A similar trend is observed with IL melting points; a minimum melting temperature is reached when there are eight carbons in the alkyl chain, as seen in Figure 4.5. Melting points of these [$C_n$mim][Br]-based ILs are mainly influenced by the packing ability of cations and anions.[45,46] When cations and anions are symmetric, they can pack closely and increase crystal energy, thus leading to higher melting points.[45,47] For example, because cations of [C_1mim][Br] and [C_2mim][Br] are more symmetrical than [C_4mim][Br] and [C_6mim][Br], their melting points are higher than those of [C_4mim][Br] and [C_6mim][Br]. Gordon and coworkers found that ionic liquids with long side chain displayed liquid crystalline behavior.[44] It consists of sheets of imidazolium rings and anions, separated by interdigitated alkyl chains.[44] The close packed mode of cations and anions leads to the increase in electrostatic force. The author also found that the closest cation C2 ¨ F-PF_6 contact in [C_{12}mim][PF_6] was 2.950 Å, slightly shorter than that of short chain [C_2mim][PF_6] (3.206 Å), which indicates ILs with longer alkyl chain have higher attractive forces between cations and anions,[51] which results in the higher melting point as well as lower the silica saturation points in ILs with the longer alkyl chains.

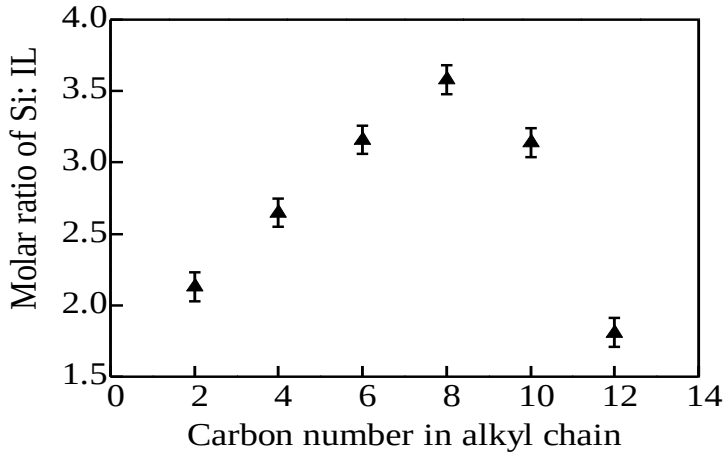

Figure 4.4 Relationship between silica saturation point and number of carbon atoms in the alkyl chain at 80 ^{o}C.

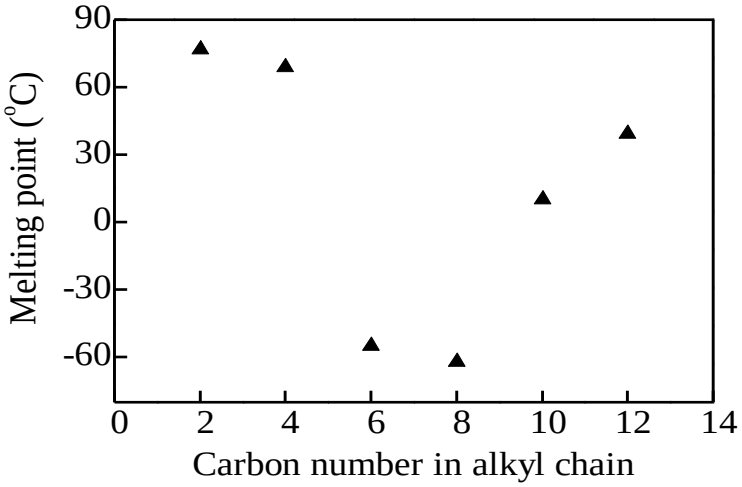

Figure 4.5 Relationship between melting point of IL and number of carbon atoms in the alkyl chain.

The relationship between silica molar solubility and molar volumes of [$C_n$mim]-based ILs is shown in Figure 4.6. With the increase of alkyl chain length, molar volumes of the ILs also increase. When the alkyl chain is with two, four, six or eight carbons, with the increase of molar volume, saturated silica solubility increases accordingly, which is as expected. It is worth noting that with the further increase of alkyl chain length from eight carbons to ten carbons, silica saturation points decrease instead of continuing to increase. The sudden decrease of silica

saturation points is possibly due to the change of packing mode when alkyl chain becomes long enough and the increase of attractive forces between cations and anions, which has been explained in the above paragraph. A similar relationship between IL molar volume and solubility has been reported by Nobel and coworkers in their studies of CO_2 in several ILs.[52] They observed that as the IL molar volume is increased from 140 cm^3/mol to 258 cm^3/mol, the solubility of CO_2 increases according. The maximum solubility is reached at an IL molar volume of 258 cm^3/mol, and the CO_2 solubility decreases with any further increase in molar volume.[52] In this paper, molar volume of [$C_n$mim][Br] at 80 ^oC increases continuously from 140 cm^3/mol to 274 cm^3/mol with the increase of alkyl chain length from two carbons to ten carbons, and the maximum saturation point is obtained when the molar volume of [$C_n$mim][Br] is 243 cm^3/mol (molar volume of [C_8mim][Br]), which is similar to the molar volume observed at the maximum CO_2 solubility.

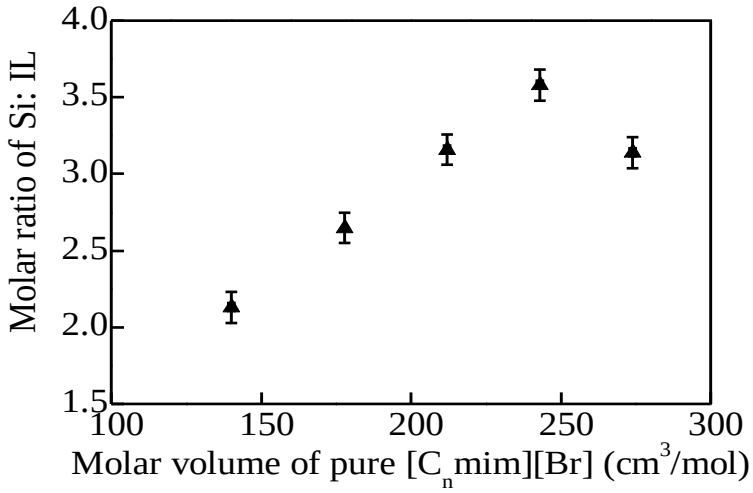

Figure 4.6 Relationship between silica saturation point and Molar volume of [$C_n$mim][Br] (n equals to 2,4,6,8 and 10) at 80 ^oC.

4.2.3.2 Influence of H connected to C2

The ionic liquids [C_2mim][Br] and [C_2mmim][Br] were used at 125^oC to investigate the influence of the acidic proton on the imidazolium ring on the silica saturation point. Results are listed in Table 4-4.The change of silica saturation solubility has the same dependence on molar volume. When the hydrogen on the C2 position is substituted by a methyl group, free volume

increases from 142 cm^3/mol to 158 cm^3/mol, but the difference in silica saturation solubility is not notable (from 2.05 to 2.38), indicating the influence due to acidic H on C2 is not significant.

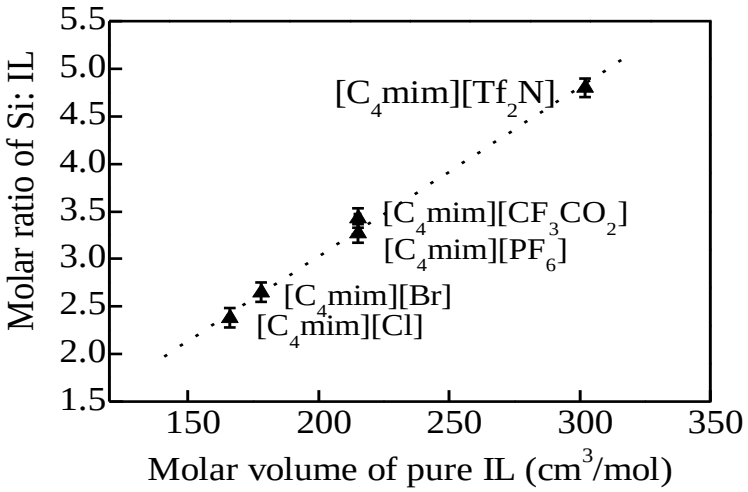

Figure 4.7 Relationship between silica saturation point in $[C_4mim]^-$-based ILs and molar volume of ILs at 80°C.

4.2.3.3 Influence of anions

Two $[C_2mim]^-$-based ionic liquids and five $[C_4mim]^-$-based ionic liquids are used to see the influence of anions on the saturations points of Syloid 63. The results are shown in Table 4-4, and the $[C_4mim]^-$ based ionic liquids results are also plotted in Figure 4-7. At 90 °C, the saturation point of $[C_2mim][Cl]$ is lower than $[C_2mim][Br]$. At 80 °C, among all of the $[C_4mim]^-$-based ionic liquids, $[C_4mim][Tf_2N]$ has the highest saturation concentration (molar ratio of silica to IL: 4.80), nearly twice the saturation solubility of Syloid 63 in $[C_4mim][Cl]$ (molar ratio of silica to IL: 2.38). Once again, the magnitude of molar volume at 80 °C corresponds quite well with the silica solubility. The ILs ranked in order of molar volume or in order of silica saturation point is the same: $[C_4mim][Tf_2N]$ > $[C_4mim][CF_3CO_2]$ ~ $[C_4mim][PF_6]$ > $[C_4mim][Br]$ > $[C_4mim][Cl]$.

4.2.3.4 Influence of temperature

The influence of temperature on silica saturation points of $[C_4mim][PF_6]$ and $[C_4mim][Tf_2N]$ is tested at varied temperatures, from 20 °C to 110 °C (or 120 °C), and the results

are shown in Table 1 and illustrated in Figure 4.8. It can be seen that with the increase in temperature of the system, more silica particles could be suspended in the ionic liquid solution for both of the ionic liquids tested.

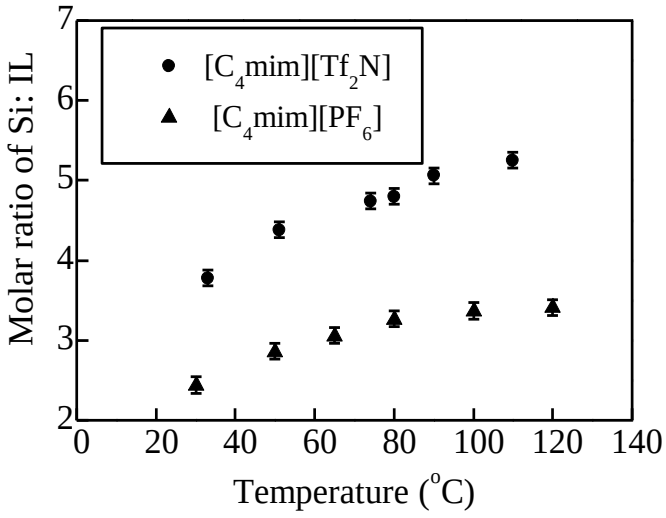

Figure 4.8 Influence of temperature on silica saturation points of $[C_4mim][PF_6]$ and $[C_4mim][Tf_2N]$.

As discussed before, the increased silica saturation in ionic liquids is probably due to the increase of molar volumes in the ionic liquids. With the increase in temperature, densities of ionic liquids decrease.[53] For example, when the temperature increases from 20 °C to 118 °C, densities of $[C_4mim][Tf_2N]$ and $[C_4mim][PF_6]$ decrease from 1.4425 g/cm^3 1.3510 g/cm^3 and from 1.3727 g/cm^3 to 1.2902 g/cm^3, respectively.[40,54,55] The decrease of density leads to bigger molar volumes and bigger free volumes. The relationship between silica saturation points and molar volumes is shown in Figure 4.9-(a). With the increase of molar volume in the ionic liquids, the molar ratio of silica to ionic liquids increases accordingly. The increase of molar volume with increase of temperature leads to the decrease of intermolecular forces, and thus increasing the silica solubility. Figure 4.9-(b) shows the relationship between silica saturation points and free volumes. Not surprisingly, with the increase of free volume, molar ratio of silica and IL increases with a similar slope for both types of ILs tested.

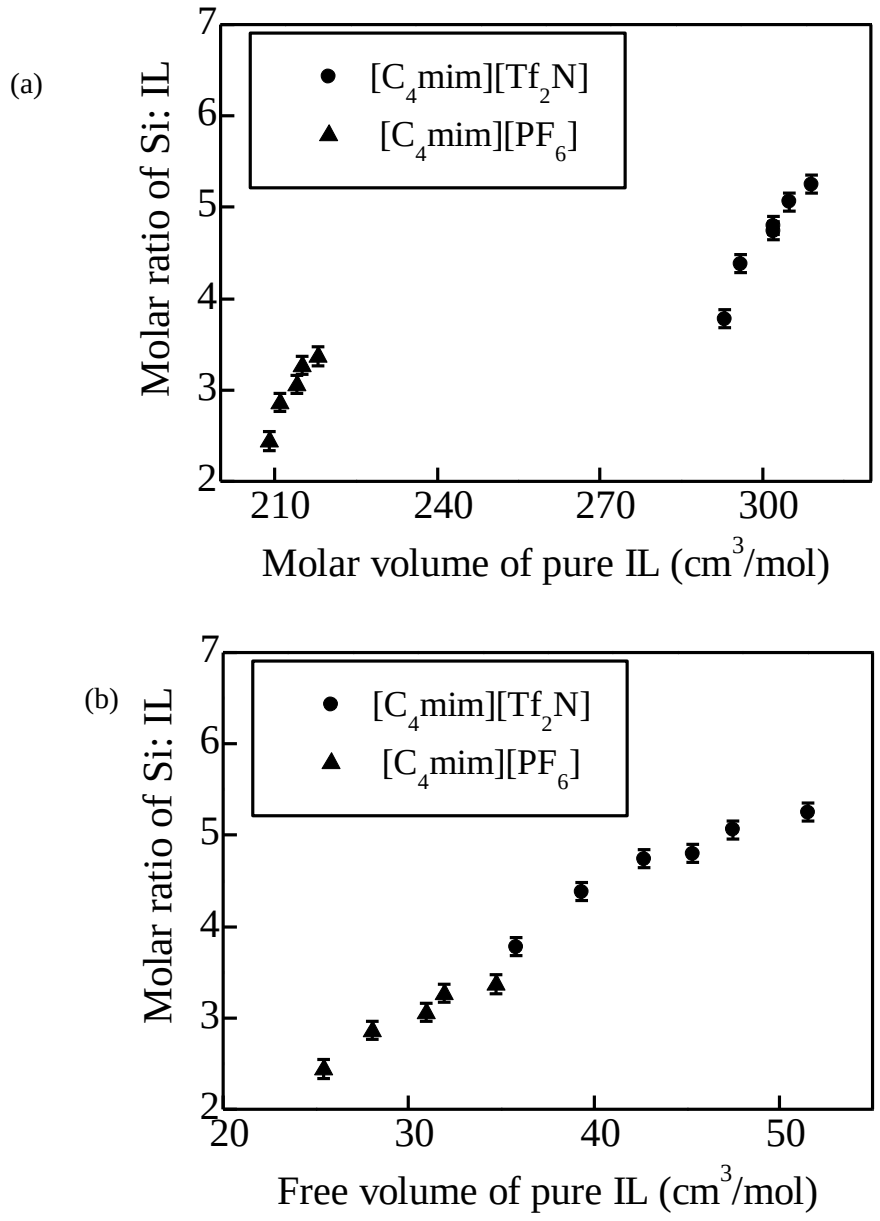

Figure 4.9 Relationship between silica saturation point and (a) molar volume of $[C_4mim][PF_6]$ and $[C_4mim][Tf_2N]$, and (b) free volume of $[C_4mim][PF_6]$ and $[C_4mim][Tf_2N]$ (for the same IL, each point represents the saturation point at a single temperature).

Viscosity is also a property determined by intermolecular forces of attraction. Generally, the stronger the intermolecular forces of attraction, the more viscous the liquid.[56] Since both the influences of temperature on viscosity of pure ionic liquids and silica saturation points are likely

due to change of intermolecular forces, it is not surprising there is excellent correlation between viscosity of pure ionic liquids and their silica saturation points, as shown in Figure 4-10.

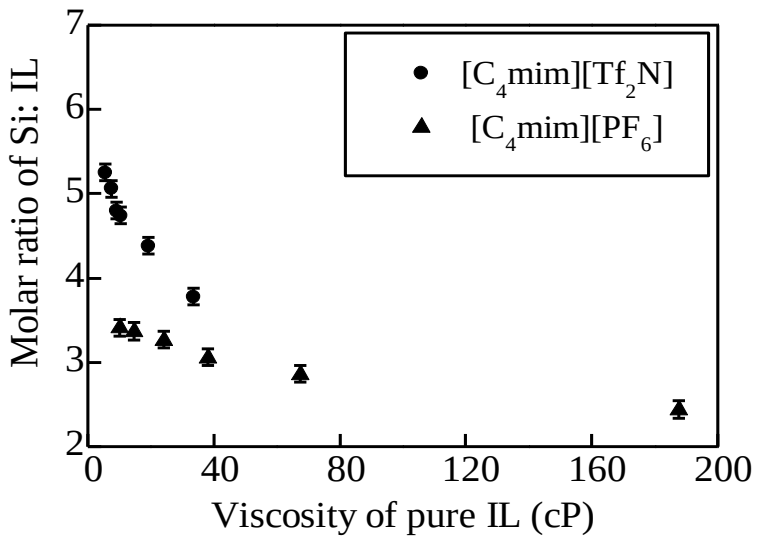

Figure 4.10 Correlation between silica saturation point and viscosities of pure [C_4mim][PF_6] and [C_4mim][Tf_2N].

4.2.3.5 Analysis on the conformation of SiO_2 particles in ionic liquids

To determine the state of the silica particles in solution, their particle sizes are measured by dynamic light scattering after being mixed with two pure ionic liquids ([C_4mim][PF_6] and [C_8mim][Br]). The concentrations of these samples are fixed at 5 wt%, much lower than the concentrations of the saturated samples. The results are shown in Figure 4-11. The spectra of dynamic light scatterings can be divided into three regimes, Rayleigh regime, Guinier regime and Porod regime, as shown in Figure 4-11. In the Guinier regime, if a graph of I(0)/I(q) and q^2, a linear line with a slope of $0.333R_g^2$ will be obtained. For a sphere particle, radius of the particle is equal to 0.77 R_g. After calculating the radius of silica particles by the previous equations, average particle size of SiO_2 particles decreased from 9 μm to 6 μm in [C_4mim][PF_6]. The decrease of particle size in [C_4mim][PF_6] is thought to result from the decomposition of SiO_2 particles by the trace amount HF known to be present in [C_4mim][PF_6]. By comparison, the particle size in [C_8mim][Br] is 9.6 μm, essentially remaining the same as the original particles, indicating that the IL not containing trace HF did not dissolve the SiO_2.

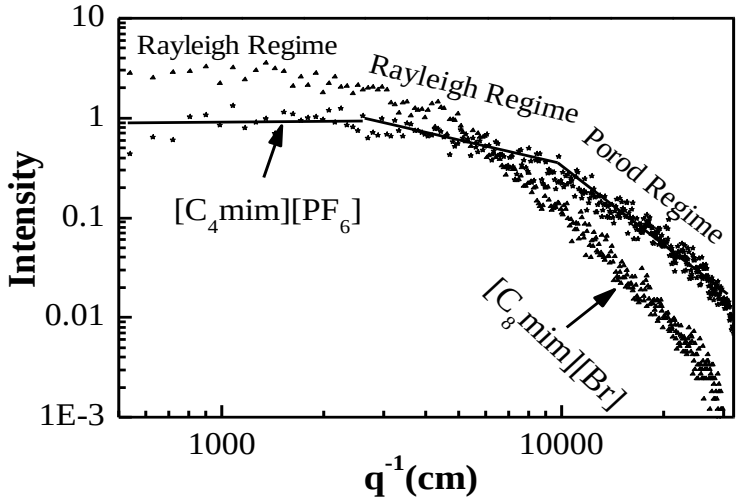

Figure 4.11 Dynamic light scattering results of [C_4mim][PF_6] and [C_8mim][Br].

Arrangement of SiO_2 particles at its free state and in two ionic liquids ([C_8mim][Br] and [C_4mim][Tf_2N]) are shown in Figure 4.12-(a), Figure 4.12-(b) and Figure 4.12-(c). The arrangements of SiO_2 particles saturated in ILs are quite uniform in these two ionic liquids. SEM images of the left powders are shown in Figure 4.12-(d). By comparing Figure 4.12-(a) and Figure 4.12-(d), it is found that there is no remarkable change in the size of SiO_2 particles after stirring with [C_4mim][Tf_2N]. Figure 4.12-(b) and Figure 4.12-(c) also show that arrangement of SiO_2 particles in [C_8mim][Br] or [C_4mim][Tf_2N] is consistent with a well packed system. The DLS results and the SEM images both give evidence that the silica particles are being suspended in the ionic liquids and not broken down unless at least a trace amount of HF is present. These findings are consistent with the observation that regardless of the ionic liquid structure, the saturation point occurs at a maximum volume fraction that is similar to packing fractions observed in close-packed systems.

(a)

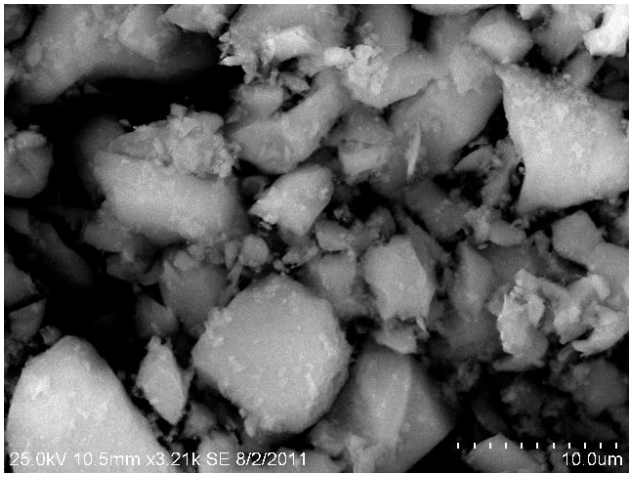
25.0kV 10.5mm x3.21k SE 8/2/2011
10.0um

(b)

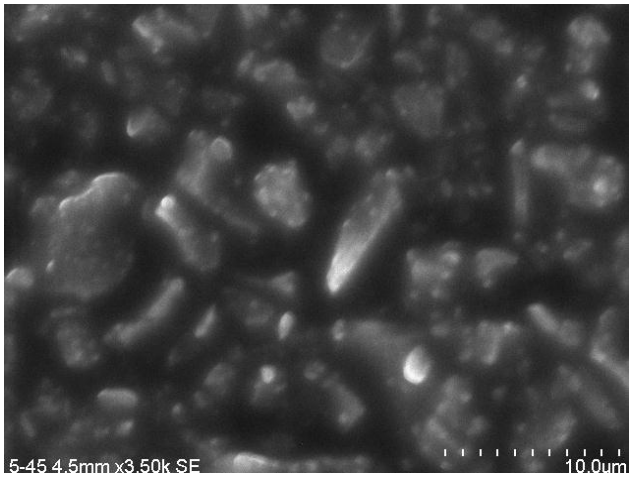
5-45 4.5mm x3.50k SE
10.0um

(c)

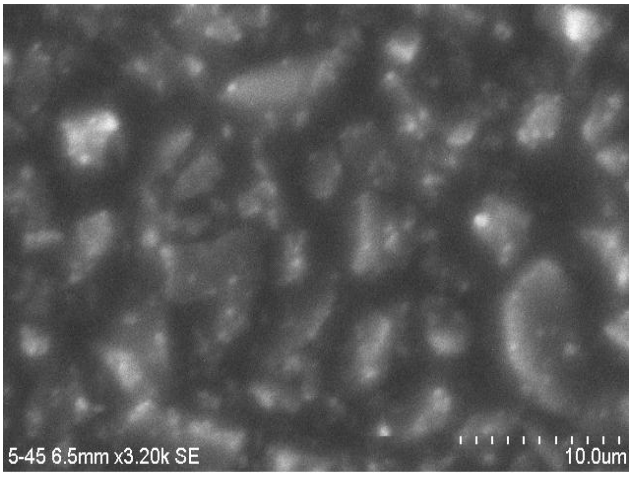
5-45 6.5mm x3.20k SE
10.0um

(d) 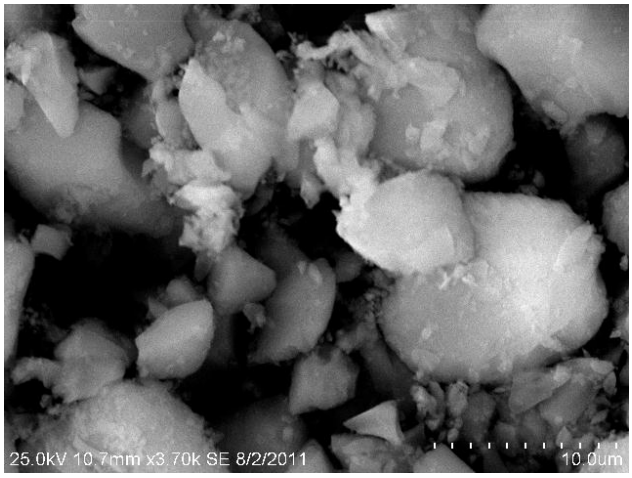

Figure 4.12 SEM photographs of (a) Syloid 63 SiO_2 particles , (b) system of Syloid 63 SiO_2 particles saturated in [C_8mim][Br], (c) system of Syloid 63 SiO_2 particles saturated in [C_4mim][Tf_2N], and (d) Syloid 63 SiO_2 particles after stirring with [C_4mim][Tf_2N] for 24 hrs and washing away [C_4mim][Tf_2N].

4.2.4 Conclusion

Saturation points of Syloid 63 silica particles in 1-alkyl-3-methylimidazolium-based ionic liquids are greatly influenced by the structures of ILs' anions and cations as evidenced by the correlations with the pure IL pure properties, such as molar volume and free volume. The silica particle saturation point is determined by a maximum volume fraction, which is consistent with a packing fraction typical of close-packed systems. In most cases, the silica particles remain the same size upon mixing in the ionic liquids, but in the case of [bmim][PF_6] which is known to react with water to form HF, a decrease in silica particle size was observed.

4.2.5 References

1. Chiappe, C.; Pieraccini, D. *J. Phys. Org. Chem.* 2005, *18*, 275-297.
2. Ngo, H. L.; LeCompte, K.; Hargens, L.; McEwen, A. B. *Thermochim. Acta* 2000, *357*, 97-102.
3. Seddon, K. R. *J. Chem. Technol. Biotechnol.* 1997, *68*, 351-356.
4. Liu, X. D.; Ma, J. M.; Zheng, W. J. *Rev. Adv. Mater. Sci.* 2011, *27*, 43-51.
5. Morris, R. E. *Top. Catal.* 2010, *53*, 1291-1296.
6. Morris, R. E. *Chem. Commun.* 2009, 2990-2998.
7. Taubert, A.; Li, Z. *Dalton Trans.* 2007, 723-727.
8. Antonietti, M.; Kuang, D. B.; Smarsly, B.; Yong, Z. *Angew. Chem. Int. Ed.* 2004, *43*, 4988-4992.
9. Han, L. J.; Wang, Y. B.; Li, C. X.; Zhang, S. J.; Lu, X. M.; Cao, M. J. *AIChE J.* 2008, *54*, 280-288.
10. Parnham, E. R.; Morris, R. E. *Acc. Chem. Res.* 2007, *40*, 1005-1013.
11. Xu, L.; Choi, E. Y.; Kwon, Y. U. *Inorg. Chem.* 2007, *46*, 10670-10680.
12. Xu, R. S.; Zhang, W. P.; Guan, J.; Xu, Y. P.; Wang, L.; Ma, H. J.; Tian, Z. J.; Han, X. W.; Lin, L. W.; Bao, X. H. *Chem. Eur. J.* 2009, *15*, 5348-5354.
13. Ma, H. J.; Tian, Z. J.; Xu, R. S.; Wang, B. C.; Wei, Y.; Wang, L.; Xu, Y. P.; Zhang, W. P.; Lin, L. W. *J. Am. Chem. Soc.* 2008, *130*, 8120-8121.
14. Parnham, E. R.; Morris, R. E. *Chem. Mater.* 2006, *18*, 4882-4887.
15. Parnham, E. R.; Morris, R. E. *J. Am. Chem. Soc.* 2006, *128*, 2204-2205.
16. Parnham, E. R. Ionothermal Synthesis: A new synthesis methodology using ionic liquids and eutectic mixtures as both solvent and template in zeotype synthesis. PhD Thesis, University of St Andrews, 2006.
17. Wheatley, P. S.; Allan, P. K.; Teat, S. J.; Ashbrook, S. E.; Morris, R. E. *J. Chem. Sci.* 2010, *1*, 483-487.
18. Ma, Y. C.; Xu, Y. P.; Wang, S. J.; Wang, B. C.; Tian, Z. J.; Yu, J. Y.; Lin, L. W. *Chem. J. Chin. Univ.* 2006, *27*, 739-741.
19. Itoh, N. *J. Electrochem. Soc.* 2009, *156*, J37-J40.

20. Safavi, A.; Maleki, N.; Iranpoor, N.; Firouzabadi, H.; Banazadeh, A. R.; Azadi, R.; Sedaghati, F. *Chem. Commun.* 2008, 6155-6157.

21. Donato, R. K.; Migliorini, M. V.; Benvegnu, M. A.; Stracke, M. P.; Gelesky, M. A.; Pavan, F. A.; Schrekker, C. M. L.; Benvenutti, E. V.; Dupont, J.; Schrekker, H. S. *J. Sol-Gel Sci. Technol* 2009, *49*, 71-77.

22. Ueno, K.; Lnaba, A.; Kondoh, M.; Watanabe, M. *Langmuir* 2008, *24*, 5253-5259.

23. Ueno, K.; Hata, K.; Katakabe, T.; Kondoh, M.; Watanabe, M. *J. Phys. Chem. B* 2008, *112*, 9013-9019.

24. McKeen, J. C.; Davis, M. E. *J. Phys. Chem. C* 2009, *113*, 9870-9877.

25. Wang, L.; Xu, Y. P.; Wei, Y.; Duan, J. C.; Chen, A. B.; Wang, B. C.; Ma, H. J.; Tian, Z. J.; Lin, L. W. *J. Am. Chem. Soc.* 2006, *128*, 7432-7433.

26. Gaillon, L.; Sirieix-Plenet, J.; Letellier, P. *J. Solution Chem.* 2004, *33*, 1333-1347.

27. Cadena, C.; Anthony, J. L.; Shah, J. K.; Morrow, T. I.; Brennecke, J. F.; Maginn, E. J. *J. Am. Chem. Soc.* 2004, *126*, 5300-5308.

28. Golovanov, D. G.; Lyssenko, K. A.; Vygodskii, Y. S.; Lozinskaya, E. I.; Shaplov, A. S.; Antipin, M. Y. *Russ. Chem. Bull.* 2006, *55*, 1989-1999.

29. Ye, C. F.; Shreeve, J. M. *J. Phys. Chem. A* 2007, *111*, 1456-1461.

30. Jenkins, H. D. B.; Roobottom, H. K.; Passmore, J.; Glasser, L. *Inorg. Chem.* 1999, *38*, 3609-3620.

31. Golovanov, D. G.; Lyssenko, K. A.; Antipin, M. Y.; Vygodskii, Y. S.; Lozinskaya, E. I.; Shaplov, A. S. *Cryst. Growth Des.* 2005, *5*, 337-340.

32. Wang, J. J.; Wang, H. Y.; Zhang, S. L.; Zhang, H. H.; Zhao, Y. *J. Phys. Chem. B* 2007, *111*, 6181-6188.

33. Yan, F.; Texter, J. *Chem. Commun.* 2006, 2696-2698.

34. Domanska, U.; Bogel-Lukasik, E.; Bogel-Lukasik, R. *Chem. Eur. J.* 2003, *9*, 3033-3041.

35. Sun, A. J.; Zhang, J. L.; Li, C. X.; Meng, H. *Chin. J. Chem.* 2009, *27*, 1741-1748.

36. Buffeteau, T.; Grondin, J.; Danten, Y.; Lassegues, J. C. *J. Phys. Chem. B* 2010, *114*, 7587-7592.

37. Tokuda, H.; Hayamizu, K.; Ishii, K.; Abu Bin Hasan Susan, M.; Watanabe, M. *J. Phys. Chem. B* 2004, *108*, 16593-16600.

38. Katsuta, S.; Shiozawa, Y.; Imai, K.; Kudo, Y.; Takeda, Y. *J. Chem. Eng. Data* 2009, *55*, 1588-1593.

39. Fredlake, C. P.; Crosthwaite, J. M.; Hert, D. G.; Aki, S.; Brennecke, J. F. *J. Chem. Eng. Data* 2004, *49*, 954-964.

40. Jacquemin, J.; Husson, P.; Padua, A. A. H.; Majer, V. *Green Chem.* 2006, *8*, 172-180.

41. Li, W. J.; Zhang, Z. F.; Han, B. X.; Hu, S. Q.; Xie, Y.; Yang, G. Y. *J. Phys. Chem. B* 2007, *111*, 6452-6456.

42. Strechan, A. A.; Paulechka, Y. U.; Blokhin, A. V.; Kabo, G. J. *J. Chem. Thermodyn.* 2008, *40*, 632-639.

43. Fan, W.; Zhou, Q.; Sun, J.; Zhang, S. J. *J. Chem. Eng. Data* 2009, *54*, 2307-2311.

44. Gordon, C. M.; Holbrey, J. D.; Kennedy, A. R.; Seddon, K. R. *J. Mater. Chem.* 1998, *8*, 2627-2636.

45. Krossing, I.; Slattery, J. M.; Daguenet, C.; Dyson, P. J.; Oleinikova, A.; Weingartner, H. *J. Am. Chem. Soc.* 2006, *128*, 13427-13434.

46. Trohalaki, S.; Pachter, R. *OSAR Comb. Sci.* 2005, *24*, 485-490.

47. Lopez-Martin, I.; Burello, E.; Davey, P. N.; Seddon, K. R.; Rothenberg, G. *ChemPhysChem* 2007, *8*, 690-695.

48. Hanke, C. G.; Price, S. L.; Lynden-Bell, R. M. *Mol. Phys.* 2001, *99*, 801-809.

49. Torquato, S.; Truskett, T. M.; Debenedetti, P. G. *Phy. Rev. Lett.* 2000, *84*, 2064-2067.

50. Chung, Y. W. *Introduction to Materials Science and Engineering*; CRC Press: Boca Raton, FL, USA, 2007.

51. Fuller, J.; Carlin, R. T.; Delong, H. C.; Haworth, D. *J. Chem. Soc., Chem. Commun.* 1994, 299-300.

52. Camper, D.; Bara, J.; Koval, C.; Noble, R. *Ind. Eng. Chem. Res.* 2006, *45*, 6279-6283.

53. Jacquemin, J.; Nancarrow, P.; Rooney, D. W.; Gomes, M. F. C.; Husson, P.; Majer, V.; Padua, A. A. H.; Hardacre, C. *J. Chem. Eng. Data* 2008, *53*, 2133-2143.

54. Roberts, N. J.; Seago, A.; Carey, J. S.; Freer, R.; Preston, C.; Lye, G. J. *Green Chem.* 2004, *6*, 475-482.

55. Widegren, J. A.; Laesecke, A.; Magee, J. W. *Chem. Commun.* 2005, 1610-1612.

56. Whitten, K. W.; Davis, R. E.; Peck, L. M.; Stanley, G. G. *Chemistry*, 8th ed.; Brooks/Cole Publishing Co.: Pacific Grove, CA, USA, 2006.

4.3 Solubility of Aluminophosphates' Precursors in Ionic Liquids

4.3.1 Introduction

4.3.1.1 Introduction to ionic liquid and aluminophosphates

Room temperature ionic liquids or ionic liquids are a group of chemicals, composed of solely cations and anions. Most of the cations are large and asymmetric; they could not pack very closely with the anions. As a result, lattice energy between cations and anions is lowered and melting points of ionic liquids are generally lower than 100 ^{o}C, with a few as low as -96 ^{o}C.[1-4] Besides their low melting points, most of them have negligible vapor pressure at high temperatures, compared with common solvent. As a result, the wide liquid range of ionic liquids makes them ideal for applications where common solvent are not suitable.[5-11] Recently, a new method called ionothermal synthesis is invented by using ionic liquids solvents to synthesize materials.[12] Porous aluminophosphates are one type of those materials synthesized ionothermally.[13-23] In ionothermal synthesis of aluminophosphates, ionic liquids are used as the solvent and sometimes at the same time structure directing agent.[13,24] Substituting water with ionic liquids in the synthesis could make the use of high-pressure vessel unnecessary and has the potential to make new framework structures due to the vast number of ionic liquids by different combinations of cations and anions.[18,25]

4.3.1.2 Introduction to aim of this section

The aim of this section is to investigate the solubility of precursors of alumophosphates in ionic liquids. Since most of the ionothermal synthesis is taken place in 1-alkyl-3-methylimidazolium bromide ([$C_n$mim][Br]), [C_6mim][Br] is chosen as the solvent in the solubility tests. The most common precursors for AlPOs are $Al(OiPr)_3$ and H_3PO_4. As a result, solubilities of $Al(OiPr)_3$, pure H_3PO_4 and H_3PO_4 (85 wt%) in [C_6mim][Br] are tested. Experimentally determined solubilities are compared with ideal solubility calculated by solid liquid equilibrium equation and activity coefficients of $Al(OiPr)_3$ at different temperatures are calculated. Influences of the presence of H_3PO_4 and H_2O on solubility of $Al(OiPr)_3$ are

investigated. These results would be helpful to understand the interaction between precursors and ionic liquid, and interaction between different precursors of microporous aluminophosphates.

4.3.2 Experimental description

4.3.2.1 Preparation of ionic liquids

[C_2mim][Br], [C_4mim][Br] and [C_6mim][Br] were synthesized according to standard method. This method involves reacting 1-alkylbromide with 1-methylimidazole in acetonitrile for 2-6 days at 40 ^oC to get crude [$C_n$mim][Br]. The mixture of [$C_n$mim][Br] and acetonitrile are then mixed with activated carbon which is separated by filtration after 24 hours. After passing through an acidic activated aluminum oxide column, the mixture is dried for about 4 days at a temperature from 40 ^oC to 60 ^oC until the water content of the products was lower than 500 ppm, as confirmed by Karl-fischer titration. Liquid NMR was used to check the purity of the products.

4.3.2.2 Source of $Al(OiPr)_3$ and phosphoric acid

$Al(OiPr)_3$ (labeled impurity 98 wt%) was bought from Fisher and used as received. Pure phosphoric acid or phosphorus pentoxide was also bought from Fisher and used to measure the solubility of pure phosphoric acid in ionic liquid. It was white crystal and the labeled purity is 99 wt%.

4.3.2.3 Solubility measurement

Sample 1, 2 and 3 are mixtures of pure $Al(OiPr)_3$ and [C_6mim][Br] with weight ratio 1: 19. Sample 5, 6 and 7 are mixtures of $Al(OiPr)_3$, H_3PO_4 and [C_6mim][Br] with different initial weight ratio. Sample 8 are mixtures of $Al(OiPr)_3$, H_3PO_4, [C_6mim][Br] and water. All of the above samples are mixed at 25 ^oC for four hours and centrifuged for 3 hours at a specific temperature to ensure all of the un-dissolved particles in the solutions are separated. The model of centrifuge is Eppendorf 5810R . These samples are centrifuged at an angular velocity of 3000 rpm. Then concentration of $Al(OiPr)_3$ is measured by Atomic Absorption Spectroscopy (AAS). The AAS used in this dissertation is AA 240 manufactured by Varian, Inc with a GTA 120 graphite tube atomizer and a cold vapor generation accessory Varian Model VGA65.

Sample 4 is a mixture of H_3PO_4 and $[C_6mim][Br]$. Initially, H_3PO_4 is added into $[C_6mim][Br]$ and the mixture is stirred until the solution becomes homogeneous. Then the mixture is left unstirred for 24 hours and separation of phases is observed. The total concentration of phosphorus in the top layer of the mixture was determined using inductively coupled plasma optical emission spectrometer (ICP-OES 720) from Varian Inc. at wavelength of 178. 222nm.

4.3.3 Results and analysis

4.3.3.1 Experimental result

After the undissolved particles are separated from the solution, the final weight percent of $Al(OiPr)_3$, H_3PO_4, $[C_6mim][Br]$ and H_2O are listed in Table 4-5. For sample 4, concentration of H_3PO_4 in the top layer of the solution is also given in Table 4-5.

Table 4-5 Initial concentration and final concentration of the mixtures and the centrifuge temperature.

ID.	Initial concentration				Final concentration				Temp.
	$Al(OiPr)_3$ wt %	H_3PO_4 wt %	$[C_6mim][Br]$ wt %	H_2O wt %	$Al(OiPr)_3$ wt %	H_3PO_4 wt %	$[C_6mim][Br]$ wt %	H_2O wt %	^oC
1	5	0	95	0	0.42	0	99.58	0	20
2	5	0	95	0	0.46	0	99.54	0	20
3	5	0	95	0	1.83	0	98.17	0	40
4	5	0	95	0	1.93	0	98.07	0	40
5	5	0	95	0	4.56	0	95.44	0	80
6	0	83	17	0	0	44.92	55.08	0	20
7	4.6	7	88.4	0	1.1	7.2	91.7	0	20
8	4.4	13.1	82.5	0	1.4	13.6	85.1	0	20
9	3.8	22.9	73.2	0	1.8	23.4	74.8	0	20
10	4.41	6.35	88.12	1.12	1.9	6.52	90.43	3.05	20

4.3.3.2 Binary System

The binary system of $Al(OiPr)_3$ and $[C_6mim][Br]$ with an initial weight ratio of 1: 19 are centrifuged at 20 ^oC, 40 ^oC and 80 ^oC, separately. The concentrations of $Al(OiPr)_3$ in the solution are 0.42-0.46 wt%, 1.83-1.93 wt% and 4.56 wt% after the undissolved particles are removed from the mixtures. These numbers are lower than the initial concentration and indicate the

solubility of $Al(OiPr)_3$ in $[C_6mim][Br]$ is low. The low solubility demonstrates the interaction between $Al(OiPr)_3$ and $[C_6mim][Br]$ will not inhibit the interaction between $Al(OiPr)_3$ and H_3PO_4 in the formation process of AlPOs. The influence of temperature on the solubility of $Al(OiPr)_3$ in $[C_6mim][Br]$ is shown in Figure 4.13. With the increase of temperature, solubility $Al(OiPr)_3$ in $[C_6mim][Br]$ increases almost linearly.

After phase separation in the mixture of H_3PO_4 and $[C_6mim][Br]$, solubility of H_3PO_4 in IL-rich phase is 44.92 wt%. Another two experiments were tested with initial concentration of H_3PO_4 lower than 44.92 wt%; one is 40 wt%, the other is 30 wt%. No phase split was observed for these two samples, proving the saturation solubility of H_3PO_4 in $[C_6mim][Br]$ is higher than 40 wt%. This result is used to maximize yield of AlPOs (see section 6.1.3.4) by increasing concentration of H_3PO_4 nearly to the saturation concentration in the reaction gel of AlPOs.[26]

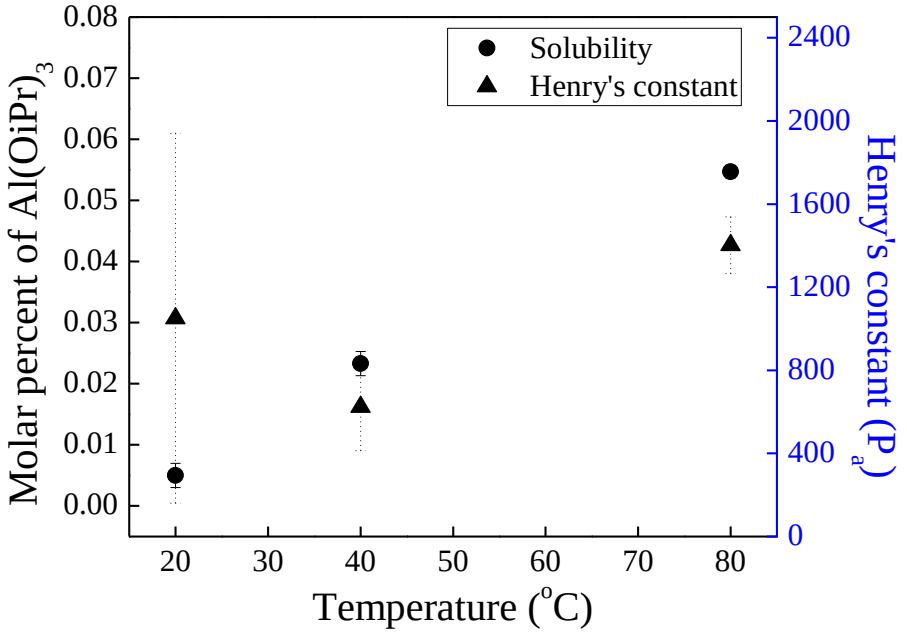

Figure 4.13 Influence of temperature on solubility of $Al(OiPr)_3$ in $[C_6mim][Br]$.

4.3.3.2.1 Ideal solubility of $Al(OiPr)_3$ and H_3PO_4 in $[C_6mim][Br]$

The ideal solubility of $Al(OiPr)_3$ and H_3PO_4 in $[C_6mim][Br]$ is modeled by standard solid-liquid equilibrium (SLE) models since the precursors have relatively high melting temperatures. The general SLE equation[27] is given below:

$$\ln\left(\frac{f_i^s}{f_i^{scl}}\right)=\left[\frac{\Delta_{fus}\underline{H}(T_{tp,i})}{R}\right]\left(\frac{1}{T_{tp,i}}-\frac{1}{T}\right)+\left(\frac{\Delta_{fus}Cp_i}{R}\right)\left[\frac{T_{tp,i}}{T}-1-\ln\left(\frac{T_{ip,j}}{T}\right)\right]-\frac{\Delta_{fus}\underline{V}}{RT}(P-P_{tp}) \qquad \textbf{Equation 4-1}$$

where $\frac{f_i^s}{f_i^{scl}}=x_i\gamma_i$. If the triple point temperature ($T_{tp,i}$) can be approximated by the melting temperature (T_m) and the $\Delta_{fus}Cp_i$ terms are negligible relative to the $\Delta_{fus}\underline{H}$ terms, the equations can be simplified to

$$\ln\left(\frac{f_i^s}{f_i^{scl}}\right)=\left[\frac{\Delta_{fus}\underline{H}(T_{tp,i})}{R}\right]\left(\frac{1}{T_{tp,i}}-\frac{1}{T}\right)=\left[\frac{\Delta_{fus}\underline{H}}{R}\right]\left(\frac{1}{T_m}-\frac{1}{T}\right)=\left[-\frac{\Delta_{fus}\underline{H}}{RT_m}\right]\left(\frac{T_m}{T}-1\right) \qquad \textbf{Equation 4-2}$$

The constants used to calculate ideal solubility and ideal solubility of $Al(OiPr)_3$ and H_3PO_4 at different temperatures are listed in Table 4-6. Heat of fusion for $Al(OiPr)_3$ is obtained by differential scanning calorimetry and heat of fusion for H_3PO_4 is retrieved from literature.[28] The ideal solubility of each component is obtained by assuming activity coefficient is equal to one. The ideal solubility of H_3PO_4 at 20 ^oC is 67.5 mol% = 45.46 wt%. From experiment, the solubility of H_3PO_4 in $[C_6mim][Br]$ is 44.95 wt%, very close to the simulation result from SLE model. But the solubilities of $Al(OiPr)_3$ in $[C_6mim][Br]$ are much lower than the ideal solubilities regardless of the temperature.

Table 4-6 Constants used to calculate ideal solubility by SLE model and ideal solubilities of $Al(OiPr)_3$ and H_3PO_4 in $[C_6mim][Br]$ at different temperatures.

Material	T_m (^oC)	$\Delta_{fus}\underline{H}$ (J/g)	$\Delta_{fus}\underline{H}$ (J/mol)	MW (g/mol)	Ideal solubility (mol %)			Ideal solubility (wt%)		
					20 ^oC	40 ^oC	80 ^oC	20 ^oC	40 ^oC	80 ^oC
$Al(OiPr)_3$	138.2	21.265	4343.376	204.25	59.9	67.1	81.1	38.59	46.18	64.35
H_3PO_4	42.4	136.73	13400	98	67.5				45.46	

4.3.3.2.2 Calculation of activity coefficient and Henry's constant using experimental data

If the solution behaves ideally, the solubility depends only on the solute properties and not on the solvent. Activity coefficient is used to account for the dependence of solubility on the solvent. Activity coefficient of $Al(OiPr)_3$ in $[C_6mim][Br]$ at different temperatures are calculated based on SLE models.

$$\ln(\frac{f_i^s}{f_i^{scl}}) = \ln(x_i\gamma_i) = \left[\frac{\Delta_{fus}\underline{H}(T_{tp,i})}{R}\right](\frac{1}{T_{tp,i}} - \frac{1}{T}) = \left[\frac{\Delta_{fus}\underline{H}}{R}\right](\frac{1}{T_m} - \frac{1}{T}) = \left[-\frac{\Delta_{fus}\underline{H}}{RT_m}\right](\frac{T_m}{T} - 1)$$

Equation 4-3

The constants used in this equation are listed in Table 4-6 and the activity coefficients of $Al(OiPr)_3$ at 20 ^oC, 40 ^oC and 80 ^oC are listed in Table 4-7. From Table 4-7, it can be seen that activity coefficient for $Al(OiPr)_3$ in $[C_6mim][Br]$ is bigger than one and the magnitude increases with the increase in temperature. Deviation of activity coefficient from one indicates $Al(OiPr)_3$ does not behave ideally in $[C_6mim][Br]$.

Table 4-7 Information for calculation of Henry's constant.

ID.	Molar percent of $Al(OiPr)_3$ mol. %	Partial pressure of $Al(OiPr)_3$ P_a	Temp. ^oC	Henry's constant P_a	Activity coefficient
1	0.0547±0.001	76.72±7.40[30]	80	1402±137	15.249
2	0.0233±0.002	14.53±4.73[30*]	40	624±210	125.065
3	0.0050±0.002	5.25±3.98[30*]	20	1050±890	118.918

*: Extrapolated from the data in the literature[30]

Henry's constant, an important thermodynamic property of a substance, could be calculated based on Henry's law given partial pressure of the solute in the gas phase and solubility of this solute in the liquid phase. This law was proposed in 1803 by William Henry.[29] In mathematical form, Henry's law is presented as $H_A = \frac{P_A}{c_A}$, where P_A is the partial pressure of solute in the gas phase, c_A is the molarity of solute in the liquid phase and H_A is Henry's constant. Pressure of $Al(OiPr)_3$ is measured and reported by Bleyerveld and his coworkers at a temperature from 80 ^oC to 126 ^oC.[30] Saturated pressures of $Al(OiPr)_3$ at 20 ^oC and 40 ^oC are extrapolated from the linear relationship between saturated pressure and temperature reported by Bleyerveld.[30] The extrapolated pressures at 20 ^oC and 40 ^oC are low and with big uncertainties. Henry's constant at 80 ^oC is calculated by Equation 4-4 and Henry's constants at different temperatures are listed in Table 4-7.

$$\frac{(76.72 \pm 7.40)Pa}{(0.0547 \pm 0.001)mol\%} = 1402 \pm 137Pa$$

Equation 4-4

Dr. Wick in Louisiana Technology University used molecular models to simulate the free energy of solvation of $Al(OiPr)_3$ in $[C_6mim][Br]$. He calculated the free energy to be -6.4 kcal/mol at 80 ^oC, while the experimental value obtained in this study is -9.5 kcal/mol calculated from Henry's constant at 80 ^oC. The two numbers are very close with each other.

4.3.3.3 Ternary system

Table 4-8 Initial concentration and final concentration of the ternary system and the centrifuge temperature.

ID.	Initial concentration				Final concentration				Temp.
	$Al(OiPr)_3$ wt %	H_3PO_4 wt %	$[C_6mim][Br]$ wt %	H_2O wt %	$Al(OiPr)_3$ wt %	H_3PO_4 wt %	$[C_6mim][Br]$ wt %	H_2O wt %	^oC
7	4.6	7	88.4	0	1.1	7.2	91.7	0	20
8	4.4	13.1	82.5	0	1.4	13.6	85.1	0	20
9	3.8	22.9	73.2	0	1.8	23.4	74.8	0	20

Table 4-8 shows the initial concentration and final concentration of the ternary systems (sample 7, sample 8 and sample 9). These samples are mixtures of three components, $Al(OiPr)_3$, H_3PO_4 and $[C_6mim][Br]$. Solubility of $Al(OiPr)_3$ is tested at 20 ^oC. Concentration of H_3PO_4 in the mixture is calculated by assuming the ratio of H_3PO_4 to $[C_6mim][Br]$ is the same as the initial ratio since the initial concentration of H_3PO_4 is much lower than the saturation concentration. For these samples, initial weight ratio of $Al(OiPr)_3$ to IL is kept the same, around 1:19, but concentration of H_3PO_4 keeps increasing. The influence of concentration of H_3PO_4 can be seen in the final concentration of $Al(OiPr)_3$. With the increase of concentration of H_3PO_4 in the mixture, concentration of $Al(OiPr)_3$ in the IL-rich phase also increases, from 1.1 wt% to 1.4 wt%, then to 1.8 wt%. As also observed by solid state NMR (see section 5.1.3.2), at 20 ^oC, $Al(OiPr)_3$ begins to interact with H_3PO_4 in $[C_6mim][Br]$. Since H_3PO_4 has high solubility in $[C_6mim][Br]$ and it has interaction with $Al(OiPr)_3$, $Al(OiPr)_3$ has higher solubility in $[C_6mim][Br]$ with the presence of H_3PO_4. Figure 4.14 is the ternary diagram for equilibrium weight ratio of $Al(OiPr)_3$: H_3PO_4: $[C_6mim][Br]$ and weight composition of reaction gel for SIZ-1, a crystalline porous material. From Figure 4.14, it can be seen that concentration of $Al(OiPr)_3$ in the reaction gel of SIZ-1 and equilibrium concentration in the mixtures of $Al(OiPr)_3$, H_3PO_4 and $[C_6mim][Br]$ are similar.

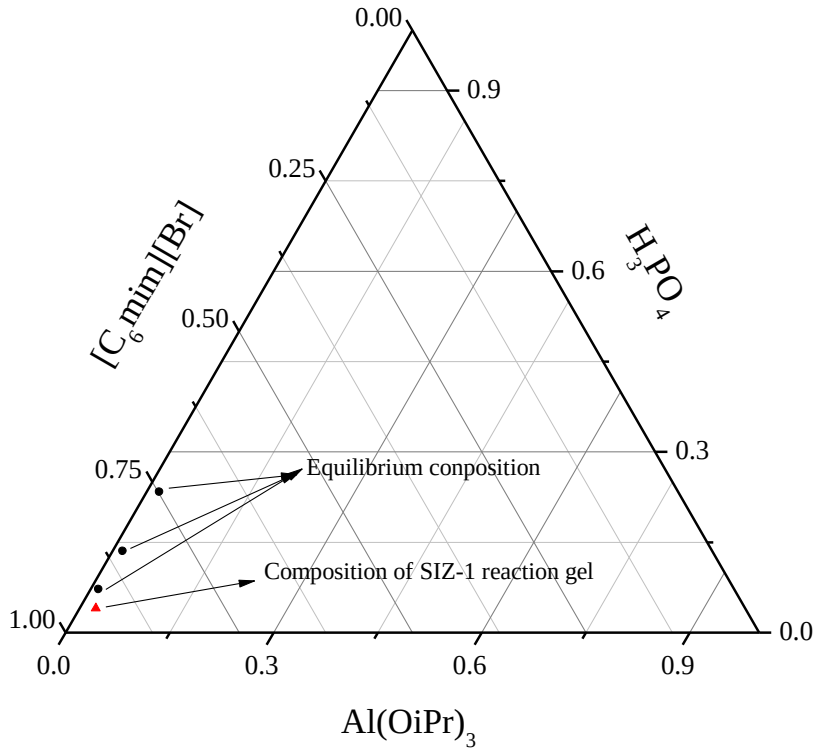

Figure 4.14 Ternary diagram for equilibrium weight ratio of $Al(OiPr)_3$: H_3PO_4: $[C_6mim][Br]$ and weight composition of reaction gel for SIZ-1.

4.3.3.4 Quaternary system

Initial concentration and final concentration of the quaternary system (including $Al(OiPr)_3$, H_3PO_4, H_2O and $[C_6mim][Br]$) are shown in Table 4-9. Concentration of each component in the quaternary system (sample 10) is very similar to those in sample 7, except the presence of water in sample 10. It seems that the small amount of water has an influence on solubility of $Al(OiPr)_3$ in the mixture. $Al(OiPr)_3$ could hydrolyze with the presence of water and the formation of Al(OH) could probably leads to the increase of its solubility.

Table 4-9 Initial concentration and final concentration of the quaternary system and the centrifuge temperature.

ID.	Initial concentration				Final concentration				Temp.
	$Al(OiPr)_3$ wt %	H_3PO_4 wt %	$[C_6mim][Br]$ wt %	H_2O wt %	$Al(OiPr)_3$ wt %	H_3PO_4 wt %	$[C_6mim][Br]$ wt %	H_2O wt %	^oC
10	4.41	6.35	88.12	1.12	1.9	6.52	90.43	3.05	20

4.3.4 Conclusion

Aluminium isopropoxide ($Al(OiPr)_3$) and pure phosphoric acid (H_3PO_4) are dissolved in 1-hexyl-3-methylimidazolium bromide at several temperatures in order to investigate solubilities of precursors or aluminophosphates in ionic liquids. It is found that solubility of $Al(OiPr)_3$ in $[C_6mim][Br]$ is very low, lower than its concentration in a reaction gel, indicating the reaction is a heterogeneous reaction. As a comparison, pure phosphoric acid could dissolve in ionic liquid easily, up to 44 wt%. Ideal solubilities of $Al(OiPr)_3$ in solution is calculated and compared with the experimental solubility data. Parameters such as activity coefficient and Henry's constant are given. Deviation of activity coefficients from one suggests the behavior of $Al(OiPr)_3$ in $[C_6mim][Br]$ is not ideal. Solubilities of $Al(OiPr)_3$ in ternary system (including $Al(OiPr)_3$, H_3PO_4 and $[C_6mim][Br]$ and in quaternary system (including $Al(OiPr)_3$, H_3PO_4, H_2O and $[C_6mim][Br]$) are also tested. It is found that at 20 ^oC, with the increase of H_3PO_4 concentration, more $Al(OiPr)_3$ is dissolved in $[C_6mim][Br]$, indicating an interaction between H_3PO_4 and $Al(OiPr)_3$.

4.3.5 Reference

1. Krossing, I.; Slattery, J. M.; Daguenet, C.; Dyson, P. J.; Oleinikova, A.; Weingartner, H. *Journal of the American Chemical Society* **2006**, *128*, 13427-13434.
2. Rooney, D.; Jacquemin, J.; Gardas, R. L. Thermophysical Properties of Ionic Liquids. In *Ionic Liquids*, 2009; Vol. 290; pp 185-212.
3. Trohalaki, S.; Pachter, R. *Qsar & Combinatorial Science* **2005**, *24*, 485-490.
4. Zhang, S. J.; Sun, N.; He, X. Z.; Lu, X. M.; Zhang, X. P. *Journal of Physical and Chemical Reference Data* **2006**, *35*, 1475-1517.
5. Fox, M. F.; Priest, M. *Proceedings of the Institution of Mechanical Engineers Part J-Journal of Engineering Tribology* **2008**, *222*, 291-303.
6. Itoh, N. *Journal of the Electrochemical Society* **2009**, *156*, J37-J40.
7. Li, Z. J.; Chang, J.; Shan, H. X.; Pan, J. M. *Reviews in Analytical Chemistry* **2007**, *26*, 109-153.
8. McFarlane, J.; Ridenour, W. B.; Luo, H.; Hunt, R. D.; DePaoli, D. W.; Ren, R. X. *Separation Science and Technology* **2005**, *40*, 1245-1265.
9. Yagi, T.; Sasaki, S.; Mano, H.; Miyake, K.; Nakano, M.; Ishida, T. *Proceedings of the Institution of Mechanical Engineers Part J-Journal of Engineering Tribology* **2009**, *223*, 1083-1090.
10. Youngs, T. G. A.; Hardacre, C.; Holbrey, J. D. *Journal of Physical Chemistry B* **2007**, *111*, 13765-13774.
11. Zhao, H. L.; Tang, Z. X.; Zhang, Q. G.; You, J. H.; Chen, Q. D. *Progress in Chemistry* **2009**, *21*, 2077-2083.
12. Parnham, E. R.; Morris, R. E. *Accounts of Chemical Research* **2007**, *40*, 1005-1013.
13. Cooper, E. R.; Andrews, C. D.; Wheatley, P. S.; Webb, P. B.; Wormald, P.; Morris, R. E. *Nature* **2004**, *430*, 1012-1016.
14. Cai, R.; Sun, M. W.; Chen, Z. W.; Munoz, R.; O'Neill, C.; Beving, D. E.; Yan, Y. S. *Angewandte Chemie-International Edition* **2008**, *47*, 525-528.
15. Fayad, E. J.; Bats, N.; Kirschhock, C. E. A.; Rebours, B.; Quoineaud, A. A.; Martens, J. A. *Angewandte Chemie-International Edition* **2010**, *49*, 4585-4588.

16. Han, L. J.; Wang, Y. B.; Li, C. X.; Zhang, S. J.; Lu, X. M.; Cao, M. J. *Aiche Journal* **2008**, *54*, 280-288.
17. Han, L. J.; Wang, Y. B.; Zhang, S. J.; Lu, X. M. *Journal of Crystal Growth* **2008**, *311*, 167-171.
18. Morris, R. E. *Chemical Communications* **2009**, 2990-2998.
19. Parnham, E. R.; Morris, R. E. *Journal of the American Chemical Society* **2006**, *128*, 2204-2205.
20. Parnham, E. R.; Morris, R. E. *Chemistry of Materials* **2006**, *18*, 4882-4887.
21. Parnham, E. R.; Morris, R. E. *Journal of Materials Chemistry* **2006**, *16*, 3682-3684.
22. Parnham, E. R.; Wheatley, P. S.; Morris, R. E. *Chemical Communications* **2006**, 380-382.
23. Wang, L.; Xu, Y. P.; Wei, Y.; Duan, J. C.; Chen, A. B.; Wang, B. C.; Ma, H. J.; Tian, Z. J.; Lin, L. W. *Journal of the American Chemical Society* **2006**, *128*, 7432-7433.
24. Xu, Y. P.; Tian, Z. J.; Wang, S. J.; Hu, Y.; Wang, L.; Wang, B. C.; Ma, Y. C.; Hou, L.; Yu, J. Y.; Lin, L. W. *Angewandte Chemie-International Edition* **2006**, *45*, 3965-3970.
25. Seddon, K. R. "Ionic liquids: designer solvents?" International George Papatheodorou Symposium, 1999, Patras, Greece.
26. Sun, X.; Polifka, A.; Anthony, J. L. *Manuscript in preparation*,***2012***.
27. Walas, S. M. Phase Equilibria in Chemical Engineering. Butterworth: Boston, 1985.
28. Weast, R. C.; Astle, M. J.; Beyer, W. H. Handbook of Chemistry and Physics. 64th ed. CRC Press, Inc. Boca Raton, FL, 1984.
29. Ball, D. W. Physical Chemistry. Thomson Learning. Pacific Grove, CA, 2011.
30. Bleyerve.Rh; Fieggen, W.; Gerding, H. *Recueil Des Travaux Chimiques Des Pays-Bas* **1972**, *91*, 477-&.

4.4 Decomposition of Ionic Liquids by Phosphoric Acid

4.4.1 Introduction

One of the limitations of the use the ionic liquid in the ionothermal synthesis of molecular sieves is the high cost of ionic liquids. Although the commonly used 1-alkyl-3-methylimidazolium bromide or chloride ([$C_n$mim][Br] or [$C_n$mim][Cl]) are cheaper than the other ionic liquids, they are still much more expensive than water used in traditional hydrothermal synthesis. For example, the price of [C_4mim][Cl] (100 g) costs $ 185 on the website of Fisher Scientific. Several options could be used to lower the cost of ionothermal synthesis, including but are not limited to usage of self-made ionic liquid from 1-alkylimidazole and bromoalkane and reuse the ionic liquids after each synthesis. The price of materials to make [C_4mim][Cl] (100g) should be less than $ 50.

In ionothermal synthesis of aluminophosphates, the most common precursors added into ionic liquids are $Al(OiPr)_3$ and H_3PO_4. Addition of structure directing agent and other acids are optional. If ionic liquids are to be reused, after the synthesis, they should maintain their original structures and should not decompose. To the best of the author's knowledge, $Al(OiPr)_3$ will not decompose [$C_n$mim][Br] or [$C_n$mim][Cl]. Then the problem comes to H_3PO_4. Will H_3PO_4 decompose ionic liquids?

4.4.2 Experimental description

[C_2mim][Br] and [C_4mim][Br] are used as the ionic liquids to test the decomposition effect of phosphoric acid. H_3PO_4 (85 wt%) is added into [C_2mim][Br] at two different molar ratios. The molar ratio of [C_2mim][Br] to H_3PO_4 to H_2O in sample 2 is 1:00 : 0.26 : 0.25, and molar ratio in sample 3 is 1.00 : 0.16 : 0.15. They are mixed at 80 ^oC for 30 mins, and homogeneous solutions are obtained after the mixing. Then the mixtures are stored in an oven at 50 ^oC. A small portion of each solution is taken out after a certain time and analyzed by liquid ^1H NMR. These times are 16 hours, 84 hours, 204 hours, 234 hours and 426 hours. Another sample (sample 4) is made of H_3PO_4 in [C_4mim][Br] at a molar ratio of 0.255: 1:00 and stored at 150 ^oC for one hour. In

addition, a reaction gel (sample 5) with a composition of 1 $Al(OiPr)_3$: 2.55 H_3PO_4: 0.8 HCl: 40 [C_4mim][Br] is heated at 150 ^oC for 5 days and its ^1H NMR pattern is obtained and compared with standard NMR pattern of [C_4mim][Br]. The type of NMR used in this dissertation is INOVA 400. It operates at 400 MHz frequency. Chloroform-d is used as the solvent to test samples; its peak appears at 7.26 ppm. Composition of each sample and preparation conditions are listed in Table 4-10.

Table 4-10 Molar ratio of each component and preparation conditions for each sample.

Sample	H_3PO_4	$Al(OiPr)_3$	H_2O *	IL		Other		Mix T. ^oC	Store T. ^oC	Store time hr
1	-	-	-	[C_2mim][Br]		-		-	20	16,84,204,234,426
2	0.255	-	0.245	[C_2mim][Br]	1.000	-		80	50	16,84,204,234,426
3	0.160	-	0.154	[C_2mim][Br]	1.000	-		80	50	16,84,204,234,426
4	0.255	-	0.245	[C_4mim][Br]	1.000	-		80	150	1
5	0.064	0.025	0.136	[C_4mim][Br]	1.000	HCl	0.020	80	150	120

*: No H_2O is added. The small amount of H_2O comes from H_3PO_4 and HCl solutions

4.4.3 Results and discussion

4.4.3.1 Decomposition of [C_2mim][Br] by H_3PO_4 at 50 ^oC

After sample 2 and sample 3 are mixed with phosphoric acid and left at 50 ^oC for several hours to several days, a small portion of them is taken out and analyzed by ^1H NMR. Spectra of these samples are then compared with spectrum of pure [C_2mim][Br] in order to determine if there is any decompositian product. ^1H NMR spectra of sample 2 and sample 3 after storing at 50 ^oC for 426 hours compared with spectrum of pure [C_2mim][Br] are shown in Figure 4.15. The spectra of sample 2 and sample 3 after storing for 16 hours, 84 hours, 204 hours and 234 hours are in the Appendix A. Extra peaks corresponding to the decomposed products begin to form within 16 hours and the amount of decomposed products increase slowly with the increase of time, as shown in Figure 4.16. Take sample 2 for example, within 16 hours, the ratio of peak intensities between the highest peak and the highest extra peak is 28.1: 1.0 and this ratio becomes 16.0: 1.0 after 234 hours. Ratio of areas under the peaks indicate the molar ratio of H atoms attached to a specific position of undecomposed IL and the H atoms attached to a specific

position of decomposed IL. Since the peaks are sharp and narrow, ratio of peaks intensities should be similar to the ratio of area under the peaks and should be similar to the molar ratio of undecomposed IL to decomposed IL. Even after 426 hours (about 18 days), the intensities of the peaks corresponding to decomposed products are still low. The ratio of peak intensities between the highest peak and the highest extra peak is 11.2: 1.0 for sample 2 and 9.6: 1.0 for sample 3, and these ratios should be similar to the molar ratio of undecomposed IL to the decomposed IL. The big ratios indicate only a small portion of [C_2mim][Br] is decomposed by phosphoric acid. Sample 2 and sample 3 do not have a significant difference in the amount of decomposed products within the 426 hours.

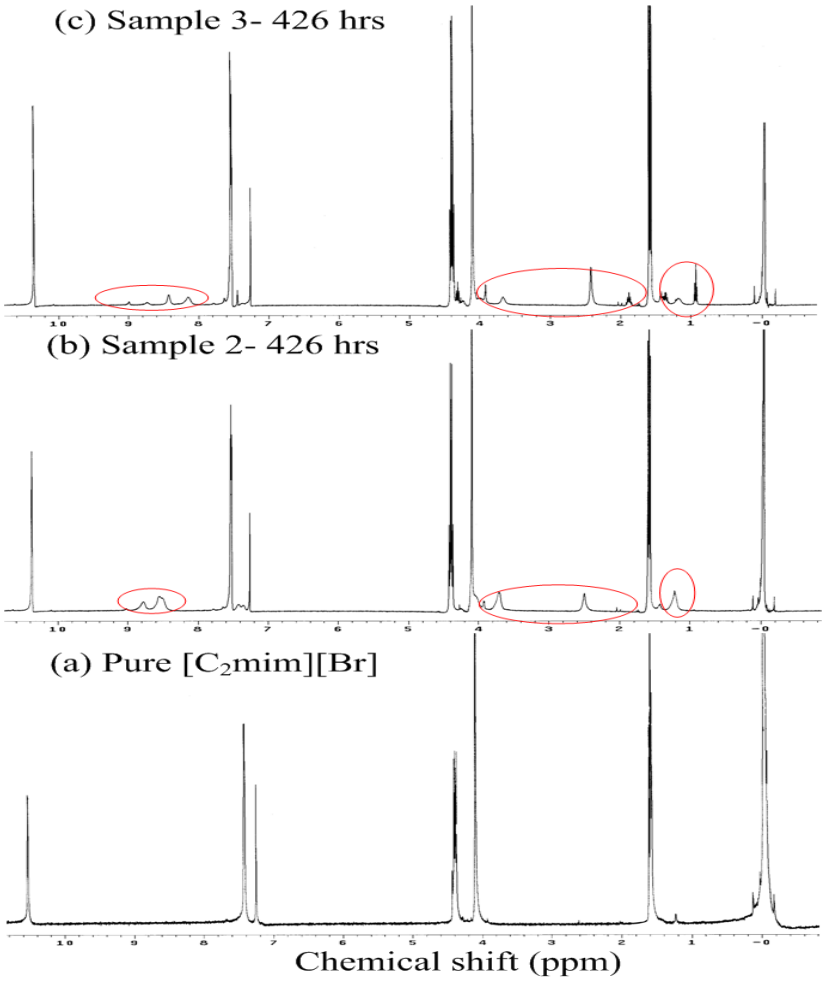

Figure 4.15 ^{1}H NMR spectra of (a) pure [C_2mim][Br], (b) sample 2 after heating for 426 hours and (c) sample 3 after heating for 426 hours.

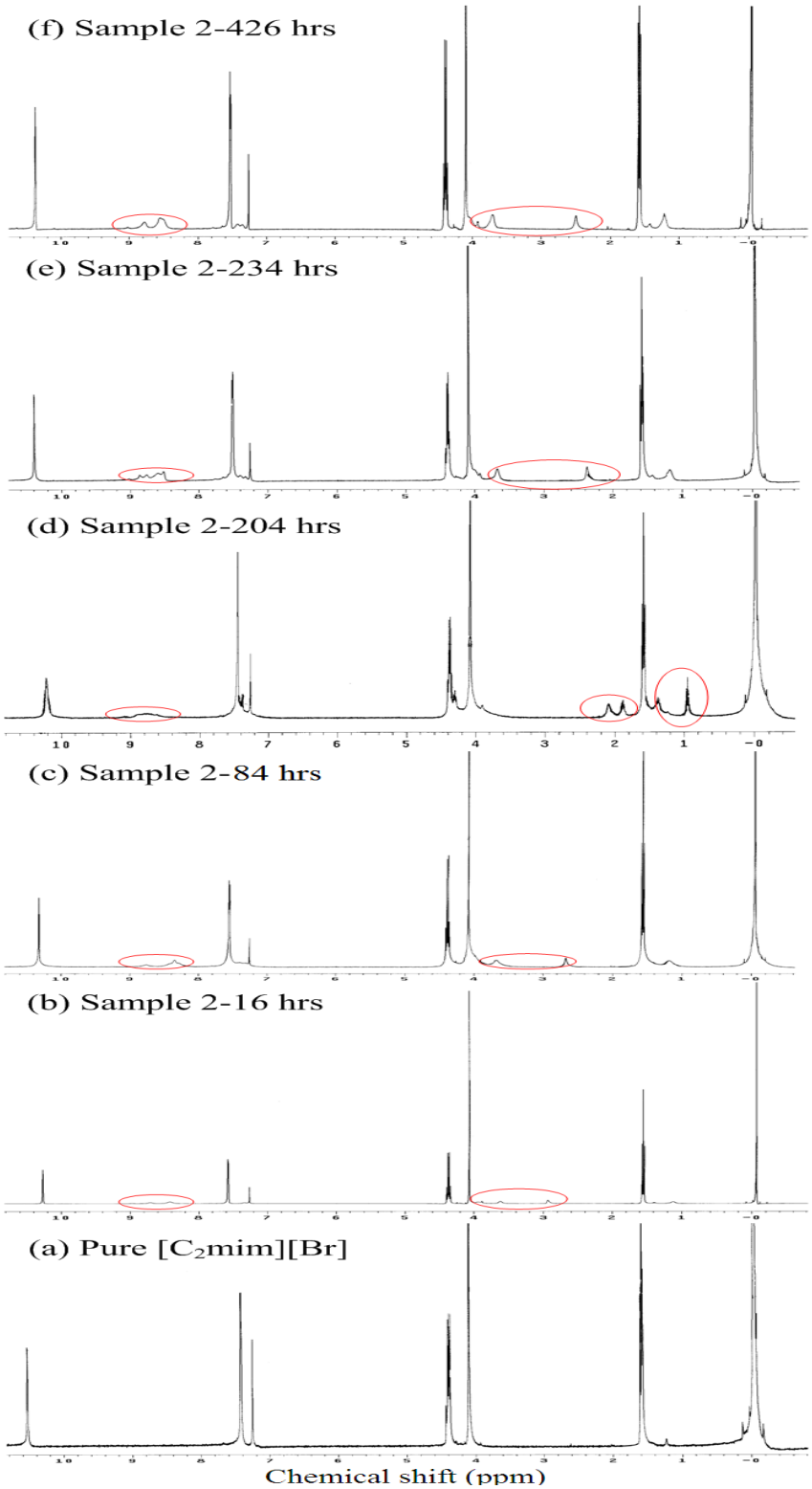

Figure 4.16 ^{1}H NMR spectra of (a) pure [C_2mim][Br] and sample 2 after heating for (b) 16 hours, (c) 84 hours, (d) 204 hours, (e) 234 hours and (f) 426 hours.

4.4.3.2 Short time decomposition effect of H_3PO_4 at 150 ^oC

In order to test the short-time decomposition effect of H_3PO_4 at reaction temperature (150 ^oC) on [C_4mim][Br], ^1H NMR spectrum of sample 4 after heating at 150 ^oC for one hour is compared with the ^1H NMR pattern of [C_4mim][Br] after heating at 150 ^oC for one hour. The spectra are shown in Figure 4.17. Only one extra peak with low intensity shows up in Figure 4.17-(c). The ratio of peak intensity between the highest peak and the highest extra peak is 37.8: 1.0 and this big ratio indicates most of [C_4mim][Br] is not decomposed either by the higher temperature or by the presence of H_3PO_4 after one hour.

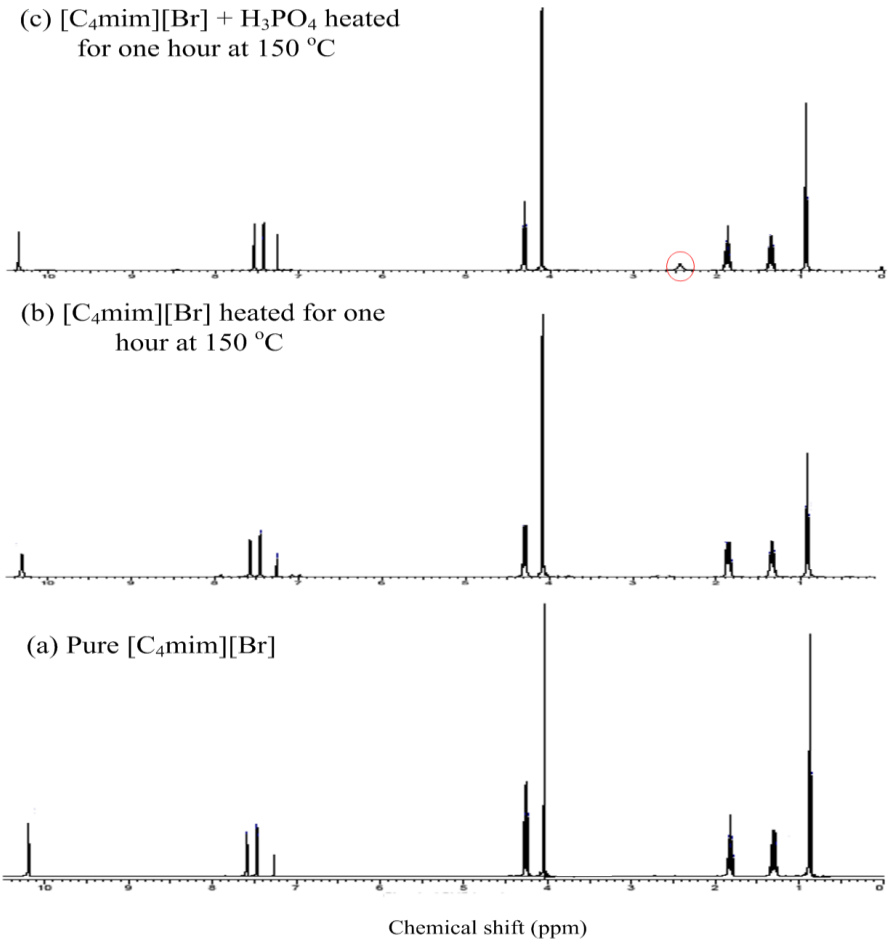

Figure 4.17 ^1H NMR spectra of (a) pure [C_4mim][Br], (b) pure [C_4mim][Br] after heating at 150 ^oC for one hour, and (c) sample 4 after heating at 150 ^oC for one hour.

4.4.3.3 Long time decomposition effect of ingredients in a reaction gel on ILs at 150 ^{o}C

In order to test the stability of [C_4mim][Br] in ionothermal synthesis of aluminophosphates, a reaction gel (sample 5) is prepared and heated at 150 ^{o}C for five days. This reaction gel could yield a crystalline structure of AEL after heating at 150 ^{o}C for five days.[1] Its spectrum is shown in Figure 4.18, along with the spectrum of pure [C_4mim][Br]. As can be seen from Figure 4.18, only one extra peak appears in Figure 4.18-(b). This peak is highly likely to be the peak corresponding to the H atoms in the dissolved aluminium isopropoxide, since the environment around H atoms in $Al(OiPr)_3$ is very similar to the H atoms whose corresponding peak is to the immediate right of the extra peak. The concentration of phosphoric acid in sample 5 is not as high as in sample 4 (molar ratio of phosphoric acid to IL is 0.064: 1.00 for sample 5 as compared to 0.255: 1.00 for sample 4). This might explain why the extra peak showing up at around 2.5 ppm in Figure 4.17-(c) is not shown in Figure 4.18-(b).

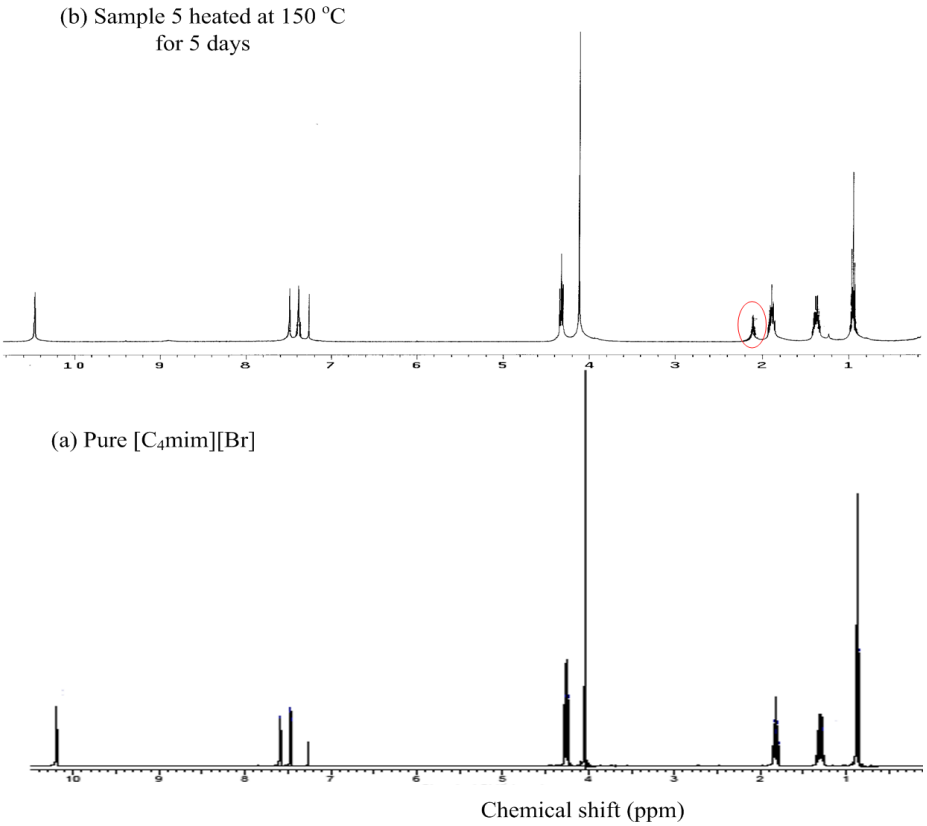

Figure 4.18 ^{1}H NMR spectra of (a) pure [C_4mim][Br] and (b) sample 5 after heating at 150 ^{o}C for 5 days.

4.4.4 Conclusion

From the comparison of NMR spectra, it can be seen that the addition of H_3PO_4 is capable of decomposing $[C_2mim][Br]$ with a molar ratio of 0.255:1.00 or 0.160:1.00 at 50 ^oC. But the decomposed amount is very small and increase very slowly with the increase of storage time. After one hour heating at 150 ^oC, spectrum of a mixture of phosphoric acid and $[C_4mim][Br]$ with a molar ratio of 0.255:1:00 only has a very small extra peak. In addition, the ^1H NMR pattern of the reaction gel composed of $Al(OiPr)_3$, H_3PO_4, HCl and $[C_4mim][Br]$ does not have much difference with the standard pattern of pure $[C_4mim][Br]$ after heating at 150 ^oC for five days, suggesting even at higher temperature, the presence of acid does not decompose much of $[C_4mim][Br]$. In conclusion, the reuse of $[C_nmim][Br]$ in ionothermal synthesis of aluminophosphates should not be prohibited by the use of H_3PO_4.

Section 4.1 is taken from the publication: Sun, X. and Anthony, J. L. "Influences of Side Chain Length of 1-Alkyl-3-Methylimidazolium Bromide on the Silica Saturation", Ionic Liquids: From Knowledge to Application, ACS Symposium Series 1030, N. V. Plechkova, R. Rogers and K. R. Seddon, eds. 2009, 189-197.

Section 4.2 is taken from the publication: Sun, X. and Anthony, J. L. “Influence of Structural Variation in Imidazolium-based Ionic Liquids on SiO2 Particle Saturation Points”, J. Phys. Chem. C, 2012, 116, 3274-3280.

Section 4.3 and 4.4 are soon to be submitted manuscripts.

4.4.5 Reference

1. Sun, X.; Polifka, A.; Anthony, J. L. *Manuscript in preparation **2012***.

Chapter 5 - Interactions between Precursors and Solvent

5.1 Effect of Structure of Ionic Liquids and Phosphoric Acid on Structure of Aluminum Isopropoxide

5.1.1 Introduction

5.1.1.1 Introduction to ionic liquids and ionothermal synthesis

Ionic liquids (ILs) are chemicals which are commonly composed of large organic cations and inorganic anions. Different from other salts, they generally have melting points which are lower than 100 ^{o}C due to the low lattice energies between cations and anions. Ionic liquids recently have found many applications in new chemical and extractive process,[1,2] fuel cells,[3] catalysis,[4,5] lubrications,[6] etc., due to their unique properties common organic solvents do not obtain. These properties include but are not limited to a wide liquid range, negligible vapor pressure for most of ILs, and numerous types of ILs could be synthesized by combining different cations and anions.[7-9]

Due to ILs' favorable properties, especially low vapor pressure, they are employed as solvent and sometimes a simultaneous structure directing agent SDA in the synthesis of microporous materials, such as silica-based zeolite and aluminophosphates.[10-12] This method is called ionothermal synthesis as a comparison to hydrothermal synthesis where water is used as the solvent. Since most of the ILs have negligible vapor pressure, synthesis of molecular sieves could be conducted in an open container and use of ILs could simplify the synthesis process by making the addition of SDA unnecessary since ILs often have structures similar to commonly used SDA in hydrothermal synthesis. The most common ILs used in ionothermal synthesis of silica-based zeolite and aluminophosphates are 1-alkyl-3-methylimidaozlium bromide ([$C_n$mim][Br]).

5.1.1.2 Introduction to interaction between precursors in ionic liquids

Much research has focused on the mechanism of molecular sieves' formation in hydrothermal synthesis, but less is known about synthesizing molecular sieves in ionic liquids.

Until now, researchers have found heating source (conventional oven vs microwave heating), water content, addition of structure directing agent (or acid) and other factors could influence the frameworks synthesized.

There are several studies on the conformation of Al atoms in the ionothermally synthesized frameworks as determined by solid state NMR. Fayad and coworkers found that without addition of SDA in the reaction gel, the final frameworks contains tetracoordinated Al (Al atoms in the framework, d=32.5 ppm), pentacoordinated Al (Al atoms in the framework with a fifth ligand, probably F^- ions, d=21 ppm) and hexacoordinated Al (tentatively assigned to water coordinated Al in the cages, d=-13 ppm).[13] Wang and coworkers obtained similar solid state NMR patterns for magnesium-containing aluminophosphate molecular sieves. They found tetracoordinated Al has an intense signal in the d=40.5 and 39.6 ppm region, pentacoordinated Al around d=28 ppm and a broad peak at d=-13 ppm corresponding to hexacoordinated Al.[14] But there is no research on coordination of Al atoms in solution for ionothermal synthesis, either after the precursor is added into the ionic liquid or after both the Al source and phosphoric acid are added into the ionic liquid. The aim of this paper is to investigate effect of ionic liquids and other precursors on the change of Al in aluminium isopropoxide ($Al(OiPr)_3$, a common Al source for molecular sieves in the aging process of ionothermal synthesis.

5.1.2 Experimental description

5.1.2.1 Preparation of ionic liquids

$[C_2mim][Br]$, $[C_4mim][Br]$ and $[C_6mim][Br]$ were synthesized according to reported methods,[15] which involves reacting 1-alkylbromide with 1-methylimidazole in acetonitrile for two to six days at 40 ^oC to get crude $[C_nmim][Br]$. The mixture of $[C_nmim][Br]$ and acetonitrile are then mixed with activated carbon which is separated by filtration after 24 hours. After passing through an acidic activated aluminum oxide column, the mixture is dried for about four days at a temperature from 40 ^oC to 60 ^oC until the water content of the products was lower than 500 ppm confirmed by Karl-Fischer titration. Liquid NMR was used to check the purity of the products.

5.1.2.2 Source of $Al(OiPr)_3$ and phosphoric acid

$Al(OiPr)_3$ is from Fisher Scientific. Before being mixed with ionic liquids, it is first dried in oven at 100 ^oC for 2 hours, and then ground into fine powder. Phosphoric acid (H_3PO_4, 85 wt%) is bought from Fisher and used as received.

5.1.2.3 Preparation of samples for ^{27}Al solid state NMR

Mixtures of IL and $Al(OiPr)_3$, and mixtures of IL and $Al(OiPr)_3$ and H_3PO_4 are stirred for four hours until the mixtures become homogeneous. Mixtures containing [C_2mim][Br] and [C_4mim][Br] (melting points of pure [C_2mim][Br] and [C_4mim][Br] are 76.9 ^oC and 69 ^oC,[16,17] respectively) are heated at 70 ^oC while stirring and mixtures containing [C_6mim][Br] (melting points of pure [C_6mim][Br] is -54.9 ^oC[18]) are stirred at room temperature (20-22 ^oC). The molar ratio of $Al(OiPr)_3$ and IL is fixed at 1:10 for all of the samples. When phosphoric acid is added, the molar ratio of $Al(OiPr)_3$ and phosphoric acid is fixed at 1:2.55. These molar ratios are very similar to those used to synthesize aluminophosphates in ionic liquids.[19] Since phosphoric acid used in this experiment is 85 wt %, water is also induced into the system. Molar ratios of $Al(OiPr)_3$, IL, H_3PO_4 and water for all of the samples are listed in Table 5-1.

Table 5-1 Molar composition of samples and their mixing temperature.

Sample ID.	$Al(OiPr)_3$	Ionic liquid		H_3PO_4	H_2O (*)	Mix temp.(^oC)
1	1	0		0	0	20
2	1	[C_2mim][Br]	10	0	0	70
3	1	[C_4mim][Br]	10	0	0	70
4	1	[C_6mim][Br]	10	0	0	20
5	1	[C_2mim][Br]	10	2.55	2.45	70
6	1	[C_4mim][Br]	10	2.55	2.45	70
7	1	[C_6mim][Br]	10	2.55	2.45	20

H_2O*: from phosphoric acid (85wt%)

5.2.2.4 Solid state NMR

Solid state NMR spectra were acquired on a Bruker Avance III 400 spectrometer (Bruker Biospin, Billerica, MA) operating at 400.1 MHz for ^1H and 104.26 MHz for ^{27}Al. The probe is a Bruker 2 channel probe with a 4 mm spinning system. Spectrometer setup uses $Al(OH)_6$ as a secondary external chemical shift reference at 0 ppm. Each sample is packed into a Kel-F insert

and inserted into a 4.0 mm zirconia rotor (Bruker Biospin, Billerica, MA). Magic angle spinning uses a sample spinning rate of 4 kHz. Excitation times of 0.60 μs are used for direct excitation. A pulse delay of 1.0 second is used. The spectral width is 50 kHz and the acquisition time is 20 ms. Proton decoupling is performed with a proton decoupling field of 64 kHz. Each data set is the sum of 14400 transients. A spectrum is acquired for each sample at 20 ^{o}C and at 70 ^{o}C.

Mixtures of IL with aluminium isopropoxide are solid or semisolid. Mixtures with aluminium isopropoxide and phosphoric acid are viscous liquids. To collect data, these samples are loaded into sealable inserts that are then placed in the solid state NMR rotors. For the liquids this is necessary at room temperature. For the semi-solid samples this is necessary to accommodate the possibility of melting at elevated temperatures. One consequence of using these inserts is a substantially lower spinning speed. These inserts could only be safely spun at 4 kHz instead of the 15 kHz that this size rotor can normally be spun. The spectra are plotted by sample and temperature.

5.1.3 Experimental result and discussion

^{27}Al NMR spectrum for each sample was collected at room temperature (20 ^{o}C) and at a higher temperature (either at 70 ^{o}C or 80 ^{o}C). ^{27}Al NMR spectra of $Al(OiPr)_3$ obtained at 20 ^{o}C and 80 ^{o}C are shown in Figure 5.1.

These spectra are used as the reference to compare with other spectra so as to indicate what the interactions between IL and $Al(OiPr)_3$, and between H_3PO_4 and $Al(OiPr)_3$ are. There is a sharp peak in the pattern of $Al(OiPr)_3$ (sample 1). This sharp peak is the peak of Al(VI). From 20 ppm to 70 ppm, there are another two broad peaks which are attributed to Al(V) and Al(IV), respectively. The intensities of the Al(V) and Al(IV) peaks are extremely low. This result indicates Al atoms in $Al(OiPr)_3$ are mainly hexacoordinated Al.

Peaks of tetracoordinated-Al (Al(IV)), pentacoordinated-Al (Al(V) and hexacoordinated-Al (Al(VI)) are listed in Table 5-2, which lists the mixing temperature and analysis temperature of each sample, location and intensity of each peak and intensity ratio of Al(IV) to Al(VI) and Al(V) to Al(VI). Intensity of peaks corresponding to Al(VI) is set to be one for each sample.

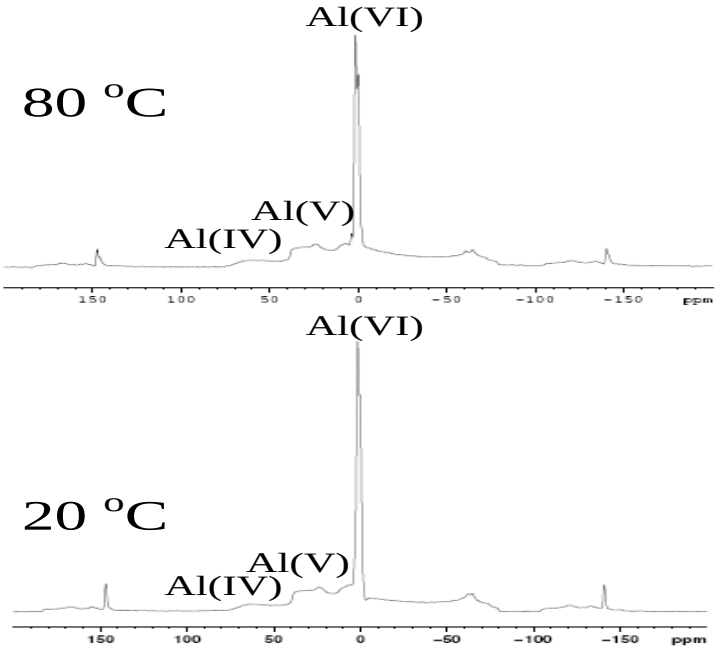

Figure 5.1 ^{27}Al NMR spectra of $Al(OiPr)_3$ at 20 °C and at 80 °C.

Table 5-2 Location and intensity of peaks corresponding to different coordinations of Al atoms at their highest intensity location tested at 20 °C and a higher temperature.

				Analysis Temp.: 70 °C (or 80 °C for sample 6)			Analysis Temp.: 20 °C		
ID.	*Desciption*	*Mix T °C*	*Al Type*	*Location ppm*	*Inten.*	*Inten. ratio*	*Location ppm*	*Inten.*	*Inten. ratio*
1	$Al(OiPr)_3$	20	Al(IV)	65	7.20E+07	**0.18**	65	6.00E+07	**0.15**
			Al(V)	24	9.50E+07	0.24	24	8.00E+07	0.2
			Al(VI)	3	4.00E+08	1	3	4.00E+08	1
2	$[C_2mim][Br]+Al(OiPr)_3$	70	Al(IV)	-	-	-	-	-	-
			Al(V)	-	-	-	-	-	-
			Al(VI)	6.1	3.8E+08	1.00	6.1	3.8E+08	1.00
3	$[C_4mim][Br]+Al(OiPr)_3$	70	Al(IV)	61.8	1.8E+08	**0.45**	66.1	2.2E+08	**0.47**
			Al(V)	33.3	2.0E+08	0.52	35.3	2.3E+08	0.49
			Al(VI)	4.6	3.9E+08	1.00	4.1	4.7E+08	1.00
4	$[C_6mim][Br]+Al(OiPr)_3$	20	Al(IV)	56.4	3.2E+08	**1.06**	-	-	-
			Al(V)	35.6	3.2E+08	1.07	-	-	-
			Al(VI)	3.0	3.0E+08	1.00	1.1	4.6E+08	1.00
5	$[C_2mim][Br]+Al(OiPr)_3+H_3PO_4$	70	Al(IV)	39.2	4.8E+08	**4.64**	39.2	3.6E+08	**2.02**
			Al(V)	6.7	1.0E+08	1.00	-	-	-
			Al(VI)	-18.6	1.0E+08	1.00	-17.1	1.8E+08	1.00
6	$[C_4mim][Br]+Al(OiPr)_3+H_3PO_4$	70	Al(IV)	38.4	4.7E+08	**8.82**	38.7	2.7E+08	**1.86**
			Al(V)	2.5	4.0E+07	0.76	2.5	6.3E+07	0.43
			Al(VI)	-17.8	5.3E+07	1.00	-16.5	1.5E+08	1.00
7	$[C_6mim][Br]+Al(OiPr)_3+H_3PO_4$	20	Al(IV)	38.6	3.6E+08	**large**	38.4	7.2E+07	**0.24**
			Al(V)	-	-	-	-	-	-
			Al(VI)	-	-	-	-15.2	3.0E+08	1.00

The interaction of ionic liquid, phosphoric acid and aluminium isopropoxide, effects of sample composition and temperature on the coordination of Al atoms in ionic liquids will be discussed in the following paragraphs.

5.1.3.1 Effect of IL on $Al(OiPr)_3$

After mixing aluminium isopropoxide with pure ionic liquids, the mixtures are scanned by ^{27}Al solid state NMR at 20 ^{o}C and 70 ^{o}C. These samples include $Al(OiPr)_3$ & $[C_2mim][Br]$, stirred at 70 ^{o}C (sample 2), $Al(OiPr)_3$ & $[C_4mim][Br]$, stirred at 70 ^{o}C (sample 3) and $Al(OiPr)_3$ & $[C_6mim][Br]$, stirred at 20 ^{o}C (sample 4). Molar ratio of $Al(OiPr)_3$ to IL is 1:10 for all of these three samples. ^{27}Al NMR spectra of these samples tested at 70 ^{o}C are shown in Figure 5.2.

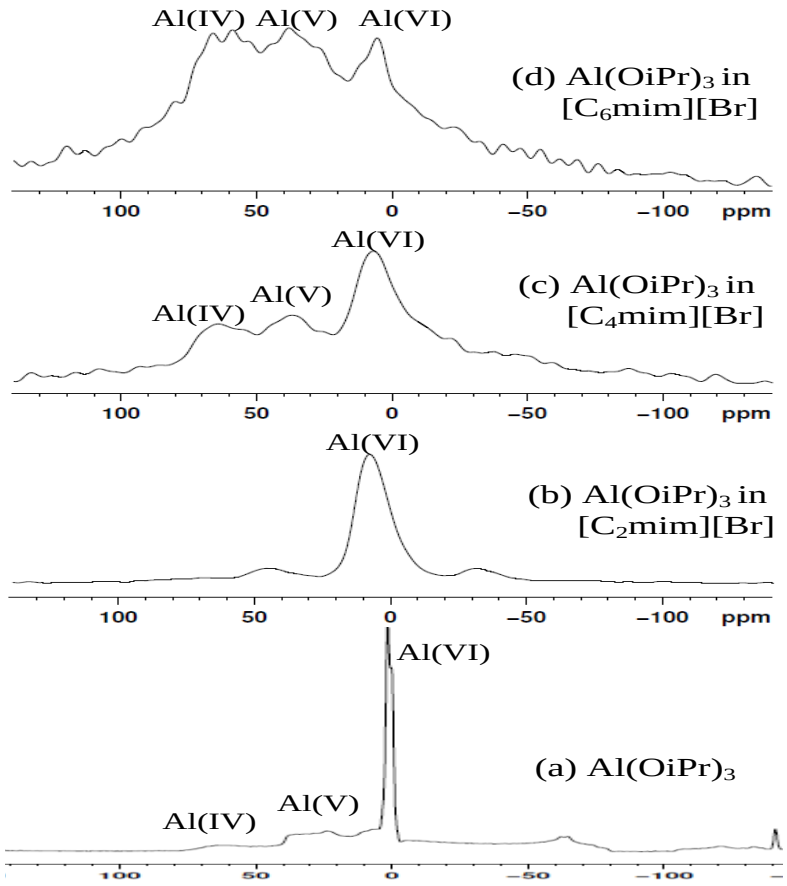

Figure 5.2 ^{27}Al NMR spectra of (a) $Al(OiPr)_3$ scanned at 80 ^{o}C, (b) $Al(OiPr)_3$ in $[C_2mim][Br]$ scanned at 70 ^{o}C, (c) $Al(OiPr)_3$ in $[C_4mim][Br]$ scanned at 70 ^{o}C and (d) $Al(OiPr)_3$ in $[C_6mim][Br]$ scanned at 70 ^{o}C.

After $Al(OiPr)_3$ is mixed with ionic liquids, peaks corresponding to pentacoordinated Al atoms and tetracoordinated Al atoms increase in intensity, notably in the mixtures of $Al(OiPr)_3$ and $[C_4mim][Br]$ or $[C_6mim][Br]$. From Table 5-2, it can be also seen that with the increase of alkyl chain length of imidazolium ring of IL, ratio of Al(IV) to Al(VI) increases from nearly 0 for $Al(OiPr)_3$ in $[C_2mim][Br]$ to 0.45 for $Al(OiPr)_3$ in $[C_4mim][Br]$, then to 1.06 for $Al(OiPr)_3$ in $[C_6mim][Br]$. In as-synthesized porous aluminophosphates, most of the Al atoms are tetracoordinated and little if any Al atoms are pentacoordinated or octacoordinated. From the above result, even without adding any mineralizer, structure directing agent or phosphoric acid, Al atoms in aluminium isopropoxide tends to change their conformation to facilitate the formation of frameworks in ionic liquids at a higher temperature.

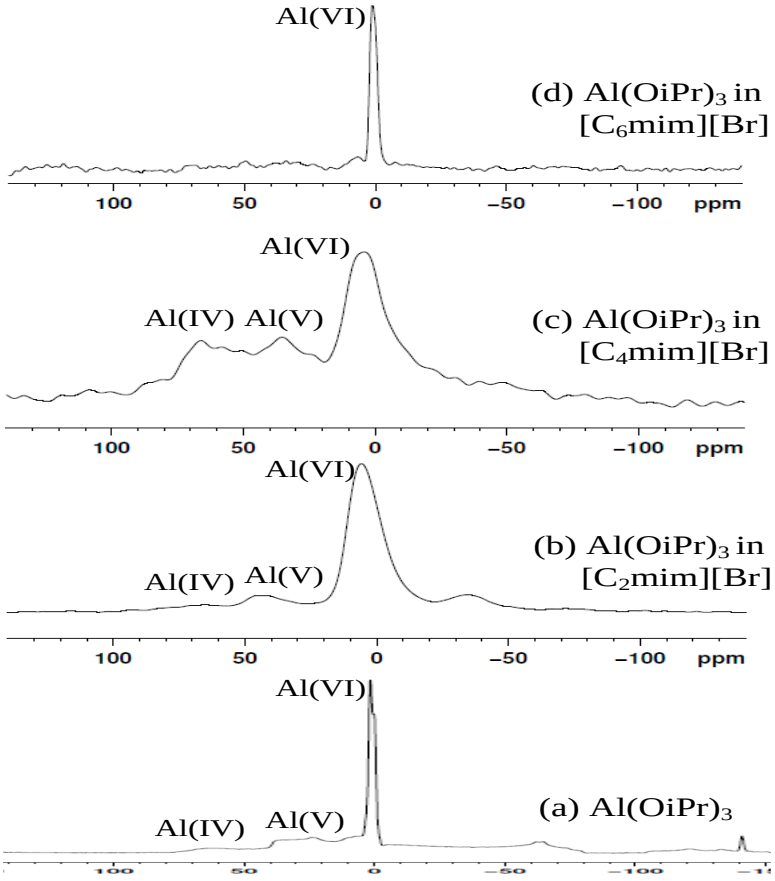

Figure 5.3 ^{27}Al NMR spectra of (a) $Al(OiPr)_3$ scanned at 20 ^{o}C, (b) $Al(OiPr)_3$ in $[C_2mim][Br]$ scanned at 20 ^{o}C, (c) $Al(OiPr)_3$ in $[C_4mim][Br]$ scanned at 20 ^{o}C and (d) $Al(OiPr)_3$ in $[C_6mim][Br]$ scanned at 20 ^{o}C.

The spectra for samples analyzed at 20 ^{o}C are shown in Figure 5.3. The trend of increasing proportions of Al(IV) and Al(V) with the increase of alkyl chain length in the imidazolium ring of ionic liquids is not seen at 20 ^{o}C. The change of Al coordination in ionic liquid is most pronounced at a higher temperature. A mixture of $Al(OiPr)_3$ and $[C_2mim][Br]$, and a mixture of $Al(OiPr)_3$ and $[C_4mim][Br]$ are stirred at 70 ^{o}C for 4 hours before scanned by solid state NMR at 20 ^{o}C. During the stirring process, the change of Al coordination has occurred and Al(VI) begins to grow into Al(V) and Al(IV). When mixture of $Al(OiPr)_3$ and $[C_6mim][Br]$ is stirred and analyzed by solid state NMR at 20 ^{o}C, the coordination of Al atoms in the mixture does not undergo dramatic change; Al(VI) does not grow into Al(V) and Al(IV).

5.1.3.2 Effect of phosphoric acid on $Al(OiPr)_3$ in IL

The influence of phosphoric acid (H_3PO_4) on the conformation of Al atoms in $Al(OiPr)_3$ dissolved in ILs was also investigated. Phosphoric acid is another important precursor for aluminophosphates. Samples 8, 10 and 12 are mixtures of $Al(OiPr)_3$ & H_3PO_4 & IL. The molar ratio of $Al(OiPr)_3$: H_3PO_4 : IL is 1: 2:55 : 10, a common composition ratio of a reaction gel to synthesize porous aluminophosphates.[19] Samples 5, 6 and 7 contains $[C_2mim][Br]$, $[C_4mim][Br]$ and $[C_6mim][Br]$, respectively.

Figure 5.4 shows the change of ^{27}Al NMR spectra of $Al(OiPr)_3$ when it is mixed with phosphoric acid and ionic liquids, scanned at 70 ^{o}C. Since the addition of H_3PO_4 causes electron density around Al atoms to increase, all of the peaks shift to the right. For the spectra of mixtures, peaks corresponding to Al(VI), Al(V) and Al(IV) shift to the location around -17 ppm, 5ppm and 39 ppm. The locations of these peaks match with the peak locations in as-synthesized aluminophosphates.[13,14,20-23] As can be seen in Figure 5.4, the intensity of Al(VI) decreases dramatically and Al(IV) increases in all of the ILs used. In sample 7, where $Al(OiPr)_3$ is mixed with H_3PO_4 and $[C_6mim][Br]$, all of the Al atoms are tetra-coordinated. From Table 5-2, it can be seen that with the increase of alkyl chain length, the ratio of Al(IV) to Al(VI) increases, from 4.64 for $Al(OiPr)_3$ in H_3PO_4 and $[C_2mim][Br]$, to 8.82 for $Al(OiPr)_3$ in H_3PO_4 and $[C_4mim][Br]$, then to only Al(IV) and no Al(VI) or Al(V) for $Al(OiPr)_3$ in H_3PO_4 and $[C_6mim][Br]$. As a comparison, the intensity ratio in $Al(OiPr)_3$ (sample 1) is only 0.18. This increasing ratio of Al(IV) to Al(VI) with the increase of alkyl chain length is the same with the trend observed in section 5.1.3.1, suggesting $[C_6mim][Br]$ could possibly accelerates the formation of Al-O-P

bonds. This behavior is consistent with the influence of alkyl chain length on formation time of crystalline materials observed in previous work.[19] It is found that with the same recipe, [C_6mim][Br] leads to the formation of porous materials in a much shorter time than [C_4mim][Br] (two hours compared with eight hours) and [C_4mim][Br] needs a much shorter time than [C_2mim][Br] for another recipe.[19]

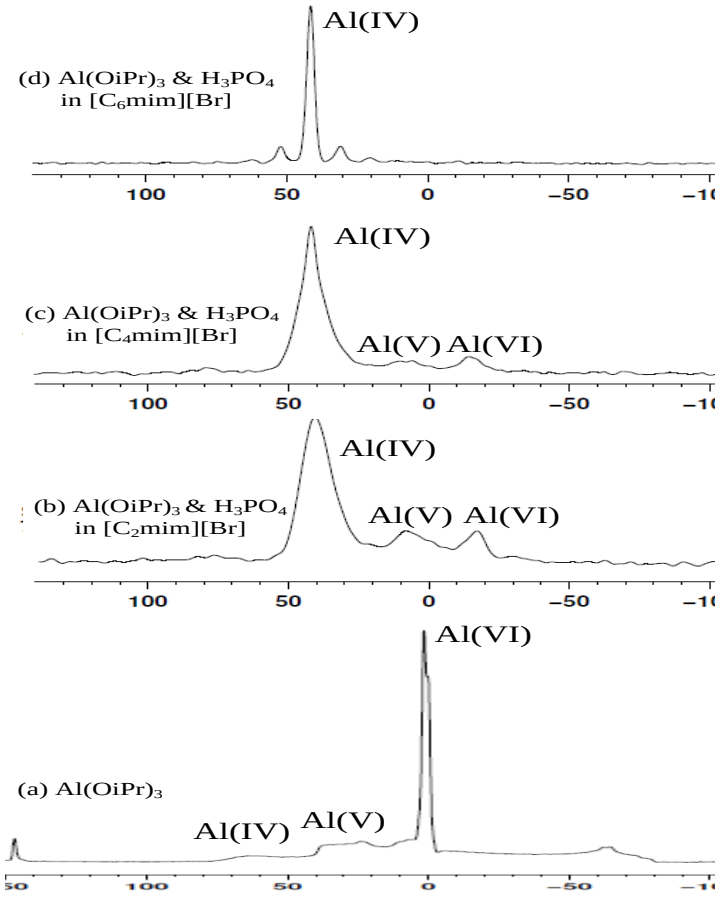

Figure 5.4 ^{27}Al NMR spectra of (a) Al(OiPr)$_3$ scanned at 80 ^{o}C, (b) Al(OiPr)$_3$ in [C_2mim][Br] and H_3PO_4 scanned at 70 ^{o}C, (c) Al(OiPr)$_3$ in [C_4mim][Br] and H_3PO_4 scanned at 70 ^{o}C and (d) Al(OiPr)$_3$ in [C_6mim][Br] and H_3PO_4 scanned at 70 ^{o}C.

Spectra of these samples scanned at 20 ^{o}C are shown in Figure 5.5. When H_3PO_4 is in the mixture, even at 20 ^{o}C, Al(VI) changes to Al(V) and Al(IV). Once again, at a low analysis temperature, the influence of a higher stirring temperature is observed to be more significant than that of the increased alkyl chain.

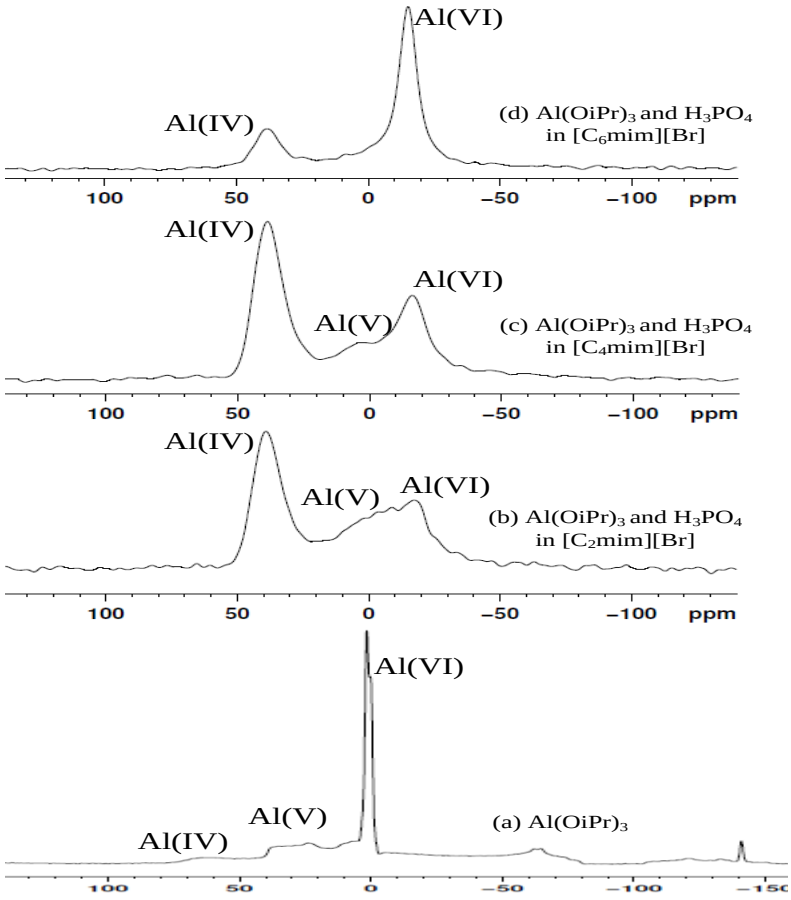

Figure 5.5 ^{27}Al NMR spectra of (a) $Al(OiPr)_3$ scanned at 20 ^{o}C, (b) $Al(OiPr)_3$ in $[C_2mim][Br]$ and H_3PO_4 scanned at 20 ^{o}C, (c) $Al(OiPr)_3$ in $[C_4mim][Br]$ and H_3PO_4 scanned at 20 ^{o}C and (d) $Al(OiPr)_3$ in $[C_6mim][Br]$ and H_3PO_4 scanned at 20 ^{o}C.

Figure 5.6 shows ^{27}Al NMR spectra of pure $Al(OiPr)_3$ (sample 1), $Al(OiPr)_3$ in $[C_4mim][Br]$ (sample 3), and $Al(OiPr)_3$ in a mixture of H_3PO_4 and $[C_4mim][Br]$ (sample 6). Except for pure $Al(OiPr)_3$, the samples are stirred at 70 ^{o}C and scanned also at 70 ^{o}C. From Figure 5.6, the influence of just $[C_4mim][Br]$ versus both $[C_4mim][Br]$ and H_3PO_4 could be observed. When there is no phosphoric acid in the mixture (sample 3), the ratio of Al(IV) to Al(VI) is higher than the ratio of pure $Al(OiPr)_3$ (0.45 versus 0.18), but the ratio is still small. With the addition of H_3PO_4 (sample 6), ratio of Al(IV) to Al(VI) increases to 8.82, and the peaks shift to right due to the increased electron density around Al atoms. The spectra of as-synthesized molecular sieves which possess Al-O-P bonds or Al-O-Si bonds are very similar to the spectra of

$Al(OiPr)_3$ in mixture of H_3PO_4 and $[C_4mim][Br]$,[20-23] indicating the aluminium in solution is in the same coordination state as it is in the final aluminophosphate material. Similar changes in the Al atoms are observed in the liquids $[C_2mim][Br]$ or $[C_6mim][Br]$.

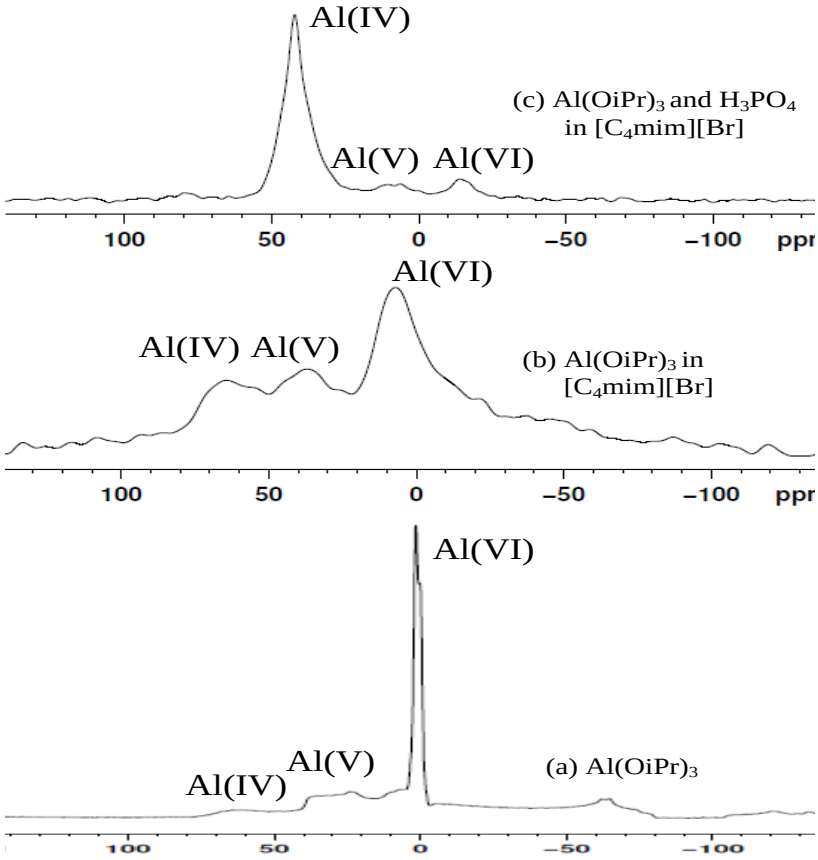

Figure 5.6 ^{27}Al NMR spectra of (a) $Al(OiPr)_3$ scanned at 80 ^oC, (b) $Al(OiPr)_3$ in $[C_4mim][Br]$ scanned at 70 ^oC and (c) $Al(OiPr)_3$ in $[C_4mim][Br]$ and H_3PO_4 scanned at 70 ^oC.

5.1.3.3 Effect of temperature on $Al(OiPr)_3$ in ionic liquids

Effect of temperature on conformation of Al atoms of $Al(OiPr)_3$ in ionic liquids is remarkable, which has been emphasized in the preceding section can be seen in the discussion of sections. Samples of $Al(OiPr)_3$ in $[C_6mim][Br]$ (sample 4) and samples of $Al(OiPr)_3$ and H_3PO_4 in $[C_6mim][Br]$ (sample 7) are used as the examples. Spectra of sample 4 scanned at 20 ^oC and at 70 ^oC are shown in Figure 5.7. With the increase of temperature from 20 ^oC to 70 ^oC, intensity ratio of Al(IV) to Al(VI) increases from nearly zero to 1.06 when $Al(OiPr)_3$ is mixed with $[C_6mim][Br]$ (sample 4). Shown in Figure 5.8 are spectra of sample 7 scanned at 20 ^oC and 70

^{o}C. When temperature is increased, nearly all of the Al (VI) disappears and only Al(IV) is left, and the ratio of Al(IV) to Al(VI) increases from 0.24 to nearly infinity, as shown in Table 5-2. Temperature clearly aids in the coordination change of aluminium atoms from Al(VI) and Al(V) to Al(IV). With addition of H_3PO_4, influence of temperature change is more significant than without addition of H_3PO_4.

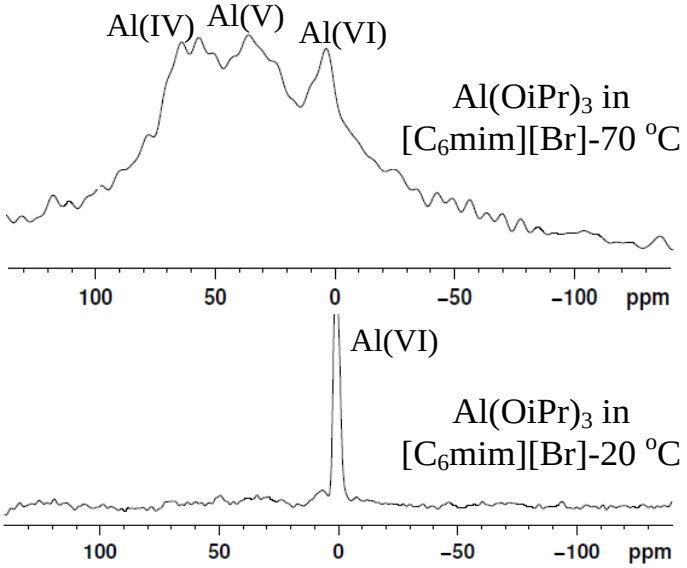

Figure 5.7 ^{27}Al-NMR spectra of Al(OiPr)$_3$ in [C$_6$mim][Br] scanned at 20 ^{o}C, and Al(OiPr)$_3$ in [C$_6$mim][Br] scanned at 70 ^{o}C.

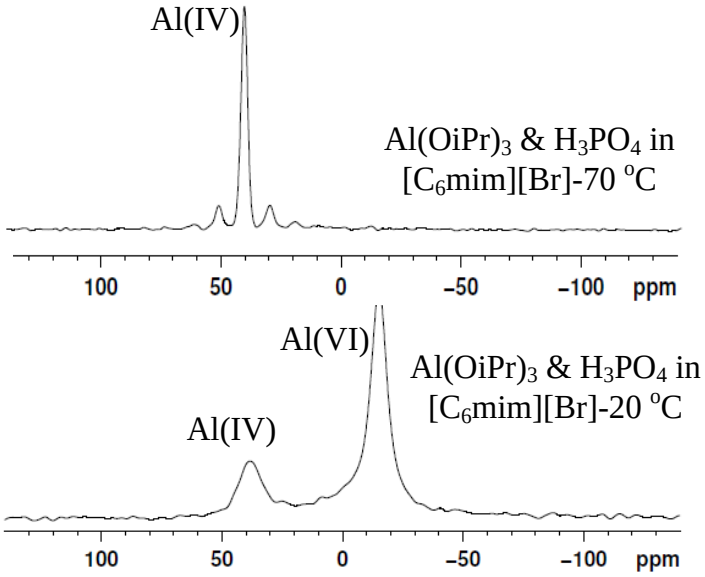

Figure 5.8 ^{27}Al NMR spectra of (a) Al(OiPr)$_3$ in [C$_6$mim][Br] and H$_3$PO$_4$ scanned at 20 ^{o}C, and (b) Al(OiPr)$_3$ in [C$_6$mim][Br] and H$_3$PO$_4$ scanned at 70 ^{o}C.

5.1.4 Conclusions

^{27}Al solid state NMR is used in this work to investigate influence of ionic liquid and phosphoric acid on the conformation of Al atoms in $Al(OiPr)_3$. The results would be helpful to understand the formation mechanism of aluminophosphates in the aging or the homogenizing process, in ionothermal synthesis. It is found that when $Al(OiPr)_3$ is mixed with an ionic liquid, at a higher temperature (70 ^oC), Al(VI) begins to change to Al(IV) and Al(V), but Al(VI) is still the dominant conformation as seen in pure $Al(OiPr)_3$. At lower temperature (20 ^oC), the change is not remarkable. When H_3PO_4 is added into the mixture, at a higher temperature (70 ^oC), tetrahedral-coordination becomes the dominant conformation of Al atoms. In addition, the peak location of Al(IV) is the same with the Al atoms in as-synthesized molecular sieves, indicating the aluminium in ILs is in the same coordination state as it is in the final aluminophosphate material. Regardless of the presence of H_3PO_4, the ratio of Al(IV) to Al(VI) increases with the increase of alkyl chain length in the imidazolium ring of ionic liquids, suggesting $[C_6mim][Br]$ could possibly accelerates the formation of Al-O-P bonds. Moreover, temperature has a great influence of conformation of $Al(OiPr)_3$ in ionic liquids. With the increase of temperature from 20 ^oC to 70 ^oC, ratio of Al(IV) to Al(VI) increases dramatically and influence of temperature is enhanced with the addition of H_3PO_4.

Section 5.1 is a soon to be submitted manuscript.

5.1.5 References

1. Meindersma, G. W.; de Haan, A. B. *Chemical Engineering Research & Design* **2008**, *86*, 745-752.
2. Earle, M. J.; Esperanca, J.; Gilea, M. A.; Lopes, J. N. C.; Rebelo, L. P. N.; Magee, J. W.; Seddon, K. R.; Widegren, J. A. *Nature* **2006**, *439*, 831-834.
3. Galinski, M.; Lewandowski, A.; Stepniak, I. *Electrochimica Acta* **2006**, *51*, 5567-5580.
4. Sheldon, R. *Chemical Communications* **2001**, 2399-2407.
5. Parvulescu, V. I.; Hardacre, C. *Chemical Reviews* **2007**, *107*, 2615-2665.
6. Minami, I. *Molecules* **2009**, *14*, 2286-2305.
7. Chiappe, C.; Pieraccini, D. *Journal of Physical Organic Chemistry* **2005**, *18*, 275-297.
8. Ngo, H. L.; LeCompte, K.; Hargens, L.; McEwen, A. B. *Thermochimica Acta* **2000**, *357*, 97-102.
9. Seddon, K. R. *Journal of Chemical Technology and Biotechnology* **1997**, *68*, 351-356.
10. Lee, J. S.; Wang, X. Q.; Luo, H. M.; Baker, G. A.; Dai, S. *Journal of the American Chemical Society* **2009**, *131*, 4596-+.
11. Han, L. J.; Wang, Y. B.; Li, C. X.; Zhang, S. J.; Lu, X. M.; Cao, M. J. *Aiche Journal* **2008**, *54*, 280-288.
12. Cooper, E. R.; Andrews, C. D.; Wheatley, P. S.; Webb, P. B.; Wormald, P.; Morris, R. E. *Nature* **2004**, *430*, 1012-1016.
13. Fayad, E. J.; Bats, N.; Kirschhock, C. E. A.; Rebours, B.; Quoineaud, A. A.; Martens, J. A. *Angewandte Chemie-International Edition* **2010**, *49*, 4585-4588.
14. Wang, L.; Xu, Y. P.; Wang, B. C.; Wang, S. J.; Yu, J. Y.; Tian, Z. J.; Lin, L. W. *Chemistry-a European Journal* **2008**, *14*, 10551-10555.
15. Gaillon, L.; Sirieix-Plenet, J.; Letellier, P. *J. Solution Chem.* **2004**, *33*, 1333-1347.
16. Golovanov, D. G.; Lyssenko, K. A.; Vygodskii, Y. S.; Lozinskaya, E. I.; Shaplov, A. S.; Antipin, M. Y. *Russ. Chem. Bull.* **2006**, *55*, 1989-1999.
17. Golovanov, D. G.; Lyssenko, K. A.; Antipin, M. Y.; Vygodskii, Y. S.; Lozinskaya, E. I.; Shaplov, A. S. *Cryst. Growth Des.* **2005**, *5*, 337-340.
18. Wang, J. J.; Wang, H. Y.; Zhang, S. L.; Zhang, H. H.; Zhao, Y. *J. Phys. Chem. B* **2007**, *111*, 6181-6188.

19. Sun, X.; Polifka, A.; Anthony, J. L. *Manuscript in preparation **2012***.
20. Xu, J.; Zhou, D.; Song, X. W.; Chen, L.; Yu, J. H.; Ye, C. H.; Deng, F. *Microporous and Mesoporous Materials* **2008**, *115*, 576-584.
21. Sakthivel, A.; Dapurkar, S. E.; Gupta, N. M.; Kulshreshtha, S. K.; Selvam, P. *Microporous and Mesoporous Materials* **2003**, *65*, 177-187.
22. Occelli, M. L.; Biz, S.; Auroux, A.; Ray, G. J. *Microporous and Mesoporous Materials* **1998**, *26*, 193-213.
23. Shen, W. L.; Yang, J.; Li, S. H.; Hu, W.; Xu, J.; Zhang, H. L.; Zou, Q.; Chen, L.; Deng, F. *Microporous and Mesoporous Materials* **2010**, *127*, 73-81.

Chapter 6 - Effect of Ionic Liquid (Molten Salts) and other Factors on Hydrothermal Synthesis of Aluminosilicate and on Ionothermal Synthesis of Aluminophosphates

6.1 Influence of Prolonged Heating Time and Type of Mineralizers on Formation of Aluminophosphates in Ionic Liquids

6.1.1 Introduction

Ionic liquids (ILs) are a group of novel solvents, whose melting points are lower than 100 ^{o}C. They are composed purely of cations and anions, most of which are bulky and with irregular shapes, preventing them from packing closely and forming crystals, thus lowering the melting point. [1-4] Ionic liquids are being used in applications such as lubricants, electrolyte in metal-air batteries, dissolving media for cellulose, and catalysts.[5-11] In addition to the desirable properties of many ILs such as negligible vapor pressure, thermal stability, and nonflammability, properties of many ILs can be tailored through judicious selection of the cations and anions to meet the requirements of different applications.[1,12-14] In theory, there are nearly endless number of ionic liquids which could be synthesized by properly combining cations and anions.[15]

Due to many of the properties of ionic liquids mentioned above, ILs are being used as the solvent and sometimes structure directing agent in the synthesis of molecular sieves.[16-18] The traditional method to synthesize molecular sieves involving dissolving precursors and often with a structure directing agent and mineralizer in water and heating the mixture for a certain time at temperatures typically between 150 ^{o}C and 200 ^{o}C. This hydrothermal process necessitates the usage of high-pressure vessels.[19-21] However, when water is substituted with ionic liquids, the negligible pressure of ILs makes the high-pressure vessel unnecessary. The approach substituting water with ILs in material synthesis is called ionothermal synthesis and was first demonstrated by Morris and coworkers in 2004.[22] Since 2004, several others have reported employing different ionic liquids as the solvent to synthesize molecular sieves. Most of the synthesis used 1-alkyl-3-methylimidazolium bromide ([$C_n$mim][Br]) with a few using 1-benzyl-3-methylimidazolium chloride, 1-butyl-3-methylimidazolium tetrafluoroborate, 1-ethyl-3-methylimidazolium

bis(trifluoromethanesulfonimide), combination of tetraethylammonium bromide and pentaerythritol, 1-butyl-3-methylimidazolium bromide/hydroxide.[17,22-39] Frameworks synthesized include SIZ-1,[22] SIZ-3,[22] SIZ-4 (CHA topology),[22] SIZ-5 (AFO topology),[22] SIZ-6,[28,35] SIZ-7 (SIV topology),[23] SIZ-8 (AEI topology),[23] SIZ-9 (SOD topology),[23] SOD,[17,39] a novel chain structure,[25] AEL,[26,27,29,40] AFI,[27,31,40-43] ATV,[27] AST,[43] LTA,[30,32,38,41] DNL-1 (structural analogue of cloverite),[36] quartz,[30] CLO,[32] cristobalite,[34,43] MFI,[35,37] tridymite[27,44] and berlinite.[45]

Ionothermal synthesis of porous aluminophosphates is investigated with emphasis on effects of different mineralizers (hydrofluoric acid and hydrochloric acid) and the phase transition of frameworks synthesized after prolonged heating. In addition, effect of alkyl chain length and precursor's ratio on structures and yield of products are also presented.

6.1.2 Experimental description

6.1.2.1 Synthesis of ionic liquids

Most of the ionic liquids used are 1-alkyl-3-methylimidazolium bromide ([$C_n$mim][Br]), including [C_2mim][Br], [C_4mim][Br] and [C_6mim][Br]. These ionic liquids were synthesized according to the method reported in literature.[46] After reacting 1-methylimidazole with alkyl-bromide at 40 ^oC (time depending on the length of alkyl chain of alkyl-bromide), the mixture passed through a granular activated carbon column and an acidic activated aluminum oxide column to remove color impurities. The final material was then dried under vacuum for more than 3 days until the water content was under 500 ppm, as determined by Karl-Fischer Titrator.

6.1.2.2 Synthesis of aluminophosphates

In the ionothermal preparation of aluminophosphates, a mixture of aluminium isopropoxide, phosphoric acid (85 wt%), hydrofluoric acid (37 wt%) or hydrofluoric acid (40 wt%) and structure directing agent (tripropylamine or dipropylamine) were added into ionic liquid and stirred at 100 ^oC for half an hour. The homogeneous solution was then charged into different Teflon liners and heated from several hours to several days, respectively. After the desired time of heating, the liners are taken out and quenched in cold water to stop

crystallization. The aluminophosphate powder was then filtrated and washed carefully with water and acetone, and allowed to dry at room temperature. These materials were synthesized according to 19 different recipes, which are shown in Table 6-1.

Table 6-1 Molar ratio of each component in the reaction gels and synthesis condition of the ionothermal recipes.

Recipe	$Al(OiPr)_3$	H_3PO_4	Acid		H_2O (*)	Ionic liquid		SDA		Temp. (^oC)
A-1	1.00	2.55	HF	0.60	3.45	$[C_4mim][Br]$	20	DPA	1.50	190
A-2	1.00	2.55	HF	0.60	3.45	$[C_4mim][Br]$	20	DPA	1.50	150
A-3	1.00	2.55	HF	0.60	3.45	$[C_4mim][Br]$	20	DPA	1.50	100
A-4	1.00	2.55	HF	0.60	3.45	$[C_6mim][Br]$	20	DPA	1.50	150
A-5	2.00	5.10	HF	0.60	5.90	$[C_4mim][Br]$	20	DPA	1.50	190
A-6	2.00	5.10	HF	0.60	5.90	$[C_2mim][Br]$	20	DPA	1.50	190
A-7	2.00	5.10	HF	0.60	5.90	$[C_4mim][Br]$	20	TPA	1.50	190
A-8	2.00	3.00	HF	0.60	3.88	$[C_2mim][Br]$	20	DPA	1.50	190
A-9	2.00	4.00	HF	0.60	4.84	$[C_2mim][Br]$	20	DPA	1.50	190
A-10	2.00	3.00	HF	0.60	3.88	$[C_4mim][Br]$	20	DPA	1.50	190
A-11	2.00	4.00	HF	0.60	4.84	$[C_4mim][Br]$	20	DPA	1.50	190
A-12	1.00	2.55	HCl	0.60	4.68	$[C_4mim][Br]$	20	DPA	1.50	190
A-13	1.00	2.55	HCl	0.80	5.42	$[C_4mim][Br]$	40	DPA	1.50	150
A-14	1.00	2.55	HCl	1.50	8.02	$[C_4mim][Br]$	20	DPA	1.50	190
A-15	2.00	5.10	HCl	0.60	6.94	$[C_4mim][Br]$	20	DPA	1.50	190
A-16	1.00	2.55	HCl	0.60	4.68	$[C_4mim][Br]$	20	-	-	190
A-17	1.00	2.55	HCl	0.80	5.42	$[C_4mim][Br]$	40	-	-	150
A-18	1.00	2.55	HCl	1.50	8.02	$[C_4mim][Br]$	20	-	-	190
A-19	1.00	2.55	-	-	2.45	$[C_4mim][Br]$	20	DPA	1.50	190

* No extra water was added. Water comes from the aqueous H_3PO_4 and acid solutions.

6.1.2.3 Characterization of the aluminophosphates

In order to determine the structures of aluminophosphates synthesized, sample powders were analyzed using an X-ray diffractometer (XRD), which was either a Bruker AXS D8 Advance model or Rigaku MiniFlex II X-ray diffractometers. The resulting patterns were compared to those available in the literature.

In order to investigate the surface of aluminophosphate, scanning electron microscope (SEM) was used by scanning the sample powder with a high-energy beam of electrons. The model is Hitachi S-3500. For those powders which do not need large magnitude of enlargement, an optical microscope (Model BX51 Olympus Inc. Tokyo, Japan) was used to observe the shape of the particles.

6.1.3 Results and discussion

Products of each recipe are synthesized three or four times to ensure reproducibility. The framework topologies synthesized with each recipe are shown in Table 6-2. They are labeled with the International Zeolite Association 3-letter code or the material name.[47] Among them, AFI, SIZ-4, AEL, tridymite, berlinite, α-cristobalite are all crystalline materials. AFI, SIZ-4 and AEL are porous structures, whereas tridymite, berlinite and α-cristobalite are dense structures. Porous structures and dense structures differ in the number of tetrahedral-coordinated atoms in a volume of 1000 $Å^3$ (T/1000 $Å^3$), higher than 21 T/1000 $Å^3$.[48,49] For example, framework type AEL has 19.2 T/1000 $Å^3$, while dense structures have much higher numbers. In addition, AFI, AEL, tridymite, berlinite and α-cristobalite have been successfully made either in hydrothermal or ionothermal synthesis. SIZ-4 has only been synthesized in ionothermal synthesis and is reported to have the topology similar to CHA.[24]

Table 6-2 Framework topologies of aluminophosphates synthesized following each recipe after heating from several hours to several days.

heating time	2 hours	4 hours	8 hours	5 days	10 days
A-1	AFI + SIZ-4	AFI + SIZ-4	AFI + SIZ-4	SIZ-4	SIZ-4
A-2	amorphous	amorphous	amorphous+peaks	SIZ-4	SIZ-4
A-3	amorphous	amorphous	amorphous	amorphous	amorphous
A-4	AEL	AEL	SIZ-4	SIZ-4	SIZ-4
A-5	AEL + AFI	AEL	AEL + SIZ-4	SIZ-4	SIZ-4
A-6	AEL	AEL	AEL	SIZ-4	SIZ-4
A-7	AEL	AEL	AEL + SIZ-4	SIZ-4	SIZ-4
A-8	amorphous	amorphous	SIZ-4	SIZ-4	SIZ-4
A-9	AEL	AEL	AEL	SIZ-4	SIZ-4
A-10	AFI + SIZ-4	AFI + SIZ-4	SIZ-4	SIZ-4	SIZ-4
A-11	AFI	AFI	AFI	SIZ-4	SIZ-4
A-12	AFI+AEL	AEL	AEL	tridymite	SIZ-4
A-13	amorphous	AEL	AEL	AEL	AEL
A-14	tridymite	tridymite	tridymite	berlinite	berlinite
A-15	AEL	AEL	AEL	berlinite	berlinite
A-16	tridymite	tridymite	tridymite	berlinite	berlinite
A-17	amorphous	amorphous	AEL	AEL	AEL
A-18	tridymite	tridymite	tridymite	berlinite	berlinite
A-19	amorphous	amorphous	AFI + amorphous	α-cristobalite	α-cristobalite

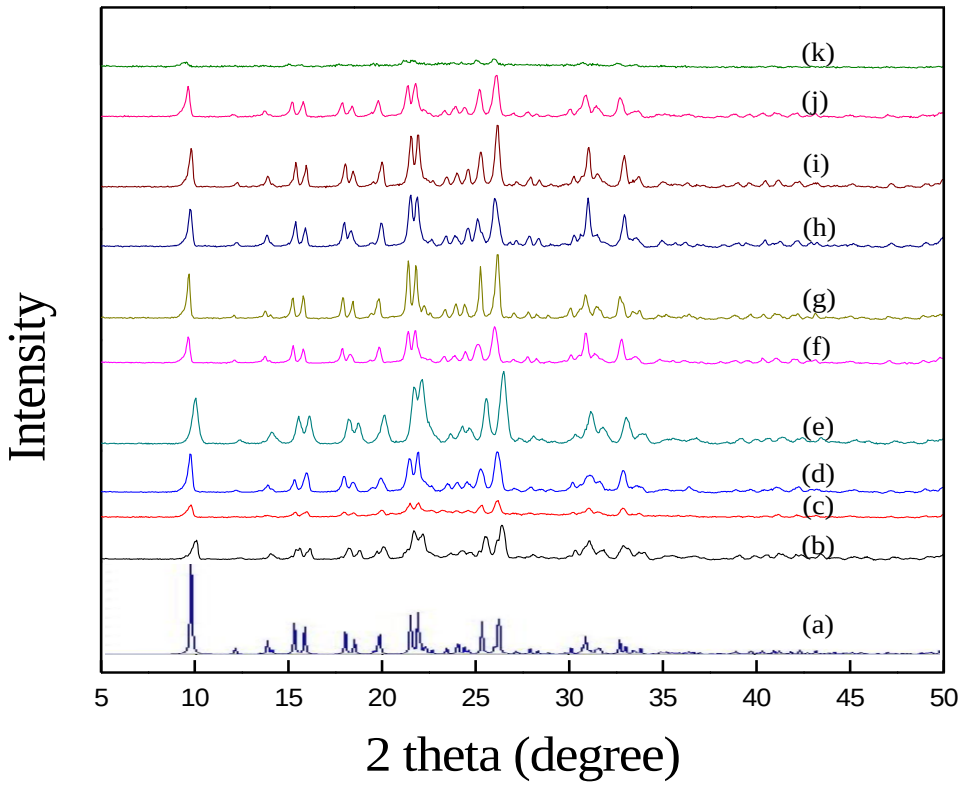

Figure 6.1 XRD patterns of (a) SIZ-4,[47] and powders made following recipe (b) A-1, (c) A-2, (d) A-4, (e) A-5, (f) A-6, (g) A-7, (h) A-8, (i) A-9, (j) A-10 and (k) A-11 after being heated for 5 days.

From Table 6-2, it can be seen that SIZ-4 and berlinite are two of the most commonly produced porous crystalline and dense materials after heating for several days. In Figure 6.1, XRD patterns of powders with pure SIZ-4 structure are listed and compared with theoretical XRD pattern of SIZ-4. As shown in Figure 1, after heating for 5 days, powders made following recipe A-1, A-2, A-4, A-5, A-6, A-7, A-8, A-9, A-10 and A-11 have the structure SIZ-4. Although the intensities of XRD patterns are different, peaks show up at the same location as the theoretical XRD pattern of SIZ-4. The similarity between these recipes is HF is used as the mineralizer. XRD patterns of materials synthesized following recipes A-15, A-16 and A-18 after heating for 5 and 10 days are compared with the theoretical pattern of berlinite, as shown in Figure 6.2. These powders all have a berlinite structure. The similarity between recipe A-15, A-16 and A-18 is that HCl is used as the mineralizer.

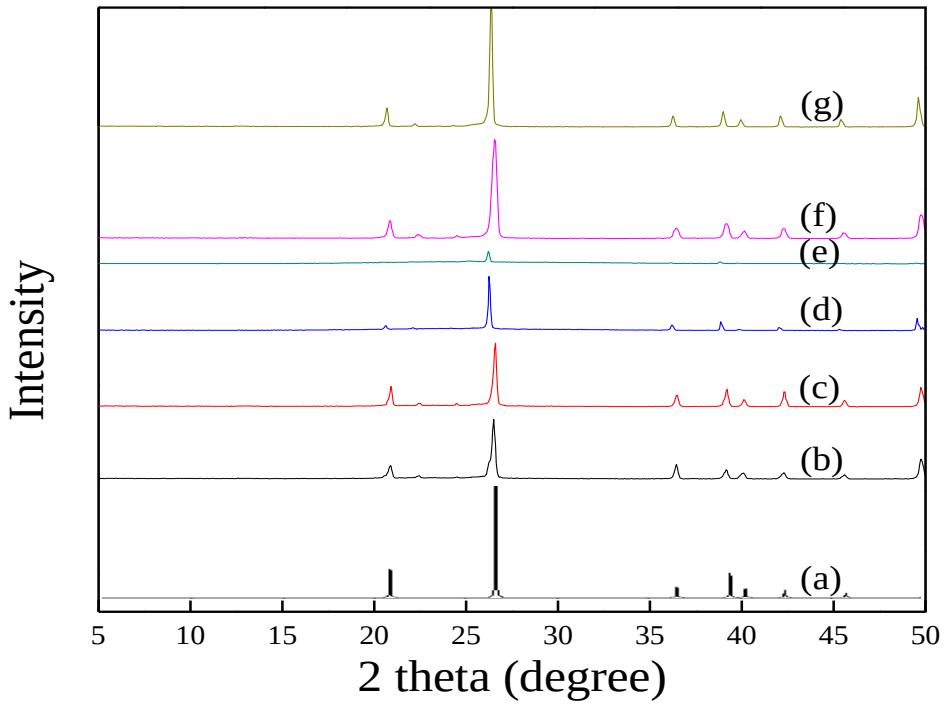

Figure 6.2 XRD patterns of (a) standard berlinite[47] and XRD patterns of A-15 heated for (b) 5 days and (c) 10 days, A-16 heated for (d) 5 days and (e) 10 days, A-18 heated for (f) 5 days and (g) 10 days.

6.1.3.1 Effects of acids

In all of these recipes, either hydrofluoric acid or hydrochloric acid is used as the mineralizer, except A-19 where there is no acid in the reaction gel. As can be seen in Table 6-2, different acids could generate different structures of powders. Most of the published ionothermal synthesis used hydrofluoric acid as the mineralizer, with a few employing no acid at all.[17,22,30] Hydrofluoric acid is a highly corrosive acid with serious health risks. As a possible substitute for hydrofluoric acid, hydrochloric acid is being used is this paper as the mineralizer in several recipes. Hydrochloric acid is one of the mineralizers commonly used in hydrothermal synthesis of molecular sieves,[50,51] but it had not been used in ionothermal synthesis for porous materials.

Recipes with hydrochloric acid as the mineralizer and dipropylamine as the structure directing agent include A-12, A-13, A-14 and A-15. All of these recipes use [C_4mim][Br] as the solvent. A-12, A-13, A-14 and A-15 differ in the molar ratio of Al: P: HCl: IL: DPA. Recipes

with hydrochloric acid as the mineralizer, but without the addition of structure directing agent, include A-16, A-17 and A-18. They are the same as A-12, A-13 and A-14, respectively, except for the absence of DPA. Products synthesized with hydrochloric acid as mineralizer, as well as molar ratio of components in the reaction gel and reaction conditions are shown in Table 6-3.

Table 6-3 Structures of aluminophosphates synthesized following recipes using HCl as the mineralizer, as well as molar ratio of components in the reaction gel and reaction conditions.

Recipe	Acid	H_2O(*)	IL	SDA		Temp	Frameworks				
						(^oC)	2 hours	4 hours	8 hours	5 days	10 days
A-12	0.60	4.68	20	DPA	1.50	190	AFI+AEL	AEL	AEL	tridymite	SIZ-4
A-13	0.80	5.42	40	DPA	1.50	150	amorphous	AEL	AEL	AEL	AEL
A-14	1.50	8.02	20	DPA	1.50	190	tridymite	tridymite	tridymite	berlinite	berlinite
A-15	0.30	3.47	10	DPA	0.75	190	AEL	AEL	AEL	berlinite	berlinite
A-16	0.60	4.68	20	-	-	190	tridymite	tridymite	tridymite	berlinite	berlinite
A-17	0.80	5.42	40	-	-	150	amorphous	amorphous	AEL	AEL	AEL
A-18	1.50	8.02	20	-	-	190	tridymite	tridymite	tridymite	berlinite	berlinite
molar ratio of Al: P = 1: 2.55; Acid: HCl; IL:[C_4mim][Br]											

From Table 6-3, it can be seen that hydrochloric acid could be used to synthesize crystalline materials. The most common structures synthesized are AEL (porous material), tridymite (dense material) and berlinite (dense material). Xu and his coworkers reported that AEL could be made with the addition of hydrofluoric acid, but if there was no acid in the reaction gel, AEL could not be synthesized.[26] From the above experiments, it can be seen that AEL can also be synthesized with the addition of hydrochloric acid, a less corrosive and volatile acid. Following recipe A-12, A-13 and A-15, the structure AEL is formed after several hours. The AEL structure changes to tridymite and berlinite if heated after 5 days for recipe A-12 and A-15. Among the recipes using HCl and DPA, only recipe A-14 leads to tridymite instead of AEL after several hours. A-14 uses more hydrochloric acid than the other recipes; as a result, there is more water in the reaction gel. The occurrence of tridymite (dense material) might be due to the increased amount of water in the excessive hydrofluoric acid. What can also been seen from Table 6-3 is the importance of the structure directing agent in ionothermal synthesis when HCl is used as the mineralizer. For A-12, when a structure directing agent (DPA) is added, porous crystalline AEL structure could be formed within several hours. But if there is no structure directing agent in the reaction gel (A-12 changed to A-16), the framework synthesized

within several hours is a dense material with tridymite structure. In addition, the framework structures formed after 5 days and 10 days are also different, tridymite (dense) and SIZ-4 (porous) compared to berlinite (dense). In addition, for A-13, when there is DPA in the reaction gel, AEL forms after 4 hours. But when there is no DPA (A-13 changed to A-17), AEL begins to appear after 8 hours.

In order to compare the effect of acid on the final structures, A-1, A-12 and A-19 are used and the products synthesized according to these recipes are shown in Table 6-4. These three recipes have the same ratio of Al: P :DPA= 1: 2.55: 1.5 and the same ionic liquid [C_4mim][Br]. They differ in the mineralizer added; A-1 uses HF, A-12 uses HCl and A-19 does not use any acid as the mineralizer. Following recipe A-1, the structures synthesized are porous materials (AFI & SIZ-4 or SIZ-4 only) whether heated for several hours or several days. However, following A-12, structures synthesized with hydrochloric acid are AFI+AEL when the heating time equals to 2 hours, and AEL when the heating time is equal to 4 hours and 8 hours, and tridymite or SIZ-4 when the heating time equals to several days. If there is no acid added into the reaction gel (A-19), only amorphous powder is formed within 4 hours heating. But after 8 hours, materials with the AFI structure begin to form and after 5 days, dense structure α-cristobalite is formed.

The recipe A-2 is the same composition as A-1 but heated at 150 ^{o}C instead of 190 ^{o}C. As expected, A-2 leads to a slower rate of formation of AFI and SIZ-4. The recipe A-13 has the same composition as A-12 but with twice the solvent and a lower heating temperature of 150 ^{o}C. The lower temperature yields crystalline AEL structures after four hours. The comparison between products of A-2 and A-13 also demonstrates different acid can lead to different structures. Frameworks made following recipe A-2 and A-13 are also shown in Table 6-4.

Table 6-4 Structures of aluminophosphates synthesized following recipes using different mineralizers, as well as molar ratio of precursors and reaction conditions.

Recipe	Acid		H_2O (*)	IL	SDA		Temp (^{o}C)	Frameworks				
								2 hours	4 hours	8 hours	5 days	10 days
A-1	HF	0.60	3.45	20	DPA	1.50	190	AFI+SIZ-4	AFI+SIZ-4	AFI+SIZ-4	SIZ-4	SIZ-4
A-2	HF	0.60	3.45	20	DPA	1.50	150	amorphous	amorphous	amorphous+peaks	SIZ-4	SIZ-4
A-12	HCl	0.60	4.68	20	DPA	1.50	190	AFI+AEL	AEL	AEL	tridymite	SIZ-4
A-13	HCl	0.80	5.42	40	DPA	1.50	150	amorphous	AEL	AEL	AEL	AEL
A-19	-	-	2.45	20	DPA	1.50	190	amorphous	amorphous	AFI+amorphous	α-cristobalite	α-cristobalite

molar ratio of Al: P = 1: 2.55; IL:[C_4mim][Br]; DPA: dipropylamine

6.1.3.2 Phase transition

It is noticeable from Table 2 that frameworks synthesized after heating for several hours have a dramatic change to another framework. The phase change in ionothermal synthesis has been documented in the literature. Wang and his coworkers noticed a short-term change of frameworks following the recipe: Al_2O_3: $2.55P_2O_5$: 0.6HF: 20[C_4mim]Br: 1.5amine (or no amine).[27] Without addition of amine, when heated at 190 ^oC, AFI (minor) + AEL (major) are formed after 1hour and only AEL is left after 4 hours heating, while at 280 ^oC, AFI (minor) +AEL (major) are made in 0.5 hour and the frameworks change to tridymite after 2 hours.[27] With addition of amine, when heated at 190 ^oC, AFI is formed after 0.5 hour and only AEL is left after 8 hours heating, while at 280 ^oC, AFI is made in 10 minutes and the frameworks change to ATV after 4 hours.[27] Here, not only the short-term phase change is investigated, but also the long-term phase change. The reaction gel of each recipe is heated from several hours to several days in order to study the change of framework in ionothermal synthesis.

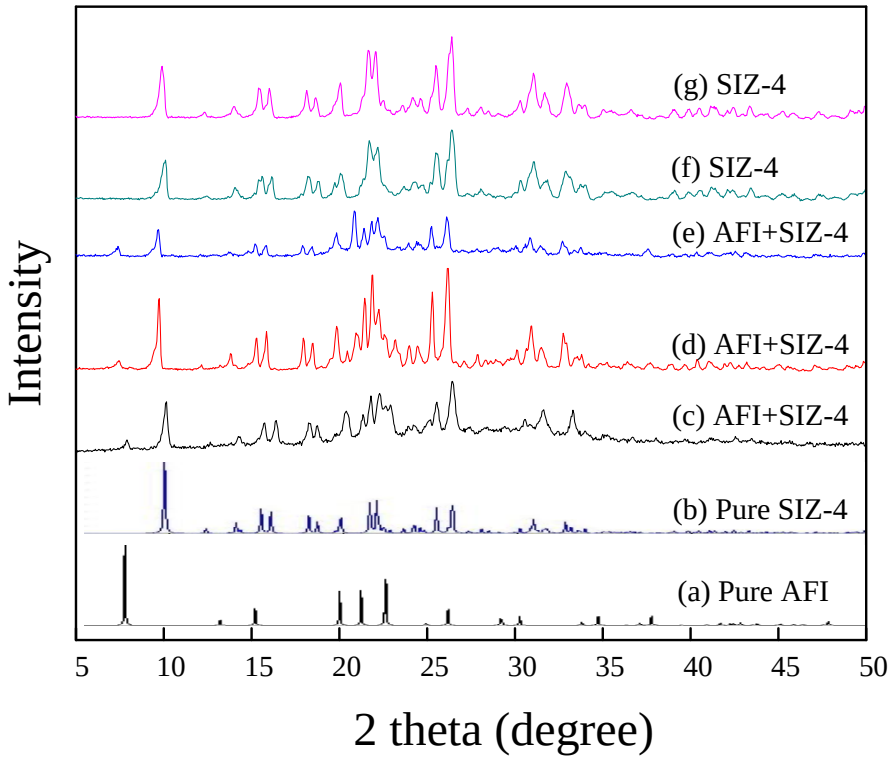

Figure 6.3 Theoretical XRD patterns of (a) AFI[47] and (b) SIZ-4[47], and XRD patterns of products synthesized following recipe A-1, heated for (c) 2 hours, (d) 4 hours, (e) 8 hours, (f) 5 days and (g) 10 days.

From Table 6-2, it can be seen that products synthesized with each recipe undergo structure change after prolonged time of heating. For those synthesized with hydrofluoric acid as mineralizer (A-1, A-2, A-3, A-4, A-5, A-6, A-7, A-8, A-9, A-10 and A-11), within several hours heating, the mostly common seen structures are AEL and a combination of AFI and SIZ-4. However, after 5 days, these structures change to SIZ-4 or berlinite. For example, change of XRD patterns of A-1 is shown in Figure 6.3. Figure 6.3-(a) and (b) are theoretical XRD patterns of AFI and SIZ-4. After heating for 2 hours, 4 hours and 8 hours, materials synthesized are with a combination of structure AFI and SIZ-4. But after further heating, up to 5 days and 10 days, structure AFI disappears and only SIZ-4 is left. XRD patterns of materials made following recipe A-1 are shown in Figure 6.3-(c), (d), (e), (f) and (g).

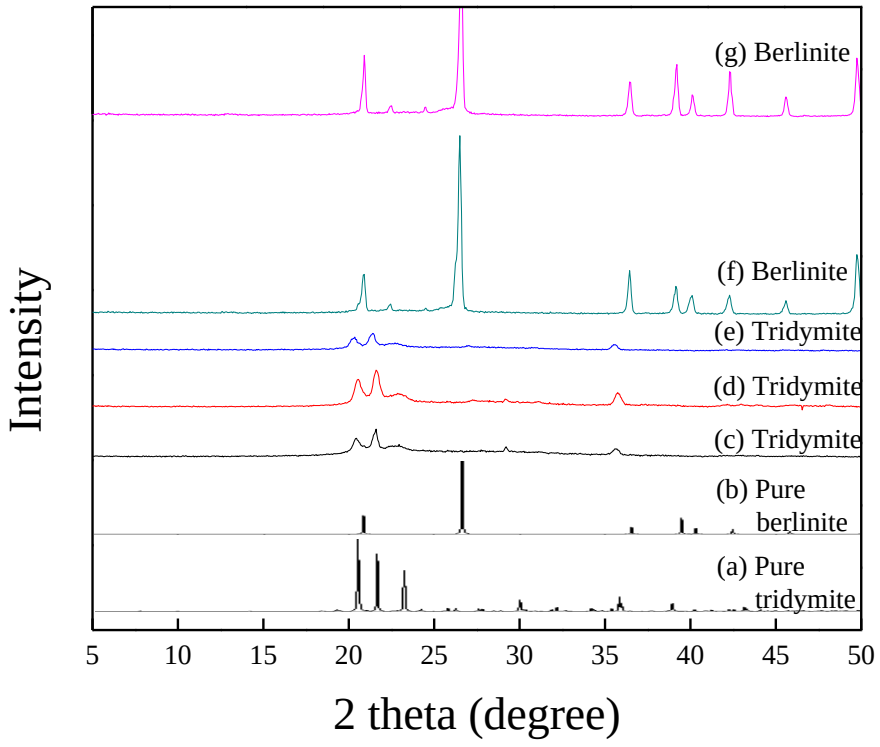

Figure 6.4 Theoretical XRD patterns of (a) tridymite and (b) berlinite,[47] and XRD patterns of products synthesized following recipe A-14, heated for (c) 2 hours, (d) 4 hours, (e) 8 hours, (f) 5 days and (g) 10 days.

In addition, for those materials synthesized with hydrochloric acid as mineralizer (from A-12 to A-18), AEL and tridymite are the most commonly synthesized materials after several hours heating, and after prolonged heating time, these structures change to berlinite or remain

unchanged for A-13 and A-18. For A-19, where no acid is added, powders synthesized with short-time heating are amorphous structure and AFI, and α-cristobalite after long-time heating. The phase transition of A-14 is shown in Figure 6.4 as an example. Figure 6.4-(a) and (b) are theoretical XRD patterns of tridymite and berlinite. After heating for 2 hours, 4 hours and 8 hours, materials produced have the tridymite structure. But after further heating up to 5 days and 10 days, structure of tridymite grows into structure berlinite.

6.1.3.3 Effect of alkyl chain length on the structures of aluminophosphates

Morris and his colleagues have reported the effect of alkyl length on the structures made. They systematically increase the number of carbon atoms in alkyl chain from 2 carbons to 5 carbons. After heating the materials from 68 hrs to 240 hrs (such as 68 hrs for $[C_2mim][Br]$ and 240 ^oC for $[C_5mim][Br]$) and at a temperature from 150 ^oC to 200 ^oC (such as at 150 ^oC for $[C_2mim][Br]$ and 200 ^oC for $[C_4mim][Br]$), they made materials with the same framework topology as SIZ-4 with the addition of HF.[24] Ma and his coworkers used $[C_nmim][Br]$ (n=2,3,4,5,6) to synthesize $GaPO_4$. Heating time is equal to 2 days or 8 days and the temperature is fixed at 180 ^oC or 150 ^oC. With the increase of alkyl chain length, the framework topology is all LTA, but with sharply decreased size, and the morphology varies from octahedron to truncated octahedron and to cube.[32] Wang and his coworkers found if $[C_2mim][Br]$ is substituted with $[C_4mim][Br]$, after heating the materials for several hours, AFI structure with 12-MR pores could be formed, while $[C_2mim][Br]$ leads to materials with smaller pores. He further suggests the possible structure-directing effect of ionic liquid based on this result.[27]

In this work, we compare effects of alkyl chain length on the short term and long term material structures. The recipes can be divided into three groups and the recipes in each group are only different in the ionic liquids used. The differences between groups are the molar ratio of precursors and heating temperatures. Synthesis condition and frameworks formed are shown in Table 6-5. In the first group, A-8 and A-10 are compared. At this synthesis condition, crystalline porous frameworks AFI and SIZ-4 begin to show up after 2 hours heating with $[C_4mim][Br]$. As a comparison, no crystalline material is formed after 4 hours heating with $[C_2mim][Br]$. In the second group, A-9 uses $[C_2mim][Br]$ as the solvent and A-11 uses $[C_4mim][Br]$ as the solvent. They lead to structure AEL and AFI, respectively, and the structures remain unchanged until 8 hours before they transform to SIZ-4. Finally, the third comparison groups include A-2

([C_4mim][Br] as the solvent) and A-4 ([C_6mim][Br] as the solvent), crystalline porous framework AEL is formed after 2 hours and this structure changes to SIZ-4 after 8 hours when [C_6mim][Br] is in the reaction gel. But no crystalline material is formed even after 8 hours when [C_4mim][Br] is used. By comparison between the two recipes in each group of recipes, it could be concluded that slightly longer alkyl chain length could possibly shorten the formation time of crystalline materials, however the slight difference of alkyl chain length has no effect on the framework topology formed after prolonged heating of time, as evidenced by the consistent SIZ-4 formed after 5 days and 10 days.

Table 6-5 Structures of aluminophosphates synthesized following recipes using different ionic liquids, as well as molar ratio of precursors and reaction conditions.

Recipe	$Al(OiPr)_3$	H_3PO_4	H_2O (*)	IL	Temp (°C)	Frameworks				
						2 hours	4 hours	8 hours	5 days	10 days
A-8	2.00	3.00	3.88	[C_2mim][Br]	190	amorphous	amorphous	SIZ-4	SIZ-4	SIZ-4
A-10	2.00	3.00	3.88	[C_4mim][Br]	190	AFI+SIZ-4	AFI+SIZ-4	SIZ-4	SIZ-4	SIZ-4
A-9	2.00	4.00	4.84	[C_2mim][Br]	190	AEL	AEL	AEL	SIZ-4	SIZ-4
A-11	2.00	4.00	4.84	[C_4mim][Br]	190	AFI	AFI	AFI	SIZ-4	SIZ-4
A-2	1.00	2.55	3.45	[C_4mim][Br]	150	amorphous	Amorphous	amorphous+peaks	SIZ-4	SIZ-4
A-4	1.00	2.55	3.45	[C_6mim][Br]	150	AEL	AEL	SIZ-4	SIZ-4	SIZ-4
molar ratio of acid: IL: SDA = 0.6: 20: 1.50; Acid: HF; SDA: DPA										

6.1.3.4 Influence of concentration of precursors in the reaction gel on the yield of products

The ionic liquid [C_6mim][Br] can dissolve up to 44 wt% pure phosphoric acid,[52] which is significantly higher than the typical concentration of phosphoric acid used in the synthesis of the aluminophosphates.[22,24,27] Recipe A-4 was used to determine whether the yield of the final product could be increased by just increasing the concentration of the precursors in solution or if the ratio of solvent to precursor would affect the final framework structure. These five new recipes (a)-(e) are shown in Table 6-6. In these recipes, heating time, temperature and amount of [C_6mim][Br] are kept the same. A-4(a), A-4(b), A-4(c) and A-4(d) only differ in the molar ratio of Al: P: IL. It should be noted that the ratio of H_2O: IL is also increased due to the increased use of phosphoric acid. A-4(e) is created by increasing every ingredient in recipe A-4(a) by a factor of four. Before calcination, weights of products synthesized are 0.275 g, 0.514 g, 0.725 g 1.392 g and 1.234g, however the frameworks are not the same, from SIZ-4 (porous) to AEL (porous) to berlinite (dense), and then to amorphous structure. The appearance of berlinite in recipes A-4(c) and A-4(d) is probably due to the increase of water concentration in the reaction gel, which was

also observed by Dr. Morris and his coworkers.[45] This result indicates in ionothermal synthesis, increasing the concentration of precursors in the reaction gel could increase the yield of products, but the solvent to precursor ratio may be necessary to retain the framework structure.

Table 6-6 Concentration of precursors and reaction conditions of revised recipes based on A-4, along with yield and frameworks synthesized.

Name	$Al(OiPr)_3$	H_3PO_4	HF	$[C_6mim][Br]$	H_2O(*)	DPA	Yield (g)	Framework
A-4(a)	1.0	2.9	0.7	20.1	3.4	1.4	0.275	SIZ-4
A-4(b)	1.9	5.0	0.7	20.0	5.7	1.5	0.514	AEL
A-4(c)	3.9	10.2	0.7	20.2	10.5	1.5	0.725	Berlinite
A-4(d)	6.0	15.5	0.7	20.0	15.8	1.5	1.392	Berlinite
A-4(e)	3.8	9.7	2.3	20.0	13.1	5.7	1.234	amorphous
Temp.: 150 ^oC, heating time: 8 hrs								

6.1.3.5 Influence of precursor's ratio on frameworks synthesized

It is known that ratio of precursors could affect the final crystal phase of zeolites in hydrothermal synthesis.[53-55] The importance of precursor's ratio is also shown in ionothermal synthesis of zeolites. For example, Zhang et al. found frameworks of aluminophosphates changes from LTA to amorphous phase the molar ratio of Al_2O_3 to P_2O_5 is systematically decreased; frameworks of gallium phosphates changes from LTA to quartz then to amorphous phase when the molar ratio of Ga_2O_3 to P_2O_5 is decreased.[30] Wang et al. found when $Al_2O(CH_3COO)_4{\cdot}4H_2O$ is used as the aluminium source and the ratio of P: Al is equal to 1: 1, the product is amorphous aluminophosphate.[56] With the increase of P: Al, AEL is gradually formed and the highest crystallinity is reached when the ratio of P: Al is 1.5: 1, but when $Al[OCH(CH_3)_2]_3$ is used as the aluminium source, the optimum ratio of P: Al is 3:1.[56]

Effect of precursor's ratio is also investigated in this work. The recipes are listed in Table 6-7. These recipes can be separated into two groups; A-10, A-11 and A-5 belong to the first group and A-9, A-10 and A-6 belong to the second group. $[C_4mim][Br]$ and $[C_2mim][Br]$ are used as the solvents for the recipes of the first group and the second group, respectively. Recipes in each group only differ in the molar ratio of Al: P. From the recipes in the first group (A-10, A-11 and A-5), it can be seen that although the frameworks synthesized within several hours are different, frameworks synthesized after several days are all SIZ-4. Increasing the ratio of Al to P is able to produce the structure of AEL within several hours. From the recipes in the second group (A-9, A-10 and A-6), frameworks synthesized within several hours are either AEL or

amorphous structures, no AFI is synthesized following recipes in the second group. After several days, all of the products changed to structure SIZ-4. Comparing recipes in the first group and second group, [C_4mim][Br] tends to produce structure AFI and [C_2mim][Br] tends to produce structure AEL within several hours heating. This finding is consistent with that published by Xu and his coworkers.[26]

Table 6-7 Ratio of precursors and reaction conditions of recipes used to investigate effect of precursor's ratio, along with frameworks synthesized after heating for different times.

Recipe	$Al(OiPr)_3$	H_3PO_4	H_2O (*)	IL		Frameworks				
						2 hours	4 hours	8 hours	5 days	10 days
A-10	2.00	3.00	3.88	[C_4mim][Br]	20	AFI+SIZ-4	AFI+SIZ-4	SIZ-4	SIZ-4	SIZ-4
A-11	2.00	4.00	4.84	[C_4mim][Br]	20	AFI	AFI	AFI	SIZ-4	SIZ-4
A-5	2.00	5.10	5.90	[C_4mim][Br]	20	AEL+AFI	AEL	AEL+SIZ-4	SIZ-4	SIZ-4
A-9	2.00	3.00	3.88	[C_2mim][Br]	20	AEL	AEL	AEL	SIZ-4	SIZ-4
A-10	2.00	4.00	4.84	[C_2mim][Br]	20	amorphous	amorphous+peaks	SIZ-4	SIZ-4	SIZ-4
A-6	2.00	5.10	5.90	[C_2mim][Br]	20	AEL+amorphous	AEL	AEL	SIZ-4	SIZ-4
hydrofluoric acid: 0.6, DPA: 1.5, Temp.: 190 ^oC										

6.1.4 Conclusion

In summary, this paper reports some new discoveries on ionothermal synthesis of zeolites, specifically porous aluminophosphates. First, hydrochloric acid is a promising mineralizer to synthesize crystalline materials in ionothermal synthesis. However, the frameworks synthesized with hydrofluoric acid and with hydrochloric acid are different. When hydrochloric acid is used as the mineralizer, structure directing agent plays an important role in deciding the framework structures after heating the reaction gels for several hours and for several days. Second, the structures synthesized within several hours will undergo dramatic changes from several hours heating to several hours heating, no matter with which acid used. Third, slightly longer alkyl chain of ILs could possibly shorten the formation time of crystalline materials, but the slight difference of alkyl chain length has no effect on the framework topology formed after prolonged heating of time. Yield of products can be raised by increasing amount of precursors in the reaction gel, but when the molar ratio of precursor to solvent reaches a limit, products synthesized are dense material instead of porous material, probably due to the increased amount of water in the reaction gel. Finally, molar ratio of precursors also has an influence on the frameworks synthesized within several hours.

6.1.5 References

1. Zhang, S. J.; Sun, N.; He, X. Z.; Lu, X. M.; Zhang, X. P. *Journal of Physical and Chemical Reference Data* **2006**, *35*, 1475-1517.
2. Rooney, D.; Jacquemin, J.; Gardas, R. L. Thermophysical Properties of Ionic Liquids. In *Ionic Liquids*, 2009; Vol. 290; pp 185-212.
3. Trohalaki, S.; Pachter, R. *Qsar & Combinatorial Science* **2005**, *24*, 485-490.
4. Krossing, I.; Slattery, J. M.; Daguenet, C.; Dyson, P. J.; Oleinikova, A.; Weingartner, H. *Journal of the American Chemical Society* **2006**, *128*, 13427-13434.
5. Zhao, H. L.; Tang, Z. X.; Zhang, Q. G.; You, J. H.; Chen, Q. D. *Progress in Chemistry* **2009**, *21*, 2077-2083.
6. Itoh, N. *Journal of the Electrochemical Society* **2009**, *156*, J37-J40.
7. Youngs, T. G. A.; Hardacre, C.; Holbrey, J. D. *Journal of Physical Chemistry B* **2007**, *111*, 13765-13774.
8. Yagi, T.; Sasaki, S.; Mano, H.; Miyake, K.; Nakano, M.; Ishida, T. *Proceedings of the Institution of Mechanical Engineers Part J-Journal of Engineering Tribology* **2009**, *223*, 1083-1090.
9. Fox, M. F.; Priest, M. *Proceedings of the Institution of Mechanical Engineers Part J-Journal of Engineering Tribology* **2008**, *222*, 291-303.
10. Li, Z. J.; Chang, J.; Shan, H. X.; Pan, J. M. *Reviews in Analytical Chemistry* **2007**, *26*, 109-153.
11. McFarlane, J.; Ridenour, W. B.; Luo, H.; Hunt, R. D.; DePaoli, D. W.; Ren, R. X. *Separation Science and Technology* **2005**, *40*, 1245-1265.
12. Wang, J. J.; Wang, H. Y.; Zhang, S. L.; Zhang, H. H.; Zhao, Y. *Journal of Physical Chemistry B* **2007**, *111*, 6181-6188.
13. Ye, C. F.; Shreeve, J. M. *Journal of Physical Chemistry A* **2007**, *111*, 1456-1461.
14. Jacquemin, J.; Husson, P.; Mayer, V.; Cibulka, I. *Journal of Chemical and Engineering Data* **2007**, *52*, 2204-2211.
15. Seddon, K. R. "Ionic liquids: designer solvents?" International George Papatheodorou Symposium, 1999, Patras, Greece.
16. Morris, R. E. *Chemical Communications* **2009**, 2990-2998.

17. Han, L. J.; Wang, Y. B.; Li, C. X.; Zhang, S. J.; Lu, X. M.; Cao, M. J. *Aiche Journal* **2008**, *54*, 280-288.
18. Parnham, E. R.; Morris, R. E. *Accounts of Chemical Research* **2007**, *40*, 1005-1013.
19. Feng, P. Y.; Bu, X. H.; Stucky, G. D. *Nature* **1997**, *388*, 735-741.
20. Meriaudeau, P.; Tuan, V. A.; Nghiem, V. T.; Lai, S. Y.; Hung, L. N.; Naccache, C. *Journal of Catalysis* **1997**, *169*, 55-66.
21. Sun, X.; King, J.; Anthony, J. L. *Chemical Engineering Journal* **2009**, *147*, 2-5.
22. Cooper, E. R.; Andrews, C. D.; Wheatley, P. S.; Webb, P. B.; Wormald, P.; Morris, R. E. *Nature* **2004**, *430*, 1012-1016.
23. Parnham, E. R.; Morris, R. E. *Journal of the American Chemical Society* **2006**, *128*, 2204-2205.
24. Parnham, E. R.; Morris, R. E. *Chemistry of Materials* **2006**, *18*, 4882-4887.
25. Parnham, E. R.; Morris, R. E. *Journal of Materials Chemistry* **2006**, *16*, 3682-3684.
26. Xu, Y. P.; Tian, Z. J.; Wang, S. J.; Hu, Y.; Wang, L.; Wang, B. C.; Ma, Y. C.; Hou, L.; Yu, J. Y.; Lin, L. W. *Angewandte Chemie-International Edition* **2006**, *45*, 3965-3970.
27. Wang, L.; Xu, Y. P.; Wei, Y.; Duan, J. C.; Chen, A. B.; Wang, B. C.; Ma, H. J.; Tian, Z. J.; Lin, L. W. *Journal of the American Chemical Society* **2006**, *128*, 7432-7433.
28. Parnham, E. R.; Wheatley, P. S.; Morris, R. E. *Chemical Communications* **2006**, 380-382.
29. Cai, R.; Sun, M. W.; Chen, Z. W.; Munoz, R.; O'Neill, C.; Beving, D. E.; Yan, Y. S. *Angewandte Chemie-International Edition* **2008**, *47*, 525-528.
30. Han, L. J.; Wang, Y. B.; Zhang, S. J.; Lu, X. M. *Journal of Crystal Growth* **2008**, *311*, 167-171.
31. Liu, L.; Li, X. P.; Xu, H.; Li, J. P.; Lin, Z.; Dong, J. X. *Dalton Transactions* **2009**, 10418-10421.
32. Ma, H. J.; Xu, R. S.; You, W. S.; Wen, G. D.; Wang, S. J.; Xu, Y.; Wang, B. C.; Wang, L.; Wei, Y.; Xu, Y. P.; Zhang, W. P.; Tian, Z. J.; Lin, L. W. *Microporous and Mesoporous Materials* **2009**, *120*, 278-284.
33. Fayad, E. J.; Bats, N.; Kirschhock, C. E. A.; Rebours, B.; Quoineaud, A. A.; Martens, J. A. *Angewandte Chemie-International Edition* **2010**, *49*, 4585-4588.
34. Xu, R. S.; Zhang, W. P.; Han, X. W.; Bao, X. H. *Chinese Journal of Catalysis* **2010**, *31*, 776-780.

35. Wheatley, P. S.; Allan, P. K.; Teat, S. J.; Ashbrook, S. E.; Morris, R. E. *Chemical Science* **2010**, *1*, 483-487.

36. Wei, Y.; Tian, Z. J.; Gies, H.; Xu, R. S.; Ma, H. J.; Pei, R. Y.; Zhang, W. P.; Xu, Y. P.; Wang, L.; Li, K. D.; Wang, B. C.; Wen, G. D.; Lin, L. W. *Angewandte Chemie-International Edition* **2010**, *49*, 5367-5370.

37. Cai, R.; Liu, Y.; Gu, S.; Yan, Y. S. *Journal of the American Chemical Society* **2010**, *132*, 12776-12777.

38. Pei, R. Y.; Xu, Y. P.; Wei, Y.; Wen, G. D.; Li, K. D.; Wang, L.; Ma, H. J.; Tian, Z. J.; Lin, L. W. *Chinese Journal of Catalysis* **2010**, *31*, 1083-1089.

39. Ma, Y. C.; Wang, S. J.; Song, Y.; Xu, Y. P.; Tian, Z. J.; Yu, J. Y.; Lin, L. W. *Chinese Journal of Inorganic Chemistry* **2010**, *26*, 1923-1926.

40. Pei, R. Y.; Tian, Z. J.; Wei, Y.; Li, K. D.; Xu, Y. P.; Wang, L.; Ma, H. J. *Materials Letters* **2010**, *64*, 2118-2121.

41. Fayad, E. J.; Bats, N.; Kirschhock, C. E. A.; Rebours, B.; Quoineaud, A. A.; Martens, J. A. *Angewandte Chemie-International Edition* **2010**, *49*, 4585-4588.

42. Ng, E. P.; Itani, L.; Sekhon, S. S.; Mintova, S. *Chemistry-a European Journal* **2010**, *16*, 12890-12897.

43. Zhao, X. H.; Wang, H.; Kang, C. X.; Sun, Z. P.; Li, G. X.; Wang, X. L. *Microporous and Mesoporous Materials* **2012**, *151*, 501-505.

44. Wang, L.; Xu, Y. P.; Wang, B. C.; Wang, S. J.; Yu, J. Y.; Tian, Z. J.; Lin, L. W. *Chemistry-a European Journal* **2008**, *14*, 10551-10555.

45. Wragg, D. S.; Slawin, A. M. Z.; Morris, R. E. *Solid State Sciences* **2009**, *11*, 411-416.

46. Gaillon, L.; Sirieix-Plenet, J.; Letellier, P. *Journal of Solution Chemistry* **2004**, *33*, 1333-1347.

47. IZA. Database of Zeolite Structures, http://www.iza-structure.org/databases/.

48. Liebau, F. *Structural Chemistry of Silicates: Structure, Bonding, and Classification*; Springer-Verlag: Berlin, Heidelberg, New York, Tokyo, 1985.

49. Liebau, F.; Gies, H.; Gunawardane, R. P.; Marler, B. **1986**, *6*, 373.

50. Pei, R. Y.; Tian, Z. J.; Wei, Y.; Li, K. D.; Xu, Y. P.; Wang, L.; Ma, H. J. *Materials Letters* **2010**, *64*, 2384-2387.

51. Huang, A. S.; Caro, J. *Microporous and Mesoporous Materials* **2010**, *129*, 90-99.

52. Sun, X.; Anthony, J. L. *Manuscript in preparation* **2012**.

53. Robson, H. *Verified Syntheses of Zeolitic Materials*, 2 ed.; Elsevier Science B. V.: Amsterdam, 2001.

54. Barrer, R. M. *Hydrothermal Chemisry of Zeolites*; Academic Press: London, 1982.

55. Wright, P. A. *Microporous Framework Solids*; The Royal Society of Chemistry: Cambridge, 2008.

56. Wang, S. J.; Hou, L.; Xu, Y. P.; Tian, Z. J.; Xu, J. Y.; Lin, L. W. *The Chinese Journal of Process Engineering* **2008**, *8*, 93-96.

6.2 Molecular Sieve Synthesis in the Presence of Tetraalkylammonium and Dialkylimidazolium Molten Salts

6.2.1 Introduction

Since the discovery of stilbite ($NaCa_2Al_5Si_{13}O_{36}.14H_2O$), the first of a group of crystalline microporous aluminosilicates discovered over 200 years ago by the Swedish scientist Cronstedt, molecular sieves have found many applications in water softening, wastewater treatment, odor control, cracking catalysts in oil industry, etc.[1-7] These stable, crystalline materials with nanometer-sized pores can have a wide range of chemical compositions, including silicate, aluminophosphate, or all-carbon molecular sieves, to name but a few.[8-11] Subsequently, there has been extensive research on the synthesis of new frameworks as well as trying to understand their mechanism of crystallization.[12-15]

Crystalline molecular sieves traditionally are prepared using hydrothermal methods. A typical zeolite synthesis would consist of a mixture of water, a source of the framework atoms, a mineralizing agent (e.g. OH^- or F^-), and a structure-directing agent (SDA).[16-20] Recently, Morris and coworkers developed an ionothermal synthesis method for several aluminophosphate molecular sieves, where an ionic liquid serves as the solvent and/or the structure directing agent.[21-23]

Both the solvent and the SDA are extremely important in the synthetic mechanism of the molecular sieves, with the role of the SDA being most widely studied. Structure directing agents have several roles during the synthesis of zeolites. They can serve only as space-holders or pore-filling agents, they can have specific interactions with the zeolite precursors that aid in directing the structure formation, or in some less common cases they can serve as templates for the final structure.[24-25] A proposed mechanism of structure directing effect on the framework formation suggests that the precursors organize around the SDAs and subsequently assemble into crystalline structures.[12, 26, 27] As a result, different SDAs usually lead to various structures. For example, in the ionothermal synthesis of AlPOs, the larger imidazolium cation $[C_4mim]^+$ leads to AFI structure which has a 12-ring channel, whereas, the smaller $[C_2mim]^+$ leads to AEL framework, which has 10-ring channel.[28] A large number of SDAs take the form of amines or tetraalkylammonium salts (e.g. [TPA][Br], DPA); the structures and sizes of those salts can be

easily altered so as to cater to variety of microporous void shapes. These SDA cations are also commonly used in ionic liquids (ILs), such as 1-methyl-3-ethylimidazolium bromide ([C_2mim][Br]) and tetramethylammonium 2,2,2-trifluoro-N-(trifluoromethylsulfonyl) acetamide ([TMA][TSAC]).[29] Unlike typical structure directing agents, the low melting points and good solvating properties also allow ILs to serve as the solvent in the synthesis reaction.[30-33]

In this work, we replaced a traditional SDA (e.g. [TPA][Br], T_{mp} = 270 ^oC[34]) with various salts while maintaining the same synthetic composition ratio. [TPA] and [TBA] are both quaternary ammonium cations and have been used as structure directing agents in molecular sieves synthesis. They have been chosen to compare the effect of alkyl chain length of SDAs on formation of silicate materials. Salts with [TBA] as the cation and different anions are also used in order to investigate the influence of different anions on the framework. The authors also replaced [TPA][Br] with the common ionic liquid 1-ethyl-3-methylimidazolium bromide [C_2mim][Br]. Two known materials were formed at the completion of the reaction depending on the salt used: either a porous silicate of MFI-type framework or the dense layered silicate magadiite.

6.2.2 Experimental procedure

Materials were prepared hydrothermally based on the method used to synthesize pure silica ZSM-5, a zeolite of MFI-type framework.[35] Water, salt (e.g. IL or SDA), base (e.g. NaOH), and silicon dioxide (e.g. Syloid 63 fumed silica) were combined in a molar ratio of 0.072 H_2O: 0.030 SDA or IL: 0.37 NaOH: 9.2 SiO_2. The molten salts/ionic liquids used include tetrabutylammonium bromide ([TBA][Br] , T_{mp} =102-104 ^oC[31]), tetrabutylammonium hexafluorophosphate ([TBA][PF_6], T_{mp} = 244-246 ^oC[36]), tetrabutylammonium nitrate ([TBA][NO_3] , T_{mp} = 118-120 ^oC[37]), tetrapropylammonium bromide ([TPA][Br], T_{mp} = 270 ^oC[34]), and 1-methyl-3-ethylimidazolium bromide ([C_2mim][Br] , T_{mp} = 79 ^oC[38]). After stirring for 2 hours, reaction mixtures were charged into Teflon-lined autoclaves, which were placed in an oven at 150 ^oC for 24 – 48 hr. The white precipitate was carefully washed with water, followed by acetone wash (for [TPA][PF_6] only), and dried in air at room temperature. Sample powders were analyzed using an X-ray diffractometer (Bruker AXS D8 Advance), and the resulting patterns were compared to those available in the literature.[39, 40]

6.2.3 Results

Each of the synthesis mixtures with the five different IL/SDAs (shown in Table 6-8) yielded a powder product; their XRD patterns are shown in Figure 6.5. Products synthesized in the presence of either tetrabutylammonium bromide ([TBA][Br]), tetrabutylammonium hexafluorophosphate ([TBA][PF_6]), tetrabutylammonium nitrate ([TBA][NO_3]), or 1-methyl-3-ethylimidazolium bromide ([C_2mim][Br]) all show main XRD peaks at $5.55^o 2\theta$, $22.5^o 2\theta$, $25.8^o 2\theta$, $26.9^o 2\theta$, and $28.25^o 2\theta$, which are characteristic of magadiite.[41] However, in the case where tetrapropylammonium bromide ([TPA][Br]), the pattern is characteristic of MFI, as expected since the reaction composition and SDA used in (4) were comparable to those in reported MFI syntheses.[42, 43] For comparison, Table 6-9 shows several previously reported synthesis conditions for both magadiite and MFI.

Table 6-8 Molar composition of reagents for preparation of magadiite and MFI in the presence of molten salts.

Product	SiO_2	H_2O	NaOH	SDA		Time (hr)	Temp.(^{o}C)	Product type
Sample-1	1.00	24.76	0.195	0.081	[TBA][Br]	44	150	magadiite
Sample-2	1.00	24.76	0.195	0.081	[TBA][PF_6]	44	150	magadiite
Sample-3	1.00	24.76	0.195	0.081	[TBA][NO_3]	44	150	magadiite
Sample-4	1.00	24.76	0.195	0.081	[TPA][Br]	44	150	MFI
Sample-5	1.00	24.76	0.195	0.081	[C_2mim][Br]	44	150	magadiite

Table 6-9 Literature molar composition of reagents for preparation of magadiite and MFI.

Literature	SiO_2	H_2O	NaOH	SDA		Other reagent		Time (hr)	Temp.(^{o}C)	Product type
40	1.00	16.67	0.333					42	150	magadiite
41	1.00	18.50	0.230					18	170	magadiite
42	1.00	20.00	0.200					48	150	magadiite
43	1.00	33.33	0.111			0.222	Na_2CO_3	72	150-160	magadiite
36	1.00	20.00	0.067	0.750	PEG 200 *	0.133	Na_2CO_3	24	150	magadiite
43	1.00	58.00	0.280					96	150	magadiite
38	1.00	22.03		0.108	[TPA][Br]	0.025	$Al_2(SO_4)_3$	144	180	MFI
						0.300	Na_2O			
						0.193	H_2SO_4			
						0.500	NaCl			
44	1.00	200		0.8	[TPA][Br]	0.5	NEt_3	96	130	MFI

45	1.00	38.00		0.100	[TPA][OH]			360	110	MFI
35	1.00	25.00	0.333			0.067	$NaAlO_2$	24	180	MFI
46	1.00	58.33	0.277	0.750	PEG 200 *	0.167	Al_2O_3	144	150	MFI

* PEG 200: Poly (ethyl glycol)

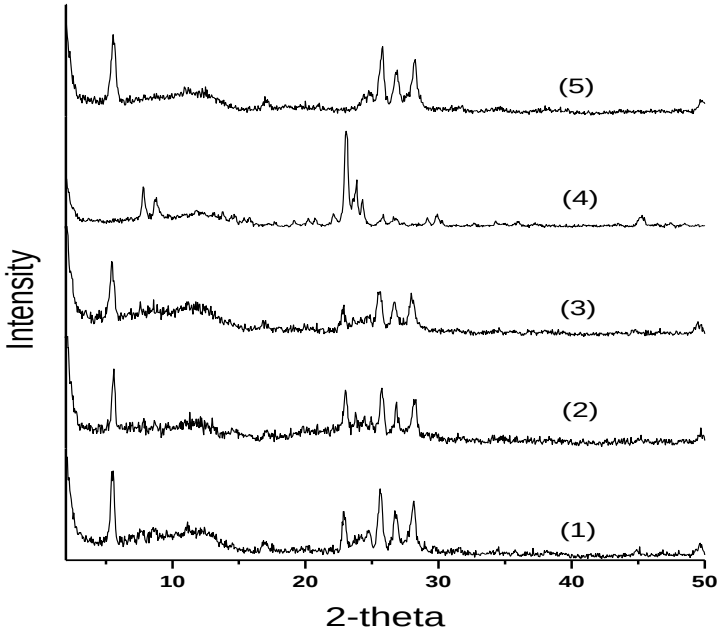

Figure 6.5 XRD patterns of products (1)-(5). Their SDAs are (1) [TBA][Br], (2) [TBA][PF_6], (3) [TBA][NO_3], (4) [TPA][Br], (5) [C_2mim][Br].

6.2.4 Discussion

Among the five salts used, only [TPA][Br] yielded a porous pure silica zeolite with the MFI-type framework ($Si_{96}O_{192}$). MFI-type material has a three dimensional pore system containing sinusoidal 10-ring channels and intersecting straight 10-ring channel,[51, 52] the structure of which is shown in Figure 6.6-(a). [TPA] is the most common cation for the synthesis of MFI-type structures.[53-56] It has been reported that favorable van der Waals interactions between the organic structure directing agent and hydrophobic silicon dioxide are the main thermodynamic driving forces for the assembly of MFI-type or similar zeolites.[12] However, by making a slight change to the cation structure by lengthening the alkyl chains from propyl to

butyl (e.g. [TBA][Br]), the MFI-type framework was no longer obtained. Clearly, the larger cation did not provide the necessary van der Waals forces to make MFI.

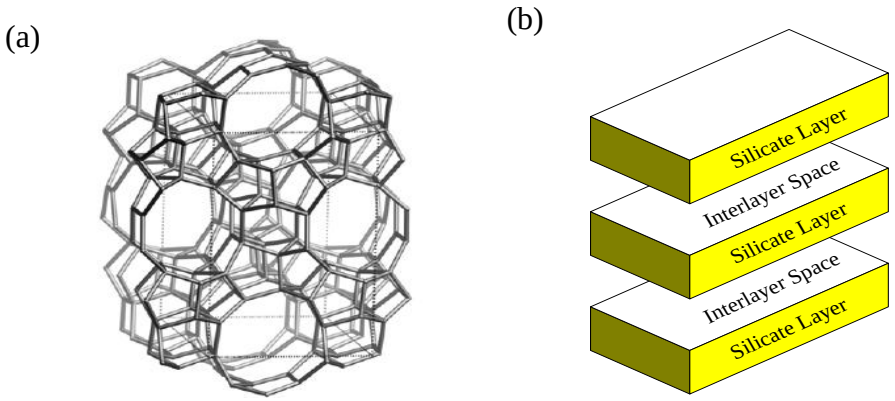

Figure 6.6 Schematic diagram of (a) the structure of MFI [53] and (b) the structure of magadiite. [54]

The syntheses with the remaining salts all resulted in the formation of magadiite ($NaSi_7O_{13}(OH)_3.4(H_2O)$), which is a dense material with silicate layer. The terminal oxygen ions of magadiite are balanced by sodium ions located between silicate layers.[59] Schematic diagram of magadiite is illustrated in Figure 6.6-(b). It is suggested that natural Na-magadiite was precipitated from the alkaline brines which were rich in silica, and low in alumina, the absence of which is of critical importance.[41] Due to magadiite's special structure, it can be used in detergent systems and catalyst support.[59, 60]

According to the literature, Na^+-magadiite is typically synthesized hydrothermally at 150 ^oC for 42 hr with molar ratios ranging from 16-58 H_2O: 0.1-0.3 NaOH: 1 SiO_2.[41, 44-46] It is noteworthy that in those reports magadiite can be synthesized without a structure directing agent. In the current work, all of the precursors and solvents are heated at 150 ^oC for 24 – 48 hr and with synthetic compositions similar to the conditions employed in producing Na^+-magadiite. In this respect, the addition of [TBA][Br], [TBA][PF_6], [TBA][NO_3] or [C_2mim][Br] neither enhanced nor inhibited the formation of the magadiite; they merely served as cosolvents. Although the salts did not serve as structure directing agents, they also did not interfere with the silica chemistry necessary for making the layered silicate. Layered silicates such as magadiite are not porous materials; however, they are recognized as being precursors to the synthesis of porous silicates.[41, 58] The fact that dense layered silicates can be synthesized in the presence of

ionic liquids bodes well for the possibility of also synthesizing a porous silicate in the presence of ILs.

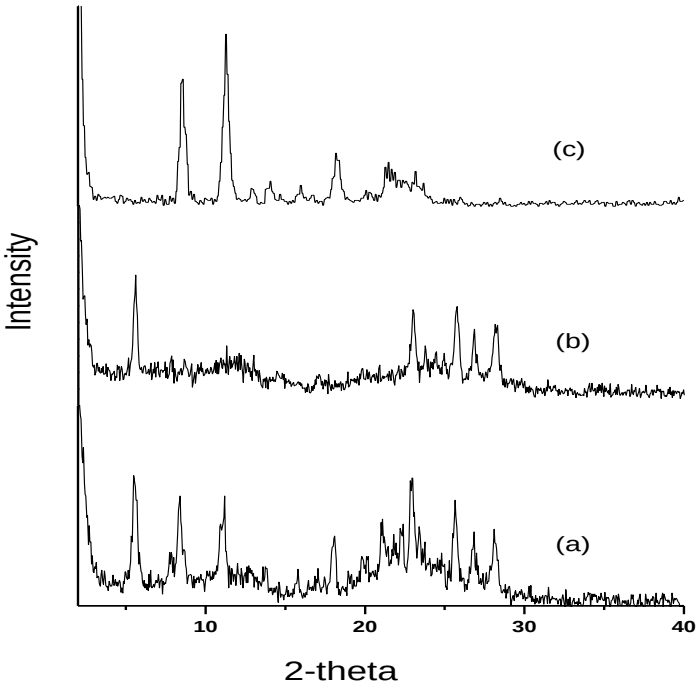

Figure 6.7 XRD patterns of (a) water washed product-2, (b) water and acetone washed product-2, and (c) [TPA][PF_6].

It is worthwhile to point out that the XRD pattern of product (2) after washing with water only was not the same as that shown in Figure 6.5. Although there are peaks characteristic of magadiite at $5.55^{o}2\theta$, $22.5^{o}2\theta$, $25.8^{o}2\theta$, $26.9^{o}2\theta$, and $28.25^{o}2\theta$, additional peaks were observed at $8.5^{o}2\theta$, $11.2^{o}2\theta$, and $18.1^{o}2\theta$, which can be seen in Figure 6.7-(a). However, after the sample was washed in acetone for 24 hr, additional peaks were no longer visible (Figure 6.7-(b)). Those additional peaks are characteristic of the salt [TBA][PF_6]; the XRD pattern of which is shown in Figure 6.7-(c). Although [TBA][PF_6] did not serve as a SDA during the synthesis process, the high intensity peaks indicate it was present in the final post-synthesis product, possibly in the interlayer space of magadiite. Unlike the other salts used in this work, salts composed of the [PF_6] anion and large organic cations are fairly hydrophobic and have a notably lower solubility in water,[61-63] which required the use of another solvent (i.e. acetone) to wash the residual [TBA][PF_6] from the final layer.

6.2.5 Conclusions

In this paper, the role of different salts with common ionic liquid cations and anions was studied in the synthesis of silicate-based molecular sieves. In the presence of [TPA][Br], a common SDA for MFI, pure-silica ZSM-5 is formed. However, with a little change to the alkyl branch of quaternary salts (e.g. [TPA][Br] to [TBA][Br]) another material, magadiite, whose synthesis commonly does not require the presence of SDA, is formed. This result affirms the importance of appropriate van der Waals forces between the precursor and structure directing agent. Also demonstrated is that the addition of tetraalkylammonium salts to the magadiite reaction mixture does not inhibit the silica chemistry involved in the formation of magadiite. This is a significant result because pillared layered minerals such as magadiite are often considered precursors to useful porous materials.

Section 6.1 is a soon to be submitted manuscript.

Section 6.2 is taken from the publication: Sun, X., King, J. and Anthony, J. L. “Molecular sieve synthesis in the presence of tetraalkylammonium and dialkylimidazolium molten salts”, J. Chem. Eng., 2009, 147, 2-5.

6.2.6 References

1. J. P. Anerousis, Chem. Eng. 83 (1976) 128-130.
2. E.L. Cooney, N.A. Booker, D.C. Shallcross, G.W. Stevens, Sep. Sci. Technol. 34 (1999) 2307-2327.
3. T.S.C. Law, C.Y.H. Chao, G.Y.W. Chan, A.K.Y. Law, Indoor Built Environ. 13 (2004) 45-51.
4. L. Li, H.F. Pan, W.B. Li, Chin. J. Catal. 23 (2002) 65-68.
5. C.F. Lin, S.S. Lo, H.Y. Lin, Y.C. Lee, J. Hazard. Mater. 60 (1998) 217-226.
6. S. Montalvo, L. Guerrero, R. Borja, L. Travieso, E. Sanchez, F. Diaz, Resour. Conserv. Recycl. 47 (2006) 26-41.
7. J. Yang, L.L. Ma, B. Shen, J.H. Zhu, Mater. Manuf. Process. 22 (2007) 750-757.
8. R.E. Morris, S.J. Weigel, Chem. Soc. Rev. 26 (1997) 309-317.
9. J. Lee, J. Kim, T. Hyeon, Adv. Mater. 18 (2006) 2073-2094.
10. Z.A.D. Lethbridge, J.J. Williams, R.I. Walton, K.E. Evans, C.W. Smith, Microporous Mesoporous Mat. 79 (2005) 339-352.
11. J.D. Epping, B.F. Chmelka, Curr. Opin. Colloid Interface Sci. 11 (2006) 81-117.
12. S.L. Burkett, M.E. Davis, J. Phys. Chem. 98 (1994) 4647-4653.
13. G. Cao, M.J. Shah, Microporous Mesoporous Mat. 101 (2007) 19-23.
14. C.S. Cundy, P.A. Cox, Microporous Mesoporous Mat. 82 (2005) 1-78.
15. J.D. Rimer, J.M. Fedeyko, D.G. Vlachos, R.F. Lobo, Chem.-Eur. J. 12 (2006) 2926-2934.
16. V.R. Choudhary, A.K. Kinage, A.A. Belhekar, Zeolites 18 (1997) 274-277.
17. M.J. Eapen, K.S.N. Reddy, V.P. Shiralkar, Zeolites 14 (1994) 295-302.
18. S.V. Awate, P.N. Joshi, V.P. Shiralkar, A.N. Kotasthane, J. Incl. Phenom. Mol. Recogn. Chem. 13 (1992) 207-218.
19. M.J. Annen, M.E. Davis, J.B. Higgins, J.L. Schlenker, J. Chem. Soc.-Chem. Commun. (1991) 1175-1176.
20. L. Massuger, C. Baerlocher, L.B. McCusker, M.A. Zwijnenburg, Microporous Mesoporous Mat. 105 (2007) 75-81.
21. E.R. Cooper, C.D. Andrews, P.S. Wheatley, P.B. Webb, P. Wormald, R.E. Morris, Nature 430 (2004) 1012-1016.
22. E.R. Parnham, R.E. Morris, J. Am. Chem. Soc. 128 (2006) 2204-2205.

23. E.R. Parnham, R.E. Morris, Chem. Mat. 18 (2006) 4882-4887.
24. G. Sastre, Phys. Chem. Chem. Phys. 9 (2007) 1052-1058.
25. G. Bonilla, I. Diaz, M. Tsapatsis, H.K. Jeong, Y. Lee, D.G. Vlachos, Chem. Mat. 16 (2004) 5697-5705.
26. A.E. Visser, R.P. Swatloski, W.M. Reichert, R. Mayton, S. Sheff, A. Wierzbicki, J.H. Davis, R.D. Rogers, Environ. Sci. Technol. 36 (2002) 2523-2529.
27. J.O. Valderrama, P.A. Robles, Ind. Eng. Chem. Res. 46 (2007) 1338-1344.
28. M. Koel, Crit. Rev. Anal. Chem. 35 (2005) 177-192.
29. F. Endres, S.Z. El Abedin, Phys. Chem. Chem. Phys. 8 (2006) 2101-2116.
30. J. A. Dean, Lange's handbook of chemistry, McGraw-Hill, New York, NY, USA, 1998.
31. A. Culfaz, U. Gunduz, H. Orbey, Cryst. Res. Technol. 28 (1993) 29-38.
32. M. M. Baizer, Organic electrochemistry, Marcel. Dekker,, New York, NY, USA, 1973.
33. R. J. Lewis Sr., Sax's dangerous properties of industrial materials, Wiley-Interscience, Malden, MA, USA, 2005.
34. I. Lopez-Martin, E. Burello, P.N. Davey, K.R. Seddon, G. Rothenberg, ChemPhysChem 8 (2007) 690-695.
35. Y. Cheng, L.J. Wang, J.S. Li, Y.C. Yang, X.Y. Sun, Mater. Lett. 59 (2005) 3427-3430.
36. O.Y. Kwon, S.Y. Jeong, J.K. Suh, J.M. Lee, Bull. Korean Chem. Soc. 16 (1995) 737-741.
37. S.T. Wong, S.F. Cheng, Chem. Mat. 5 (1993) 770-777.
38. B. Burger, K. Haas-Santo, M. Hunger, J. Weitkamp, Chem. Eng. Technol. 23 (2000) 322-324.
39. M. Liu, S. H. Xiang, Shiyou Xuebao 17 (2001) 24-29.
40. R.A. Fletcher, D.M. Bibby, Clay Clay Min. 35 (1987) 318-320.
41. K. Kikuta, K. Ohta, K. Takagi, Chem. Mat. 14 (2002) 3123-3127.
42. O.Y. Kwon, K.W. Park, Bull. Korean Chem. Soc. 25 (2004) 25-26.
43. F.X. Feng, K.J. Balkus, Microporous Mesoporous Mat. 69 (2004) 85-96.
44. T. Ban, H. Mitaku, C. Suzuki, T. Kume, Y. Ohya, Y. Takahashi, J. Porous Mat. 12 (2005) 255-263.
45. S.L. Burkett, M.E. Davis, Chem. Mat. 7 (1995) 920-928.
46. F.X. Feng, K.J. Balkus, J. Porous Mat. 10 (2003) 235-242.
47. G.T. Kokotailo, S.L. Lawton, D.H. Olson, W.M. Meier, Nature 272 (1978) 437-438.

48. D.H. Olson, G.T. Kokotailo, S.L. Lawton, W.M. Meier, J. Phys. Chem. 85 (1981) 2238-2243.
49. L.M. Huang, W.P. Guo, P. Deng, Z.Y. Xue, Q.Z. Li, J. Phys. Chem. B 104 (2000) 2817-2823.
50. W. Zhou, S.Y. Zhang, X.Y. Hao, H. Guo, C. Zhang, Y.Q. Zhang, S.X. Liu, J. Solid State Chem. 179 (2006) 855-865.
51. A.V. Goretsky, L.W. Beck, S.I. Zones, M.E. Davis, Microporous Mesoporous Mat. 28 (1999) 387-393.
52. C.A. Click, R.A. Assink, C.J. Brinker, S.J. Naik, J. Phys. Chem. B 104 (2000) 233-236.
53. C. Baerlocher, W. M. Meier, D.H. Olson, Atlas of zeolite framework types, Elsevier, Amsterdam, New York, USA, 2001.
54. G.G. Almond, R.K. Harris, K.R. Franklin, J. Mater. Chem. 7 (1997) 681-687.
55. I.V. Mitchell, Pillared Layered structures: current trends and applications, Elsevier, Amsterdam, NY, USA, 1990.
56. A. Fudala, Z. Konya, Y. Kiyozumi, S.I. Niwa, M. Toba, F. Mizukami, P.B. Lentz, J. Nagy, I. Kiricsi, Microporous Mesoporous Mat. 35-6 (2000) 631-641.
57. J.L. Anthony, E.J. Maginn, J.F. Brennecke, Journal of Physical Chemistry B 105 (2001) 10942-10949.
58. N.V. Shvedene, S.V. Borovskaya, V.V. Sviridov, E.R. Ismailova, I.V. Pletnev, Analytical and Bioanalytical Chemistry 381 (2005) 427-430.
59. W. L. F. Armarego, Purification of laboratory chemicals, Butterworth-Heinemann, Oxford, UK, 1997.

Chapter 7 - Conclusion and Recommendations

Conclusion

This project is aimed at investigating the behavior of precursors of zeolites in ionic liquids and the interaction between precursors and ionic liquids in ionothermal synthesis because these fundamental properties could be useful in the current and future synthesis of aluminophosphates. First, solubilities of different precursors, including Syloid 63 silica particles, aluminium isopropoxide and phosphoric acid in different ionic liquids are reported. Parameters such as activity coefficient and Henry's constant are also calculated. Influence of ILs' structures could make a great influence on the solubility of precursors. In addition, with the presence of phosphoric acid in ILs, more aluminium isopropoxide could be dissolved in ILs, indicating an interaction of phosphoric acid with aluminium isopropoxide in ILs. Then in order to reuse ionic liquids in ionothermal synthesis of aluminophosphates, influence of phosphoric acid on structures of ionic liquids is investigated. It is found at 50 ^{o}C, a very small amount of [C_2mim][Br] is decomposed by phosphoric acid even after 18 days. And after heated at 150 ^{o}C either for one hour or five days, the decomposed amount of [C_4mim][Br] is extremely small and negligible. As a result, the reuse of 1-alkyl-3-methylimidazolium bromides should not be hindered by the use of phosphoric acid.

Second, interaction between precursors and ILs are studied by ^{27}Al solid state NMR. The precursor is mainly aluminium isopropoxide. At room temperature, Al(VI) is the primary confirmation of aluminium atoms in aluminium isopropoxide, as compared to Al(IV) in as-synthesized molecular sieves. It is found that in [$C_n$mim][Br] (n=2, 4, 6) and at 70 ^{o}C, some Al atoms with Al(VI) confirmation begins to change to Al(IV). The change is more significant with the presence of phosphoric acid. At lower temperature, this change is not as remarkable as at 70 ^{o}C. With the increase of alkyl chain of ILs, ratio of Al(IV) to Al(VI) increases regardless at room temperature or at 70 ^{o}C, suggesting [C_6mim][Br] could possibly accelerates the formation of Al-O-P bonds.

Third, it is found that in hydrothermal synthesis, hydrochloric acid could be used as the mineralizer and the usage of hydrochloric acid yield very different structures from the usage of hydrofluoric acid. Hydrochloric acid is capable of generating both dense and porous materials.

Regardless of the acid used, frameworks synthesized after several hours always undergo a dramatic change after further heating up to ten days. A slightly longer alkyl chain of ILs could accelerate the formation of crystalline materials. Increasing concentration of precursors in the reaction gel could increase the yield, but the same framework is not retained, transforming from porous material to dense material, and the formation of dense structure when concentration of precursors reaches a limit is possibly due to increase of water content in the reaction gel. Some of these experimental results are inspired or corresponding to the results of solubility test and solid NMR experiment. For example, the founding of the maximum solubility of phosphoric acid in $[C_6mim][Br]$ leads to the experiment to increase the concentration of precursors in reaction gels in order to maximize yield. Moreover, the founding of a slight increase in alkyl chain length shortens formation of Al-O-P bond by ^{27}Al solid state NMR is consistent with the finding that a slightly longer alkyl chain of ILs could accelerate the formation of crystalline materials in ionothermal synthesis.

Finally, in the hydrothermal synthesis of silicate-based molecular sieves with the addition of different molten salts with common ionic liquid cations and anions, it is found that pure-silica ZSM-5 is formed when tripropylammonium bromide ([TPA][Br]) is used as structure directing agent (SDA), and when tributylammonium bromide, tributylammonium hexafluorophosphate, tributylammonium nitride or 1-ethyl-3-methylimidazolium bromide is used as SDA, magadiite is formed. These results demonstrate the important of appropriate van der Waals force between precursor and structure directing agent. Also shown in these results is the addition of tetraalkylammonium salts to the magadiite reaction mixture does not inhibit the silica chemistry involved in the formation of magadiite which is one of dense materials, while these materials are considered as precursors to useful porous materials.

Recommendations

^{27}Al solid state NMR is a powerful tool to investigate state change of Al atoms in ionic liquids. In this project, after $Al(OiPr)_3$ is added into ionic liquids or added into a mixture of H_3PO_4 and ionic liquids, changes of confirmation of Al atoms are studied in order to find the interaction between ionic liquids and aluminium isopropoxide and interaction between phosphoric acid and aluminium isopropoxide in ionic liquids. In most of the reaction gels,

mineralizer and structure directing agent are added and claimed to be necessary for the formation of specific frameworks. As a result, one of the recommended works is to use solid state NMR to study effect of mineralizer and structure directing agent on the confirmation change of Al atoms in $Al(OiPr)_3$.

Aluminosilicates is believed to be more difficult to synthesize in ionic liquids than aluminophosphates. The main precursors of aluminosilicates are aluminium source and silicon source. Before an empirical recipe to synthesize aluminosilicate is proposed, ^{27}Al solid state NMR could be used to find at which temperature and by adding which mineralizer, confirmation of Al in the Al source could transfer to Al(IV) with the presence of a silicon source instead of phosphoric acid. At the same time, ^{29}Si solid state NMR can also be used to monitor the change of Si atoms in the reaction gel.

In addition, since this is the first research on ionothermal synthesis using hydrochloric acid instead of hydrofluoric acid, more recipes could be created to synthesize aluminophosphates of different frameworks by hydrochloric acid. In order to prevent the occurrence of dense materials due to water in the hydrochloric acid, high concentration hydrochloric acid could be used.

Appendix A - Additional Solid State NMR Data (Corresponding to Section 4.4)

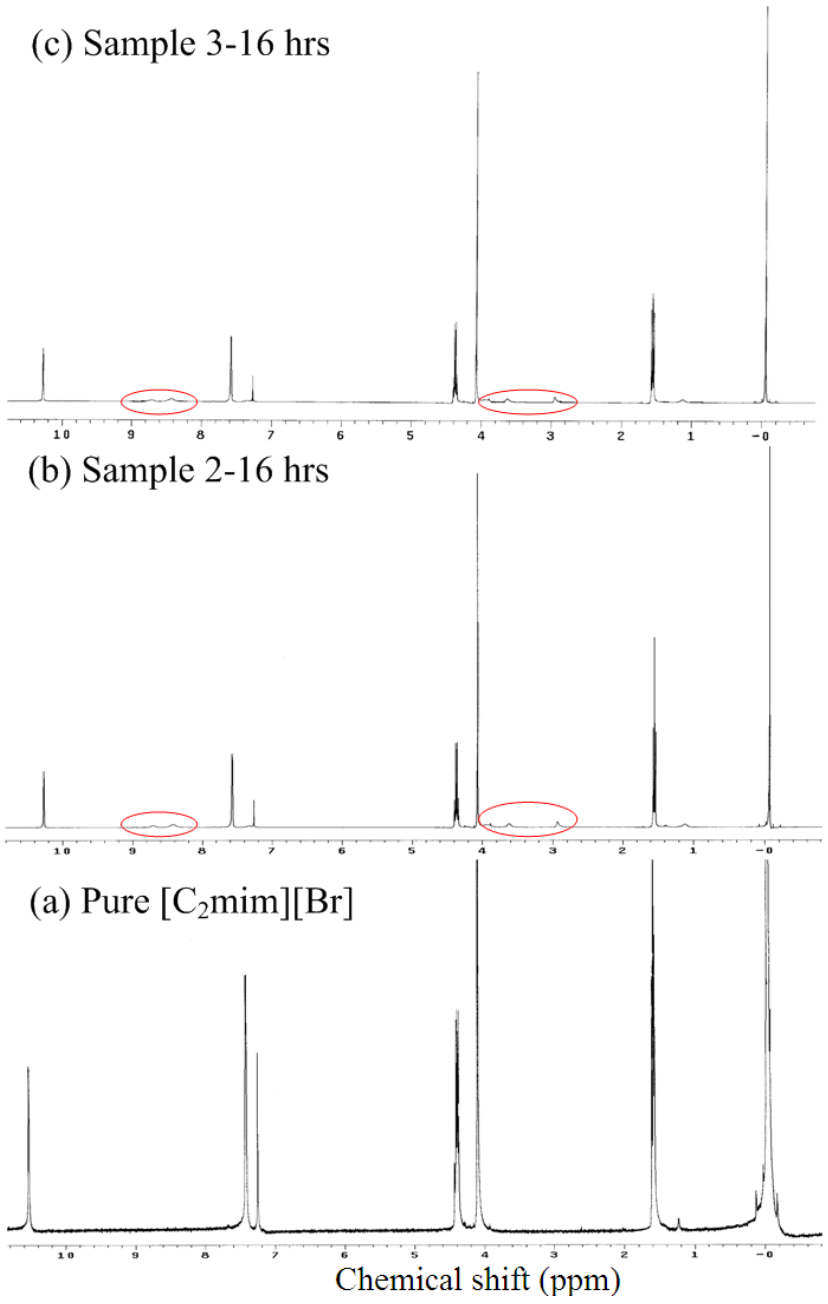

Figure 7.1 ^{1}H NMR spectra of (a) pure [C_2mim][Br], (b) sample 2 after heating for 16 hours and (c) sample 3 after heating for 16 hours.

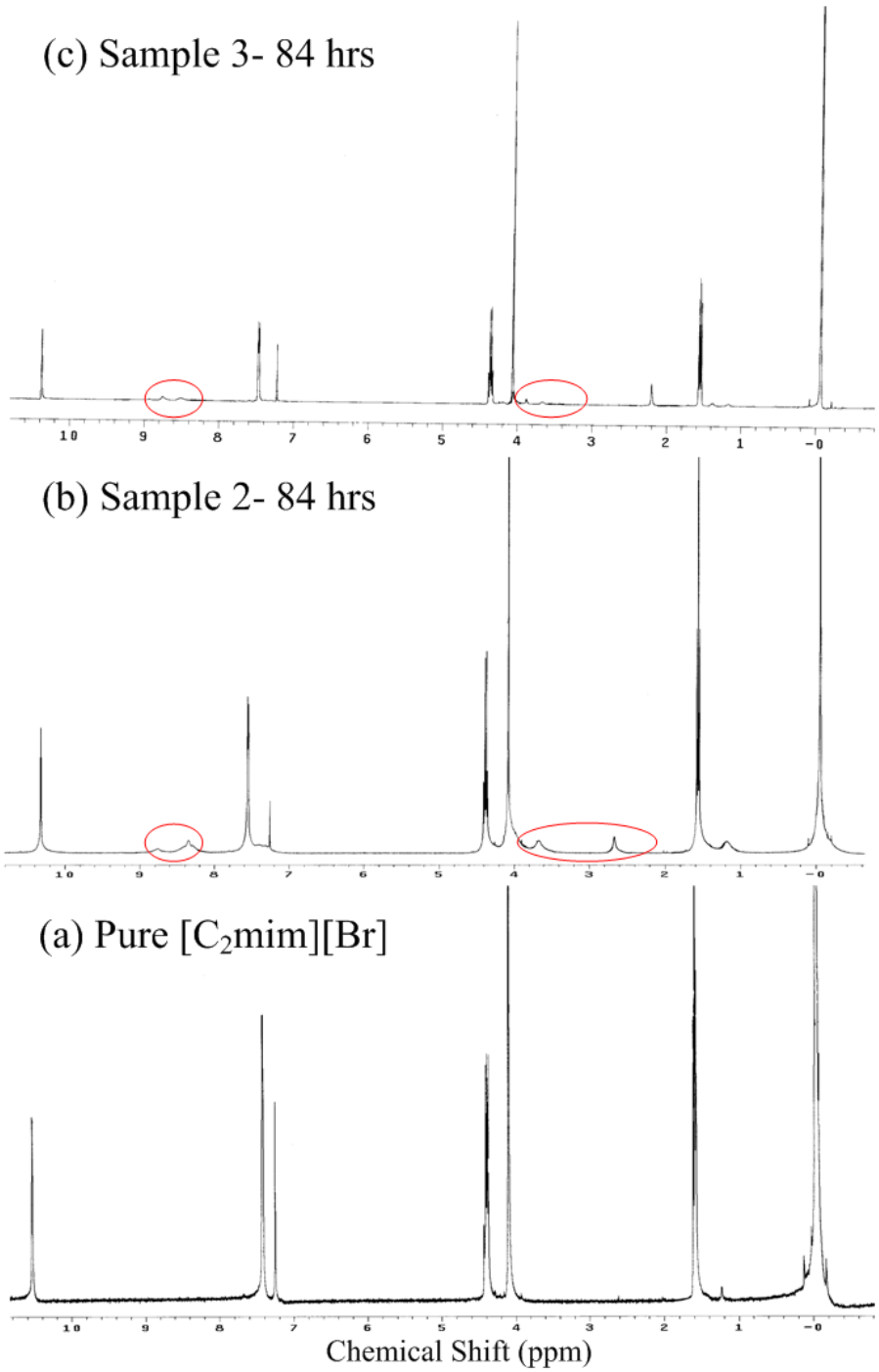

Figure 7.2 ^{1}H NMR spectra of (a) pure [C_2mim][Br], (b) sample 2 after heating for 84 hours and (c) sample 3 after heating for 84 hours.

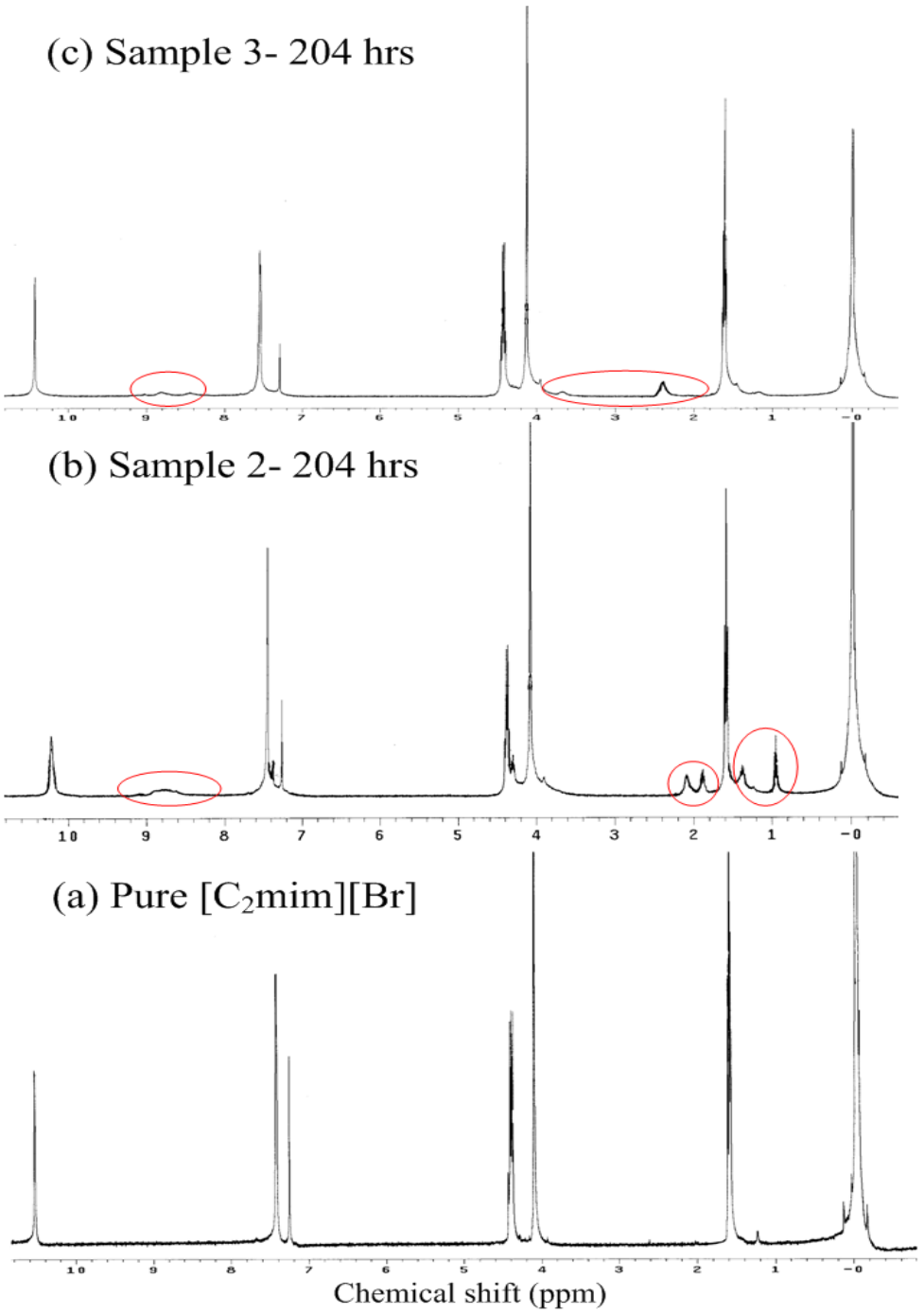

Figure 7.3 ^{1}H NMR spectra of (a) pure [C_2mim][Br], (b) sample 2 after heating for 204 hours and (c) sample 3 after heating for 204 hours.

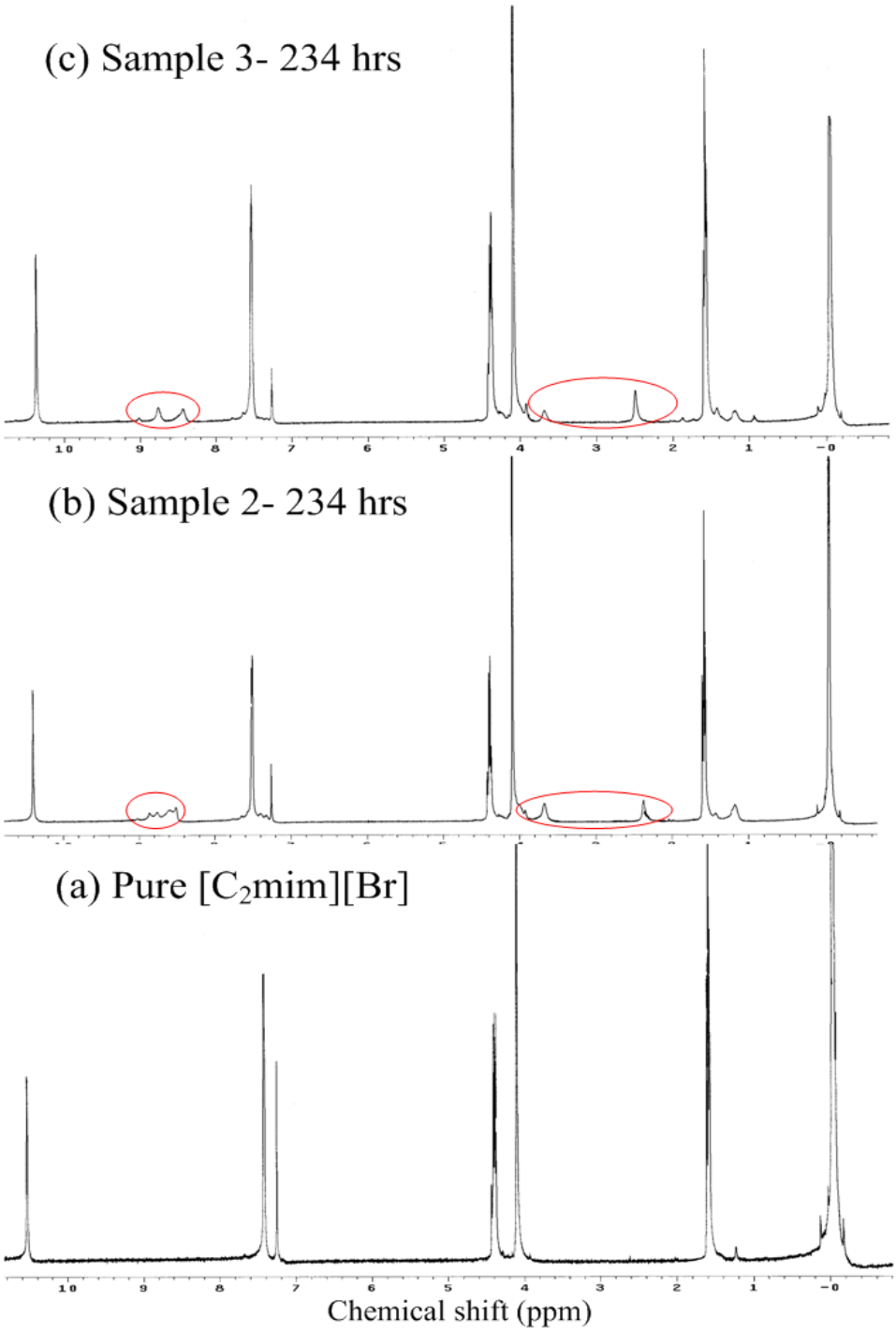

Figure 7.4 ^{1}H NMR spectra of (a) pure [C_2mim][Br], (b) sample 2 after heating for 234 hours and (c) sample 3 after heating for 234 hours.

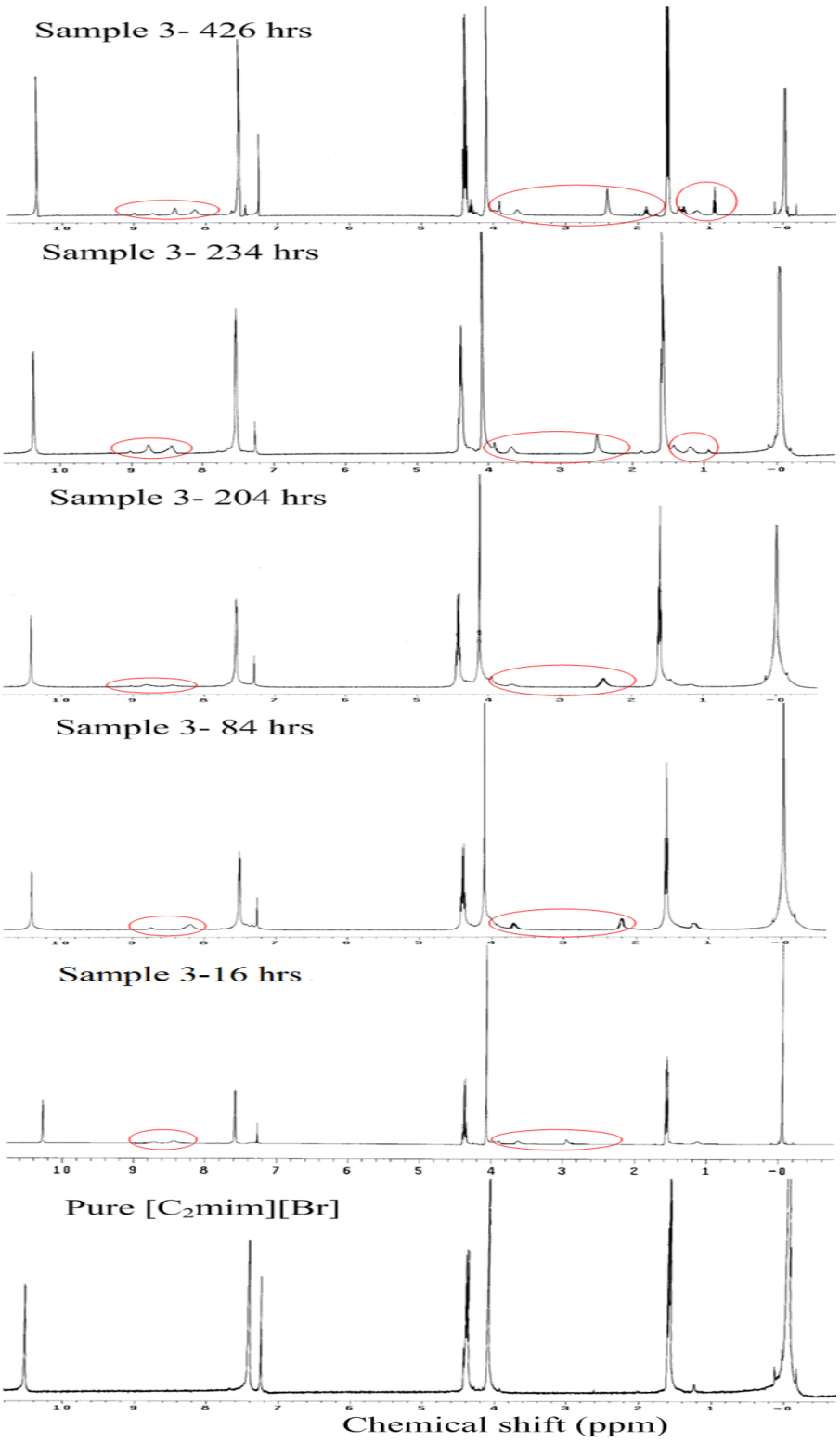

Figure 7.5 ^{1}H NMR spectra of (a) pure [C_2mim][Br] and sample 3 after heating for (b) 16 hours, (c) 84 hours, (d) 204 hours, (e) 234 hours and (f) 426 hours.

Appendix B - X-ray Diffraction Patterns for the Synthesized AlPOs (Corresponding to Section 6.1)

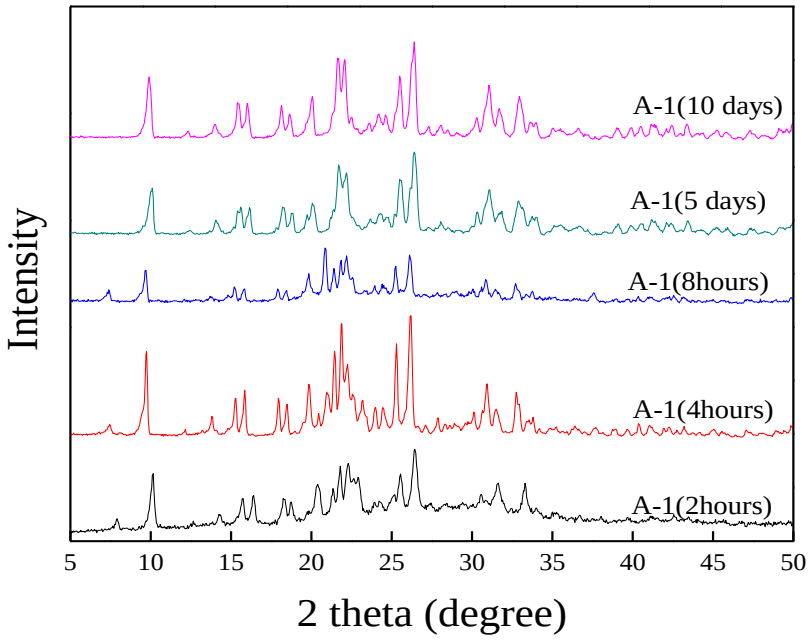

Figure 7.6 XRD patterns of products synthesized following recipe A-1, heated for (a) 2 hours, (b) 4 hours, (c) 8 hours, (d) 5 days and (e) 10 days.

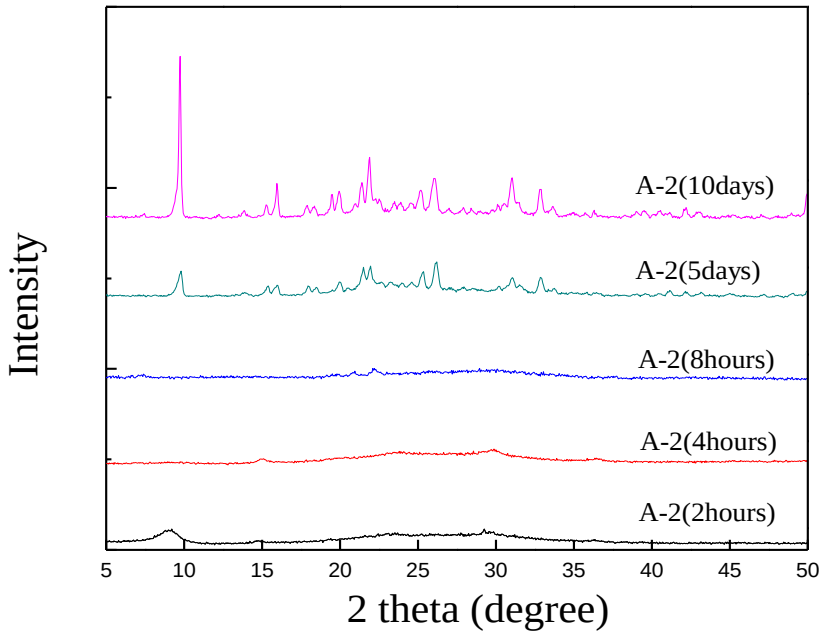

Figure 7.7 XRD patterns of products synthesized following recipe A-2, heated for (a) 2 hours, (b) 4 hours, (c) 8 hours, (d) 5 days and (e) 10 days.

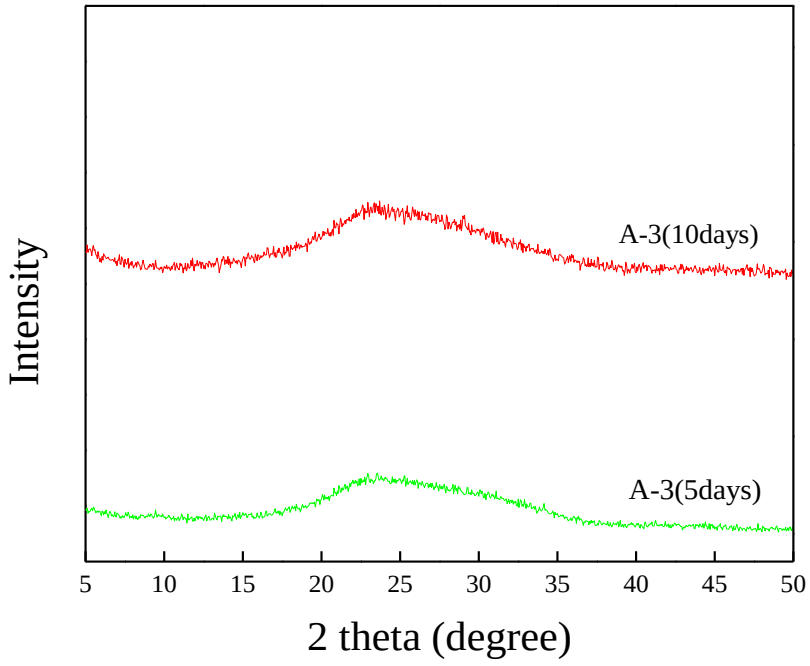

Figure 7.8 XRD patterns of products synthesized following recipe A-3, heated for (a) 5 days and (b) 10 days.

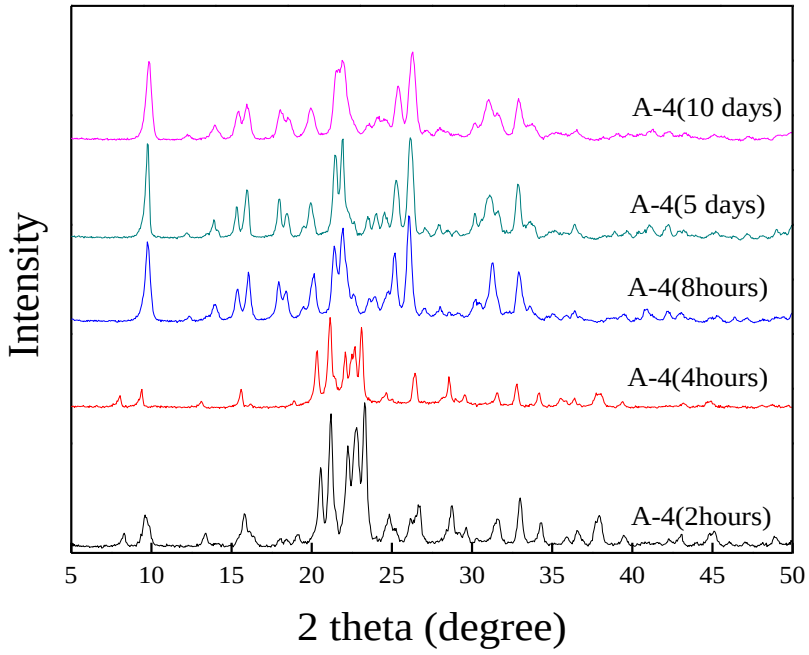

Figure 7.9 XRD patterns of products synthesized following recipe A-4, heated for (a) 2 hours, (b) 4 hours, (c) 8 hours, (d) 5 days and (e) 10 days.

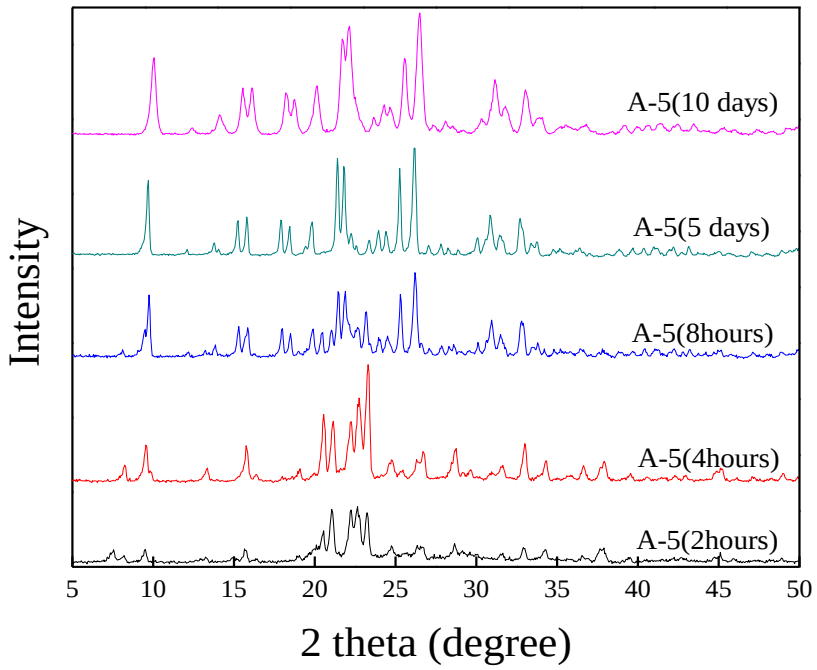

Figure 7.10 XRD patterns of products synthesized following recipe A-5, heated for (a) 2 hours, (b) 4 hours, (c) 8 hours, (d) 5 days and (e) 10 days.

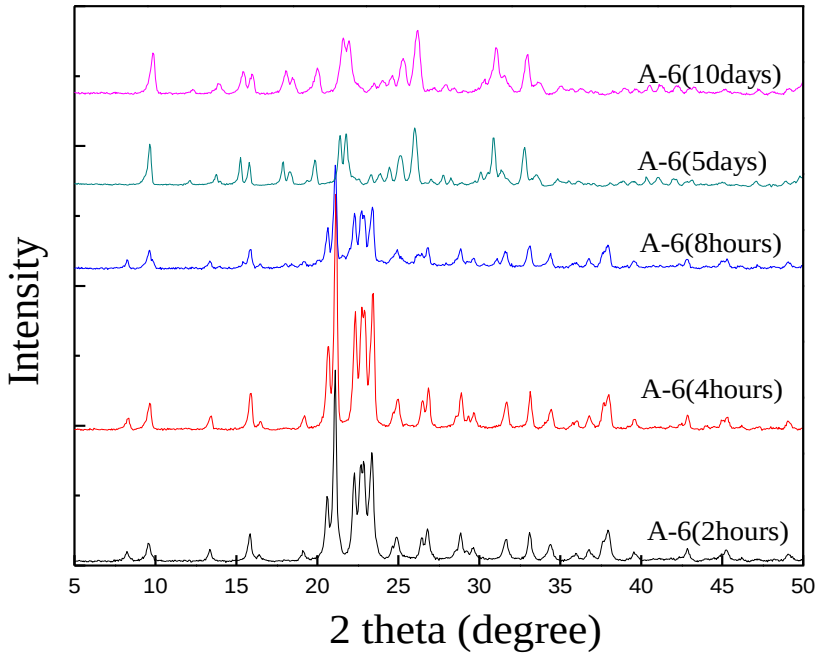

Figure 7.11 XRD patterns of products synthesized following recipe A-6, heated for (a) 2 hours, (b) 4 hours, (c) 8 hours, (d) 5 days and (e) 10 days.

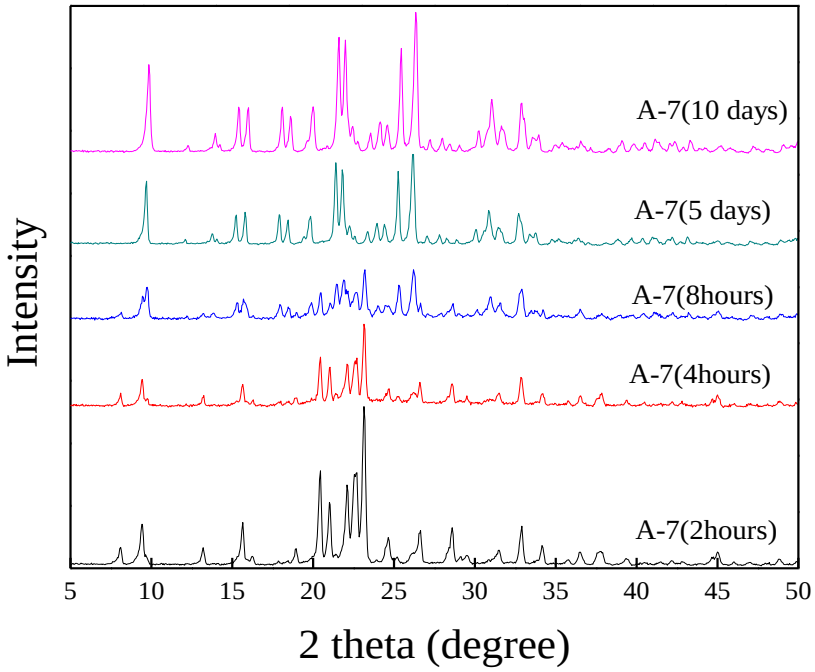

Figure 7.12 XRD patterns of products synthesized following recipe A-7, heated for (a) 2 hours, (b) 4 hours, (c) 8 hours, (d) 5 days and (e) 10 days.

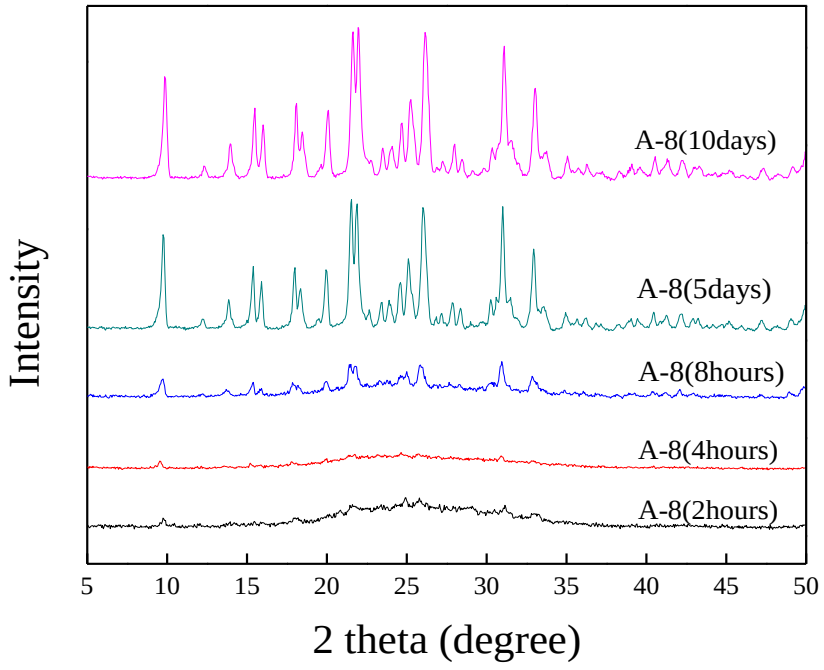

Figure 7.13 XRD patterns of products synthesized following recipe A-8, heated for (a) 2 hours, (b) 4 hours, (c) 8 hours, (d) 5 days and (e) 10 days.

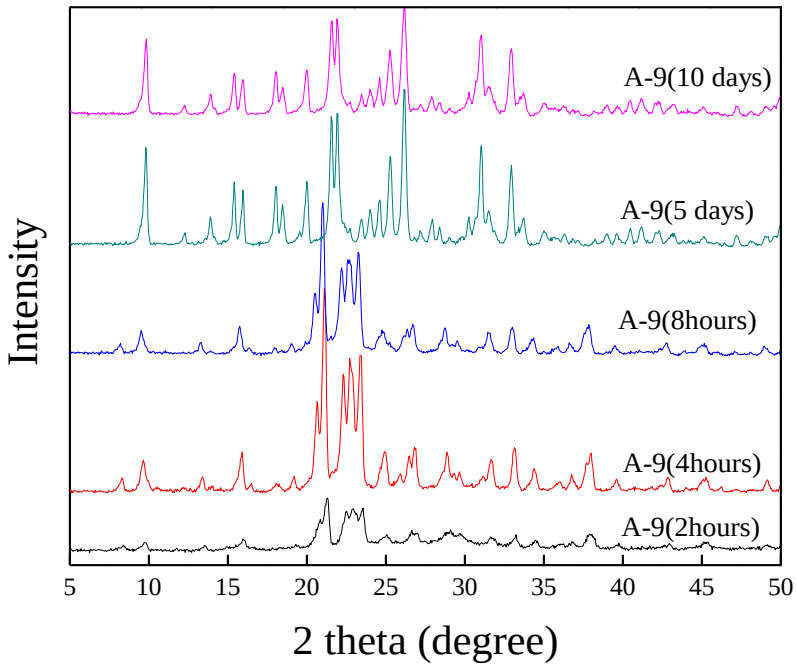

Figure 7.14 XRD patterns of products synthesized following recipe A-9, heated for (a) 2 hours, (b) 4 hours, (c) 8 hours, (d) 5 days and (e) 10 days.

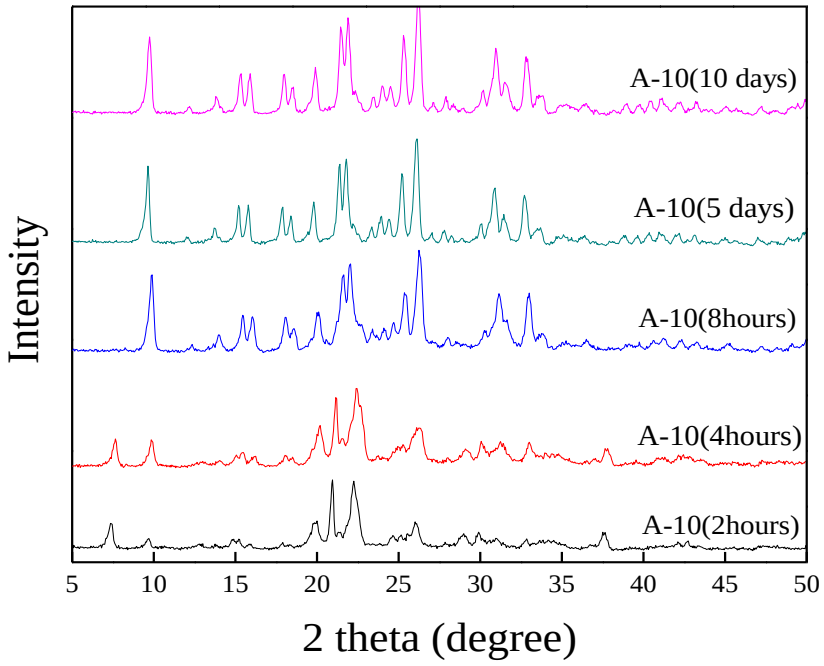

Figure 7.15 XRD patterns of products synthesized following recipe A-10, heated for (a) 2 hours, (b) 4 hours, (c) 8 hours, (d) 5 days and (e) 10 days.

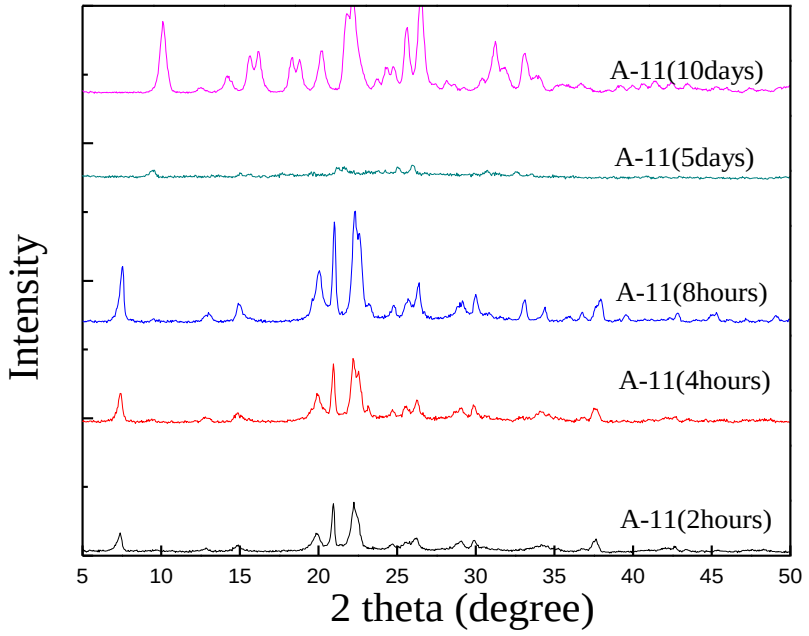

Figure 7.16 XRD patterns of products synthesized following recipe A-11, heated for (a) 2 hours, (b) 4 hours, (c) 8 hours, (d) 5 days and (e) 10 days.

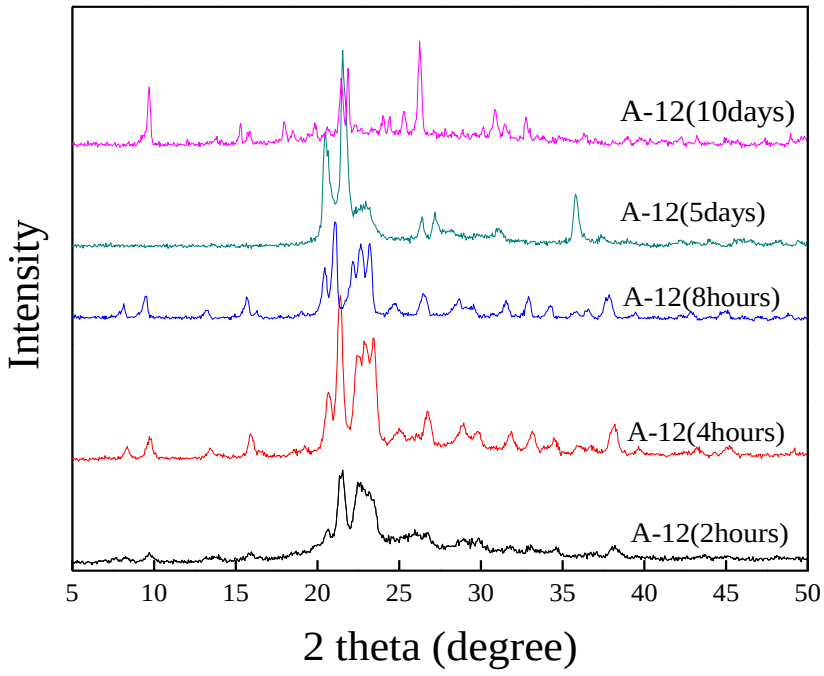

Figure 7.17 XRD patterns of products synthesized following recipe A-12, heated for (a) 2 hours, (b) 4 hours, (c) 8 hours, (d) 5 days and (e) 10 days.

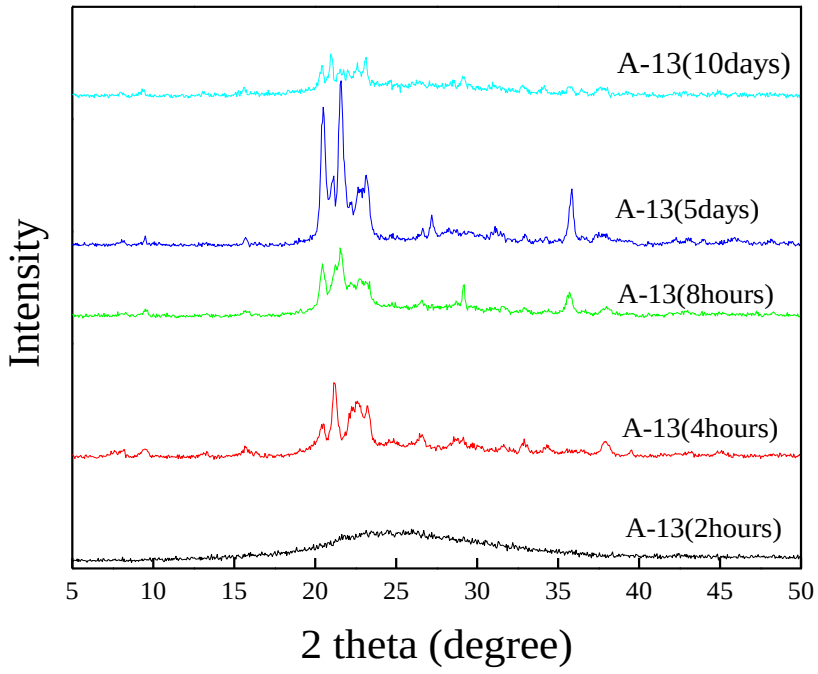

Figure 7.18 XRD patterns of products synthesized following recipe A-13, heated for (a) 2 hours, (b) 4 hours, (c) 8 hours, (d) 5 days and (e) 10 days.

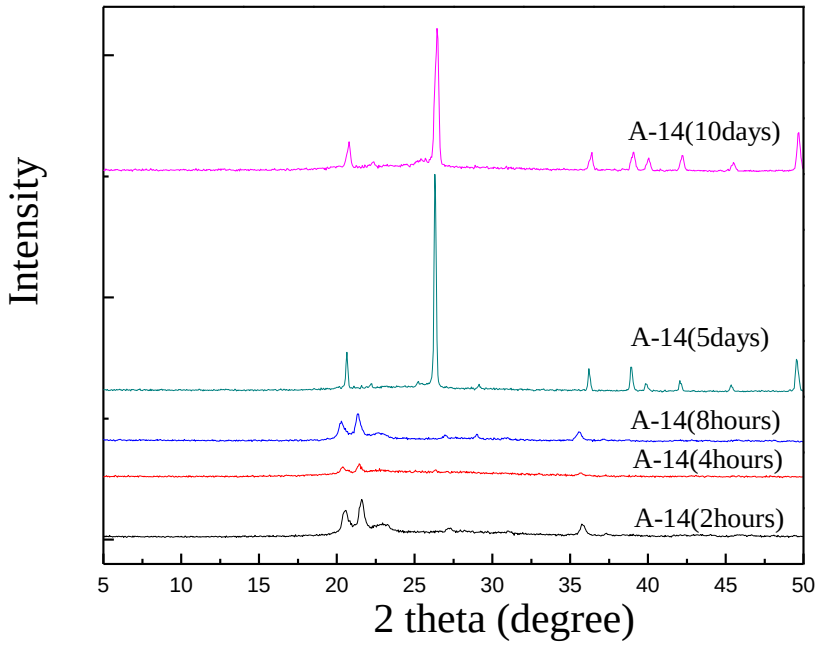

Figure 7.19 XRD patterns of products synthesized following recipe A-14, heated for (a) 2 hours, (b) 4 hours, (c) 8 hours, (d) 5 days and (e) 10 days.

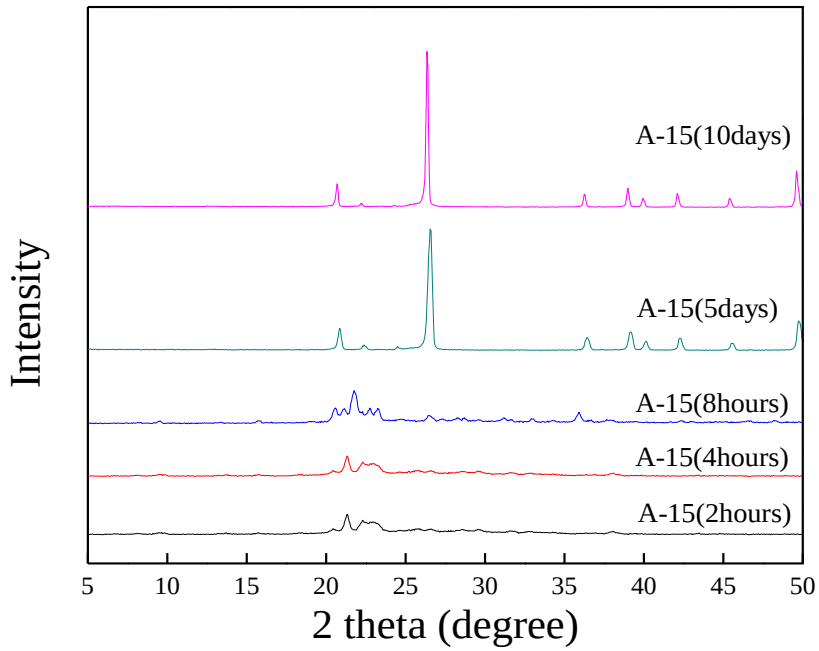

Figure 7.20 XRD patterns of products synthesized following recipe A-15, heated for (a) 2 hours, (b) 4 hours, (c) 8 hours, (d) 5 days and (e) 10 days.

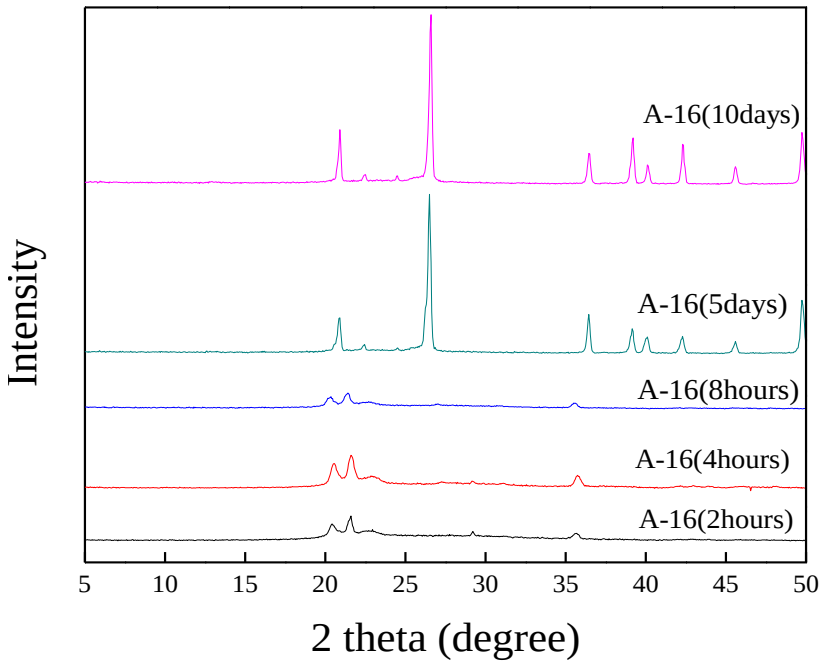

Figure 7.21 XRD patterns of products synthesized following recipe A-16, heated for (a) 2 hours, (b) 4 hours, (c) 8 hours, (d) 5 days and (e) 10 days.

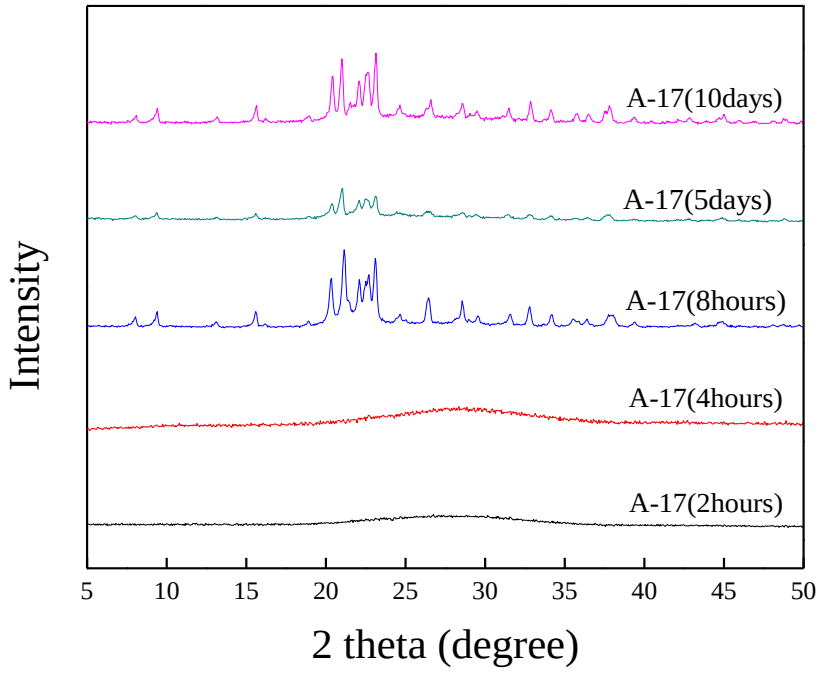

Figure 7.22 XRD patterns of products synthesized following recipe A-17, heated for (a) 2 hours, (b) 4 hours, (c) 8 hours, (d) 5 days and (e) 10 days.

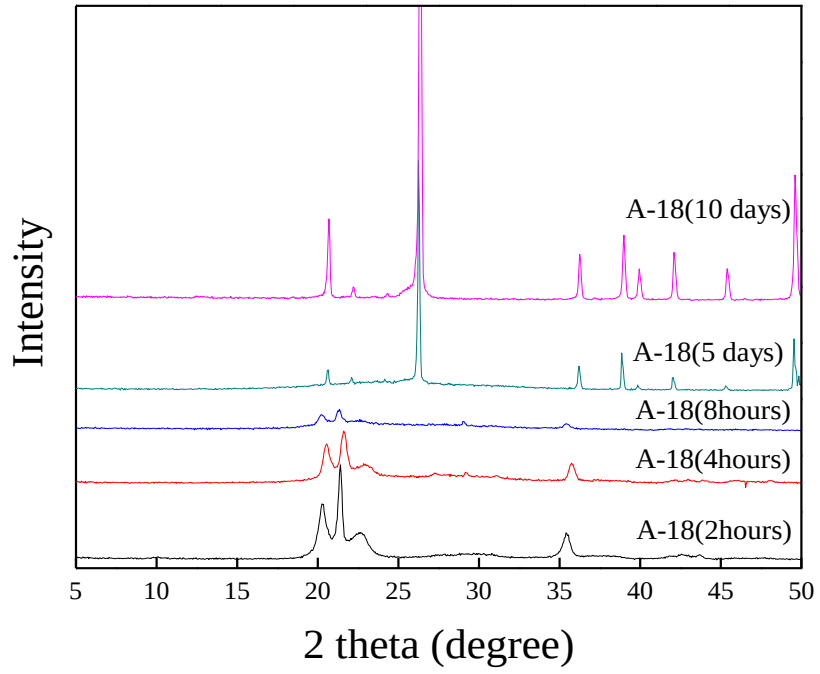

Figure 7.23 XRD patterns of products synthesized following recipe A-18, heated for (a) 2 hours, (b) 4 hours, (c) 8 hours, (d) 5 days and (e) 10 days.

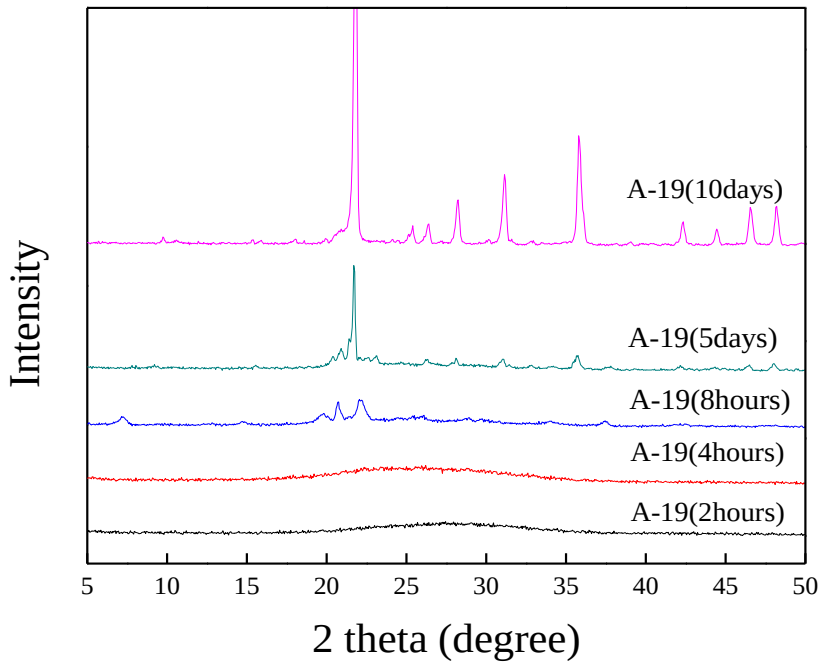

Figure 7.24 XRD patterns of products synthesized following recipe A-19, heated for (a) 2 hours, (b) 4 hours, (c) 8 hours, (d) 5 days and (e) 10 days.